

DISSECTION OF THE
HSF1-DEPENDENT STRESS RESPONSE
WITH A SPECIAL FOCUS ON THE
CHLOROPLAST HSP70 SYSTEM
IN *CHLAMYDOMONAS REINHARDTII*

Vom Fachbereich Biologie
der technischen Universität Kaiserslautern
zur Erlangung des akademischen Grades
„Doktor der Naturwissenschaften“
genehmigte Dissertation
(D386)

Kumulative Dissertation

vorgelegt von
Dipl. Biol. Stefan Schmollinger

Tag der Abgabe: 17.10.2012

Wissenschaftliche Aussprache: 30.11.2012

Prüfungskommission:

Vorsitzender: Prof. Dr. Ekkehard Neuhaus

1. Gutachter: Prof. Dr. Michael Schroda

2. Gutachter: Prof. Dr. Johannes M. Herrmann

Die Wissenschaft, richtig verstanden, heilt den Menschen von seinem Stolz;
denn sie zeigt ihm seine Grenzen.
Albert Schweitzer

TABLE OF CONTENTS

Preamble.....	- 1 -
1. Introduction	- 3 -
1.1. Chlamydomonas as a model organism	- 3 -
1.2. The heat shock response	- 3 -
1.2.1. Heat shock factors (HSFs), transcriptional regulators of the HSR	- 4 -
1.2.1.1. The complexity of the HSF gene family	- 5 -
1.2.2. Eliciting a HSF1-dependent heat shock response	- 6 -
1.2.3. Heat shock elements	- 8 -
1.2.4. Targets of transcriptional regulation	- 9 -
1.2.4.1. Plant specific targets of the HSR.....	- 10 -
1.3. Chaperones of the HSP70 family	- 11 -
1.3.1. HSP70s in the chloroplast.....	- 12 -
1.4. Reverse genetics in <i>Chlamydomonas reinhardtii</i>	- 14 -
1.4.1. Gene targeting in Chlamydomonas	- 14 -
1.4.2. RNA interference (RNAi).....	- 15 -
1.4.2.1. siRNA based tools for reverse genetics in Chlamydomonas.....	- 18 -
1.4.2.2. Artificial miRNAs increase specificity and applicability	- 18 -
1.4.2.3. Inducible knock-down approaches.....	- 20 -
1.5. Aims of this work	- 21 -
2. Summarizing discussion	- 23 -
2.1. General features of the HSR in Chlamydomonas.....	- 23 -
2.1.1. Role of cytosolic chaperones in the HSR of Chlamydomonas.....	- 23 -
2.1.2. Stress sensing and signal transduction	- 24 -
2.2. Development of an inducible amiRNA system for Chlamydomonas.....	- 27 -
2.2.1. Vector features	- 27 -
2.2.2. Application – Proof of principle	- 28 -
2.3. Identification of potential HSF1 target genes	- 30 -
2.3.1. HSF1-dependently regulated processes (Plant-specific features).....	- 30 -
2.3.2. Direct targets	- 31 -
2.3.3. Feedback control	- 32 -
2.3.4. Regulation of the stress response at the epigenetic level	- 32 -
2.4. Functional analysis of the essential chloroplast chaperone HSP70B	- 33 -
2.4.1. Consequences of chaperone depletion on the VIPP1 substrate.....	- 34 -
2.4.2. Essential functions of HSP70B	- 34 -
2.4.3. A novel approach to identify HSP70B substrates.....	- 36 -
2.4.4. Outlook.....	- 37 -
3. Articles and manuscripts.....	- 39 -

3.1.	Article 1: An inducible artificial microRNA system for <i>Chlamydomonas reinhardtii</i> ... confirms a key role for heat shock factor 1 in regulating thermotolerance.....	- 39 -
3.2.	Article 2: Transcription factor-dependent chromatin remodeling at heat shock and .. copper-responsive promoters in <i>Chlamydomonas reinhardtii</i>	- 49 -
3.3.	Article 3: A protocol for the identification of protein-protein interactions based on .. ¹⁵ N metabolic labeling, immunoprecipitation, quantitative mass spectrometry and .. affinity modulation.	- 75 -
3.4.	Manuscript 1: Dissection of the heat stress response in <i>Chlamydomonas</i> reveals a ... role for chloroplast HSP70B in stress signaling.	- 83 -
3.5.	Manuscript 2: The HSF1-dependent heat shock response in <i>Chlamydomonas</i> <i>reinhardtii</i>	- 113 -
3.6.	Manuscript 3: Stromal HSP70B is an essential protein for cell growth with functions in thylakoid assembly and amino acid metabolism.	- 149 -
4.	References.....	- 187 -
5.	Summary / Zusammenfassung.....	- 201 -
6.	Erklärung.....	- 203 -
7.	Curriculum vitae.....	- 205 -

PREAMBLE

Die vorliegende Dissertation wurde am Max Planck Institut für Molekulare Pflanzenphysiologie in Potsdam-Golm in der Arbeitsgruppe von Professor Dr. Michael Schroda angefertigt. Die Experimente, die dieser Arbeit zugrunde liegen wurden zwischen dem 01.10.2008 und dem 01.03.2012 durchgeführt. Die Dissertation ist kumulativ verfasst und besteht aus drei veröffentlichten Arbeiten, einem zur Veröffentlichung eingereichten Manuskript und zwei Manuskriptentwürfen.

Article 1: **Stefan Schmollinger**, Daniela Strenkert and Michael Schroda:

An inducible artificial microRNA system for *Chlamydomonas reinhardtii* confirms a key role for heat shock factor 1 in regulating thermotolerance.

Current Genetics, 2010, Aug, 56(4):383-9.

Article 2: Daniela Strenkert, **Stefan Schmollinger**, Frederik Sommer, Miriam Schulz-Raffelt and Michael Schroda:

Transcription factor-dependent chromatin remodeling at heat shock and copper-responsive promoters in *Chlamydomonas reinhardtii*.

The Plant Cell, 2011, Jun, 23(6):2285-301.

Article 3: **Stefan Schmollinger**, Daniela Strenkert, Vittoria Offeddu, André Nordhues, Frederik Sommer and Michael Schroda:

A protocol for the identification of protein-protein interactions based on ¹⁵N metabolic labeling, immunoprecipitation, quantitative mass spectrometry and affinity modulation.

Journal of Visualized Experiments, 2012, Sep, 67, e4083

Manuscript 1: **Stefan Schmollinger***, Miriam Schulz-Raffelt*, Daniela Strenkert, Daniel Veyel, Olivier Vallon and Michael Schroda:

Dissection of the heat stress response in *Chlamydomonas* reveals a role for chloroplast HSP70B in stress signaling.

Manuscript currently submitted for publication

Manuscript 2: **Stefan Schmollinger**, Timo Mühlhaus, Daniela Strenkert, Miriam Schulz-Raffelt, Corinna Gruber, Stefanie Schönfelder, Sebastian Klie, Björn Voss, Thorsten Kurz, Wolfgang Hess and Michael Schroda:

The HSF1-dependent heat shock response in *Chlamydomonas reinhardtii*.

Draft manuscript

Manuscript 3: **Stefan Schmollinger**, Corinna Gruber, Daniela Strenkert, Daniel Veyel, Timo Mühlhaus, Frederik Sommer, Dorothea Hemme and Michael Schroda:

Stromal HSP70B is an essential protein for cell growth with functions in thylakoid assembly and amino acid metabolism.

Draft manuscript

Zusätzlich habe ich während meiner Promotion zu zwei weiteren, bereits veröffentlichten Arbeiten beigetragen, die in dieser Arbeit nicht genauer ausgeführt werden. Diese sind im Folgenden aufgeführt.

Article 4: Daniela Strenkert, **Stefan Schmollinger** and Michael Schroda: Protocol: Methodology for chromatin immunoprecipitation (ChIP) in *Chlamydomonas reinhardtii*. Plant Methods, 2011, Nov, 3;7(1):35

Article 5: André Nordhues, Mark Aurel Schöttler, Ann-Katrin Unger, Stefan Geimer, Stephanie Schönfelder, **Stefan Schmollinger**, Mark Rütgers, Giovanni Finazzi, Barbara Soppa, Frederik Sommer, Timo Mühlhaus, Thomas Roach, Anja Krieger-Liszkay, Heiko Lokstein, José Luis Crespo and Michael Schroda:

Evidence for a role of VIPP1 in the structural organization of the photosynthetic apparatus in *Chlamydomonas*.

The Plant Cell, 2012, Feb, 24(2):637-59

1. INTRODUCTION

1.1. CHLAMYDOMONAS AS A MODEL ORGANISM

Chlamydomonas reinhardtii, a unicellular green alga, is utilized as a plant model organism to investigate cell and molecular biology since the 1950s¹. Its single chloroplast and the highly conserved structure of the photosynthetic apparatus within the green lineage combined with the ability of *Chlamydomonas* to also grow heterotrophically facilitated research especially in the field of photosynthesis, chloroplast biogenesis and nuclear control of chloroplast gene expression^{2,3}. Research on the structure of the *Chlamydomonas* flagella, their mode of operation and the underlying molecular mechanisms of their assembly provided important insights into flagella/basal body related diseases in mammals⁴.

While these fields were extensively studied in the past, the techniques developed and understanding gained for the model organism enabled research on a broad variety of plant-related topics. The common motivation to favor the simple unicellular green alga over higher plant model organisms are the advantages of a microbial-like system (fast culturing, easy perturbations) and the reduced complexity of its gene families as exemplified with stress-related protein families later on in this work. A prominent example is a *Chlamydomonas* eyespot protein, Channelrhodopsin, which is responsible for the modulation of flagellar beating to direct the alga towards optimal light intensities (phototaxis). The in-depth characterization of this protein in *Chlamydomonas* opened up a completely new field within neurosciences, now referred to as “optogenetics”. By directly transducing a light signal to the opening of an ion channel within a single protein, Channelrhodopsin allows for optical controlled, very fast induction of action potentials in neurons^{5,6}.

1.2. THE HEAT SHOCK RESPONSE

In order to maintain homeostasis and survive in a changing environment all living organisms created cellular mechanisms to cope with various natural stress conditions⁷. One of them, the heat shock response (HSR), is a highly ordered genetic response to diverse environmental and physiological stresses, as there are elevated temperatures, heavy metals, oxidants, bacterial/viral infections and toxic chemicals⁸. The occurrence of unfolded or misfolded proteins is the common molecular consequence of these various proteotoxic stresses. Beside the inability to fulfill their own functions, unfolded proteins are a constant threat to neighboring native proteins by exposing normally buried hydrophobic regions to their local environment. These regions may stabilize other proteins in unfavorable conformations and allow them to join protein aggregates. Therefore, cells need a fast defense mechanism to avoid harmful effects. The first indication for such a response to proteotoxic stress conditions was the appearance of new puffs in polytene chromosomes of larval salivary glands of *Drosophila busckii* pointing to a massive change in gene expression upon temperature shift⁹.

The major product of the HSR is a specific set of proteins, the so-called heat shock proteins (HSPs), consisting mainly of molecular chaperones and proteases. The HSP superfamily is organized by molecular mass and groups into six major families: HSP100s, HSP90s, HSP70s, HSP60s, HSP40s and small heat shock proteins (sHSPs)¹⁰. Whereas some of these proteins are exclusively present under stress conditions, many of them also have essential proofreading function in protein biogenesis and protein homeostasis under normal growth conditions^{11,12}. They play roles in the assisted folding of newly synthesized or denatured proteins, in the resolving of protein aggregates, in translocating proteins across membranes and in assembling and disassembling of protein complexes. Furthermore, they target proteins to the protein degradation machinery and modulate many signal transduction pathways¹³⁻¹⁶.

1.2.1. HEAT SHOCK FACTORS (HSFs), TRANSCRIPTIONAL REGULATORS OF THE HSR

The heat shock response in eukaryotes is regulated at the transcriptional level by the activity of a specialized family of transcription factors, the so-called heat shock factors (HSFs)¹⁷⁻¹⁹. Their basic domain architecture is highly conserved and consists of three functional domains: The N-terminal DNA binding domain, which is the most conserved part of HSF proteins, an oligomerization domain and a C-terminal transactivation domain²⁰. An overview of the structure of the DNA binding domain and HSF domain organization from different organisms is provided in Figure 1A/B.

The DNA binding domain (DBD) consists of a three α -helix bundle that is capped by a four-stranded antiparallel β -sheet^{21,22}. In addition, HSFs can contain a “wing”, a long, flexible turn between β -sheet three and four, consisting of 15 amino acids, present only in non-plant species^{23,24}. DNA contact is mainly mediated by the central helix-turn-helix motif consisting of helix two and three of the α -helix bundle and the turn in between. Amino acids from the so-called recognition helix (helix three), especially a highly conserved arginine residue, mediate direct contact to nucleotides in the major groove of the DNA²². The wing of the DBD is not participating in the protein-DNA interface, as known from other “winged” helix-turn-helix proteins. Instead, it participates in the oligomerization interface²².

HSFs bind to their target DNA only when assembled into trimers²⁵. Mainly responsible for the oligomerization is the second conserved region adjacent to the DBD. The oligomerization domain consists of two hydrophobic heptad repeat regions (HR-A/B). They are α -helical regions with hydrophobic amino acids (mainly leucine, isoleucine, valine) at every seventh position thus creating a hydrophobic patch on one side of the helix, similar to leucine zippers^{25,26}. Three of these patches from individual HSF monomers allow trimerization, presumably via a triple-stranded α -helical coiled-coil interaction²⁷.

Within the C-terminal transactivation domain (CTAD), proper localization and interaction with the transcription machinery and enhancer proteins is realized in order to promote transcription²⁸. A conserved motif consisting of an Aromatic, large Hydrophobic and

an Acidic amino acid residue (AHA) plays a major role in the transactivation process^{28,29}.

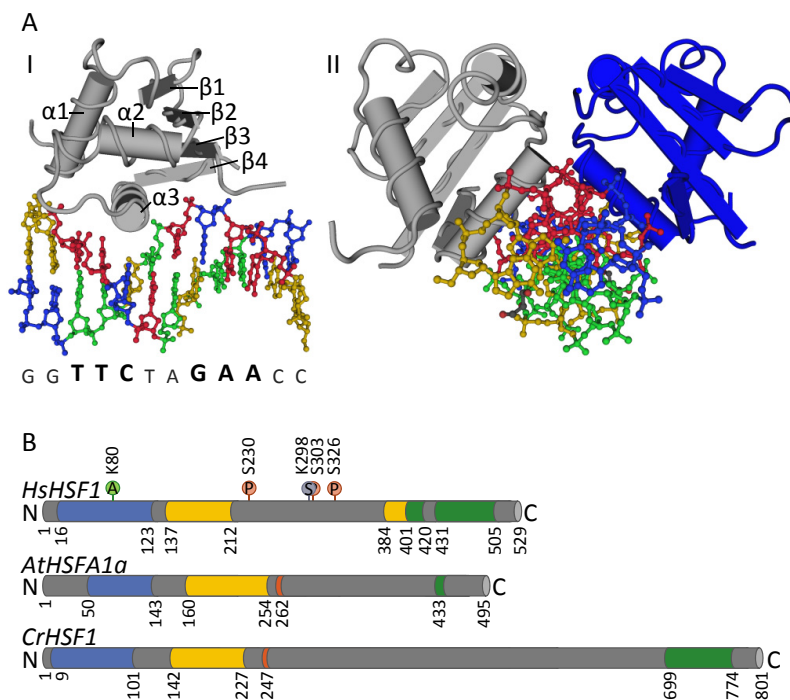


Figure 1: Structural features of HSFs

A: DNA binding domain of *Kluyveromyces lactis*: Structure of the HSF DNA binding domain attached to DNA as determined by Littlefield and Nelson, 1999. The stereo views of the DNA binding domain attached to a HSE were generated with Cn3D (NCBI). The α -helices of the three α -helix bundle are labeled $\alpha1$, $\alpha2$ and $\alpha3$, respectively; the β strands are labeled $\beta1$, $\beta2$, $\beta3$ and $\beta4$. The first view is looking down on α -helix 3, the recognition helix positioned in the major groove of the DNA over the G of the first nGAAn binding site. The second view is looking down on the DNA, showing two DNA binding domains attached to the nnGAAnnTTCnn locus.

B: Domain architecture of HSFs: HSFs from *Homo sapiens* (*HsHSF1*), *Arabidopsis thaliana* (*AtHSFA1a*) and *Chlamydomonas reinhardtii* (*CrHSF1*). The conserved DNA binding domains (blue), the hydrophobic heptad repeat regions involved in intra- or intermolecular helix-helix interactions (yellow), the nuclear localization signal (red) and C-terminal activating elements (green) are presented. The known phosphorylated (P, red), acetylated (A, green) and sumoylated (S, blue) amino acid residues in *HsHSF1* involved in activation and attenuation are denoted.

1.2.1.1. THE COMPLEXITY OF THE HSF GENE FAMILY

Heat shock factors are highly conserved among all eukaryotes and are distinguished from other transcription factors by their highly conserved DNA binding domain. Regarding the number of HSFs and the presence and arrangement of domains many differences are found between different species.

The best-studied HSF systems are found within mammals. Four different HSFs exist in vertebrates, whereas not all are present throughout this subphylum. HSF1 and HSF2 are ubiquitous while HSF4 is found only in mammals and HSF3 is specific for avian species⁷. *HSF1* is expressed in almost all cell types at all developmental stages and is essential for the induction of HSPs in response to proteotoxic stress conditions³⁰. HSF2 is not able to bind to HSP promoters alone, but in addition to HSF1, thereby modulating HSP gene expression, both in a stimulating and repressing way³¹.

In the green lineage the family of heat shock factors is extraordinarily complex with for example 21 members in *Arabidopsis thaliana* and 25 members in rice (*Oryza sativa*) and maize (*Zea mays*)³²⁻³⁴. Therefore, HSFs were classified into three distinct subclasses (A, B and C) according to the spacing between the HR-A and HR-B region and the presence (A) or absence

(B, C) of the AHA motifs in their transactivation domains³⁴. Whereas non-plant HSFs and HSFs of plant class B contain no additional amino acids in between HR-A and HR-B, seven amino acids were added to plant class C HSFs and twenty-one to members of plant class A HSFs³⁴. The latter were identified as activators of *HSP* gene expression, and thus are essential for plants to cope with proteotoxic stresses^{35,36}. HSFs of plant class B modulate *HSP* gene expression in a similar way as already described for HSF2 in the vertebrate system. They act as co-activators or repressors of transcription promoted by plant class A HSFs. Tomato HSF1 is an example for a co-activating B-type plant HSF. Acting in concert with an A-type HSF, tomato HSF1, expression of target genes is strongly increased upon stress treatment³⁷. In contrast, Arabidopsis AtHsf1 is a repressor of gene expression. Lacking a short histone like motif in its CTAD necessary for transcriptional activation, this B-type HSF is repressing AtHsf1 promoted transcription of *HSP* genes^{37,38}. In addition, A-type HSFs are assembling into hetero-oligomeric supercomplexes, as demonstrated for tomato HSF1a and HSF1b, to further increase expression of *HSP* genes^{39,40}. Furthermore, the composition of the expressed HSF pool depends on the prevailing stress condition⁴¹. Taken together, plants developed a highly variable acclimation strategy to proteotoxic stress conditions enabling specialized fine tuning to different chaperoning needs.

On the opposite, only a single HSF is sufficient for regulation of thermotolerance in *Saccharomyces cerevisiae*, *Chlamydomonas reinhardtii*, *Drosophila melanogaster* and *Caenorhabditis elegans*. This is especially remarkable in case of the single HSF of *Chlamydomonas*, which is phylogenetically located at the origin of the green lineage. *Chlamydomonas* HSF1 has a high similarity to the domain architecture of plant class A HSFs, containing a 21 amino acid insertion between the HR-A and B region and also AHA motifs in the CTAD. Another typical feature of plant HSFs is their inducibility upon stress treatment. As *Chlamydomonas* HSF1 shares this trait with plant HSFs it is clearly distinct from the other single HSFs of worm, fly and yeast²⁴. On the other hand, *Chlamydomonas* HSF1 is also distinct from plant HSFs. It is constitutively trimeric, similar to yeast HSF, while plant HSFs trimerize upon occurrence of proteotoxic stresses, similar to the single HSF in *Drosophila* and mammalian HSFs.

1.2.2. ELICITING A HSF1-DEPENDENT HEAT SHOCK RESPONSE

The triggering of a HSF-dependent stress response is a complex process and is differently realized in various organisms. Upon stress, all HSFs are activated in a multistep process, which can include the resolving of repressing protein-protein interactions, oligomerization, post-translational modifications, translocation into the nucleus and stress-dependent accumulation of *HSF* mRNA¹⁹. The current model of eliciting and attenuating a stress response is summarized in Figure 2.

Whereas yeast and *Chlamydomonas* HSFs are constitutively present in a trimeric state already under normal growth conditions, controlling the transition from the monomeric to the oligomeric HSF plays a major role during the activation of HSFs from plants, *Drosophila melanogaster* and mammals^{24,25,42}. Their HSFs are present as monomers which are detained

from trimerization under non-stress conditions by a third conserved hydrophobic heptad repeat region within the C-terminal transactivation domain (HR-C). Formation of an intramolecular coiled-coil between the HR-C and HR-A/B regions prevents HSF trimer formation and also transcription of target genes at ambient temperatures^{42,43}. Consistent with a regulation at the level of HSF trimerization, chaperones of the HSP90 family are bound to HSF monomers under non-stress conditions in human cell lines⁴⁴. Trimerization is inhibited presumably by favoring the folding into the HR-C containing intramolecular coiled-coil instead of to an oligomerization competent state⁴⁵. Upon stress, HSP90 chaperones are recruited from unfolded/misfolded proteins and therefore release the previously bound HSF monomers which in turn are able to trimerize.

The direct interaction between the HS transcription factor and a chaperone is an elegant mechanism to directly transduce the chaperone need of the cell to increased gene expression. There is good evidence that this type of regulation is also taking place during other stages of the HSF activation process and is also involved in the attenuation of the HSF dependent heat stress response¹⁹. HSP90 containing complexes were not only shown to bind to HSF monomers to inhibit trimerization, but also to bind to HSF trimers, thus affecting the ability to bind to DNA⁴⁶. HSP70 containing complexes, when present in excess, presumably recognize HSF trimers as a substrate. The binding of HSP70 to the C-terminal transactivation domain of HSF1 is realized directly by its substrate binding domain and is also ATP dependent,

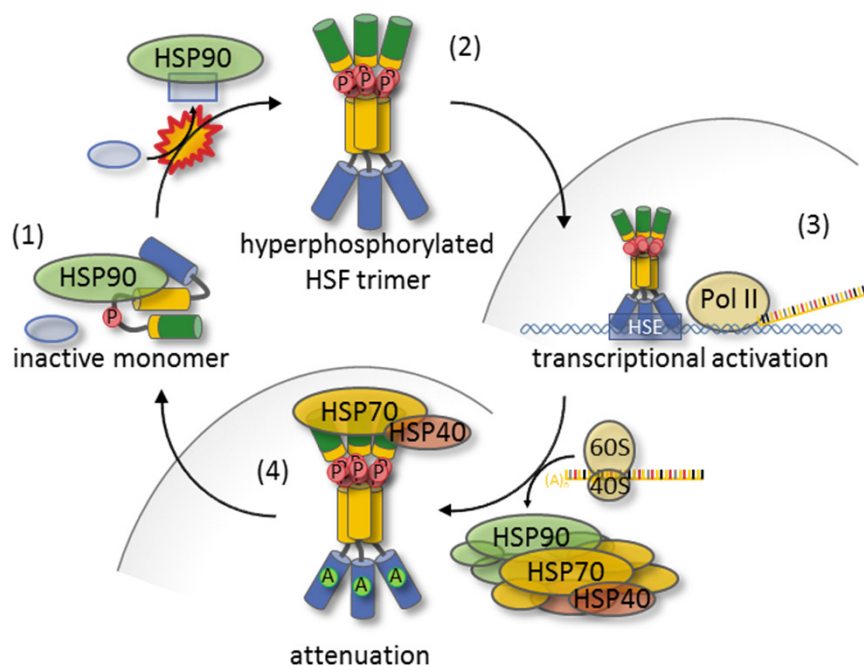


Figure 2: HSF1 activation cycle

Current model of the activation cycle of mammalian HSFs: Under ambient conditions, HSF monomers are bound by HSP90s that inhibit trimer formation (1). Upon stress, unfolded proteins recruit HSP90s, releasing HSF monomers which subsequently trimerize (2). HSF trimers are then hyperphosphorylated and translocated into the nucleus where they bind to HSEs in promoters of stress related genes (3). Once protein homeostasis is restored, the HSR is attenuated (4) through the binding of free chaperones of the HSP70 and 40 class to the transactivation domain of HSFs (decreasing transactivation capacity) and the acetylation of lysine 80 in the DNA binding domain (lowering DNA binding affinity). Adapted from¹⁹.

as is true for other HSP70 substrates. In contrast to the HSP90 containing complexes, DNA binding of HSF is not affected when in complex with HSP70. Instead, the trans-activating effect on gene expression is reduced, thus allowing the repression of DNA-bound HSF complexes⁴⁷.

Furthermore, HSFs are subject of multiple post-translational modifications (included in Figure 1A) that modulate HSF activity, including acetylation of a lysine within the DBD, phosphorylation of several serine residues and sumoylation of lysine residues¹⁹. HSF is already constitutively phosphorylated at several positions under normal growth conditions, but undergoes additional phosphorylations upon stress-treatment⁴⁸. Two of the stress-inducible phosphorylations, at serine 230 and 326 of human HSF1, are positively influencing stress regulation^{48,49}. The opposite was shown for phosphorylation of serine 303 and 307, which is constitutively present and responsible for repression of transactivation at ambient temperatures⁵⁰. Sumoylation of lysine 298 in human HSF1 is negatively influencing the transactivation of target genes and is thought to modulate the HSR⁵¹. Acetylation within the DBD is negatively affecting the DNA binding affinity of human HSF1 and therefore seems to play an important role during attenuation of the stress response⁵².

In parallel, also the localization of HSF1 is highly regulated and plays an important role during the activation cycle. Upon activation of the stress response, HSF is re-localized from the cytosol into the nucleus and/or to distinct regions within the nucleus, so-called stress granules⁵³.

1.2.3. HEAT SHOCK ELEMENTS

Trimeric HSFs bind with high affinity to specific *cis*-acting sequences in promoter regions, so-called heat shock elements (HSEs). In general, HSEs consist of at least three alternating inverted repeats of the pentameric sequence nGAAn, which is recognized by a HSF trimer (Figure 3). Each pentamer is bound by one DNA binding domain in the major groove of the DNA^{22,54-56}. Consistent with a regulation at the level of trimerization, the binding affinity of a single HSF monomer to a single nGAAn is rather weak. High-affinity DNA binding premises the presence of three binding sites as well as trimerized HSF²². HSEs are highly conserved throughout evolution and can be transferred between distantly related organisms while retaining their regulatory pattern⁵⁷.

In principle, there are three different types of HSEs. In perfect HSEs the pentamers are directly connected in an inverted orientation (nTTCnnGAAnnTTCn or nGAAnnTTCnnGAAn), while in gap-type HSEs there is one, in step-type HSEs there are two 5-p insertions between the nGAAn pentamers^{54,58,59}. While there seems to be a certain flexibility in the distance between the pentamers contacted by a single trimer, the (multiple of) 5 bp spacing between the pentamers is crucial for HSF binding. A proper spacing allows positioning of the binding nucleotides on one side of the DNA double-helix and therefore allows binding of the, in terms of turning, sterically limited trimer⁵⁸. Whereas yeast HSF1 is capable of binding all three types of HSEs, regulation of the target genes is different between the HSE types. For example, in gap-type

controlled genes in yeast the temperature needs to be higher to induce the gene to a full extent (39°C compared to 37°C for perfect HSEs)⁶⁰. Moreover, gene induction is dependent on a different part of the transactivation domain thereby indicating the need of different co-activators for transactivation at the different HSEs⁶⁰.

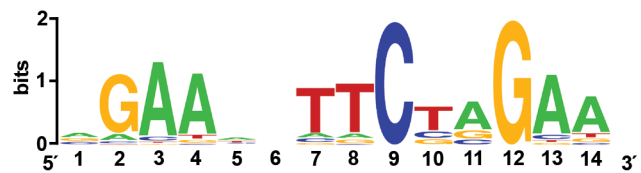


Figure 3: Heat shock elements

The position-specific weight matrix (PSWM) of heat shock elements in *Drosophila melanogaster* is derived from a genome-wide ChIP-seq study and illustrated with WebLogo²⁷⁰. From⁶⁷.

Therefore a single HSF, together with a

limited number of co-activator proteins, is capable of individually controlling different sets of genes, a principle referred to as combinatorial control^{61,62}. Furthermore, HSEs differ in their conservation to the nGAAn consensus and the position of the HSE within the promoter relative to the transcriptional start site. These alterations offer a way to differently express various *HSP* genes also within the perfect, gap-type and step-type group of target genes.

Additionally, most HSF-regulated genes harbor more than one HSE within their promoter regions, thereby allowing the binding of multiple HSFs in a cooperative manner^{22,63}. The trimeric nature of the HSFs thereby has interesting consequences as there are two distinct binding interfaces, referred to as head-to-head (nGAAn to nTTCn) and tail-to-tail (nTTCn to nGAAn) orientation depending on the bordering pentamers of the two connected HSEs. Cooperativity between two HSFs is more pronounced when the neighboring pentamers are in the tail-to-tail conformation^{22,64}.

1.2.4. Targets of transcriptional regulation

The set of genes regulated in response to the onset of the proteotoxic stress determines the acclimation strategy used and therefore is extensively studied in various organisms⁶⁵⁻⁶⁸. Different experimental approaches have been used in the past to determine HSF targets either directly via Electrophoretic Mobility Shift Assays (EMSA) or Chromatin Immunoprecipitation (ChIP), or indirectly by identifying genes differentially expressed between wild-type and *hsf* mutants upon the onset of different proteotoxic stresses. Genome wide analysis with microarrays and next-generation sequencing techniques allowed to extend the initial set of regulated genes, which was mainly consisting of molecular chaperones and proteins involved in protein degradation. HSF-binding to promoters of genes involved in cell wall biosynthesis, signal transduction, small molecule transport and energy metabolism was demonstrated upon stress treatment in yeast⁶⁶. In *Drosophila*, genes involved in general metabolism, signaling and gene expression were shown to be directly regulated by HSF1⁶⁹. In mammalian cells, HSF1 was shown to regulate the expression of proteins from the extracellular matrix, for example collagen COL4A6⁶⁵. In general, in all studies binding of HSF to promoter regions correlated well with stress-induced mRNA expression. Only in mammalian cells a small fraction of HSF1-bound genes was not induced upon heat stress, indicating the need of additional activator

proteins in these organisms to induce gene expression⁶⁵.

1.2.4.1. PLANT SPECIFIC TARGETS OF THE HSR

Plants harbor many HSFs, demonstrating the need of these organisms for a fine-tuned stress response. To elucidate the targets of transcriptional activation is rather complicated in a situation like this, as many closely related transcription factors potentially take over and also alter the response in the respective knock-out strains. Nevertheless, several studies were carried out where expression profiling in knock-out strains of individual HSFs compared to wild type was used to identify genes regulated by the individual factors upon stress treatment.

Double knock-out of *Arabidopsis* *HSFA1a* and *HSFA1b* resulted in the differential expression of 112 genes⁶⁸. Surprisingly only few of the identified genes belong to the classical group of expected proteins, such as chaperones, co-chaperones, other HSFs and proteases. Instead, other pathways were identified as targets of HSF-dependent activation for example carbohydrate metabolism (the Raffinose family oligosaccharide (RFO) pathway). RFOs have been found before to increase drought tolerance as potential osmoprotective substances⁷⁰. In contrast to *HSFA1a/b*, analysis of the transcriptome of *HSFA2* knock-out plants in *Arabidopsis* revealed the central role of this transcription factor in the control of several chaperones from different classes within all compartments of the cell (sHSPs, HSP70s, HSP100s)⁷¹. Furthermore, an interesting link was found to the detoxification of reactive oxygen species (ROS), given that *HSFA2* directly controls the expression of *APX2*, an ascorbate peroxidase. While *APX1* is the predominant APX isoform within the cytosol of *Arabidopsis* under ambient conditions, this protein is heat-labile and replaced by *APX2* under proteotoxic conditions⁷². All aerobic organisms use these kind of enzymes which use ascorbate to reduce hydrogen peroxide for the detoxification of ROS evolving during respiration in mitochondria. Photosynthetic organisms are especially prone to ROS damage because they harbor a second source of ROS with the photosynthetic electron transport chain. Expression profiling in *HSFB1/B2b* double knock-out revealed that this transcription factor is not involved in HSP regulation at all⁷³. Instead, this HSF indirectly represses the expression of genes that protect *Arabidopsis* from pathogens (Pdf1.2a, Pdf1.2b).

1.3. CHAPERONES OF THE HSP70 FAMILY

Several proteins need assistance in folding not only upon proteotoxic stresses but also at ambient conditions. Originally identified in cells upon exposure to heat (Heat Shock Proteins), chaperones of the HSP70 class offer the cell various functions for protein quality control under all conditions. HSP70 chaperones assist in folding of newly synthesized polypeptide chains, translocate proteins across cell membranes and assemble, disassemble or modify protein complexes^{11,15,74,75}.

An N-terminal ATPase domain (~45 kDa) and a C-terminal substrate-binding domain (~25 kDa) build up the conserved core of all HSP70 proteins. Affinity for substrates and ATPase activity are functionally connected and regulated by specific co-chaperones (illustrated in Figure 4). When ATP is bound in the nucleotide binding pocket of the ATPase domain, the substrate binding domain is forced into an open conformation, with only little affinity for substrates⁷⁶. In this conformation, a specific class of co-chaperones, the so-called J-domain proteins (JDP), has a high affinity for HSP70s. These co-chaperones bind to their substrates and transfer them to the HSP70 chaperone to assist in folding⁷⁷. The conserved J-domain is thereby the domain interacting with HSP70s⁷⁸. Beside the eponymous J-domain, JDPs are highly variable and outnumber in almost any organism the rather limited number of different HSP70s⁷⁹. Therefore, and because of different substrate specificities, JDPs are thought to organize the wide range of substrates and consequently determine the functions of HSP70s⁸⁰. Beside delivering different substrates to the substrate binding domain of HSP70s, JDPs additionally stimulate HSP70s ATPase activity^{81,82}. Hydrolysis of ATP induces a conformational change in the substrate binding domain of HSP70s towards a closed conformation with high substrate affinity. This leads to a tight binding of the presented substrate. In the ADP state, nucleotide exchange factors (NEF), the second important class of co-chaperones, exhibit a high affinity for HSP70s. Several types of NEFs can be distinguished, the bacterial GrpE, the eukaryotic Bag1, Bag2, Hsp110/Grp170 and HspBP class. While structure and binding sites at HSP70s of all NEFs are completely different, all NEFs, with the exception of HspBP, increase the rate

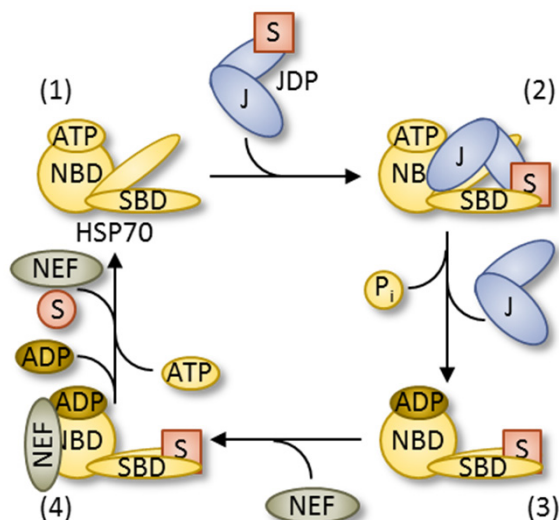


Figure 4: Functional cycle of HSP70s (see text for details):

(1) Initially, ATP is bound to the nucleotide binding domain (NBD) of HSP70, the substrate binding domain (SBD) is in an open conformation. J-Domain proteins (JDP) recruit unfolded substrates (S) to the SBD of HSP70s (2). ATP hydrolysis leads to a tight binding of the substrate (3). Subsequent binding of nucleotide exchange factors (NEF) promotes the replacement of ADP by ATP and release of folded substrates (4).

of ADP release and subsequent ATP binding of HSP70s in a similar way, by stabilizing similar conformations of the ATPase domain^{83,84}. The exchange of the nucleotide again promotes a transition of the substrate binding domain, this time back to the open conformation with low substrate affinity. Upon nucleotide exchange, HSP70 has completed the cycle and is ready to start a new cycle. How folding is promoted in the substrate during binding to HSP70s is still under debate. An attractive hypothesis by Goloubinoff and coworkers suggests that HSP70s do not contribute to the folding process at all, but act as unfoldases of presented misfolded substrates⁸⁵. Tight binding, driven by ATP hydrolysis, forces the misfolded substrate into a different, rather unfolded conformation. The unfolded substrate contains more free energy and therefore has a second chance to spontaneously fold to its native state. If spontaneous folding is not successful, chaperone-mediated unfolding will be repeated until the substrate finally reaches the native state. This mechanism, although ATP consuming for every cycle of unfolding, is still several thousand times less expensive than degradation and resynthesis of the protein. As an additional function, simple binding of chaperones to hydrophobic patches reduces the chance of aggregation, an important process during stress referred as ‘holdase’ activity¹⁵.

In general, substrates of HSP70s are recognized by a 4 to 5 amino acid long hydrophobic patch, that is flanked by basic amino acids⁸⁶. Exposure of hydrophobic amino acids to the aqueous phase is generally very rare in native, soluble proteins, since the building out of buried hydrophobic cores is a major driving force of protein folding. The binding motif is quite general, statistically it can be found every 36 amino acids in virtually any protein, and therefore allows HSP70s to bind and subsequently unfold almost all proteins when necessary⁸⁶.

1.3.1. HSP70S IN THE CHLOROPLAST

HSP70s are present in all compartments of the eukaryotic cell including the chloroplast. In the past, research has focused especially on mitochondria, the cytosol and the ER while only little effort was taken to understand plastidic HSP70s, especially those in the stroma⁸⁷. The so far best studied HSP70 system within the chloroplast is found in *Chlamydomonas reinhardtii*⁸⁸. Here, there is only a single major HSP70 localized in the stroma, termed HSP70B⁸⁹. The *HSP70B* gene was found to be upregulated by dark-light transitions and upon different environmental stress conditions like heat shock, high light and photoinhibition⁸⁹⁻⁹¹. Antisense and overexpression *Chlamydomonas* strains were used to investigate HSP70B function during photoinhibition. Here, HSP70B was found to play an important role in photoprotection of PSII core subunits during stress and in the repair of damaged PSII centers during the recovery process⁹¹. Further functional characterization has proven to be difficult. Mutants lacking stromal HSP70s could not be obtained so far in any plant organism and constitutive knock-down approaches failed to reduce protein levels beyond 80% of wild-type levels⁹¹⁻⁹³. Therefore, different approaches were taken to investigate the function of plastidic HSP70s. Initial approaches using co-

immunoprecipitations and comparative genomics led to the identification of several co-chaperones and also of a target of stromal HSP70B in *Chlamydomonas*.

At first, the nucleotide exchange factor in the stroma was identified and termed CGE1 (Chloroplast GrpE homolog 1)^{94,95}. CGE1 binds to HSP70B as a dimer, similar to its bacterial ancestor GrpE. Interestingly, the *CGE1* gene is expressed in two splice variants, resulting in the addition of two extra amino acids close to the N-terminal tail when translated from the longer transcript⁹⁵. This longer splice variant has a higher affinity for HSP70B and was shown to be the dominant isoform at elevated temperatures, while the short one is more abundant at ambient temperatures⁹⁴.

At least five different J-domain proteins are present in the chloroplast of *Chlamydomonas*, termed Chloroplast DnaJ homologs (CDJ) one to five. Four of these proteins have been subject of closer investigation⁹⁶⁻⁹⁸. CDJ1 groups into JDP class I that in addition to the J-domain contains a glycine-rich and a cysteine-rich region including four zinc fingers⁹⁹. Class I JDPs are generally believed to deliver unfolded substrates and to have a broad substrate spectrum⁷⁹. In contrast to CDJ1, CDJ2 does not contain the glycine-rich and zinc-finger domains and therefore groups into class III of J-domain proteins. CDJ2 seems to be a JDP with a specific function with VIPP1 as prominent substrate that is presented to HSP70B⁹⁶. VIPP1 is present in the cell as monomers, dimers and high molecular weight oligomers. These constitute rings of an approximate diameter of 28-37 nm that may further assemble into rod-shaped complexes^{96,100}. HSP70B was shown to catalyze the assembly and disassembly of these oligomeric complexes. CDJ3-5 are also of JDP class III proteins but contain a bacterial ferredoxin domain harboring a 4Fe/4S cluster in addition to the J-domain⁹⁷. CDJ3 is strongly induced when cells are shifted from dark into the light and is associated with RNA. It was therefore hypothesized that CDJ3 uses its Fe/S cluster to redox-dependently recruit HSP70B to complexes controlling transcription/translation that are subsequently modulated by the chaperone⁹⁷.

Similar to mitochondrial HSP70s, chloroplast HSP70B needs an additional co-chaperone to reach its native state, the HEP2 protein (HSP70 Escort Protein 2). HEP2 most likely is required for the folding of HSP70B into the native state after its import into the chloroplast¹⁰¹. In contrast, the mitochondrial homolog HEP1 appears to bind to the ATPase and linker domains of mitochondrial HSP70s in the ADP state to prevent also self-aggregation during the running chaperoning cycle^{102,103}.

HSP70B was also found to interact with a chaperone of the HSP90 class, HSP90C^{104,105}. In other compartments, especially the ER and the cytosol, HSP70-HSP90 complexes are ubiquitous and especially important in regulating proteins involved in signaling, like receptors, transcription factors and kinases¹⁰⁶.

Further functional assignments were made in higher plants (*Physcomitrella patens* and *Arabidopsis thaliana*). Stromal HSP70 proteins were found to interact with components of the chloroplast import machinery^{92,93}. Consequently, the import rate of precursor proteins was affected in respective mutant strains with reduced functional HSP70 content.

1.4. REVERSE GENETICS IN *CHLAMYDOMONAS REINHARDTII*

The recent release of the complete nuclear genome sequence of *Chlamydomonas* uncovered more than 15.000 protein coding genes, most of them with so far unknown function¹⁰⁷. With the nuclear genome all three genomes of *Chlamydomonas* are sequenced by now and are tractable and amenable to molecular analysis¹⁰⁷⁻¹⁰⁹. Different methods for transformation of the genomes have been set up: particle gun bombardment is used for transforming any of the three genomes¹¹⁰⁻¹¹², agitation with glass beads drives DNA into the nuclear and chloroplast genomes^{113,114} and electroporation allows to manipulate the nuclear genome¹¹⁵. Furthermore, the genome sequence of *Chlamydomonas* enabled *in silico* analyses like comparative genomic studies for the identification of various new plant related genes, for example the members of the “GreenCut2”, containing 311 out of 597 genes with unknown function, conserved only in organisms with plastids¹¹⁶. Consequently, the development of reverse genetics strategies to study the function of these interesting unknown genes became increasingly important and several new reverse genetics methods have been developed for *Chlamydomonas*^{117,118}.

1.4.1. GENE TARGETING IN *CHLAMYDOMONAS*

Different strategies have emerged in various organisms to provide gene-specific mutants. Targeted gene knock-out can be achieved by homologous recombination or the creation and screening of randomly generated insertional or chemically induced mutant libraries¹¹⁹.

Homologous recombination (HR) is a cellular mechanism used during cell growth for the repair of DNA double-strand breaks, damaged replication forks, and during telomere maintenance. During meiosis, HR is used to generate diversity among the progeny by recombining different alleles and ensuring correct chromosome segregation¹²⁰. A homologous template DNA sequence is thereby used to restore, in case of the endogenous repair mechanism, or manipulate, in case of a biotechnological application, a specific genomic DNA sequence¹²⁰. As a tool in reverse genetics it therefore allows a broad range of applications: Gene knock-out can be achieved by creating null alleles with the insertion of a selectable marker into the coding sequence. In-detail gene characterization is done using *in vitro* modified sequences (knock-in) to alter single amino acids. Introducing in-frame reporter genes or affinity tags allows for example to determine subcellular localization and to identify interacting proteins^{121,122}. Especially in yeast HR is applied regularly and very successfully. For example, in-frame insertion of the coding sequence of the green fluorescent protein (GFP) directly at the position of the stop codon in all open reading frames (ORFs) via HR enabled the subcellular localization of ~75% of the yeast proteome and generated a library of immeasurable value for detailed research^{122,123}. In *Chlamydomonas*, HR is routinely used to modify the plastidic genome¹²⁴. However, in the nuclear genome HR is a very inefficient process, as it is in most higher eukaryotes where random insertion into the genome dominates HR¹²⁵. A method using single-stranded DNA as template has been developed by the group of Peter Hegemann, which

allowed for a strong increase in the ratio of homologous towards non-homologous integration to about 1-2 %^{126,127}. Unfortunately, these improvements have not established HR as a routine tool for reverse genetics approaches in *Chlamydomonas*.

Sequence-indexed, insertional mutant libraries facilitate gene function analysis in many model organisms. A prominent example is the *Agrobacterium tumefaciens*-derived T-DNA mutant collection of *Arabidopsis thaliana*¹²⁸. The labor intense and cost-intensive long-term culturing/storing of *Chlamydomonas* so far limited similar attempts in this alga. Therefore, in the past, immediate screening in phenotypically pre-selected mutant collections allowed for the identification of gene specific mutants^{117,129}. Pazour and Whitman used a forward genetic strategy to select for strains with phenotypes in motility and then probed within the subset of mutants for the integrity of their specific target genes¹²⁹. More recently, the group of Arthur Grossman has further improved this strategy by allowing the identification of DNA inserts at any non-essential gene locus without previous phenotypic pre-selection¹¹⁷. To ensure knock-out in specific target genes, a large number of mutants must be created and screened in a short-term period. They therefore developed a PCR-based screening strategy to identify specific knock-outs among 100.000 independent mutant strains using pools of different sizes. Although this method is still quite labor intensive and limited to non-essential genes, it will definitely lead to a large number of knock-out mutants especially in previously unstudied genes lacking obvious phenotypes.

Chemical compounds like ethyl methanesulfonate (EMS), or physical damage mediated by radiation, increase the frequency especially of point mutations or deletions in genomes of different organisms¹³⁰. In addition to loss-of-function mutations, chemical mutagens generate a wide range of mutations allowing in-depth characterization of the mutated genes. Specifically designed high throughput screening systems allow for the identification of point mutations in genes of interest, for example TILLING (Targeting Induced Local Lesions In Genomes)^{131,132}. Methods for radiation induced mutagenesis combined with TILLING are currently under development in the group of Krishna Niyogi but, up to now, have not been published for *Chlamydomonas*.

1.4.2. RNA INTERFERENCE (RNAi)

The most popular reverse genetics strategies in *Chlamydomonas reinhardtii* are based on RNA interference (RNAi)¹³³⁻¹³⁵. In contrast to *in cis* acting gene targeting methods these strategies act *in trans* and do not require the modification of the target gene locus itself. RNAi is an evolutionary conserved endogenous mechanism for silencing gene expression that uses 20-30 bp small RNA (sRNA) guiding molecules to target complementary nucleic acids¹³⁶⁻¹³⁹. The sRNA is thereby directly bound by a protein of the Argonaute protein family which itself is incorporated into the RISC (RNA Induced Silencing Complex) or RITS (RNA Induced Transcriptional Silencing) effector complexes. Silencing is thereby not restricted to fine-tune endogenous gene expression but also controls transposable elements in the genome and is

widely used as a defense mechanism against intruding nucleic acids^{140,141}.

RNAi mechanisms are subdivided into three major classes (siRNA, miRNA, piRNA), depending on the origin of the guiding sRNA molecule. These pathways are illustrated in Figure 5. Small interfering RNAs (siRNA) originate from: (1) long, almost perfectly matching double-stranded RNAs which again originate either from extended endogenous inverted repeats (also termed hairpin RNAs, hpRNAs) (2) from transposable elements that either contain inverted repeats within their flanking regions or are clustered in altered orientation (3) from a gene (not necessarily from a single locus) transcribed in sense and antisense direction (bidirectional transcription) (4) from overlapping genes on opposite DNA strands (cis natural antisense transcripts - cisNATs) (5) from the activity of RNA-dependent RNA polymerases (RdRPs)¹⁴²⁻¹⁴⁴. These long dsRNAs are then processed to 21-22 nucleotide short, double-stranded siRNAs with a two-nucleotide 3' overhang by a tandem ribonuclease domain of the RNaseIII family in a protein called Dicer¹⁴⁵. One of the two strands of the double-stranded siRNA, the so-called guide strand, which has a lower thermodynamic stability at the 5' end, is then ultimately incorporated into the Argonaute protein, while the other strand (also-called passenger strand) is rapidly degraded^{146,147}. Such siRNA-guided Argonaute effector complexes then identify their targets by Watson-Crick base pairing matching to the siRNA guide strand.

In contrast, micro RNAs (miRNAs) originate from non-protein-coding genes whose DNA polymerase II derived long transcripts fold into imperfectly matching dsRNAs. These primary miRNA precursors (pri-miRNAs) form a complex, stem-loop containing secondary structure¹⁴⁸⁻¹⁵³. Whereas multiple siRNAs are processed from a single siRNA precursor, miRNA precursors result in a single miRNA species. In animals, the pri-miRNAs are processed in the nucleus by a second RNaseIII domain-containing enzyme called Drosha first to ~70 bp long, so-called pre-miRNAs¹⁵⁴. The latter are exported and further processed in the cytosol by Dicer to the mature ~22 bp short miRNA¹⁵⁵. In contrast to that, there is only a single enzyme in plants (Dicer-like 1 (DCL1)) that is located in the nucleus and catalyzes both steps in miRNA maturation¹⁵⁶. The double stranded miRNA is then incorporated into an Argonaute protein and processed to miRNA/miRNA* similar to the guide/passenger strand mechanism described for the siRNAs.

The third class of small guiding RNAs is termed piRNAs because of their association with Piwi proteins, a subclass of proteins within the Argonaute protein family¹⁵⁷⁻¹⁶². piRNA precursors are localized within specialized clusters in the genome and include no dsRNA intermediate during their maturation^{163,164}. Consequently, they are directly synthesized from single-stranded RNA templates by the intrinsic Piwi RNase activity in a Dicer-independent pathway^{164,165}.

There are several distinct effector mechanisms for RNAi-induced silencing including mRNA degradation, inhibition of translation and silencing of the gene locus, also summarized in Figure 5. mRNA degradation can be achieved directly via an intrinsic RNaseH domain of the Argonaute protein itself^{166,167}. The target RNA molecule is thereby cut in the middle of the sRNA directed site, between nucleotide 10 and 11, as counted from the 5' end of the

sRNA guide¹⁴³. If not degraded, translation of target mRNAs is reduced or even completely blocked. Several different mechanisms are used for this purpose that are still under debate^{168,169}. One mechanism currently discussed is the competitive binding of the Argonaute protein itself to the 7-methylguanosine cap of mRNAs. This conserved cap structure of eukaryotic mRNAs has to be bound by an eukaryotic initiation factor (eIF4F) in order to convey translation¹⁷⁰. Another mechanism used is miRNA-mediated de-adenylation of poly(A) tails. When this structure of mRNAs is missing the poly(A)-binding protein cannot bind which is also affecting stability of the initiation complex leading to less pronounced translation^{171,172}. Additionally, the RNAi machinery can directly inhibit mRNA synthesis by halting elongation of nascent transcripts or affecting the chromatin state at the target gene locus¹⁷³⁻¹⁷⁵. For example, facultative heterochromatin formation is induced and responsible for transcriptional silencing of transposons in near-centromere located regions in the genome of *Schizosaccharomyces pombe*¹⁷⁴.

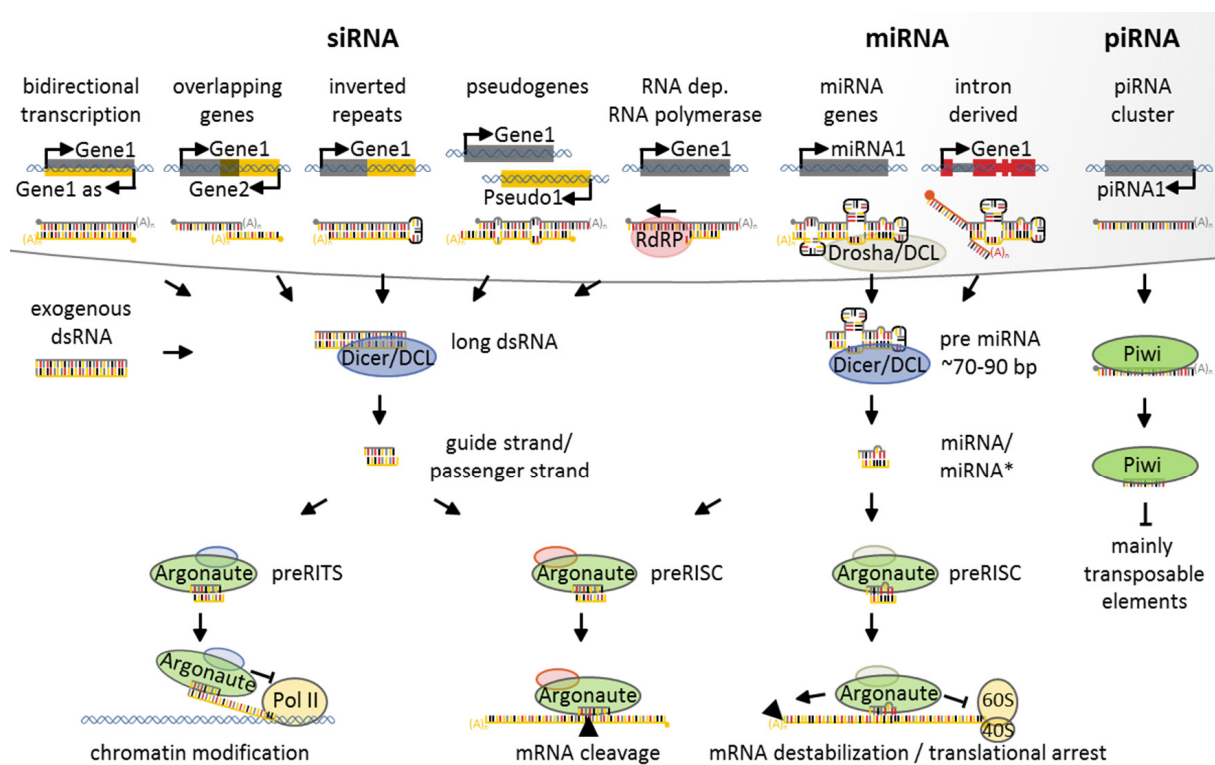


Figure 5: Biogenesis of small RNAs

Small interfering RNAs (siRNA): The processing of endo-siRNA originating from various sources (see text for details) requires a Dicer/DCL type nuclease in the cytosol before loading the ~21-bp double-stranded siRNA onto an Argonaute protein. The siRNA is finally mounted onto an Argonaute protein and integrated into the RNA Induced Silencing Complex (RISC) or RNA Induced Transcriptional Silencing complex (RITS). Accordingly, target mRNAs are degraded (RISC) or the target locus is silenced (RITS).

MicroRNAs (miRNA): Primary transcripts of miRNAs (pri-miRNAs) originate from RNA polymerase II transcribed miRNA genes or from intron regions of host genes. Processing involves Drosha and Dicer in animals, Dicer-like proteins in plants (DCL) and results in ~22 bp miRNA/miRNA* duplexes (see text for details). After their loading onto Argonaute proteins, miRNAs cause translational arrest or target mRNA destabilization in animals or mRNA cleavage in plants.

PIWI-interacting RNA (piRNA): piRNAs are processed Dicer-independently from single-stranded RNA precursors originating largely from particular intergenic regions known as piRNA clusters. Most probably, piRNAs are directly processed by proteins of an Argonaute subfamily, the Piwi proteins. piRNAs are most of the times involved in the silencing of transposable elements. Adapted from²⁷¹.

1.4.2.1. siRNA BASED TOOLS FOR REVERSE GENETICS IN CHLAMYDOMONAS

While the mechanism of downregulation became evident at the beginning of the 21st century, RNAi-based methods had been routinely used for gene targeting much earlier, especially in plants^{137,176}. First indications for an existing RNA silencing mechanism in *Chlamydomonas* were found in the late 1990s. Cerrutti and coworkers observed a rapid degradation of the *aadA* mRNA (conferring spectinomycin resistance) when *Chlamydomonas* cells were not cultivated under selective pressure¹⁷⁷. The transcription rate was unaffected and furthermore the production of an antisense transcript was observed, probably originating from an endogenous promoter at the integration site. The first RNAi based knock-down approach in *Chlamydomonas* was then applied two years later with a successful underexpression of HSP70B, a nuclear encoded 70kDa chaperone targeted to the chloroplast, with an antisense RNA producing construct⁹¹. The expression of the antisense RNA from a strong promoter led to mildly reduced basal levels of the endogenous *HSP70B* mRNA (50-80 % of wild-type levels) and likewise protein levels (~80 % of wild-type levels), thus allowing the characterization of HSP70B especially in situations where chaperone protein levels needed to be adjusted quickly (i.e. after heat shock treatment, dark-light transition or during photoinhibition)⁹¹. Two years later, Fuhrmann and colleagues used the already gained knowledge about the RNAi mechanism and demonstrated the efficient downregulation of the Chlamyopsin (*COP*) gene with a hairpin construct directly generating dsRNA¹⁷⁸. In the following years, constructs of both types have been applied successfully in several reverse genetics experiments¹³⁴.

1.4.2.2. ARTIFICIAL MIRNAS INCREASE SPECIFICITY AND APPLICABILITY

Several problems are inherent to siRNA-based silencing strategies. Primary siRNAs, products of the introduced dsRNA generating construct, target in 50-70% of the cases other mRNAs, in addition to the intended target, albeit with a lower but sufficient affinity for downregulation¹⁷⁹. The binding of the siRNA-guided RISC complex to (off-)target mRNAs in plants is followed by recruitment of RdRPs to the cleaved mRNA. The RdRP synthesizes dsRNA which in turn is a target for the RNAi machinery. Thereby resulting so-called secondary siRNAs have a high affinity for their respective targets, and therefore lead to efficient downregulation of additional mRNAs, a phenomenon called off-target down-regulation, transitivity, or spreading¹⁸⁰. In *Chlamydomonas*, a severe problem for siRNA-based approaches is silencing of the inverted repeat constructs, thereby reducing the time when the gene of interest is underexpressed to only a few weeks¹⁸¹.

In order to increase the specificity of RNAi-based reverse genetics methods the group of Detlef Weigel redesigned the guiding part of endogenous miRNAs of *Arabidopsis thaliana* and created so called artificial miRNAs (amiRNAs)¹⁸². miRNAs in animals lead to translational arrest of a large number of target mRNAs, due to a limited complementarity between the miRNA guide and the target mRNAs in the seed region of the miRNA (base 2-8 of the 21-24

bp miRNA). In contrast, miRNAs in plants require a high level of homology with their target throughout the complete sequence for efficient binding and subsequent degradation, thus allowing their use for specific reverse genetics approaches¹⁸³. In contrast to long dsRNA that lead to the production of multiple small siRNAs, the single guiding RNA within the miRNA stem-loop structure allows a precise prediction of the potential target and off-targets of the amiRNAs¹⁸⁴.

miRNAs were believed to have evolved within multicellular organisms until the discovery of miRNAs in deep sequencing analyses of the small RNA population of *Chlamydomonas*^{185,186}. Two independent groups have then established the amiRNA technique for the specific silencing of *Chlamydomonas* genes^{118,187}. Examples of all types of amiRNA constructs present in *Chlamydomonas* at the beginning of this work are illustrated in Figure 6. The *Chlamydomonas* transcriptome was added to the web microRNA designer (WMD) tool developed by the group of Detlef Weigel to allow for a convenient, automated amiRNA design for any target gene. Especially off-targeting, optimal parameters for amiRNA maturation, and

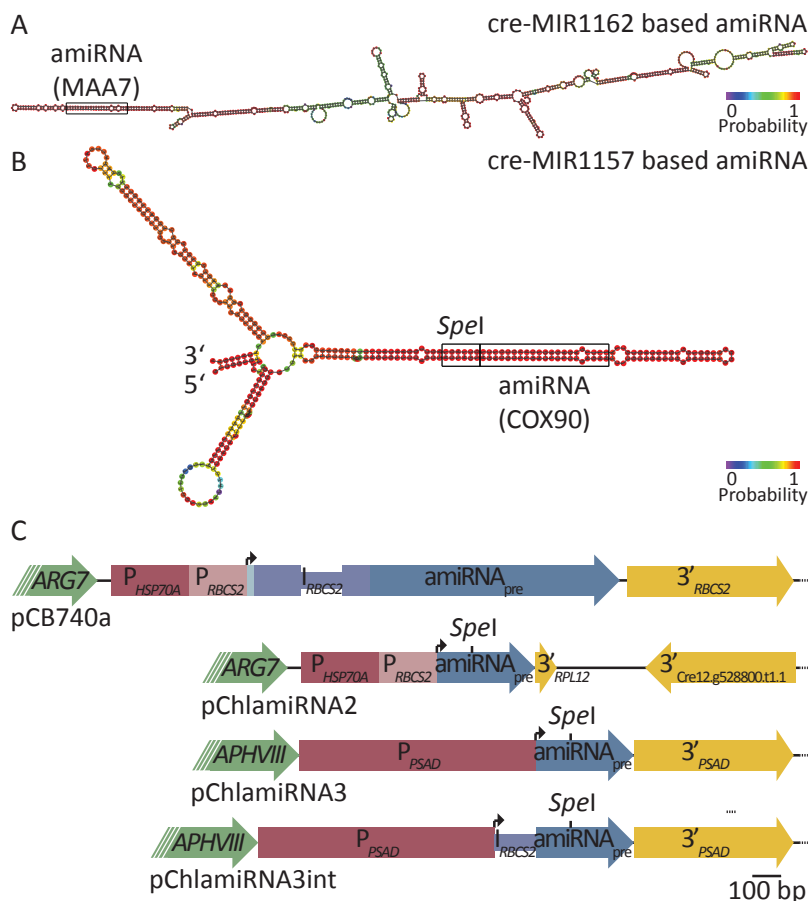


Figure 6: amiRNAs in *Chlamydomonas reinhardtii*

A: cre-MIR1162 based amiRNA: Secondary structure of the amiRNA precursor used by Zhao and coworkers to target the *MAA7* mRNA¹⁸⁷. The 22-bp framed region is altered compared to the natural cre-MIR1162 and is finally incorporated into the effector complexes. Structure prediction was performed by RNAfold on the Vienna RNA webserver²⁷². Centroid structure drawing encoding base-pair probabilities with a color code. For unpaired regions the color denotes the probability of being unpaired.

B: cre-MIR1157 based amiRNA: Secondary structure of the amiRNA precursor targeting *COX90* based on the vector developed by Molnar and colleagues¹¹⁸. The introduced *Spel* site allowing for simplified cloning is highlighted, as is the miRNA/miRNA* region.

C: Different constructs for targeted knock-down using amiRNA in *Chlamydomonas*: The selection marker (green), promoter (red), 5'UTR (light blue), transcribed region (blue) and terminators (yellow) are drawn to size. For selection either the *ARG7* gene, conferring arginine prototrophy, or *AphVIII*, conferring resistance against Paromomycin, are used. Promoters from the *PSAD* gene as well as the *HSP70A/RBCS2* tandem promoter drive the expression of the modified precursor (amiRNA_{pre}) of cre-MIR1162 (pCB740a) and cre-MIR1157 (all other constructs). To increase expression, the first intron of *RBCS2* (*I_{RBCS2}*) was cloned into pCB740 and pChlamiRNA3int^{118,187,273}.

thermodynamic stability of the amiRNA/mRNA duplex are considered by the WMD tool ^{118,184}. Yijun Qi's group adapted the backbone of miRNA 1162 for constitutive down-regulation of the tryptophan synthase (*MAA7*) and the two genes encoding the small subunit of Rubisco (*RBCS1/RBCS2*) with a single amiRNA ¹⁸⁷. miRNA 1162 was chosen because of its high expression level throughout different cell types. Both constructs led to down-regulation of their respective target genes and to the occurrence of expected phenotypes. Whereas the construct targeting *MAA7* led to the silencing of the *MAA7* gene in about 95% of all transformants, the two-gene-targeting construct against the highly expressed *RBCS1/2* genes was less effective (~45 %) ¹⁸⁷.

Based on the precursor of the endogenous miRNA 1157, Attila Molnar and colleagues developed two vectors using different promoters and selection markers for the constitutive expression of amiRNAs in *Chlamydomonas*. miRNA 1157 is also highly expressed in vegetative cells and gametes, both under autotrophic and heterotrophic growth conditions ¹⁸⁶. In general, these constructs are more advanced than those from the Yi group. They do not rely on the terminator sequence from the *RBCS2* gene, which potentially promotes antisense RNA synthesis *in vivo* ¹⁸⁸. Instead, the construct harbors two different terminator sequences (*RPL12* and *192566* terminator), one to terminate the regular amiRNA precursor and the second to avoid antisense RNA production from nearby promoters behind the amiRNA at the site of integration. To facilitate cloning, a *SpeI* restriction site was introduced directly in front of the (guiding) miRNA coding sequence. This allows the use of dsDNA oligos with 5' and 3' *SpeI* compatible ends to introduce the amiRNA instead of a PCR-based cloning procedure.

As a byproduct, all of the amiRNA constructs are much shorter than the long, inverted-repeat constructs generating siRNAs. This increases the number of successful transformations of the complete construct and therefore knock-down strains (up to ~95% in case of *MAA7* gene) ¹⁸⁷. Furthermore, miRNAs are not prone to self-silencing in *Chlamydomonas*, probably also a result of the reduced length ¹¹⁸.

1.4.2.3. INDUCIBLE KNOCK-DOWN APPROACHES

Assigning gene function on the basis of a phenotype observed in constitutive knock-out/down mutants may be corrupted by the appearance of strong secondary phenotypes that conceal the primary function of the target protein. Additionally, constitutive knock-out/down does not allow to assess functions of essential proteins. Furthermore, multicellular eukaryotes, but also single-celled organisms differentiating into different cell types, need specialized knock-down tools for the targeting of genes in specific situations to further dissect their function. These situations include distinct tissues, different developmental stages or the activation of specific genetic programs like stress responses or acclimation to nutrient availability. To tackle these demands, RNAi constructs driven from specialized, inducible promoters allow for a developmental or conditional resolving of phenotypes and have proven their benefit to gene characterization in several higher plant species ¹⁸⁹.

An ideal inducible knock-down system should provide strong repression under non-

inducing conditions, high expression levels upon activation, and should not influence the organism by the method of induction. A simple example for such a system is the AlcR/AlcA regulon. It utilizes a two-component system consisting of the AlcR regulator and the *AlcA* promoter region from *Aspergillus nidulans*, a filamentous fungus¹⁹⁰. The AlcR transcription factor is activated in the presence of ethanol/acetaldehyde and subsequently binds to regulatory elements within target gene promoters, for example the *AlcA* promoter encoding an alcohol dehydrogenase. The binding of AlcR leads to a strong induction of gene expression and therefore allows the utilization of ethanol as a carbon source in the fungus^{190,191}. AlcR itself harbors all necessary features for the recognition of the inducing compound and induction of gene expression, therefore no additional factors are required for this system in order to control any attached DNA sequence¹⁹². A hairpin RNAi construct in tobacco was successfully controlled with the AlcR/AlcA system and used to target genes in the chlorophyll biosynthesis pathway¹⁹³. Furthermore, this system was also applied to control the first amiRNA in higher plants, and was successfully targeting *GUN4* alone and *CPC/TRY/EPC2* simultaneously¹⁸². In *Chlamydomonas*, so far no inducible amiRNA system was applied. The only so far reported inducible knock-down approach used an endogenous regulator to control an inverted repeat construct producing siRNAs. Under the control of the inducible *NIT1* promoter the centrin gene was successfully knocked down¹⁹⁴.

1.5. AIMS OF THIS WORK

In a previous study, HSF1 was identified as a key regulator of the heat stress response (HSR) in *Chlamydomonas*²⁴. The aim of this thesis was therefore to dissect the HSF1-dependent HSR in more detail. Three different approaches should provide further insights into the subject. (1) A pharmaceutical approach: challenging different steps during activation and attenuation of the stress response with specific inhibitors was expected to allow for a deeper understanding of the regulation and stress sensing processes. (2) A microarray-based transcriptome analysis in wild-type and knock-down strains should allow for the identification of plant-specific target genes of HSF1. (3) Preliminary results pointed to a role of HSP70B in stress signaling of the chloroplast, which I was to examine more closely in *HSP70B* knock-down strains. Especially the essential nature of stromal HSP70s made it necessary to develop an inducible system for targeted knock-down in order to achieve a higher degree of underexpression. The advantages of the newly developed amiRNA system by Molnar *et al.* were therefore to be combined with an inducible promoter (*NIT1*) to enable the time-resolved analyses of phenotypes¹¹⁸.

2. SUMMARIZING DISCUSSION

2.1. GENERAL FEATURES OF THE HSR IN CHLAMYDOMONAS

So far, only little evidence is provided in the literature on the elementary principles of the heat shock response (HSR) in *Chlamydomonas*²⁴. We therefore first used a pharmaceutical approach and applied several inhibitors to *Chlamydomonas* cell cultures affecting different steps in the activation and attenuation of the stress response (Manuscript 1). This strategy was already successfully used before in *Chlamydomonas* to dissect the nitrogen deprivation/blue light signaling pathway resulting in gametogenesis¹⁹⁵.

I will briefly summarize the state of the research on this project at the beginning of my PhD. Initial studies already showed that *Chlamydomonas* HSF1 is multiply phosphorylated upon the onset of heat stress²⁴. The application of a competitive inhibitor of protein kinases, staurosporine, to heat shocked cells demonstrated that phosphorylation of HSF1 is affecting the ability of HSF1 to promote transcription at target promoters (Manuscript 1, Figure 1). The initial trigger that leads to activation of the HSR appears to be the accumulation of unfolded proteins. Feeding with an arginine analog, canavanine, that impedes the formation of a normal secondary structure, resulted in the activation of HSF1 at ambient temperatures (Manuscript 1, Figure 3). Application of an inhibitor of cytosolic protein synthesis (cycloheximide) revealed that for attenuation of the HSR specific proteins have to be synthesized *de novo* after the onset of heat stress (Manuscript 1, Figure 2).

Taken together, the results so far strongly suggested that the general features of the HSR known from mammalian systems are also valid for *Chlamydomonas*. First, the HSR is elicited by the occurrence of unfolded proteins. Second, in the absence of regulation at the level of trimerization, phosphorylation plays an essential role in the activation of HSF1. And finally, the synthesis of nuclear-encoded proteins (presumably chaperones and/or phosphatases) is necessary for attenuation of the stress response.

2.1.1. ROLE OF CYTOSOLIC CHAPERONES IN THE HSR OF CHLAMYDOMONAS

We wanted to investigate the role of molecular chaperones in signalling or relaying the stress state of the cell to HSF1, a process first uncovered in mammalian systems that is also conserved in higher plants^{45,196}. Cytosolic HSP70A was already found to interact with HSF1, but the interaction was sustained during the heat shock treatment²⁴. Besides HSP70s, especially HSP90s are known from other systems to bind to HSFs at ambient conditions^{44,45}. This interaction between HSP90 and HSF plays a central role in current models of the activation of the HSR because directly connecting the occurrence of unfolded proteins to the activation of the HSF (Figure 2). This system represents an elegant mechanism for stress sensing and subsequent signal transduction¹⁹.

We therefore aimed to investigate whether cytosolic HSP90A played a role in the

HSR of *Chlamydomonas*. For this, we first used co-immunoprecipitation (CoIP) to investigate whether there was a direct interaction between HSP90A and HSF1 in *Chlamydomonas* (Manuscript 1, Figure 6). Indeed, I could detect a weak interaction between HSF1 and HSP90A in the absence of stress. Surprisingly, I could show that HSP90A, like HSP70A, binds to HSF1 also after the onset of heat stress (Manuscript 1, Figure 6). HSP90s in higher plants bind to HSF via the C-terminus, probably recognizing HSF as a substrate¹⁹⁶. As a second approach, I therefore applied two inhibitors, radicicol and geldanamycin, that specifically inhibit HSP90 activity (Manuscript 1, Figure 4 and 5). When added at ambient conditions to *Chlamydomonas* cell cultures, both inhibitors were successful in eliciting a stress response at high concentrations. The inhibitor-induced stress response was not as pronounced and not as immediate as the HSR elicited upon heat stress.

Taken together, HSP90A is an important player in the *Chlamydomonas* HSR and contributes to the HSF1-dependent activation of target genes. From our data, i.e. the constitutive interaction between HSF1 and HSP90A and the slow induction of the inhibitor-induced stress response, we would not propose a direct function of HSP90A in stress signal transduction or stress sensing. Especially the activation of HSF by radicicol and geldanamycin is discussed in the literature as evidence for a direct role of HSP90s in relaying the stress response to HSFs^{19,197}. In general, HSP90s are not required for general protein folding but interact preferentially with a specific subset of partially folded, metastable proteins¹⁹⁸⁻²⁰⁰. Inhibiting HSP90s therefore may result in the release and aggregation of its client proteins, which might be sufficient to induce a HSF-dependent stress response at ambient conditions. As this induction would depend on the accumulation of unfolded/aggregated proteins, our observations on the slow induction of the HSR upon geldanamycin/radicicol feeding might be explained by a buffering through other chaperone classes.

We therefore rather propose an indirect role of HSP90A in modulating the HSR in *Chlamydomonas*. The direct interaction of HSP90A with HSF1 may assist in the HSF1-directed assembly or disassembly of protein complexes, for example to initiate or pause transcription. A recent report in *Drosophila* supports this hypothesis by directly linking HSP90 to a protein involved in sustainment of paused DNA polymerase II also at HSF1 regulated promoters²⁰¹.

2.1.2. STRESS SENSING AND SIGNAL TRANSDUCTION

When the HSP90A/HSF1 complex is not involved in sensing and relaying the stress signal to HSF1, what could be the sensor? Recently, there was compelling evidence that a calcium channel is involved in eliciting a HSR in the moss *Physcomitrella patens*²⁰². The authors proposed that temperature changes affect membrane-fluidity which in turn regulates Ca²⁺ influx via a Ca²⁺ channel across the plasma membrane. Ca²⁺ inflow again activates a calmodulin-dependent stress kinase to eventually mediate HSF1 hyperphosphorylation²⁰³. Also this hypothesis represents an elegant mechanism for stress sensing, however it is challenging our view that unfolded proteins trigger the stress response in *Chlamydomonas*.

To test whether inflow of extracellular calcium plays a role in stress sensing we applied two extracellular Ca^{2+} chelators, EGTA and BAPTA, to washed *Chlamydomonas* cells and studied the influence on HSF1 target gene expression upon stress treatment (Manuscript 1, Figure 7). Intriguingly, BAPTA and EGTA produced different results concerning the involvement of calcium influx on the stress response. BAPTA was able to delay the induction of stress-related genes and consequently reduced thermotolerance, while EGTA failed to affect the stress response, even at 40 times higher concentrations than necessary to affect Ca^{2+} influx in *Chlamydomonas*²⁰⁴. Both inhibitors have a comparable preference for Ca^{2+} over other ions but BAPTA binds Ca^{2+} about 100 times faster than EGTA²⁰⁵. It might therefore be possible that the Ca^{2+} pools employed for the HSR are only transiently available and therefore only accessible to BAPTA. Alternatively, Ca^{2+} pools might be accessible to BAPTA for other reasons, for example sterical limitations. Another explanation might be, that BAPTA, in contrast to EGTA, is known to also affect processes independent of its Ca^{2+} binding properties²⁰⁶. Therefore BAPTA might interfere with stress responsive pathways at other instances than Ca^{2+} influx, for example a membrane-bound sensor that is not a channel. Ca^{2+} influx might play a role in stress signaling also in *Chlamydomonas*, but is it the sensor? Interestingly, HSP90 inhibitors induced a stress response in moss at ambient conditions that is dependent on Ca^{2+} influx²⁰². This could imply that stress sensing is realized by a chaperone-bound (HSP70 and/or HSP90) client protein, in the simplest case the Ca^{2+} channel itself, that is released from an inhibiting complex upon occurrence of stress. The stress-dependent Ca^{2+} influx further amplifies the signal, finally resulting in HSF1 phosphorylation.

Temperature stress has a severe impact on chloroplasts and results in decreased photosynthesis rates and carbon fixation under stress conditions^{207,208}. Therefore, acclimation of the chloroplast to elevated temperatures is a necessity in photosynthetic organisms. In other compartments, i.e. in mitochondria and the ER, proteotoxic stress is handled individually, each in a separate, HSF-independent pathway^{209,210}. Surprisingly, the use of antisense constructs targeting HSP70B revealed that underexpressing strains are affected in the entire cell's HSR (Manuscript 1, Figures 8-10). In addition, several plastidic chaperone genes are directly controlled at the transcriptional level by HSF1, as judged from the reduction of their transcripts in *HSF1*-underexpressing strains, for example *ClpB3*, *HSP22F*, *HSP90C* and *HSP70B* (Article 2, Figure 1 and Manuscript 2, Figure 2)²⁴ as well as the direct binding of HSF1 to promoters of the plastidic chaperone genes *CLPB3* and *HSP22F* (Article 2, Figure 3 and Manuscript 2, Figure 6). These results suggest, that in contrast to other compartments the stress state of the chloroplast is integrated into the HSF1-dependent HSR.

A summary of our current working model of the HSF1-dependent stress response in *Chlamydomonas* is presented in Figure 7: when the amount of unfolded/misfolded proteins exceeds the chaperoning capacity of the cell, the stress sensor is released from an inhibiting, chaperone-containing complex. The released sensor releases a signal cascade that is amplified via Ca^{2+} influx and finally results in the activation of HSF1 via hyper-phosphorylation by a stress kinase. The simplest conceivable scenario would require only two components: A stress-

sensing Ca^{2+} channel that would be directly bound by inhibiting chaperones, and a calmodulin-dependent kinase (CaMK), that directly phosphorylates HSF1. Hyper-phosphorylated HSF1 binds to HSEs within target gene promoters to enhance the chaperoning capacity in the cell. Attenuation is also realized via post-translational modification of HSF1. The stress kinase is inactivated when surplus chaperones inhibit the sensor again and, additionally, a phosphatase is either *de novo* synthesized or activated to actively remove necessary phosphorylations from active HSF1. The phosphatase should also require chaperone activity to ensure proteostasis before attenuation. HSP70A/HSP90A complexes attached to HSF1 are necessary, for example by recruiting DNA Polymerase II in order to convey transcription. The chloroplast-derived signal is integrated either at the level of the cytoplasmic stress sensor or later on during signal transduction, or might completely independently result in further modification of HSF1, allowing a fine-tuning of the response.

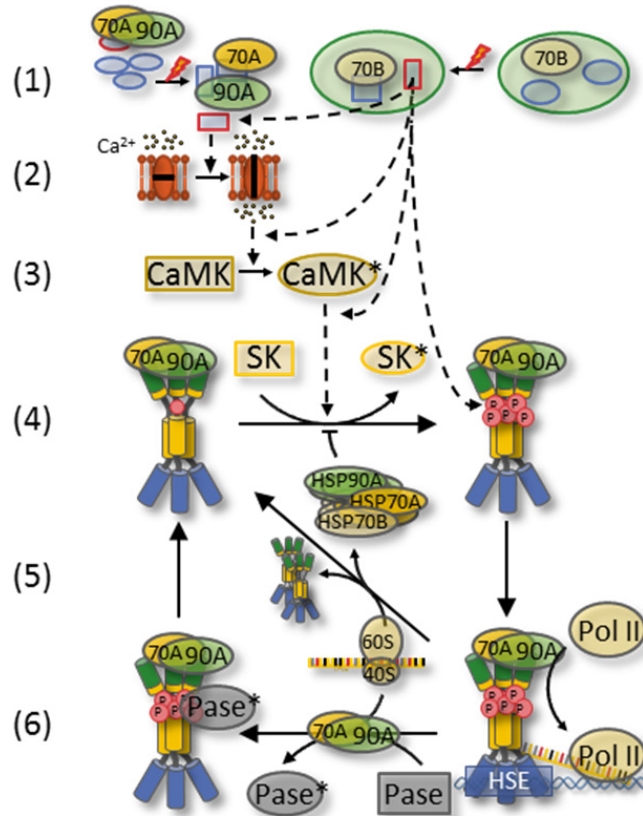


Figure 7: Current working model of the HSF1-dependent HSR in Chlamydomonas

Native proteins (blue circles) unfold upon the occurrence of a proteotoxic stress and accumulate in the cytosol and chloroplast (1). Chaperones (among others: HSP70B (chloroplast), HSP90A and HSP70A (cytosol)) are attracted by the unfolded proteins (blue squares) and release the stress sensor (red square) from an inhibiting complex. The activated sensor (red square) activates a signal cascade that includes Ca^{2+} influx via a membrane-bound Ca^{2+} channel (2) and the activation of a calmodulin dependent kinase (CaMK) (3). Inactive HSF1 trimers (4) are transferred into hyper-phosphorylated, activated trimers by a stress kinase (SK). HSF1 binds to heat shock elements (HSEs) within promoters of stress-related genes to promote transcription (5). Adjusting the chaperoning capacity to the specific need during proteotoxic conditions finally results in inactivation of the stress kinase by depleting unfolded proteins from the cytosol and the chloroplast (5).

A phosphatase (Pase), that requires chaperoning activity to reach an active conformation, dephosphorylates and consequently inactivates HSF1 in the attenuation phase (6). HSP70A/HSP90A complexes attached to HSF1 contribute to HSF1-mediated transcriptional regulation, for example by recruiting DNA Polymerase II (Pol II) in order to convey transcription.

2.2. DEVELOPMENT OF AN INDUCIBLE AMIRNA SYSTEM FOR CHLAMYDOMONAS

In order to further dissect the stress response, especially the HSP70B-related signaling component from the chloroplast, a more efficient knock-down system was to be employed. Stromal HSP70s have been demonstrated to be essential in higher plants and might also be essential in *Chlamydomonas*, as judged from poor underexpression in constitutive antisense strains^{91,211}. In order to study essential processes requiring HSP70B that so far escaped conventional knock-out or antisense strategies, inducible underexpression is the method of choice^{193,212-214}. During my PhD thesis I therefore extended the *Chlamydomonas* toolkit by an inducible artificial microRNA (amiRNA) system (Article 1). amiRNAs have several advantages over hairpin-derived RNAi silencing tools as already pointed out in the introduction. They offer a high level of specificity and are less prone to self-silencing¹¹⁸.

2.2.1. VECTOR FEATURES

The vector on which my amiRNA construct (summarized in Figure 8) is derived from a recently developed constitutive amiRNA system for *Chlamydomonas*¹¹⁸. This vector offers a convenient cloning strategy for routine application which is also featured by the inducible system now. The region in the miRNA precursor (cre-1157) targeting the gene of interest is small enough (~90 bp) to allow direct synthesis of the miRNA*/ miRNA cassettes as DNA oligonucleotides. When the oligos are synthesized with a 2-bp overhang on either side compatible with a *SpeI* digestion site they can directly be inserted into the restriction site of the vector. Termination is realized by a region consisting of two inverted 3' UTRs to prevent read-through transcription from nearby promoters close to the 3' end¹¹⁸. For selection, the *ARG7* gene from *Chlamydomonas* is used, which restores arginine prototrophy in arginine auxotrophic mutant strains.

To ensure a tight control, the choice of the promoter controlling expression of the amiRNA construct is the most crucial step for the inducible knock-down system. The use of transgenic systems is rather difficult in *Chlamydomonas* as constructs containing foreign DNA sequences are readily silenced¹⁷⁷. Therefore, the choice is limited to inducible endogenous systems. In addition, the mechanism of induction should not interfere with gene expression in related pathways, which is especially difficult when studying stress responses, and should also allow for a convenient use in the lab. Copper responsive promoters, for example that of cytochrome c6 (*CYC6*), have been used before in *Chlamydomonas* for inducible gene expression²¹⁵. However, inducing copper deficiency requires long-term cultivation on copper-free medium, a procedure that makes it complicated to find the exact point of induction of the amiRNA. The addition of Ni²⁺/Co²⁺ is also inducing copper responsive promoters, but is also known to induce the expression of stress responsive genes²¹⁶. Other well-characterized inducible promoters are also not suitable, for example the promoter of the carbonic anhydrase, *CAH1*, that requires high levels of CO₂ for repression, a tedious and expensive procedure in the

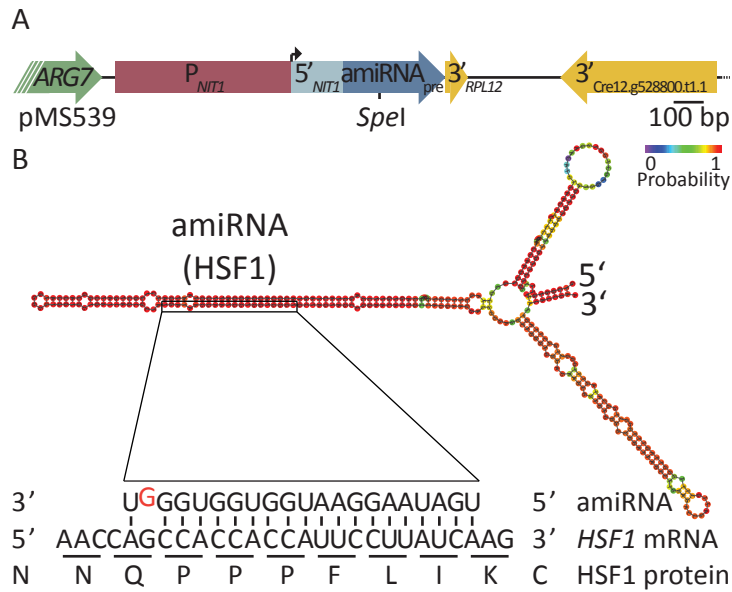
lab. Activating the promoter of arylsulfatase (*ARS*) induction requires depletion from sulfur, which is cheap and easy to control but results in pleiotropic phenotypes, for example PSII depletion, starch accumulation and growth arrest^{217,218}. We therefore took advantage of the tight regulation of the *NIT1* promoter to control the expression of the amiRNA (Article 1). This promoter has already proven to be suitable for inducible expression in *Chlamydomonas* and also of an RNAi hairpin construct^{194,219}. The native *NIT1* promoter drives expression of nitrate reductase (NR) catalyzing the reduction of nitrate to nitrite, the first step in nitrate assimilation²²⁰. If available, ammonium is the preferred nitrogen source, as it requires the least energy for assimilation²²¹⁻²²³. The *NIT1* promoter is therefore tightly controlled on the by the NIT2 transcription factor which serves as an activator in the presence of nitrate as sole nitrogen source^{220,224}. In addition, ammonium directly represses the expression of the *NIT1* gene by a so far unknown mechanism²²¹.

Ammonium and nitrate are both natural sources of nitrogen for *Chlamydomonas*, thus their utilization should be an integral part of acclimation to nutrient availability and should not elicit stress responses. Indeed, I carefully studied the expression of stress related genes upon switching the nitrogen source and did not find increased stress gene expression in the long term (Manuscript 3, Figure 3 and 6). However, switching the nitrogen sources requires at least three centrifugation steps to completely exchange the growth media, a process shown to transiently induce stress genes (Article 1, Figure 3). This is certainly a disadvantage of the system, but as target protein depletion requires much more time (Article 1, Figure 3B) the transient induction of stress genes is unlikely to affect the interpretation of phenotypes. Nevertheless, a proper empty vector control needs to be included in all experiments using this system.

2.2.2. APPLICATION – PROOF OF PRINCIPLE

So far, only the strong constitutive *PSAD* and *HSP70A-RBCS2* promoters were used to drive amiRNA expression in *Chlamydomonas*^{118,187}. During my PhD thesis I successfully applied the nitrogen source dependent expression of amiRNAs targeting *HSF1* and *HSP70B* (Article 1, Manuscript 3). Expression of both amiRNAs successfully decreased the levels of the respective mRNAs and corresponding protein levels. Furthermore, VIPP1, VIPP2, HSP90C, and SECA protein levels were successfully reduced using similar constructs in our group, as well as the levels of PETO and CAS in the labs of Olivier Vallon and Michael Hippler, respectively^{90,225}.

The level of depletion strongly varied for the different target proteins, probably depending on the abundance of the target mRNA in the cell. Especially for highly expressed genes, like *VIPP1* and *CAS*, corresponding protein levels could not be decreased to the same extent as with strong constitutive promoters^{90,225}. As the degree of downregulation of the target gene is strongly depending on the expression level of the amiRNA this might indicate that the induced *NIT1* promoter is not as strong as the constitutive *HSP70A-RBCS2* tandem promoter^{182,226}. In addition, the number of underexpressing strains displaying phenotypes is

**Figure 8: inducible amiRNAs**

A: Construct for inducible amiRNA expression (pMS539): The selection marker (*ARG7*, green), promoter (*NIT1*, red), 5'UTR (light blue), transcribed precursor (*amiRNA_{pre}*, blue) and terminators (yellow) are drawn accurate to size.

B: amiRNA targeting HSF1: Secondary structure of the amiRNA precursor targeting *HSF1* based on the vector developed by Molnar and colleagues¹¹⁸. Sequences of the miRNA incorporated into Argonaute proteins, the region targeted in the *HSF1* mRNA, and deduced amino acid sequence of the DNA-binding domain of HSF1 are shown.

significantly smaller when the inducible system is used. About 5 % of the strains that express the *ARG7* gene showed also reduced levels of *HSF1* or *HSP70B* and corresponding phenotypes. The constitutive constructs produced phenotypes in almost every second transformant^{118,187}. The smaller number of transformants can be explained by the *HSP70A-RBCS2* tandem promoter driving all the constitutive amiRNA constructs, where the *HSP70A* promoter was shown to increase the chance that close-by promoters are expressed at a random integration site in the genome (transcriptional state enhancer)^{91,227-229}. Taken together, compared to the constitutive *HSP70A-RBCS2* promoter-driven constructs, *NIT1*-controlled construct are less strong expressed in fewer transformants.

The time-resolved analysis of phenotypes plays an important role when using inducible knock-down strains, especially when it comes to essential genes where there is only a limited time frame to study gene-specific phenotypes. I therefore studied the dynamics of underexpression for *HSF1* and *HSP70B*. *HSF1* mRNA was declining already 1-2 hours after switching the nitrogen source while protein levels start to decline 6-8 hours after the switch (Article 1, Figure 2 and 3). After about 24 hours, almost no protein was detectable anymore. The half-life of HSF1 protein correlated thereby largely with the doubling time of the cells, indicating that HSF1 seems to be a quite stable protein that is diluted out by growth. In terms of the kinetics, similar results were obtained for HSP70B (Manuscript 3, Figure 2 and 5). It seems that acclimation to the altered nitrogen availability takes a few hours until cells are able to divide again (Manuscript 3, Figure 1 and 6). Indeed a strong induction of the *NIT1* gene was observed within the first hours on nitrate-containing medium, while in the long term *NIT1* expression is maintained at a basal level (Article 1, Figure 3). Therefore, within a limited time frame, between 4 and 24 hours after the exchange of the nitrogen source, target protein levels decline gradually and allow for a detailed characterization of phenotypes.

Inducible knock-down strains using the *NIT1* promoter can also be used to study gain of function phenotypes. For example, when HSF1 protein is depleted, after shifting cells grown on nitrate back to ammonium, cells regain thermotolerance (Article 1, Figure 4). Here,

the addition of ammonium to nitrate-containing media is also sufficient to repress the *NIT1* promoter, therefore not requiring any centrifugation steps. Surprisingly, protein levels recover much more slowly than they deplete (Article 1, Figure 4). Moreover, induction seems to be more a stepwise than a gradual procedure, as judged from basically no recovery of HSF1 protein within the first 24 hours. We therefore assume that miRNAs remain loaded on Argonaute for a considerable time period and suppress mRNA levels of *HSF1*.

2.3. IDENTIFICATION OF POTENTIAL HSF1 TARGET GENES

In order to identify potential plant-specific target genes of HSF1, we used RNAi and amiRNA mediated knock-down and compared the transcriptome between wild-type and *hsf1* mutant strains upon stress treatment using microarrays and qRT-PCR (Manuscript 2)^{230,231}. Compared to the current state of the *Chlamydomonas* genome (version 5, published online in June, 2012) that includes the information from several recently performed RNAseq studies, the used microarrays developed in 2008 cover about 45% of all known genes²³¹. This is still suitable to identify pathways affected by HSF1 depletion but, of course, is not sufficient to provide a complete dataset of potentially *HSF1*-regulated genes.

2.3.1. HSF1-DEPENDENTLY REGULATED PROCESSES (PLANT-SPECIFIC FEATURES)

In total, 978 genes were differentially expressed upon heat shock in HSF1 knock-down compared to wild type strains (Manuscript 2, Figure 1). To identify plant-related pathways, a bin enrichment analysis was conducted among these differentially expressed genes. For classification, the *Chlamydomonas* MapMan ontology was used in its most recent version²³². Four of the most general categories were overrepresented in the dataset, namely tetrapyrrole biosynthesis (19), stress (20), redox regulation (21) and protein (29) (Manuscript 2, Figure 4).

Several members of the canonical, heat stress gene families (chaperones and proteases) are found within two of these categories: protein.folding (29.6) and stress.abiotic (20.2)⁸⁷. Not surprisingly, genes encoding chaperones showed the strongest induction upon heat shock which was abolished in HSF1-depleted strains (Manuscript 2, Figure 4C). In contrast to previous studies carried out in *Arabidopsis*, genes encoding members of all chaperone families (sHSPs, HSP60s, HSP70s, HSP90s, HSP100s) were found to be regulated by HSF1 and all bins containing chaperone-encoding genes were found to change significantly dependent on HSF1 (Manuscript 2, Table 1). Among the significant HSF1-dependently regulated genes, several are coding for chloroplast chaperones and co-chaperones, further confirming the role of HSF1 in acclimation of chloroplast protein homeostasis during heat stress (Manuscript 2, Table 1).

While transcript levels from genes of the stress, redox regulation and protein categories increase HSF1-dependently upon stress treatment, as expected for a transcription factor known as activator, expression of genes within the tetrapyrrole group is HSF1-dependently reduced. Repression of chlorophyll biosynthesis upon different stress conditions was quite

frequently observed in higher plants and it is widely believed that this repression limits the generation of reactive oxygen species (ROS) ²³³⁻²³⁵. So far, involved transcriptional regulators have not been identified. However, analysis of promoter regions of several genes involved in tetrapyrrole biogenesis did not reveal potential HSEs. Therefore one can only speculate on the role of HSF1 in repressing the expression of these genes upon heat shock. One explanation might be that HSF1 controls the expression of a specific repressor binding to the promoter regions of genes from the tetrapyrrole biosynthesis pathway.

Beside tetrapyrrole biosynthesis, there is a second category of proteins enriched that performs plant-specific processes: protein targeting (29.3). Especially, transcripts from translocons involved in transport into the chloroplast and into mitochondria are HSF1-dependently increased upon heat shock (Manuscript 2, Table 2). In addition, two genes involved in protein transport within the chloroplast are HSF1-dependently increased, both of which are involved in the biogenesis of thylakoid membrane proteins: *FFC* (Fifty-Four-Chloroplast Homologue), a subunit of the chloroplast signal recognition particle involved in LHC integration in thylakoids, and *TATA*, a subunit of the Sec independent twin-arginine translocon in the thylakoid membrane ²³⁶.

2.3.2. DIRECT TARGETS

The set of differentially expressed genes contains a number of candidates that are increasingly expressed upon HSF1 depletion, for example the tetrapyrrole biosynthesis genes already mentioned above. This type of regulation is rather indirectly dependent on HSF1, a transcription factor known as an activator of transcription. In addition, high affinity targets are still able to recruit remaining HSF1 in knock-down strains and consequently are not significantly differentially expressed. To identify direct HSF1 targets we therefore performed a clustering approach within the whole dataset (not only the significant regulated subset), searching for genes increasingly expressed upon heat shock (Manuscript 2, Figure 5). 581 candidates were identified showing a unique expression signature qualifying them for being controlled by HSF1. At a limited number of interesting loci we analyzed promoter regions for the presence of heat shock elements (HSE) and performed chromatin immunoprecipitation (ChIP) experiments with antibodies against HSF1 to directly probe for HSF1 binding *in vivo*.

Promoters from four out of nine tested genes were directly bound by HSF1: *HSP70G*, *HSF1*, *CLPB3* and *MPA1* (Manuscript 2, Figure 6B). Two of the genes, *HSP70G* and *CLPB3*, encode for chaperones probably located in the ER and in the chloroplast, respectively. Only little is known about the third gene (*MPA1*). In *Chlamydomonas*, *MPA1* is strongly induced in phosphate depleted cells lacking *PSR1*, the transcription factor necessary for acclimation to phosphate-limiting conditions ²³⁷. *MPA1* is homologous to yeast *DCR2* (30% identical and 46% similar residues), a phosphatase involved in regulating the unfolded protein response (UPR) in the ER ²³⁸. The UPR in yeast is regulated by the trans-membrane kinase/endonuclease *Ire1*. This protein oligomerizes upon occurrence of unfolded proteins in the ER and subsequently is

auto-phosphorylated *in trans* at the cytoplasmic side²³⁹. The phosphorylated Ire1 protein is capable of processing an intron in the mRNA of the transcription factor HAC1, necessary for the proper translation and subsequent transcriptional activation of the UPR target genes²⁴⁰. The MPA1 homolog DCR2 was found to dephosphorylate Ire1 and therefore to inactivate the UPR²³⁸. Consequently, transcriptional activation of MPA1 by HSF1 might be used to inactivate the UPR in response to heat stress.

2.3.3. FEEDBACK CONTROL

The last, very interesting promoter region identified as a direct target of HSF1 is the *HSF1* promoter itself (Manuscript 2, Figure 6B). A unique feature of the HSR in plants compared to all other so far studied organisms is the heat shock inducibility of *HSF* genes^{241,242}. For the first time we observed that HSF1 is directly responsible for its induction. The additional HSF1 synthesized during heat shock (see Figure 7, step 5) might either further enhance transcription (positive feedback loop) or contribute to the attenuation of the HSR, as newly synthesized, unphosphorylated and therefore inactive HSF1 might compete with activated hyper-phosphorylated HSF1 already present during stress for target gene promoter binding (negative feedback loop).

To understand the role of the additionally produced HSF1 protein, we made use of the properties of our inducible amiRNA system and performed a heat shock experiment where production of additional HSF1 was abolished (Manuscript 2, Figure 7). We could show that the additional HSF1 protein was necessary to further enhance transcription of target genes and therefore is required for a positive feedback loop. It might be possible that the additional protein is necessary to also induce a second set of targets with lower affinity binding sites. Within higher plants, the network of HSFs is extraordinary complex. Several HSFs are expressed only upon stress treatment, consequently modulate the HSR and therefore allow for fine-tuning of the stress response. In *Chlamydomonas* with only a single inducible HSF, this type of regulation is already realized and therefore might represent the initial evolutionary event that enables the more fine-scaled stress response in plant systems.

2.3.4. REGULATION OF THE STRESS RESPONSE AT THE EPIGENETIC LEVEL

The promoter regions of *CDJ1*, *TIC40*, *TIC110*, *FFC* and *LHCBM9* were not directly bound by HSF1 (Manuscript 2, Figure 6). However, all of them harbor HSEs comparable to those within promoters that showed HSF1 binding. In *Drosophila*, the chromatin surrounding the HSE has to be in a specific configuration in order to allow HSF1 binding⁶⁷. Especially acetylation of lysine residues of histones H3 and H4 played an important role in this regulation.

We therefore analyzed chromatin structure at ambient and elevated temperatures in exemplary stress-responsive promoters (Article 2 and Manuscript 2). At ambient conditions there was virtually no difference between the chromatin state of HSF1-occupied promoters and those that don't show HSF1 binding (Manuscript 2, Figure 6). We therefore conclude that,

in contrast to *Drosophila*, specific chromatin modifications in the proximity of HSEs are not influencing the binding of HSF1 to promoters in *Chlamydomonas*. We rather hypothesize that either the presence of additional, so far unknown *cis* elements, or nucleosome positioning determine HSF1 binding. The latter hypothesis is supported by the observation that HSEs within the (HSF1-bound) *HSP70A* promoter are found within the nucleosome linker region²⁴³.

In general, we found HSF1-bound heat shock genes to be highly regulated at the chromatin level upon switching to elevated temperatures. Especially acetylation of lysines at histones H3 and H4 is increased and the positioning of nucleosomes is altered (Article 2, Figure 4 and Manuscript 2, Figure 6)²⁴³. Thereby, HSF1 binding is preceding the modification of the histones as well as eviction/sliding of nucleosomes (Article 2, Figure 5). Interestingly, genes that are activated upon heat shock but are not directly bound by HSF1 showed also no alterations at the chromatin level (Manuscript 2, Figure 6 and S2). This indicates that indeed a different mechanism is used for the activation of these genes upon heat shock.

2.4. FUNCTIONAL ANALYSIS OF THE ESSENTIAL CHLOROPLAST CHAPERONE HSP70B

After the successful development of the inducible amiRNA construct, we applied the system for the characterization of the stromal chaperone HSP70B (Manuscript 3). Using this technique, protein levels of HSP70B were decreased to ~ 20% of wild type levels about 24 hours after switching the nitrogen source. Coincidentally, 24 hours after exchanging the nitrogen source, cells stopped to divide and growth arrested (Manuscript 3, Figure 2). Reduced growth rates upon depletion of HSP70B by 20% were also reported in a previous study⁹¹. Despite tremendous effort, knock-down strains with further reduced protein levels could not be obtained (Michael Schroda, personal communication). In addition, a knock-out of a stromal HSP70 (Hsp70-2) was lethal in the moss *Physcomitrella patens*⁹³ and simultaneous knock-out of the two stromal Hsp70s from *Arabidopsis* (cpHsc70-1 and cpHsc70-2, 91% identity) did also not yield viable progeny²¹¹. Taken together, functions inherent to stromal HSP70s seem to be essential for cell growth throughout the green lineage.

Several observations were made indicating that *Chlamydomonas* cells are reversibly arrested in growth and not irreversibly damaged, at least within the first 48 hours after induction of the amiRNA: first, when HSP70B levels were allowed to recover, no obvious differences in growth rates were observed between inducible knock-down strains and wildtype in the subsequent days (Manuscript 3, Figure 2). Second, cells accumulate large amounts of starch when arrested in growth (Manuscript 3, Figure 4 and S2), indicating that metabolism is still generating energy for sugar synthesis and storage. Starch accumulation is frequently observed in nutrient limited, growth-arrested *Chlamydomonas* cells²⁴⁴. And last, microscopy analyses and cell measurements showed that cells are intact and cell size is increased in HSP70B knock-down strains, demonstrating that cells are indeed viable but fail to divide (Manuscript 3, Figure 2 and S4).

2.4.1. CONSEQUENCES OF CHAPERONE DEPLETION ON THE VIPP1 SUBSTRATE

The so far only known substrate of the HSP70B chaperone system in the chloroplast of *Chlamydomonas* is the VIPP1 protein⁹⁶, where HSP70B catalyzes the interconversion between oligomeric and monomeric states¹⁰⁰. VIPP1 is strongly accumulating in inducibly HSP70B depleted cells (Manuscript 3, Figure 3), starting already early upon depletion of HSP70B. This clearly indicates that VIPP1 function is affected in HSP70B depleted cells, resulting in a feedback in order to increase levels of functional VIPP1. This is supported by the increased expression of the VIPP2 protein upon HSP70B depletion, a homolog of VIPP1 only present in green alga and moss (Manuscript 3, Figure 3). VIPP2 is only weakly expressed at ambient conditions and was shown to be expressed at high levels only in VIPP1 knock-down strains and after high light exposure⁹⁰.

Additional phenotypes of VIPP1 knock-down strains are also found in inducibly HSP70B depleted cells, for example high light sensitivity (Manuscript 3, Figure 4) and, more specifically, aberrant structures at the origin of thylakoid membranes (Manuscript 3, Figure 5). Interestingly, the distribution between VIPP1 oligomers and monomers is distorted in inducible HSP70B knock-down strains (Manuscript 3, Figure 4 and S2). Depending on the HSP70B protein level, lower molecular weight isoforms of VIPP1 are depleted, while higher molecular weight isoforms increase strongly. Apparently, the dynamic interconversion between monomers and oligomers catalyzed by HSP70B is crucial for the function of VIPP1.

2.4.2. ESSENTIAL FUNCTIONS OF HSP70B

HSP70B is the only prominent HSP70 in the stroma of the *Chlamydomonas* chloroplast and therefore probably involved in a plethora of processes²⁴⁵. It is therefore hard to determine which function of HSP70B eventually is responsible to what extent for the growth arrest. Two functions were assigned to HSP70B in previous studies, assembly/disassembly of VIPP1 oligomers and a role in photoprotection and repair of PSII core subunits during photoinhibition^{91,100}. PSII protein levels, as well as other proteins from photosystems, seem to be only slightly affected within the first 36 hours of HSP70B depletion (Manuscript 3, Figure S5). Photosynthesis is also a dispensable process for *Chlamydomonas*, as it can grow on acetate that is included in our standard medium²⁴⁶. Knock-down strains of VIPP1 were also characterized previously and did not show significant growth defects at ambient conditions⁹⁰. Therefore, affecting the repair process of PSII and VIPP1 function in general is rather unlikely to directly cause the observed growth-arrest in HSP70B knock-down strains.

In higher plants, stromal HSP70s were found to contribute to the import of nuclear encoded proteins into the chloroplast^{92,93}. This is an essential process, as judged from phenotypes of knock-out plants depleted from central proteins of the TIC and TOC translocons²⁴⁷⁻²⁴⁹. Accumulation of preproteins that still include the N-terminal extension was found in mutants defective in transport, as the transit peptide normally is cleaved off in the stroma

after successful import^{250,251}. However, within our protein analyses we followed many nuclear-encoded chloroplast proteins in HSP70B-depleted cells, i.e. VIPP1/2, CGE1, CDJ1/2/4, HSP90C and did not observe the accumulation of unprocessed isoforms. We therefore conclude that potential functions of HSP70B in import are also either minor or can be fully compensated by other chaperones, i.e. ClpC, and therefore contributes only weakly to the growth arrest phenotype.

From the data gathered in this work, we would therefore propose two processes that potentially contribute to the growth arrest: a nutrient-limitation induced growth arrest, resulting from misfolding of HSP70B-dependent substrates involved in biosynthetic processes, and a stress-response induced growth arrest, probably resulting from unfolding and aggregation of HSP70B substrates in general.

Essential processes carried out by the chloroplast are the assimilation of nutrients (C, N, S) and their conversion into building blocks for cell growth (i.e. amino acids, fatty acids and nucleotides)²⁵². Especially starch accumulation and ATG8-mediated autophagy is observed in response to nutrient limitation, two phenotypes we observed also in inducibly HSP70B depleted cells (Manuscript 3, Figure 5, 6 and S6)^{244,253}. We therefore tested if the addition of amino acids is capable of reverting the growth-arrested phenotype. Among 8 amino acids tested, specifically the addition of arginine at concentrations similar to those provided to auxotrophic strains allowed HSP70B-depleted cells to resume exponential growth (Manuscript 3, Figure 7 and S7). Arginine is the only amino acid that is actively imported into *Chlamydomonas* cells, probably because of the absence of proper transporters for other amino acids^{254,255}. We therefore cannot exclude that amino acids that did not rescue the growth arrest phenotype would do so if properly imported.

There are several possibilities at which level arginine might rescue the HSP70B depletion induced growth arrest. Arginine anabolism might be directly impaired, as several steps of arginine biosynthesis are localized in the chloroplast²⁵⁶. In addition, *Chlamydomonas* can grow on arginine as sole nitrogen source, so nitrogen fixation might be non-functional in HSP70B-depleted cells²⁵⁴. Nitrate fixation requires uptake of nitrate into the cytosol via a specific transporter where subsequent reduction to nitrite is taking place, catalyzed by nitrate reductase (NR)²²¹. A second transporter imports nitrite into the chloroplast where the nitrite reductase (NiR) reduces nitrite to ammonium, which is ATP dependently incorporated into glutamate creating glutamine by an enzyme called glutamine synthetase (GS). Glutamine is converted together with 2-oxoglutarate to two molecules of glutamate by an enzyme called glutamate synthase (GOGAT) as the final step of nitrogen fixation.

While the initial steps take place in the cytosol, NiR, GS and GOGAT might depend on HSP70B as they are located in the chloroplast. However, *Chlamydomonas* can use several amino acids as alternative nitrogen sources. Most of them are not imported into the cell, but are substrates of an unspecific extracellular amino acid oxidase/deaminase that produces ammonium in the extracellular space, which is subsequently imported and incorporated into glutamate via GS/GOGAT^{257,258}. However, the addition of several amino acids to HSP70B-

depleted cells that were previously shown to serve as substrate of the amino acid deaminase (lysine, valine, leucine, isoleucine, methionine) did not result in a release of the growth arrest (Manuscript 3, Figure S7). This pathway would bypass the plastidic NiR, but obviously is not sufficient to rescue the growth arrest.

Arginine itself is degraded to proline, allowing the assimilation of three nitrogen molecules. The first two are generated by arginase, generating ornithine from arginine and releasing urea, which is degraded to ammonium and incorporated into glutamate, also requiring the GS/GOGAT cycle. The last nitrogen is directly incorporated into glutamate from ornithine by ornithine aminotransferase, and therefore allows to bypass the GS/GOGAT cycle for nitrogen assimilation. However, ornithine was not able to revert the growth arrest phenotype when fed to HSP70B-depleted cells (Manuscript 3, Figure 7), indicating that bypassing GS/GOGAT is also not sufficient to suppress the phenotype. However, in this case, we cannot exclude that uptake of ornithine is also not possible for *Chlamydomonas* and GS/GOGAT is still the growth limiting factor that is bypassed by arginine uptake. Taken together, additional research is required to identify the substrate, either GS/GOGAT or the enzyme in arginine biosynthesis that directly requires HSP70B for proper function.

Two stress responses, the HSF1-dependent HSR and macroautophagy, were activated in HSP70B depleted cells (Manuscript 3, Figure 6 and S6). Both stress responses are known to induce a growth-arrest also in *Chlamydomonas* ^{259,260}. In a previous study in yeast, HSF1 was closely linked to TOR (Target Of Rapamycin) kinase ²⁶¹, a central regulator of cell growth in response to nutrient availability and environmental cues ²⁶². Moreover, a recent study in human cell lines showed that HSF1 is directly phosphorylated by TOR kinase and that this phosphorylation is necessary for HSF1 activation, indicating that TOR is also involved in eliciting the HSR ²⁶³. Autophagy is also activated in nutrient-limited, growth-arrested cells via the TOR signaling pathway ^{260,264}. It is therefore possible that the induction of the HSR and macroautophagy is a consequence from nutrient limitation and a TOR-mediated growth-arrest.

2.4.3. A NOVEL APPROACH TO IDENTIFY HSP70B SUBSTRATES

Previous attempts to identify targets of HSP70B did not reveal candidate proteins that would explain the observed phenotype. In order to find the substrates of the HSP70B chaperone machinery in biosynthetic pathways, a new method has to be developed, allowing for the specific identification of interacting proteins (Article 3). HSP70-substrate interactions are only transient, depend on PTMs, correct protein stoichiometry and often require co-chaperones (J-domain proteins) for their delivery to the chaperone. We were therefore working with cell lysates that should closely reflect the *in vivo* situation, and used a co-immunoprecipitation (CoIP) approach to find specific targets of HSP70B ^{265,266}. Novel interaction partners are then identified in an untargeted way by tandem mass spectrometry (LC-MS/MS). However, this strategy is often perturbed by a high false positive discovery rate, mainly derived from the

high sensitivity of modern mass spectrometers that confidently detect traces of unspecifically precipitating proteins. It therefore requires tedious verification of candidate interaction partners to prove specific interactions. Alternatively, a recently developed method based on stable isotope labeling and the use of knock-down mutants allows to quantitatively distinguish between specific interacting proteins and contaminants²⁶⁷.

I introduced two improvements to the original method to allow for identification of interaction partners of HSP70B in *Chlamydomonas*: (1) ¹⁵N metabolic labeling was used instead of labeled amino acids to quantify precipitated proteins. ¹⁵N metabolic labeling is much cheaper and can be applied to plants, fungi and bacteria that are prototrophic for amino acids. In addition, the problem of arginine-to-proline interconversion for quantification of the mass spectrometry data does not apply^{104,268}. (2) Affinity modulation by ATP/ADP was used to reduce the amount of specifically precipitated proteins instead of using knock-down mutants. HSP70s are known to specifically interact with their co-chaperones and substrates in an ATP-dependent manner. Binding to substrates is thereby more pronounced in the ADP state (closed conformation of the substrate binding domain, Figure 4)²⁶⁹. This strategy has several advantages over the use of knock-down strains. Two different concentrations of the target protein are present in the experiment when using knock-down and wildtype strains, requiring a careful titration of the antibodies to allow for quantitation. Moreover, knock-down of a target protein has consequences on the expression of related proteins, as demonstrated for example for the VIPP1 protein in case of HSP70B (Manuscript 3, Figure 3), and therefore might hamper distinguishing true from false interaction partners.

So far, I was able to demonstrate that this method is indeed able to capture interacting proteins dependent on the bound nucleotide (ATP/ADP). As a proof of principle, the specific interaction of HSP70B with its nucleotide exchange factor CGE1 in the ADP state was successfully demonstrated (Article 3, Figure 2 and 3).

2.4.4. OUTLOOK

The identification of the link to biosynthetic processes is one of the major findings in this work. To further establish this connection of HSP70B in general and especially in arginine biosynthesis or nitrogen assimilation will be one of the upcoming challenges in this project. However, specific substrates so far escaped our approach and make it necessary to further improve the method especially in terms of sensitivity.

In addition, the VIPP1 protein, the so far only known target of HSP70B, was strongly accumulating in HSP70B knock-down strains, probably resulting from a feedback to increase functional levels of VIPP1. Other targets might accumulate in a similar manner, so candidates can be derived from studying proteome dynamics upon HSP70B depletion. Such an experiment would also allow to study other aspects of this study in more detail, for example the accumulation of pre-proteins (transit peptides) to study the influence on chloroplast import.

3. ARTICLES AND MANUSCRIPTS

3.1. ARTICLE 1: AN INDUCIBLE ARTIFICIAL MICRORNA SYSTEM FOR *CHLAMYDOMONAS REINHARDTII* CONFIRMS A KEY ROLE FOR HEAT SHOCK FACTOR 1 IN REGULATING THERMOTOLERANCE.

Authors:

Stefan Schmollinger, Daniela Strenkert and Michael Schroda

Journal:

Current Genetics, 56(4):383-9.

Date:

2010, August

Contribution to:

Figure 1

Figure 2

Figure 3

Figure 4

Curr Genet (2010) 56:383–389
DOI 10.1007/s00294-010-0304-4

TECHNICAL NOTE

An inducible artificial microRNA system for *Chlamydomonas reinhardtii* confirms a key role for heat shock factor 1 in regulating thermotolerance

Stefan Schmollinger · Daniela Strenkert ·
Michael Schroda

Received: 19 January 2010 / Revised: 19 April 2010 / Accepted: 19 April 2010 / Published online: 7 May 2010
© Springer-Verlag 2010

Abstract Several RNA silencing strategies employing antisense or inverted repeat constructs have been applied to *Chlamydomonas reinhardtii*. Problems inherent to these strategies, like off-target effects by unpredictable generation of siRNAs, were solved previously by constructs allowing for routine expression of specific artificial microRNAs (amiRNAs). Yet missing was a routine tool for inducible amiRNA expression, which to establish was the aim of this work. For this, we equipped a recently developed amiRNA expression vector with the *NIT1* promoter, which is repressed by ammonium and activated by nitrate. We tested this conditional amiRNA vector with heat shock factor 1 (*HSF1*) as target. *HSF1* transcripts in transformants were already reduced ~2 h after transfer from ammonium to nitrate-containing medium. In contrast, HSF1 protein levels declined only ~8 h after the shift and were strongly reduced after 24 h, suggesting that HSF1 is a stable protein and diluted out by growth. HSF1 levels recovered partly when transformant cells were shifted back to ammonium for 72 h. Transformants developed thermosensitivity only on nitrate and thermosensitivity correlated with strong reduction in HSF1 levels, hence supporting our earlier conclusion that HSF1 is a key regulator for thermotolerance in *Chlamydomonas*.

Keywords Nitrate reductase · Inducible expression · Artificial microRNA · *Chlamydomonas* · Heat shock factor · Thermosensitivity

Communicated by A. Grossman.

S. Schmollinger · D. Strenkert · M. Schroda (✉)
Max-Planck-Institut für Molekulare Pflanzenphysiologie,
Am Mühlenberg 1, 14476 Potsdam-Golm, Germany
e-mail: Schroda@mpimp-golm.mpg.de

Introduction

The steadily growing number of sequenced genomes has strongly facilitated the identification of interesting genes by comparative genomics, which in turn creates a demand for efficient reverse genetics approaches for gene function analyses. The latter are facilitated by indexed mutant libraries and RNA silencing tools that meanwhile are available for many organisms. However, assigning gene function on the basis of a phenotype observed in constitutive knock-out/down mutants may be corrupted by the appearance of strong secondary phenotypes that conceal the primary effect. Moreover, functions of essential genes cannot be studied. Both drawbacks of constitutive knock-out/down mutants can be remedied by inducible RNA silencing tools, which allow for kinetically resolving the development of phenotypes and are available e.g. for several higher plant species (Moore et al. 2006).

Chlamydomonas reinhardtii has long been used as a plant model organism for studying various aspects in cell biology (Harris 2008). The main advantages of *Chlamydomonas* are its simple handling, short generation time and easy genetics. Moreover, it is yet the only organism that allows genetic manipulation of its three genomes (chloroplast, mitochondrial and nuclear), which are all sequenced (Merchant et al. 2007). Compared to higher plants, gene families in *Chlamydomonas* in general are much less complex, therefore facilitating functional genomics (Schroda 2004). Finally, a plethora of molecular tools have been developed for *Chlamydomonas* in recent years. For example, vectors for the expression of antisense and inverted repeat constructs have been successfully implemented (Schroda 2006), including an inverted repeat construct under control of the inducible *NIT1* promoter (Koblenz and Lechtreck 2005). However, inverted repeat constructs are

extremely prone to silencing (Yamasaki et al. 2008) and give rise to unpredictable siRNAs that may have off-target effects (Xu et al. 2006). The recent finding of microRNAs in *Chlamydomonas* (Molnar et al. 2007; Zhao et al. 2007) has prompted the development of vectors mediating the expression of artificial microRNAs (amiRNAs) that contain a defined, target specific miRNA and apparently are not prone to silencing (Molnar et al. 2009; Zhao et al. 2009). Here, we report the development of a vector for *Chlamydomonas* that combines conditional gene expression via the *NIT1* promoter with the advantages of amiRNA specificity. To demonstrate the efficiency of this inducible amiRNA system, we have targeted the *HSF1* mRNA and confirm the role of HSF1 as key regulator of the stress response in *Chlamydomonas*.

Materials and methods

Strains and culture conditions

Chlamydomonas reinhardtii strain cw15-325 (cw₄ mt⁺ arg7 nit1⁺ nit2⁺), kindly provided by R. Matagne (University of Liège, Belgium), was used as recipient strain for transformation with *HSF1*-amiRNA construct pMS540 (see below) and control construct pCB412 (Schroda et al. 1999). Strains were grown mixotrophically in tris–acetate-phosphate (TAP) medium (Harris 2008) on a rotatory shaker at 25°C and $\sim 30 \mu\text{E m}^{-2} \text{s}^{-1}$. The TAP medium was supplemented with 50 mg L⁻¹ of arginine when required.

Vector construction

At first, 791 bp of 5' sequence from the *NIT1* gene were amplified by PCR using primers 5'-ATGGaTcCATcTAGAGGTGACCCGCCAGCC-3' and 5'-TGGTggcCatTtAAAgGctagCGGACTCTCGAGC-3' (lower case letters indicate nucleotides altered to introduce recognition sites for restriction enzymes *Bam*HI-*Xba*I-*Bsr*EII and *Msc*I-*Nhe*I into forward and reverse primer, respectively), and plasmid pMN24 as template (Fernandez et al. 1989). The 791 bp PCR product, consisting of promoter and 5' UTR sequences, was digested with *Xba*I and *Msc*I and ligated into *Xba*I/*Msc*I-digested pMS179 (Schulz-Raffelt et al. 2010), yielding pMS287. Next, 138 bp of microRNA sequence were amplified by PCR using primers 5'-GAGATCTAGAGGTGTTGGGTC-3' and 5'-aaaCCatggACTAGTAGCTGGAACACTGC-3' (lower case letters indicate nucleotides altered to introduce recognition sites for restriction enzymes *Xba*I and *Nco*I into forward and reverse primer, respectively), and plasmid pChlamiRNA2 as template (Molnar et al. 2009). The PCR product was digested with *Xba*I and *Nco*I and ligated into *Nhe*I/*Nco*I-digested

pMS287, generating pMS538. Finally, pMS538 was digested with *Xba*I and *Spe*I to release an 878-bp 5'-*NIT1*/microRNA fragment, which was ligated into *Xba*I/*Spe*I-digested, shrimp alkaline phosphatase-treated pChlamiRNA2 to yield pMS539.

The miRNA targeting *Chlamydomonas HSF1* was designed according to the detailed instructions given by Molnar et al. (2009) using the WMD2 tool at <http://wmd2.weigelworld.org> (Ossowski et al. 2008). Resulting oligonucleotides 5'-ctagtACCCACCACCATTCCCTAATCAAtcgcgtgatcgccaccatgggggtggtggtgatcagcgcTGTATAAGGAATGGTGGTGGGTg-3' and 5'-ctagcACCCACCACCATTCC TTATCAtagcgtgatcaccaccaccatgggtccgatcagcagagaTGATTAGGAATGGTGGTGGGTa-3' (uppercase letters indicate miRNA*/miRNA sequences) were annealed by boiling and slowly cooling-down in a thermocycler and ligated into *Spe*I-digested pMS539, yielding pMS540. Screening for correct clones was done as described by Molnar et al. (2009). pMS540 was linearized by digestion with *Hind*III and transformed into *Chlamydomonas* strain cw 15-325 by vortexing with glass beads (Kindle 1990).

Shifts from repressive to inducing conditions

For RNA and protein gel blot analyses, cells were grown in 100 mL of TAP–NH₄Cl medium to a maximal density of $\sim 5 \times 10^6$ cells/mL. Cells were centrifuged at 2,500g for 4 min at 25°C. The cell pellet was resuspended twice in 50 mL TAP–N medium in a 50-mL falcon tube and centrifuged at 3,100g for 2 min at 25°C to remove remaining TAP–NH₄Cl. The cells were resuspended in TAP–KNO₃ to a density of 2×10^6 cells/mL and if necessary, diluted during the experiment to ensure that cell densities never exceeded 6×10^6 cells/mL. RNA extraction and hybridization were performed as described previously (Liu et al. 2005). Probes used for hybridization were: a 805-bp fragment from the *NIT1* gene which was amplified by RT-PCR with primers 5'-ATGCTGAAGAAGAGCATTGGC-3' and 5'-CCATCAGGTTCCAGGTGATCA-3' on RNA isolated from TAP–KNO₃ grown cells; a 2,358-bp *Nhe*I-*Xba*I fragment from the *HSF1* gene; the full length ~ 1 -kb cDNA of *CBLP2*. Radioactive signals were detected using BAS-IP MS2040 phosphorimager plates (Raytest), scanned with a Typhoon TRIO + phosphorimager with ImageQuant TL Software (Amersham Biosciences) and quantified using the Quantity One 4.5.1 program (Bio-Rad). Protein extraction and gel blot analysis were done as reported in (Willmund and Schroda 2005). Antisera used were against *Chlamydomonas HSF1* (Schulz-Raffelt et al. 2007) and CF1 β (Lemaire and Wollman 1989). For phenotype analyses, cells were grown in TAP–NH₄Cl medium to a density of $\sim 6 \times 10^6$ cells/mL at $\sim 30 \mu\text{E m}^{-2} \text{s}^{-1}$ and diluted into TAP–NH₄Cl or TAP–KNO₃ medium to a density of

$\sim 10^5$ cells/mL 2 days before the experiment. Cells were then grown again to a density of $\sim 3 \times 10^6$ cells/mL and 50 μ l were spotted on TAP agar plates containing 7.5 mM KNO_3 or 7.5 mM NH_4Cl , respectively, as nitrogen source. Plates were incubated at $30 \mu\text{E m}^{-2} \text{s}^{-1}$ for 3 days at 25°C , which if indicated were interspersed with two 2-h incubations at 40°C in the light (heat shocks were done in 24-h intervals).

Shifts from inducing to repressive conditions

Cells were grown for 3 days in TAP- KNO_3 medium to a density of $\sim 4 \times 10^6$ cells/mL at $\sim 30 \mu\text{E m}^{-2} \text{s}^{-1}$ and diluted into TAP- KNO_3 or TAP- NH_4Cl medium to a density of $\sim 10^5$ cells/mL and grown for another 3 days. Protein extraction and immunoblot analysis were done as described above. For phenotype analysis, cells were grown for 3 days in TAP- KNO_3 medium to a density of $\sim 4 \times 10^6$ cells/mL at $\sim 30 \mu\text{E m}^{-2} \text{s}^{-1}$ and diluted into TAP- KNO_3 or TAP- NH_4Cl medium to a density of $\sim 10^5$ cells/mL. After another 3 days of growth in TAP- KNO_3 or TAP- NH_4Cl medium, respectively, cultures were split and either continued to be incubated at 25°C , or heat-shocked at 40°C for 2 h in the light. 50 μ l ($\sim 2 \times 10^5$ cells) were spotted on TAP agar plates containing 7.5 mM KNO_3 or 7.5 mM NH_4Cl , respectively, as nitrogen source. Plates were incubated at $\sim 30 \mu\text{E m}^{-2} \text{s}^{-1}$ for 3 days at 25°C .

Results

Two independent groups recently reported on vectors for the specific downregulation of Chlamydomonas genes by artificial microRNAs (amiRNAs) (Molnar et al. 2009; Zhao et al. 2009). Both groups employed the strong constitutive *HSP70A-RBCS2* promoter to drive expression of modified precursors of natural Chlamydomonas miRNAs. The vectors generated by Molnar et al. also allow for the convenient design of amiRNAs based on the WMD web tool (Ossowski et al. 2008) and for easy cloning of designed oligonucleotides into a unique *SpeI* site engineered into the miRNA precursor. To further improve this convenient tool, we replaced the *HSP70A-RBCS2* promoter in pChlamiRNA2 (Molnar et al. 2009) with the *NITI* promoter, which controls expression of the Chlamydomonas nitrate reductase gene (Fernandez et al. 1989) (Fig. 1a). The *NITI* gene is repressed when cells are grown with ammonium and induced with nitrate as nitrogen source (Quesada and Fernandez 1994). This regulation is mediated by sequences present in the region 282 nt upstream from the translational start site of the *NITI* gene and is maintained in a transgene setting (Ohresser et al. 1997). Hence, while fully supporting the convenient designing and cloning

concept of Molnar et al., modified vector pMS539 should allow for conditional amiRNA expression based on the nitrogen source used.

To test the usefulness of pMS539, we designed an amiRNA targeting the coding region of the heat shock factor 1 (*HSF1*) transcript and cloned it into pMS539 to generate pMS540 (Fig. 1a). We chose the *HSF1* gene as target because Chlamydomonas strains with strongly reduced HSF1 levels were found to be viable under non-stress conditions, but were severely thermosensitive (Schulz-Raffelt et al. 2007), hence providing a simple screen for strains with low HSF1 levels. pMS540 was transformed into a cell wall deficient, arginine auxotrophic strain containing functional copies of the *NIT1* and *NIT2* genes. The *NIT2* gene encodes a transcription factor that is required for nitrate signalling on the *NIT1* promoter (Camargo et al. 2007). Transformants were selected for arginine prototrophy. Of 100 transformants that were grown on TAP- KNO_3 plates and subjected to two 2-h heat shock treatments, six appeared to be thermosensitive (data not shown). In one of these transformants, HSF1 accumulated to wild-type levels (Fig. 1b), thus thermosensitivity might have arisen from integration of the vector into another gene essential for thermotolerance, like *HSP101* (Sanchez and Lindquist 1990). Two of the six transformants had moderately reduced HSF1 levels and three had very low HSF1 levels (Fig. 1b). Accordingly, the latter three were highly thermosensitive (Fig. 1c).

We next wanted to test whether reduced HSF1 levels and thermosensitivity correlated with nitrate-induced expression of pMS540. For this, we grew a transformant generated with the empty vector and two pMS540 transformants (#5 and #22) with strong phenotypes using ammonium or nitrate as nitrogen source and analysed their HSF1 protein levels and thermosensitivity. As expected, HSF1 protein levels were only reduced in the transformants grown on nitrate, whereas they were unaffected in control cells grown on either nitrogen source or in transformants grown on ammonium (Fig. 2a). Accordingly, both pMS540 transformants were thermosensitive only on nitrate, but not on ammonium, whereas the control was thermotolerant on either nitrogen source (Fig. 2b).

Next, we aimed at following the kinetics of HSF1 down-regulation induced by shifting the nitrogen source from ammonium to nitrate. To this end, we monitored *HSF1* mRNA levels within the first 8 h and HSF1 protein levels within the first 24 h after the shift. We observed a decline in *HSF1* mRNA levels around 2 h after the shift, right after expression of the native *NITI* transcript had peaked (Figs. 3a, b; Quesada and Fernandez 1994). Hence, as observed by Molnar et al. (2009) and Zhao et al. (2009), amiRNAs in Chlamydomonas apparently act by impacting the level of transcript accumulation. We consistently

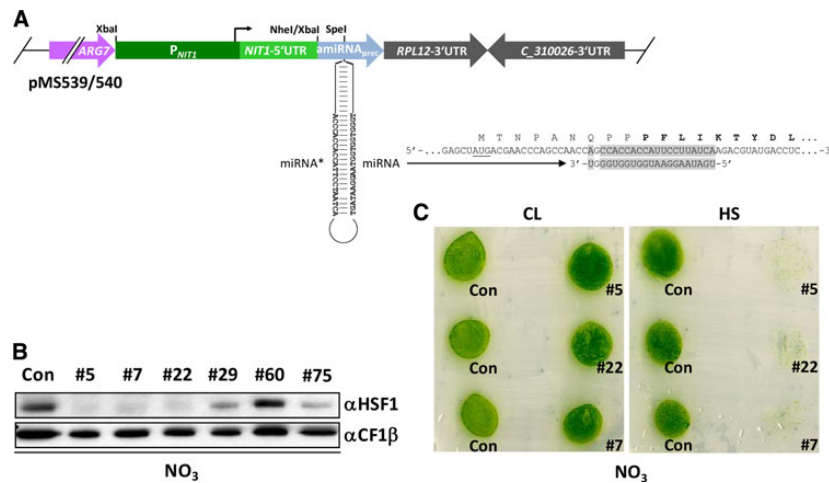


Fig. 1 Construct for the conditional expression of an *HSF1*-amiRNA and preliminary analysis of *HSF1*-underexpressing strains. **a** Schematic drawing of inducible amiRNA construct pMS540 and its target region in the *HSF1* transcript. Construct pMS540 is based on pChlamiRNA2 (Molnar et al. 2009), which itself is a derivative of pCB740 (Schroda et al. 1999). pMS540 contains the *ARG7* gene as selectable marker, 465 nt of *NITI* promoter sequence, 294 nt of *NITI* 5' UTR connected to the modified precursor of natural miRNA cre-MIR1157, and the two 3' UTRs from *RPL12* and estExt_fgenes2_pg.C_31002 as inverted terminator. The amiRNA generated by pMS540 targets the region coding for the extreme N-terminal part of *HSF1*, which includes the *HSF1* DNA-binding domain (shown in *bold letters*). Base-pairing nucleotides of the amiRNA and *HSF1*

mRNA are shaded in *grey*. **b** Immunoblot analysis of transformants with reduced *HSF1* protein levels. Total protein corresponding to 2 μ g chlorophyll was extracted from control cells (*Con*) and six pMS540 transformants grown directly in TAP with 7.5 mM KNO_3 as nitrogen source to a density of $\sim 5 \times 10^6$ cells mL^{-1} and separated on a 10% SDS-polyacrylamide gel. Levels of *HSF1* protein relative to loading control *CF1 β* were analysed by immunoblotting. Control cells are the cw15-325 recipient strain transformed with the *ARG7* gene (pCB412) alone. **c** Analysis of thermotolerance of control and *HSF1*-amiRNA strains. Cells were spotted on TAP- KNO_3 agar plates and incubated in the light for 3 days continuously at 25°C (CL) or interspersed with two 2-h heat shock treatments at 40°C (HS)

observed that transcript levels of *HSF1* and heat shock genes increase at varying extent shortly after changing the medium (Fig. 3b, data not shown). Most likely, centrifugation and washing steps stress cells slightly. At the protein level, a clear decline in *HSF1* levels in transformants #5 and #22 was observed only 8 h after shifting cells to nitrate-containing medium, while *HSF1* was strongly reduced 24 h after the shift (Fig. 3c). As expected, no change in *HSF1* levels after shifting the nitrogen source was observed in control cells.

Finally, we asked whether *HSF1*-amiRNA strains were able to reconstitute *HSF1* levels and thermotolerance when the nitrogen source was shifted back from nitrate to ammonium. For this, *HSF1* levels were monitored in control cells and transformants #5 and #22 that, after growth on nitrate for 3 days, were shifted to ammonium as nitrogen source. As shown in Fig. 4a, this treatment resulted in a gradual recovery of *HSF1* levels in transformants #5 and #22, although wild-type *HSF1* levels were not fully recovered even after cells were grown for 3 days on ammonium. This might be due to a slow translation rate of *HSF1* transcripts under non-stress conditions. Alternatively, Argonaute proteins loaded with the *HSF1*-miRNA might be stable and

continue to affect *HSF1* transcripts until diluted out by growth. In any case, as shown in Fig. 4b, the partly recovered *HSF1* levels in transformant #5 were sufficient to re-establish thermotolerance that was lost when cells were grown on nitrate.

Discussion

In this work, we extend the Chlamydomonas toolkit by an inducible artificial microRNA (amiRNA) vector. In this vector, amiRNA expression is mediated by the *NITI* promoter, which is repressed when cells are grown on ammonium and induced when they are grown on nitrate as nitrogen source (Fig. 3a; Ohresser et al. 1997; Quesada and Fernandez 1994). The *NITI* promoter has already been employed successfully in Chlamydomonas to drive inducible expression of an inverted repeat construct targeting centrin (Koblenz and Lechtreck 2005). However, the construction of inverted repeat constructs is tedious, as it requires gene dependent, multi-step cloning strategies. Moreover, siRNAs generated from inverted repeat constructs are unpredictable and may have off-target effects

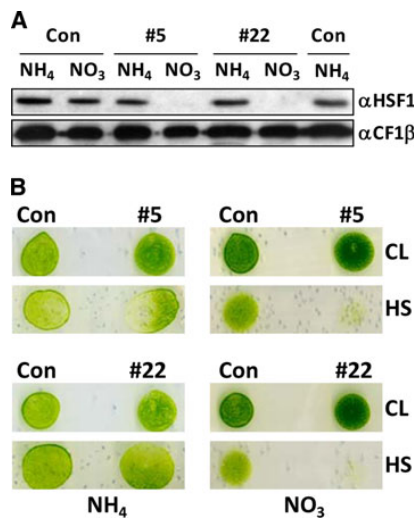


Fig. 2 Analysis of HSF1 expression levels and phenotype of *HSF1*-amiRNA strains under repressive and inducing conditions. **a** HSF1 expression levels in *HSF1*-amiRNA strains. Two independent pMS540 transformants (#5 and #22) and control cells transformed with the empty vector (*Con*) were grown with KNO₃ or NH₄Cl as nitrogen source. Total protein corresponding to 2 μg chlorophyll was extracted, separated on a 10% SDS-polyacrylamide gel, and levels of HSF1 protein relative to loading control CF1β were analysed by immunoblotting. **b** Analysis of thermotolerance of control and *HSF1*-amiRNA strains under repressive and inducing conditions. Cells were spotted on TAP-NH₄Cl and TAP-KNO₃ agar plates and treated as described in Fig. 1C

(Xu et al. 2006). Our vector is based on a construct developed by Molnar et al. (2009), which allows for the convenient cloning of amiRNAs that can easily be designed and tested for specificity by the WMD web tool (Ossowski et al. 2008). Hence, our vector combines easy cloning with conditional expression of specific amiRNAs regulated by physiological concentrations of natural nitrogen sources.

Using the strong constitutive *HSP70A-RBCS2* promoter to drive amiRNA expression, Molnar et al. (2009) and Zhao et al. (2009) observed strong phenotypes in 16–72% of transformants obtained for the four target genes investigated. In contrast, only 5% of transformants generated with *NIT1* promoter-driven *HSF1*-amiRNA exhibited a thermo-sensitive phenotype. Koblenz and Lehtreck (2005) also observed generally weaker phenotypes in transformants containing the inverted repeat construct under control of the *NIT1* promoter as compared to the *HSP70A-RBCS2* promoter. As the degree of downregulation of the target gene correlates with the amiRNA expression level (Molnar et al. 2007; Ossowski et al. 2008), the higher numbers of transformants with strong phenotypes reported previously for amiRNA constructs might be due to on average higher promoter activity of *HSP70A-RBCS2* compared to *NIT1*. Alternatively, this effect might be due to the ability of the

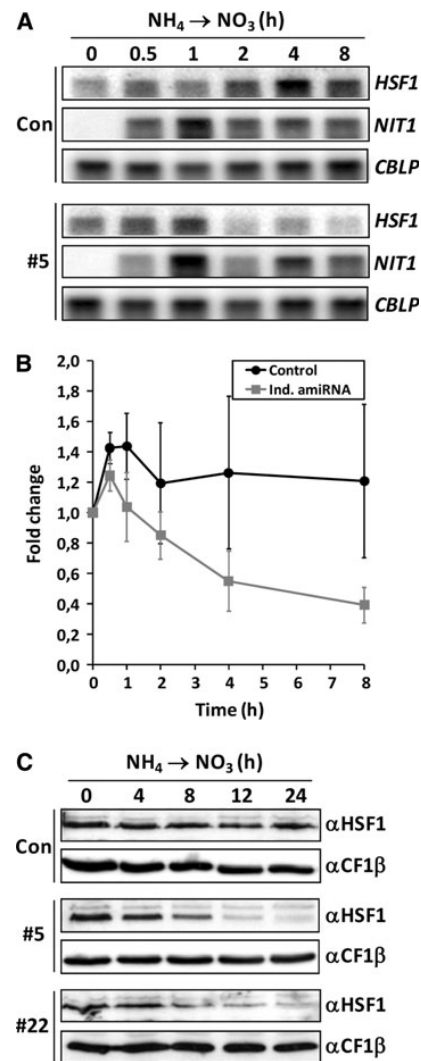


Fig. 3 Time course analysis of the expression of selected gene products in *HSF1*-amiRNA cells after shifting to inducing conditions. **a** Analysis of mRNA expression in *HSF1*-amiRNA strains. Control cells transformed with the empty vector (*Con*) and *HSF1*-amiRNA strain #5 were grown in TAP-NH₄Cl and transferred to TAP-KNO₃. Total RNA was isolated from samples taken from both cultures at the time points indicated and accumulation of the *HSF1* and *NIT1* transcripts relative to loading control *CBLP2* was monitored by northern analysis. **b** Quantification of *HSF1* mRNA levels. Signals from *HSF1* corrected for unequal loading on the basis of *CBLP2* signals were quantified from northern experiments described in Fig. 3a and plotted as fold change relative to the first time point. Three experiments with control cells and five with *HSF1*-amiRNA strains #5 and #22 were considered. Error bars depict the standard error of the mean. **c** Time resolved analysis of HSF1 protein levels. Control cells (*Con*) and *HSF1*-amiRNA strains #5 and #22 were grown in TAP-NH₄Cl and transferred to TAP-KNO₃. Total protein corresponding to 2 μg chlorophyll was extracted from samples taken from both cultures at the time points indicated, separated on a 10% SDS-polyacrylamide gel, and accumulation of HSF1 relative to loading control CF1β was monitored by immunoblotting

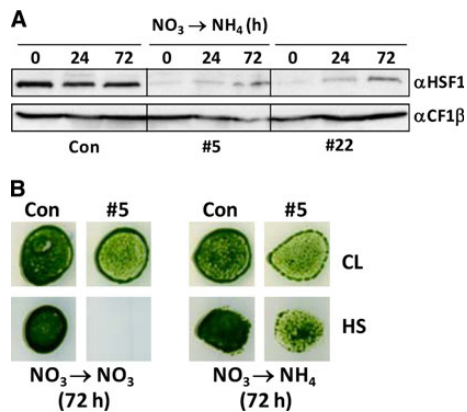


Fig. 4 Analysis of HSF1 protein levels and thermotolerance after shifting *HSF1*-amiRNA cells from inducing to repressive conditions. **a** Time resolved analysis of HSF1 protein levels. Control cells transformed with the empty vector (*Con*) and *HSF1*-amiRNA strains #5 and #22 were grown for 72 h in TAP-KNO₃ and transferred to TAP-NH₄Cl. Total protein corresponding to 2 μg chlorophyll was extracted from samples taken from both cultures at the time points indicated, separated on a 10% SDS-polyacrylamide gel, and accumulation of HSF1 relative to loading control CF1β was monitored by immunoblotting. **b** Analysis of thermotolerance of control and *HSF1*-amiRNA cells. Control cells and *HSF1*-amiRNA strain #5 were grown in TAP-KNO₃ for 72 h and transferred back to TAP-KNO₃ (*left panel*) or to TAP-NH₄Cl (*right panel*) for another 72 h. Cell cultures were split and incubated either at 25°C (CL) or at 40°C (HS) for 2 h. Aliquots from treated cultures were then spotted onto TAP-KNO₃ and TAP-NH₄Cl agar plates, respectively, and incubated for 3 days to estimate the survival rate

HSP70A promoter to act as transcriptional state enhancer, i.e., to improve the chance that a randomly integrated transgene is expressed (Lodha et al. 2008; Schroda et al. 2002). In light of the frequently observed silencing of transgenes in *Chlamydomonas* (Schroda 2006), it may be worth mentioning that nitrate-induced downregulation of HSF1 and thermosensitivity in transformants #5 and #22 could be fully reproduced even after maintaining them on TAP-NH₄Cl for 9 months.

We have frequently observed a slight induction of stress genes apparently resulting from centrifugation and washing steps required for shifting the nitrogen source (Fig. 3b). This certainly is a disadvantage of using the *NIT1* promoter for regulated amiRNA expression. However, as effects on target protein accumulation occur only several hours later (Figs. 3c, 4a), the inflicted brief stress is unlikely to affect the development of phenotypes arising from downregulation of the specific target protein given that the target protein has a low turnover rate. Moreover, the stress will similarly affect control cultures for which cells are shifted back to ammonium so that any effect of stress induction on the observed phenotypes can be readily determined. Despite these potential disadvantages inherent to using the

NIT1 promoter to regulate amiRNA expression, the *NIT1* promoter has several advantages over other characterised, inducible *Chlamydomonas* promoters such as those for cytochrome c6 (Quinn et al. 2003), *CAH1* encoding a periplasmic carbonic anhydrase (Kucho et al. 1999), or *HSP70A* encoding a cytosolic Hsp70 (Schroda et al. 2000): (i) it is very tightly regulated (Fig. 3a; Quesada and Fernandez 1994); (ii) induction by shifting the nitrogen source is simple to perform and may be used to monitor the development of loss of function phenotypes (NH₄ → NO₃; Fig. 3c) or gain of function phenotypes (NO₃ → NH₄; Fig. 4); (iii) induction is persistent and does not inflict long-term physiological stress to the cells. The latter aspect is important in light of the long induction times required for diluting out a stable protein to low levels (Fig. 3c) or to re-establish wild-type levels of the target protein (Fig. 4a). However, it should be kept in mind that frequently used *Chlamydomonas* strains, like CC124, are *nit1*⁻ *nit2*⁻ and therefore cannot grow on nitrate (Harris 2008).

In addition to demonstrating a proof of principle, the inducible downregulation of HSF1 and the development of the resulting thermosensitive phenotype caused by the expression of our amiRNA transcript allow us to draw two more conclusions: (i) HSF1 levels decline by a factor of ~2 every ~8 h (Fig. 3c), the latter roughly corresponding to the generation time of *Chlamydomonas* (Harris 2008). Hence, HSF1 must be a stable protein and reduction in HSF1 levels appears to result from a simple dilution by growth after amiRNA-mediated removal of *HSF1* transcript abolishes synthesis of new HSF1. (ii) Even though the specific *HSF1*-amiRNA targeted a different region in the *HSF1* transcript than our previously reported *HSF1*-inverted repeat construct (Schulz-Raffelt et al. 2007), a similar level of thermosensitivity was induced. This corroborates our earlier findings that HSF1 is a key regulator of the stress response in *Chlamydomonas*.

Acknowledgments We thank Steve Miller for critically reading the manuscript, Attila Molnar for construct pChlamRNA2 and helpful advice, and Olivier Vallon for the antiserum against CF1β. This work was supported by the Max Planck Society and grants from the Deutsche Forschungsgemeinschaft (Schr 617/5-1) and the Bundesministerium für Bildung und Forschung (Systems Biology Initiative FORSYS, project GoFORSYS).

References

- Camargo A, Llamas A, Schnell RA, Higuera JJ, Gonzalez-Ballester D, Lefebvre PA, Fernandez E, Galvan A (2007) Nitrate signaling by the regulatory gene NIT2 in *Chlamydomonas*. *Plant Cell* 19:3491–3503
- Fernandez E, Schnell R, Ranum LP, Hussey SC, Silflow CD, Lefebvre PA (1989) Isolation and characterization of the nitrate reductase structural gene of *Chlamydomonas reinhardtii*. *Proc Natl Acad Sci USA* 86:6449–6453

- Harris EH (2008) The *Chlamydomonas* sourcebook: introduction to *Chlamydomonas* and its laboratory use, 2nd edn. Academic Press, San Diego
- Kindle KL (1990) High-frequency nuclear transformation of *Chlamydomonas reinhardtii*. Proc Natl Acad Sci USA 87:1228–1232
- Koblentz B, Lechtreck KF (2005) The *NIT1* promoter allows inducible and reversible silencing of centrin in *Chlamydomonas reinhardtii*. Eukaryot Cell 4:1959–1962
- Kucho K, Ohyama K, Fukuzawa H (1999) CO(2)-responsive transcriptional regulation of CAH1 encoding carbonic anhydrase is mediated by enhancer and silencer regions in *Chlamydomonas reinhardtii*. Plant Physiol 121:1329–1338
- Lemaire C, Wollman FA (1989) The chloroplast ATP synthase in *Chlamydomonas reinhardtii*. I. Characterization of its nine constitutive subunits. J Biol Chem 264:10228–10234
- Liu C, Willmund F, Whitelegge JP, Hawat S, Knapp B, Lodha M, Schroda M (2005) J-domain protein CDJ2 and HSP70B are a plastidic chaperone pair that interacts with vesicle-inducing protein in plastids 1. Mol Biol Cell 16:1165–1177
- Lodha M, Schulz-Raffelt M, Schroda M (2008) A new assay for promoter analysis in *Chlamydomonas* reveals roles for heat shock elements and the *TATA* box in *HSP70A* promoter-mediated activation of transgene expression. Eukaryot Cell 7:172–176
- Merchant SS, Prochnik SE, Vallon O, Harris EH, Karpowicz SJ, Witman GB, Terry A, Salamov A, Fritz-Laylin LK, Marechal-Drouard L, Marshall WF, Qu LH, Nelson DR, Sanderfoot AA, Spalding MH, Kapitonov VV, Ren Q, Ferris P, Lindquist E, Shapiro H, Lucas SM, Grimwood J, Schmutz J, Cardol P, Cerutti H, Chanfreau G, Chen CL, Cognat V, Croft MT, Dent R, Dutcher S, Fernandez E, Fukuzawa H, Gonzalez-Ballester D, Gonzalez-Halphen D, Hallmann A, Hanikenne M, Hippler M, Inwood W, Jabbari K, Kalanon M, Kuras R, Lefebvre PA, Lemaire SD, Lobanov AV, Lohr M, Manuell A, Meier I, Mets L, Mittag M, Mittelmeier T, Moroney JV, Moseley J, Napoli C, Nedelcu AM, Niyogi K, Novoselov SV, Paulsen IT, Pazour G, Purton S, Ral JP, Riano-Pachon DM, Riekhof W, Rymarquis L, Schroda M, Stern D, Umen J, Willows R, Wilson N, Zimmer SL, Allmer J, Balk J, Bisova K, Chen CJ, Elias M, Gendler K, Hauser C, Lamb MR, Ledford H, Long JC, Minagawa J, Page MD, Pan J, Pootakham W, Roje S, Rose A, Stahlberg E, Terauchi AM, Yang P, Ball S, Bowler C, Dieckmann CL, Gladyshev VN, Green P, Jorgensen R, Mayfield S, Mueller-Roeber B, Rajamani S, Sayre RT, Brokstein P, Dubchak I, Goodstein D, Hornick L, Huang YW, Jhaveri J, Luo Y, Martinez D, Ngau WC, Otiillar B, Poliakov A, Porter A, Szajkowski L, Werner G, Zhou K, Grigoriev IV, Rokhsar DS, Grossman AR (2007) The *Chlamydomonas* genome reveals the evolution of key animal and plant functions. Science 318:245–250
- Molnar A, Schwach F, Studholme DJ, Thuenemann EC, Baulcombe DC (2007) miRNAs control gene expression in the single-cell alga *Chlamydomonas reinhardtii*. Nature 447:1126–1129
- Molnar A, Bassett A, Thuenemann E, Schwach F, Karkare S, Ossowski S, Weigel D, Baulcombe D (2009) Highly specific gene silencing by artificial microRNAs in the unicellular alga *Chlamydomonas reinhardtii*. Plant J 58:165–174
- Moore I, Samalova M, Kurup S (2006) Transactivated and chemically inducible gene expression in plants. Plant J 45:651–683
- Ohresser M, Matagne RF, Loppes R (1997) Expression of the arylsulphatase reporter gene under the control of the *nit1* promoter in *Chlamydomonas reinhardtii*. Curr Genet 31:264–271
- Ossowski S, Schwab R, Weigel D (2008) Gene silencing in plants using artificial microRNAs and other small RNAs. Plant J 53:674–690
- Quesada A, Fernandez E (1994) Expression of nitrate assimilation related genes in *Chlamydomonas reinhardtii*. Plant Mol Biol 24:185–194
- Quinn JM, Kropat J, Merchant S (2003) Copper response element and Crr1-dependent Ni(2+)-responsive promoter for induced, reversible gene expression in *Chlamydomonas reinhardtii*. Eukaryot Cell 2:995–1002
- Sanchez Y, Lindquist SL (1990) HSP104 required for induced thermotolerance. Science 248:1112–1115
- Schroda M (2004) The *Chlamydomonas* genome reveals its secrets: chaperone genes and the potential roles of their gene products in the chloroplast. Photosynth Res 82:221–240
- Schroda M (2006) RNA silencing in *Chlamydomonas*: mechanisms and tools. Curr Genet 49:69–84
- Schroda M, Vallon O, Wollman FA, Beck CF (1999) A chloroplast-targeted heat shock protein 70 (HSP70) contributes to the photoprotection and repair of photosystem II during and after photoinhibition. Plant Cell 11:1165–1178
- Schroda M, Blocker D, Beck CF (2000) The *HSP70A* promoter as a tool for the improved expression of transgenes in *Chlamydomonas*. Plant J 21:121–131
- Schroda M, Beck CF, Vallon O (2002) Sequence elements within an *HSP70* promoter counteract transcriptional transgene silencing in *Chlamydomonas*. Plant J 31:445–455
- Schulz-Raffelt M, Lodha M, Schroda M (2007) Heat shock factor 1 is a key regulator of the stress response in *Chlamydomonas*. Plant J 52:286–295
- Schulz-Raffelt M, Schmollinger S, Skupin A, Strenkert D, Veyel D, Vallon O, Ebenhöf O, Schroda M (2010) Dissection of the stress response in *Chlamydomonas* reveals a role for chloroplast HSP70B in stress signalling. Submitted
- Willmund F, Schroda M (2005) HEAT SHOCK PROTEIN 90C is a bona fide Hsp90 that interacts with plastidic HSP70B in *Chlamydomonas reinhardtii*. Plant Physiol 138:2310–2322
- Xu P, Zhang Y, Kang L, Roossinck MJ, Mysore KS (2006) Computational estimation and experimental verification of off-target silencing during posttranscriptional gene silencing in plants. Plant Physiol 142:429–440
- Yamasaki T, Miyasaka H, Ohama T (2008) Unstable RNAi effects through epigenetic silencing of an inverted repeat transgene in *Chlamydomonas reinhardtii*. Genetics 180:1927–1944
- Zhao T, Li G, Mi S, Li S, Hannon GJ, Wang XJ, Qi Y (2007) A complex system of small RNAs in the unicellular green alga *Chlamydomonas reinhardtii*. Genes Dev 21:1190–1203
- Zhao T, Wang W, Bai X, Qi Y (2009) Gene silencing by artificial microRNAs in *Chlamydomonas*. Plant J 58:157–164

3.2. ARTICLE 2: TRANSCRIPTION FACTOR-DEPENDENT CHROMATIN REMODELING AT HEAT SHOCK AND COPPER-RESPONSIVE PROMOTERS IN *CHLAMYDOMONAS REINHARDTII*.

Authors:

Daniela Strenkert, **Stefan Schmollinger**, Frederik Sommer, Miriam Schulz-Raffelt and Michael Schroda

Journal:

The Plant Cell, 23(6):2285-301.

Date:

2011, June

Contribution to:

Figure 1 A

Supplemental Figure 2 A and C

Statistical analysis of Figure 3, 4, 7, 8

Transcription Factor–Dependent Chromatin Remodeling at Heat Shock and Copper-Responsive Promoters in *Chlamydomonas reinhardtii*^{WIOA}

Daniela Strenkert, Stefan Schmollinger, Frederik Sommer, Miriam Schulz-Raffelt,¹ and Michael Schroda²

Max-Planck-Institut für Molekulare Pflanzenphysiologie, D-14476 Potsdam-Golm, Germany

How transcription factors affect chromatin structure to regulate gene expression in response to changes in environmental conditions is poorly understood in the green lineage. To shed light on this issue, we used chromatin immunoprecipitation and formaldehyde-assisted isolation of regulatory elements to investigate the chromatin structure at target genes of HSF1 and CRR1, key transcriptional regulators of the heat shock and copper starvation responses, respectively, in the unicellular green alga *Chlamydomonas reinhardtii*. Generally, we detected lower nucleosome occupancy, higher levels of histone H3/4 acetylation, and lower levels of histone H3 Lys 4 (H3K4) monomethylation at promoter regions of active genes compared with inactive promoters and transcribed and intergenic regions. Specifically, we find that activated HSF1 and CRR1 transcription factors mediate the acetylation of histones H3/4, nucleosome eviction, remodeling of the H3K4 mono- and dimethylation marks, and transcription initiation/elongation. By this, HSF1 and CRR1 quite individually remodel and activate target promoters that may be inactive and embedded into closed chromatin (*HSP22F/CYC6*) or weakly active and embedded into partially opened (*CPX1*) or completely opened chromatin (*HSP70A/CRD1*). We also observed HSF1-independent histone H3/4 deacetylation at the *RBCS2* promoter after heat shock, suggesting interplay of specific and presumably more generally acting factors to adapt gene expression to the new requirements of a changing environment.

INTRODUCTION

Living organisms may acclimate to abiotic stress by the up- and downregulation of specific sets of genes. Since chromatin remodeling plays an important role in the regulation of gene expression in all eukaryotes examined to date (Kouzarides, 2007; Li et al., 2007), we are interested in how chromatin remodeling affects gene expression in plant systems as a consequence of changes in environmental conditions. We studied this issue in the unicellular green alga *Chlamydomonas reinhardtii*. *Chlamydomonas* has the advantage that changes in environmental conditions may be homogeneously and instantaneously applied to all cells in a cell culture. Moreover, in contrast with land plants, *Chlamydomonas* cells are not differentiated into different cell types or organized into different tissues. The stress responses on which our studies focus, those permitting acclimation to heat shock and copper deficiency, are well characterized in *Chlamydomonas* and therefore well suited for investigations into transcriptional regulation at the chromatin level (Merchant et al., 2006; Schulz-Raffelt et al., 2007).

¹ Current address: Centre National de la Recherche Scientifique, Unité Mixte de Recherche 6191, Commissariat à l'Énergie Atomique et aux Énergies Alternatives Cadarache, 13108 Saint-Paul-lez-Durance, France.

² Address correspondence to schroda@mpimp-golm.mpg.de.

The author responsible for distribution of materials integral to the findings presented in this article in accordance with the policy described in the Instructions for Authors (www.plantcell.org) is: Michael Schroda (Schroda@mpimp-golm.mpg.de).

^{WIOA} Online version contains Web-only data.

^{Open Access} Open Access articles can be viewed online without a subscription. www.plantcell.org/cgi/doi/10.1105/tpc.111.085266

The heat shock response is regulated by evolutionarily conserved heat shock transcription factors (HSFs), which are activated by hyperphosphorylation and bind as trimers to cis-regulatory motifs known as heat shock elements (HSEs) (Sorger and Pelham, 1988; Sorger and Nelson, 1989). HSEs contain at least three 5'-nGAAn-3' repeats in alternating orientations and are present in the promoters of heat shock genes in a diverse set of organisms (Pelham, 1982). As deletion of HSEs from the *Chlamydomonas HSP70A* promoter entirely abolishes its heat shock inducibility, HSEs are also clearly indispensable for the regulation of the heat shock response in *Chlamydomonas* (Lodha et al., 2008). *Chlamydomonas* contains a single canonical HSF (HSF1), which possesses all features typical for plant (class A) HSFs and represents a key regulator of the stress response in this alga (Schulz-Raffelt et al., 2007). Like in the yeast *Saccharomyces cerevisiae* (but in contrast with the situation for other organisms), *Chlamydomonas* HSF1 forms trimers constitutively and becomes activated by hyperphosphorylation. The two heat shock genes investigated in this work are *HSP70A* and *HSP22F*. *HSP70A* encodes a cytosolic chaperone, which is constitutively expressed and further induced after heat shock (Müller et al., 1992). *HSP22F* encodes a small heat shock protein that is most likely targeted to the chloroplast (Schroda and Vallon, 2008) and only expressed under stress conditions like heat shock (this work).

The copper response regulator (CRR1) is the key regulator of copper homeostasis in *Chlamydomonas* as it mediates activation and repression of target genes of the copper response pathway. CRR1 contains a plant-specific DNA binding domain named SBP that recognizes defined copper response elements (CuREs) with a 5'-GTAC-3' core sequence. CRR1 binding to the CuREs within the *CYC6*, *CPX1*, and *CRD1* promoters leads to

transcriptional activation of these genes (Quinn and Merchant, 1995; Kropat et al., 2005; Sommer et al., 2010). The *CYC6* gene encodes cytochrome c6 (Merchant and Bogorad, 1986), which substitutes for the copper-containing plastocyanin in photosynthetic electron transport under copper deficiency conditions (Wood, 1978; Merchant and Bogorad, 1987). The *CPX1* gene encodes coprogen oxidase (Quinn et al., 1999), and the *copper response defect1* (*CRD1*) gene encodes a plastid-localized putative diiron protein that is required for the synthesis of protochlorophyllide (Moseley et al., 2000; Tottey et al., 2003). Hence, the *CPX1* and *CRD1* gene products both are involved in tetrapyrrole biosynthesis.

Chromatin structure is dictated in large part by posttranslational modifications of the unstructured N termini of histones (Luger, 2003; Kouzarides, 2007). Of the many known histone modifications, several are especially intensely studied because they are consistently associated with increased or reduced levels of transcription. These include acetylation of histone H3 at Lys-9 and -14, of histone H4 at Lys-5/8/12/16 and methylation of histone H3 at Lys-4 (Li et al., 2007).

Histone Lys acetylation is mediated by histone acetyltransferases, which in turn are recruited by transcription factors that bind to *cis*-regulatory elements on the underlying DNA (de la Cruz et al., 2005). Histone acetylation again may be recognized by proteins containing bromodomains (Owen et al., 2000) or tandem PHD fingers (Zeng et al., 2010) that may themselves be histone acetyltransferases, factors with ATP-dependent chromatin remodeling activity like SNF2 or Brahma, or components of chromatin remodeling complexes like CHRAC, SAGA, or RSC (Aalfs and Kingston, 2000).

Methyl marks are deposited by methyl-transferases that may, for example, be recruited by the Ser5-phosphorylated RNA polymerase II to target methylation of nucleosomes at the 5' ends of active genes (Krogan et al., 2003; Ng et al., 2003). Lys methylation is recognized by proteins containing chromodomains, WD40 repeats, or PHD fingers via aromatic cages, which allow discriminating between mono-, di-, and trimethylated lysines (Couture et al., 2006; Li et al., 2006; Ruthenburg et al., 2006). ING2 (inhibitor of growth) is an example of a protein that harbors a PHD finger that recognizes trimethylated Lys-4 at histone H3, which is typically present at promoters of highly transcribed genes (Peña et al., 2006). ING2 in turn may recruit the mSin3a-histone deacetylase complex to repress active genes in response to DNA damage (Shi et al., 2006).

With the goal of determining the relationship between chromatin state and transcriptional activation of heat shock and copper-regulated genes in *Chlamydomonas*, we monitored transcription factor binding, nucleosome occupancy, and levels of histone H3/4 acetylation and histone H3 Lys 4 (H3K4) mono- and dimethylation at heat shock and copper-regulated genes using chromatin immunoprecipitation (ChIP), while in parallel monitoring changes in RNA abundance by quantitative real-time RT-PCR (qRT-PCR). The gene encoding the small subunit of ribulose-1,5-bisphosphate carboxylase/oxygenase 2 (*RBCS2*) was included as control. We also used formaldehyde-assisted isolation of regulatory elements (FAIRE) (Giresi et al., 2007) to obtain additional information concerning the chromatin state under different environmental conditions. Combined, these

approaches provided us with insights into the underlying mechanisms of chromatin remodeling preceding transcriptional activation in *Chlamydomonas*.

RESULTS

HSF1 Is Required for Target Gene Activation by Heat Shock

To study the role of the HSF1 transcription factor in regulating chromatin structure at its target genes, we needed *hsf1* mutant strains. As a stable *hsf1* knockout mutant is not available, we generated strains that are downregulated for HSF1 using RNA interference (RNAi) and artificial microRNA (amiRNA) approaches as described previously (Schulz-Raffelt et al., 2007; Schmollinger et al., 2010). *HSF1*-RNAi and *HSF1*-amiRNA strains were both selected on the basis of thermosensitivity and therefore contained similarly low levels of residual HSF1 protein (Figure 1A; see Supplemental Figure 1A online). As expected, the downregulation of HSF1 strongly impaired but did not entirely abolish the transcription of HSF1 target genes under heat stress: compared with control strains, heat shock-induced transcript accumulation for *HSP70A*, *HSF1*, and *HSP22F* in these lines was reduced on average from ~6.5-fold to ~2.5-fold, ~16-fold to ~2.7-fold, and ~840-fold to ~6.6-fold, respectively (Figure 1B; see Supplemental Figure 1B online). Heat shock had no effect on the accumulation of *RBCS2* and *CYC6* transcripts in control and HSF1-underexpressing lines (Figure 1B).

HSF1 Binds to the Control Regions of the *HSP70A* and *HSP22F* Promoters

To characterize the interaction of HSF1 with its predicted target promoters, we performed ChIP assays on control and *HSF1*-RNAi/amiRNA lines with an affinity-purified polyclonal antiserum against HSF1 (Schulz-Raffelt et al., 2007; see Supplemental Figures 2A and 2B online). Reduced HSF1 accumulation in cells used for ChIP was verified prior to each experiment (Figure 1A). The amounts of precipitated DNA fragments from the *HSP70A*, *HSP22F*, *RBCS2*, and *CYC6* promoters were subsequently quantified by quantitative real-time PCR (qPCR); the amplified regions of the genes are summarized in Figure 2. The specificity of the ChIPs was verified by comparing signals obtained with antibodies against HSF1 with those obtained with antibodies against VIPP2 as a control (see Supplemental Figures 2C and 2D online). In control strains, under nonstress conditions, ChIP with HSF1 antibodies enriched the *HSP70A* and *HSP22F* promoter fragments ~3.4- and ~2-fold, respectively, compared with the *RBCS2* and *CYC6* promoters (Figure 3). Heat shock led to ~13.3- and ~8-fold enrichments of *HSP70A* and *HSP22F* promoter fragments, respectively, compared with *RBCS2* and *CYC6* promoters. Under nonstress conditions, ~1.6 times less *HSP70A* promoter fragments was precipitated from *HSF1*-RNAi/amiRNA strains compared with the control strain, while no change was observed in the amount of precipitated *HSP22F* promoter fragments. Under heat shock conditions, ~3-fold less *HSP70A* promoter fragments was precipitated in *HSF1*-RNAi/amiRNA strains compared with the control strain and enrichment

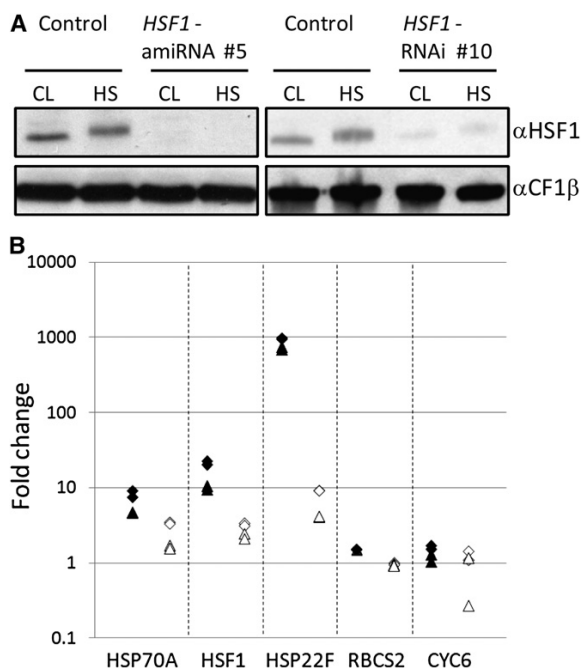


Figure 1. Analysis of Protein and Transcript Levels in HSF1-Under-expressing Strains Prior to ChIP Analysis.

(A) HSF1 abundance is reduced in *HSF1*-amiRNA and -RNAi strains. Control, *HSF1*-amiRNA, and *HSF1*-RNAi lines were kept under nonstress conditions (CL) or subjected to heat shock (HS) for 30 min. Whole-cell proteins were extracted, and proteins corresponding to 2 μ g chlorophyll were separated by SDS-PAGE and analyzed by immunoblotting using antisera against HSF1 and CF1 β (as loading control).

(B) Accumulation of selected transcripts in control and *HSF1*-RNAi/amiRNA cells. RNA was extracted from nonstressed cells and cells subjected to a 30-min heat shock for analysis by qRT-PCR using the comparative CT method with *CBLP2* as control gene. Primer efficiencies and qRT-PCR end products (amplicons) for all target transcripts are presented in Supplemental Figure 3 online. Shown are fold changes in transcript accumulation between stressed versus nonstressed conditions in control (black) and *HSF1*-RNAi/amiRNA lines (white), respectively. Three technical replicates each from *HSF1*-RNAi line #10 (triangles) and *HSF1*-amiRNA line #5 (diamonds) were performed.

of *HSP22F* promoter fragments was completely abolished. These data suggest that HSF1 constitutively binds to the *HSP70A* promoter, but not the *HSP22F* promoter, and that binding at both promoters increases \sim 4-fold during heat stress. Moreover, HSF1 appears to have a higher affinity for the *HSP70A* promoter than for the *HSP22F* promoter, as judged from the binding of residual HSF1 to *HSP70A* but not to *HSP22F* in *HSF1*-RNAi/amiRNA strains.

HSF1 Appears to Be Responsible for Nucleosome Remodeling

To analyze whether HSF1 affects nucleosome occupancy at its target promoters, we performed ChIP with antibodies against the

C terminus of core histone H3, which is known not to be modified. For a better comparability of biological replicates, we normalized values resulting from qPCR quantification of precipitated DNA fragments relative to those obtained for amplification of 10% input DNA and to the values obtained for the *CYC6* promoter. The *CYC6* promoter is inactive in the presence of copper (Quinn and Merchant, 1995), which explains why heat shock had no effect on mRNA expression, nucleosome occupancy, or histone modifications at *CYC6* (Figure 1B; see Supplemental Figures 4B and 5A online).

In nonstressed control cells, nucleosome occupancy at the heat shock gene promoters was 30 to 50% lower than at the *CYC6* promoter. Heat shock led to a further reduction of nucleosome occupancy by \sim 1.6-fold at the *HSP22F* promoter and by \sim 10-fold at the *HSP70A* promoter (Figure 4A; see Supplemental Figure 4A online). The latter result was consistent with the observation that much lower levels of *HSP70A* promoter fragments were precipitated with antibodies against modified histones from heat shock samples compared with nonstressed controls (see below). In the *HSF1*-RNAi/amiRNA strains, we observed the same \sim 10-fold reduction of nucleosome occupancy at the *HSP70A* promoter after heat shock as seen in the control strain, whereas the reduction of nucleosome occupancy at the *HSP22F* promoter was less pronounced. This suggested

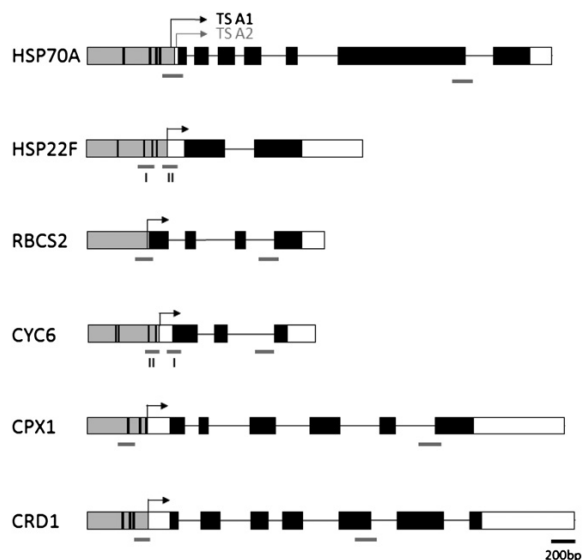


Figure 2. Regions Amplified from Chromatin Immunoprecipitates by qPCR.

Shown are the six genes investigated in this study. Promoter regions are indicated by gray boxes, transcriptional start sites (TS) by arrows, translated regions by black boxes, untranslated regions by white boxes, and introns by thin lines. The *HSP70A* promoter has two transcriptional start sites designated TSA1 and TSA2 (von Gromoff et al., 2006). Vertical black lines designate putative HSEs in the *HSP70A* and *HSP22F* promoter regions and putative CuREs in the *CYC6*, *CPX1*, and *CRD1* promoters. Gray bars designate the regions amplified by qPCR (if not indicated otherwise, region I was used by default for *HSP22F* and *CYC6*).

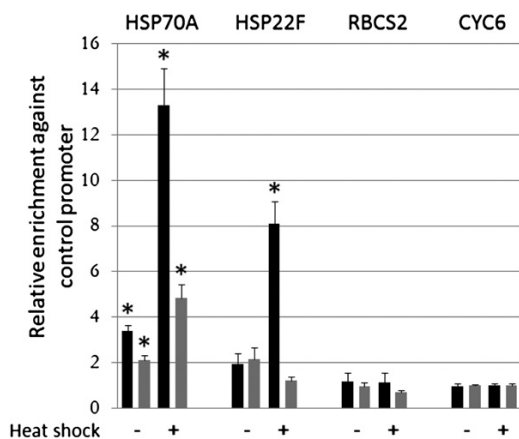


Figure 3. HSF1 Binds to Promoters *HSP70A* and *HSP22F*.

ChIP was done on control (black bars) and HSF1-underexpressing strains (gray bars) grown under nonstress conditions or subjected to a 30-min heat shock. From DNA fragments precipitated with α HSF1 antibodies the promoter regions shown in Figure 2 were amplified by qPCR. The enrichment relative to 10% input DNA was calculated and normalized to the values obtained for the *CYC6* promoter. Error bars indicate standard errors of the mean of two biological replicates, with each analyzed in triplicate. HSF1-underexpressing strains analyzed were *HSF1*-RNAi line #10 and *HSF1*-amiRNA line #5. Asterisks indicate the significance of change compared with the *CYC6* promoter in control cells under nonstress conditions (*t* test, *P* value \leq 0.01).

that HSF1 was to some extent responsible for reducing nucleosome occupancy at the *HSP22F* promoter. This may be true also for the *HSP70A* promoter but might be concealed by its higher affinity for HSF1, leading to binding of the residual HSF1 present in *HSF1*-RNAi/amiRNA strains (Figure 3).

Interestingly, nucleosome occupancy at the *RBCS2* promoter increased by \sim 20% after heat shock (Figure 4A). As this effect was observed equally in control and *HSF1*-RNAi/amiRNA strains, it appears to be independent of HSF1.

HSF1 Promotes Increased Levels of Histone H3/H4 Acetylation at Heat Shock Gene Promoters

The levels of histone H3 and H4 acetylation and the methylation state of Lys-4 (K4) at histone H3 are known to be crucial marks for the regulation of euchromatic genes. Hence, we wanted to determine whether HSF1 binding to the heat shock gene promoters influences levels of H3/4 acetylation and H3K4 mono- and dimethylation of local nucleosomes. We first performed ChIP analyses using antibodies against di-acetylated histone H3 and tetra-acetylated histone H4. We chose to generally express histone modifications (e.g., Figure 4B) relative to the abundance of nucleosomes at the DNA fragment investigated (Figure 4A) to account for variations in nucleosome occupancy.

Strikingly, in control cells, histone H3 was acetylated at \sim 14-fold higher levels at the *HSP70A* promoter than at the *CYC6* promoter (Figure 4B). Although the low nucleosome occupancy

of the *HSP70A* promoter during heat shock makes correct quantification of histone modifications difficult, H3 acetylation levels appeared to be equally high under nonstress and stress conditions. By contrast, histone H3 acetylation levels at the *HSP70A* promoter were \sim 35 to 50% lower in *HSF1*-RNAi/amiRNA strains under nonstress and stress conditions, thus pointing to a role of HSF1 in promoting histone H3 acetylation. In contrast with the *HSP70A* promoter, histone H3 acetylation levels at the *HSP22F* promoter under nonstress conditions were only slightly elevated when compared with the *CYC6* promoter. Levels of H3 acetylation at the *HSP22F* promoter were the same in control cells as in the *HSF1*-RNAi/amiRNA strains under nonstress conditions but increased more than 3-fold in the control strain following heat shock, while they did not increase at all in the *HSF1*-RNAi/amiRNA strains. Again, these results point to a role of HSF1 in promoting H3 acetylation at heat shock gene promoters. Histone H3 acetylation levels at the *RBCS2* promoter were \sim 4-fold higher than at the *CYC6* promoter and tended to decline during heat shock. As the effect was similar in control and *HSF1*-RNAi/amiRNA strains, it appears to be HSF1 independent.

ChIP analyses using antibodies against acetylated H4 yielded similar results. In control cells under nonstress conditions, histone H4 at the *HSP70A* promoter was acetylated at \sim 10-fold higher levels than histone H4 at the *CYC6* promoter (Figure 4C). Although difficult to assess accurately, levels of H4 acetylation of the few nucleosomes remaining on *HSP70A* promoter fragments tended to increase even more during heat shock. This tendency was not observed in *HSF1*-RNAi/amiRNA strains, thus suggesting a role of HSF1 also in promoting H4 acetylation. In control cells, histone H4 acetylation levels at the *HSP22F* promoter were \sim 2- and \sim 16-fold higher than at the *CYC6* promoter during nonstress and heat shock conditions, respectively (Figure 4C). By contrast, in *HSF1*-RNAi/amiRNA strains under nonstress conditions, H4 acetylation levels at the *HSP22F* promoter were as low as at the *CYC6* promoter, and during stress, they were only \sim 7-fold higher, supporting the conclusion that HSF1 is required for H4 acetylation at the heat shock gene promoters. Under nonstress conditions, histone H4 acetylation levels at the *RBCS2* promoter were even \sim 6-fold higher than at the *CYC6* promoter, but during heat shock dropped to the same low levels as at the *CYC6* promoter. Since this effect was observed in both control and *HSF1*-RNAi/amiRNA strains, it appears to be HSF1 independent.

Under nonstress conditions, histone H3K4 dimethylation levels at the *CYC6* and *HSP22F* promoters were comparable, whereas they were \sim 3- and \sim 8-fold lower at the *HSP70A* and *RBCS2* promoters than at *CYC6*, respectively (Figure 4D). Heat shock appeared to result in an \sim 2.7-fold increase in H3K4 dimethylation levels at the *HSP70A* promoter; however, given the low nucleosome occupancy at the *HSP70A* promoter during heat shock, this observation may not be meaningful. In control cells, H3K4 monomethylation levels were comparable at promoters *CYC6*, *HSP22F*, and *RBCS2* under nonstress and heat shock conditions (Figure 4E). By contrast, H3K4 monomethylation was \sim 6-fold lower at the *HSP70A* promoter than at *CYC6* under nonstress conditions but seemed to increase \sim 4-fold during heat shock. As for dimethylation of H3K4, this result might not be

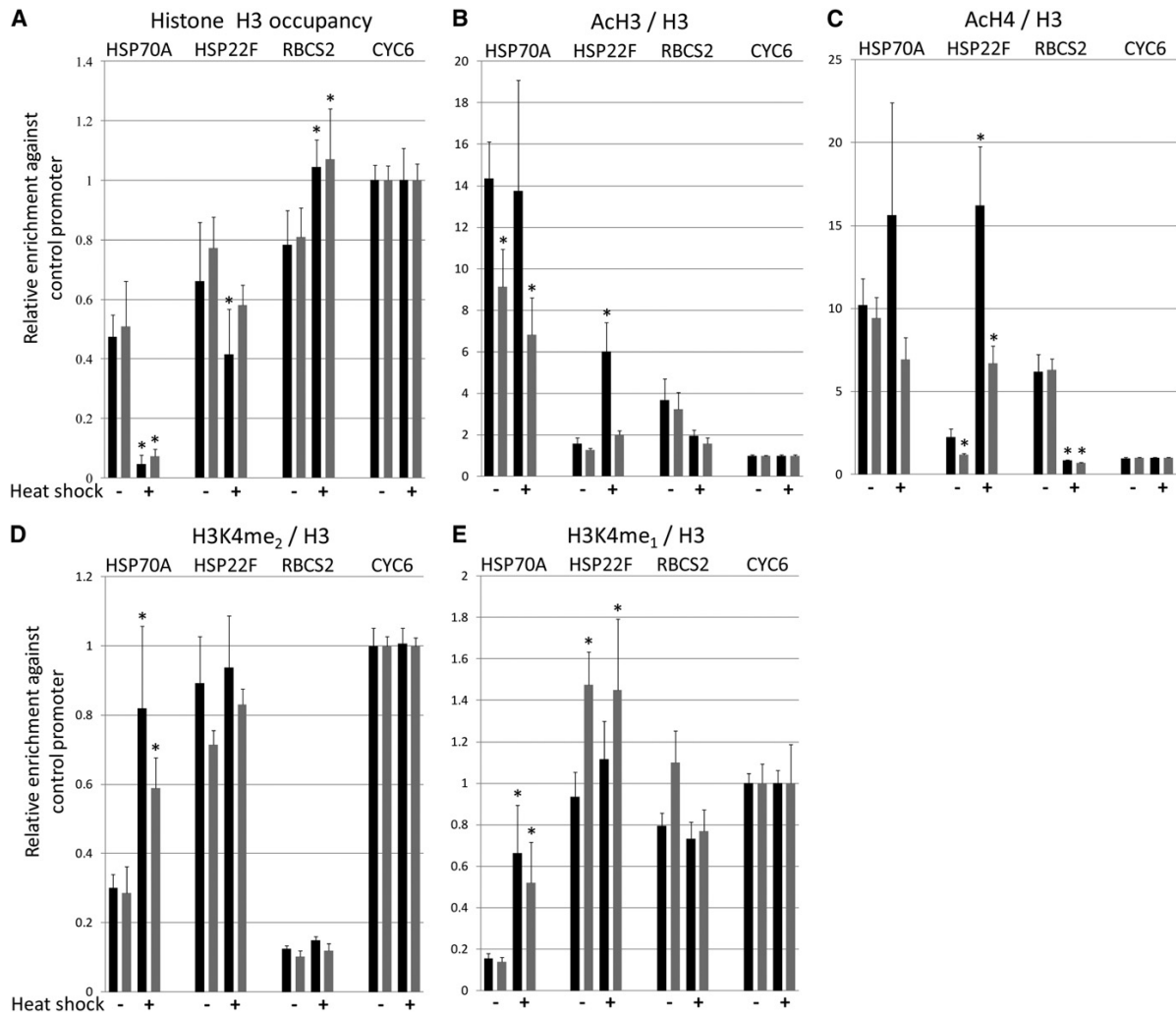


Figure 4. Analysis of Nucleosome Occupancy and Histone Modifications at Heat Shock-Responsive and Control Promoters.

(A) Nucleosome occupancy declines at heat shock gene promoters after heat shock. ChIP was done as described in Figure 3 but using antibodies against the unmodified C terminus of histone H3 to determine nucleosome occupancy at the indicated promoters in control (black bars) and HSF1-underexpressing strains (gray bars).

(B) HSF1 promotes acetylation of histone H3 at the *HSP70A* and *HSP22F* promoters. ChIP was done using antibodies against acetylated Lys-9 and -14 of histone H3.

(C) HSF1 promotes acetylation of histone H4 at the *HSP22F* promoter. ChIP was done using antibodies against acetylated Lys-5, -8, -12, and -16 of histone H4.

(D) HSF1 has no effect on histone H3 dimethylation at the heat shock gene promoters. ChIP was done using antibodies against dimethylated Lys-4 at histone 3 (H3K4).

(E) HSF1 might reduce histone H3 monomethylation at the *HSP22F* promoter. ChIP was done using antibodies against monomethylated Lys-4 at histone 3 (H3K4).

qPCR data from the experiments in **(B)** to **(E)** are given relative to the nucleosome occupancy at the respective promoter region (data from **(A)**). Error bars indicate standard errors of the mean of two biological replicates, with each analyzed in triplicate. Asterisks indicate the significance of change at the respective promoter compared with control cells under nonstress conditions (*t* test, *P* value ≤ 0.05).

meaningful because few nucleosomes remain on *HSP70A* promoter fragments under heat shock conditions. While the same patterns of H3K4 dimethylation were observed in control and *HSF1*-RNAi/amiRNA strains and therefore appeared not to depend on HSF1, levels of H3K4 monomethylation were higher at the *HSP22F* promoter under nonstress and stress conditions in the *hsf1* mutant compared with control cells. This suggests that HSF1 might be responsible for the reduced levels of monomethylation at the *HSP22F* promoter.

HSF1 Binding at the *HSP22F* Promoter Precedes Histone Acetylation/Eviction and Transcriptional Activation

To gain mechanistic insights into how transcriptional activation by HSF1 is mediated in *Chlamydomonas*, it is necessary to resolve when exactly after onset of heat stress the processes of transcription factor binding, histone modification, histone eviction, and transcription take place. Under nonstress conditions, the *HSP22F* gene is not transcribed, HSF1 does not bind to the promoter, nucleosome occupancy is relatively high, and histones H3 and H4 contain low levels of acetylation (Figures 3 and 4; see Supplemental Figure 2D online). Hence, the *HSP22F* gene appears to be an ideal target to study the sequence of events leading to transcriptional activation by heat stress. To this end, we performed a time-course analysis of HSF1 binding, histone occupancy, and histone H3/4 acetylation at the *HSP22F* promoter and of *HSP22F* mRNA accumulation within the first 10 min after exposing control cells to heat stress. This analysis revealed that occupation of the *HSP22F* promoter by HSF1 is detectable already 30 s after the onset of heat shock, which correlates with an ~2-fold increase in levels of histone H4 acetylation (Figure 5). Within 60 s after onset of heat stress, HSF1 has already reached ~30% of its maximal occupancy at the *HSP22F* promoter and acetylation levels of histones H3 and H4 have increased ~2- and ~5.6-fold, respectively, which coincides with a reduction of histone occupancy by ~35%. Note that almost identical results were obtained when a region located at the *HSP22F* transcriptional start site rather than at the HSEs was amplified from chromatin precipitates (region II of *HSP22F* in Figure 2; see Supplemental Figure 6A online). As a strong increase in *HSP22F* transcript levels was detected only 2 min after onset of heat stress, nucleosome remodeling at the *HSP22F* promoter is more likely a prerequisite for rather than a consequence of transcription.

Nucleosome Remodeling at Promoters of Copper-Responsive Genes Depends on CRR1

To elucidate whether our results from HSF1-mediated chromatin remodeling at heat shock promoters can more generally be applied to other *Chlamydomonas* promoters responsive to changes in environmental conditions, we extended our studies to the copper response. In contrast with the situation for HSF1, a mutant harboring a stable knockout of the gene encoding the key regulator of copper homeostasis, CRR1, is available (Eriksson et al., 2004). As expected, the induction of CRR1 target genes *CYC6*, *CPX1*, and *CRD1* after copper depletion was entirely abolished in the *crr1* knockout mutant (Figure 6), hence corroborating the results reported previously by Kropat et al. (2005). The

variation in CRR1 target gene expression levels in control (*CRR1*⁺) cells under copper-depleted conditions is due to slight variations in residual copper ion concentrations in the cell cultures.

As we were not able to immunoprecipitate native or green fluorescent protein-tagged CRR1, we could not directly test for preloading of copper-responsive promoters by CRR1. Hence, we had to limit our analysis to the investigation of nucleosome occupancy and histone modifications in control and *crr1* mutant strains under copper-replete and copper deprivation conditions. This time, we normalized qPCR quantification values relative to those obtained for the *RBCS2* promoter, whose associated expression levels, nucleosome occupancy, and histone modifications remained unaffected by copper starvation (see Supplemental Figure 5B online). In control and *crr1* mutant cells, nucleosome occupancy under copper-replete conditions was similar between the *CYC6* and *RBCS2* promoters, whereas it was 40 to 60% lower at the *CPX1* and *CRD1* promoters (Figure 7A). In control cells, copper depletion led to a 1.3- to 2-fold reduction of nucleosome occupancy at the *CYC6*, *CPX1*, and *CRD1* promoters, whereas no such effect was observed in *crr1* mutant cells. These results suggest that, similar to what was observed for HSF1 at the *HSP22F* promoter, CRR1 appeared to be responsible for reducing nucleosome occupancy at copper-responsive promoters.

CRR1 Promotes Higher Levels of Histone H3/H4 Acetylation and Lower Levels of H3K4 Mono- and Dimethylation at the *CYC6* and *CPX1* Promoters

We next asked whether CRR1, like HSF1, promotes histone acetylation at its target promoters. As shown in Figure 7B, this is indeed the case for some targets: in control cells, after copper depletion, H3 acetylation increased at the *CYC6* and *CPX1* promoters by factors of ~4 and ~1.6, respectively, whereas this effect was not observed in the *crr1* mutant. No changes in histone H3 acetylation levels were observed at the *CRD1* promoter. Interestingly, under copper-replete conditions, H3 acetylation levels were ~2-fold lower at the *CYC6* promoter than at the *RBCS2* promoter, whereas they were ~1.5- and 2.5-fold higher at the *CPX1* and the *CRD1* promoters, respectively, than at *RBCS2*.

A similar picture was obtained for H4 acetylation. Here, under copper-replete conditions, acetylation levels at the *CYC6* and *CPX1* promoters were ~6- and ~3-fold lower, respectively, than at the *RBCS2* promoter. After copper depletion, however, H4 acetylation at *CYC6* and *CPX1* increased more than 8-fold relative to copper-replete conditions (Figure 7C). This effect was not observed in the *crr1* mutant, indicating that H4 acetylation of nucleosomes at the *CYC6* and *CPX1* gene promoters is mediated by the CRR1 transcription factor. Histone H4 acetylation at the *CRD1* promoter was independent of both copper availability and CRR1: in all strains and under all conditions tested, it was ~2.5-fold higher than at the *RBCS2* promoter.

To get an estimate on how much the region that was chosen within the target promoter for amplification from chromatin immunoprecipitates influenced the results, we analyzed nucleosome occupancy and H3/4 acetylation at a different region of the *CYC6* promoter in control and *crr1* mutant cells under

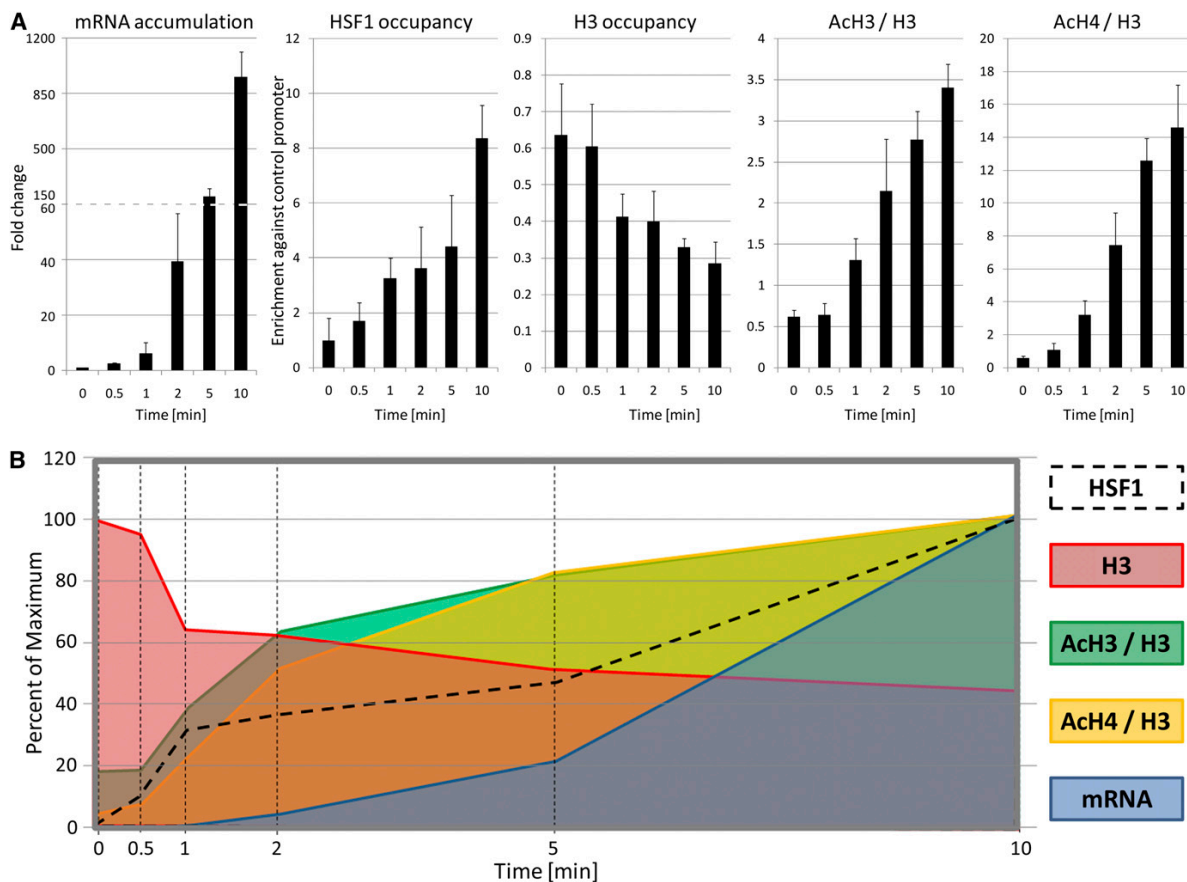


Figure 5. Analysis of the Sequence of Events at the *HSP22F* Promoter within the First 10 min after Onset of Heat Stress.

(A) HSF1 binding precedes chromatin remodeling and transcription. Control cells were subjected to heat stress, and samples for RNA extraction and ChIP were taken immediately prior to the temperature shift and at the indicated time points after shift from 25 to 40°C. *HSP22F* mRNA levels were quantified by qRT-PCR as described in Figure 1B. Shown are fold changes in transcript accumulation relative to the nonstressed state. Values derive from two biological replicates, with each analyzed in triplicate. ChIP was done as described in Figure 3, again amplifying region I of the *HSP22F* promoter (Figure 2). The enrichment relative to 10% input DNA was calculated and normalized to the values obtained for the *CYC6* promoter. Error bars indicate standard errors of two biological replicates, each analyzed in triplicate.

(B) Graphical overview of the sequence of events at the *HSP22F* promoter after onset of heat stress. The data from **(A)** are given as percentage of the respective maximal values.

copper-replete conditions and after copper depletion (region II of the *CYC6* promoter in Figure 2). While histone occupancy was ~1.7-fold higher within the *CYC6* 5' untranslated region (region I) than at the relevant copper-responsive elements (region II), CRR1-dependent reduction in nucleosome occupancy and relative increases in H3/4 acetylation were the same at both regions (see Supplemental Figure 6B online). Combined with the results obtained for the two different regions analyzed within the *HSP22F* promoter (Figure 2; see Supplemental Figure 6A online), these data indicate that the chromatin state at the actual promoter regions appears to spread into the flanking regions.

Under copper-replete conditions, the *CYC6* and *CPX1* promoters are associated with 7- to 8-fold higher levels of histone

H3K4 dimethylation than the *RBCS2* promoter, and the *CRD1* promoter possesses ~2.5-fold higher levels than *RBCS2* (Figure 7D). At the *CYC6* and *CPX1* promoters, H3K4 dimethylation levels decreased ~2-fold in response to copper depletion. This effect was not as pronounced in the *crr1* mutant, suggesting a role for the CRR1 transcription factor in mediating remodeling of the dimethylation mark. H3K4 dimethylation levels at the *CRD1* promoter were the same regardless of copper or CRR1 availability.

Under copper-replete conditions, levels of histone H3K4 monomethylation were ~2.5-fold higher at the *CYC6* promoter than at the *RBCS2* promoter but ~2-fold lower at the *CPX1* and *CRD1* promoters than at *RBCS2* (Figure 7E). Interestingly, in

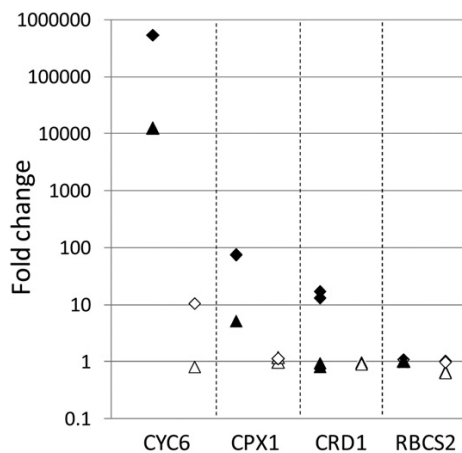


Figure 6. Accumulation of Selected Transcripts in Control and *crr1* Mutant Cells.

Transcript accumulation in copper-replete versus copper-depleted control (black) and *crr1* mutant cells (white) was assessed by qRT-PCR as described in Figure 1B. Values shown are from two biological replicates (triangles and diamonds), each analyzed in triplicate.

response to copper depletion, H3K4 monomethylation levels decreased by a factor of ~ 10 at the *CYC6* promoter and by a factor of ~ 2 at the *CPX1* and *CRD1* promoters. These effects were largely abolished in the *crr1* mutant, suggesting that CRR1 also plays a role in remodeling of the H3K4 monomethylation mark.

FAIRE Analysis Indicates That Transcription Factor-Mediated Chromatin Remodeling Occurs at Target Promoters

Our ChIP results suggest that the HSF1 and CRR1 transcription factors under inducing conditions mediate chromatin remodeling toward an open chromatin structure at the heat shock and copper-responsive promoters, respectively. To test this conclusion using a second assay, we employed the FAIRE technique. FAIRE is a non-antibody-based method that involves formaldehyde cross-linking of DNA-protein complexes and that enriches for DNA fragments that correspond to regions of open chromatin structure (Giresi et al., 2007).

As shown in Figure 8A, ~ 2.5 times more *HSP70A* than *HSP22F* promoter fragments were enriched by FAIRE (relative to input DNA) in nonstressed cells, indicating that the *HSP70A* promoter is constitutively in a more open conformation than the *HSP22F* promoter. Furthermore, enrichment of *HSP70A* and *HSP22F* promoter fragments was ~ 1.5 - and ~ 2 -fold greater, respectively, for control cells subjected to heat shock relative to nonstressed cells, while there was no enrichment for *HSP22F* promoter fragments in heat-shocked *HSF1*-amiRNA cells, relative to nonstressed cells. Interestingly, in control and *crr1* mutant cells grown under copper-replete conditions, roughly the same quantity of *CYC6*, *CPX1*, and *CRD1* promoter fragments were enriched by FAIRE (Figure 8B), and these amounts were comparable to

those obtained for the inactive *HSP22F* promoter (Figure 8A). Copper depletion led to a 1.6- to 2-fold increase in FAIRE-enriched fragments of the *CYC6*, *CPX1*, and *CRD1* promoters, but there was no enrichment of these promoter fragments in *crr1* mutant cells (Figure 8B). When compared with ChIP, FAIRE indicated a more pronounced opening of chromatin structure at the *CRD1* promoter in copper-depleted control cells (cf. Figures 7A and 8B). This might be explained by the comparably low sensitivity of the *CRD1* gene to copper depletion (Figure 6), which might prevent a clearer detection of changes in nucleosome occupancy. Overall, the data obtained from these FAIRE experiments corroborate the ChIP results reported above, namely, that HSF1 and CRR1 transcription factors mediate chromatin remodeling at their target promoters.

Gene-Wide Analysis of the Distribution of Chromatin Marks

To gain insights into general aspects of chromatin organization in *Chlamydomonas*, we compared the distribution of chromatin marks throughout representative parts of the six genes analyzed in this study, including promoter, transcribed, and two intergenic regions (see Figure 2 for promoter and transcribed regions assayed). As a general trend, we observed lower histone occupancy, higher levels of histone H3/4 acetylation, and lower levels of H3K4 monomethylation at promoter regions of active genes compared with levels at inactive promoters and at transcribed and intergenic regions (Figure 9). H3K4 monomethylation appears to be particularly high in the 3' region of actively transcribed genes. No distinct pattern was observed for H3K4 dimethylation, except for a potential enrichment in promoter regions of inactive genes.

DISCUSSION

We employed the ChIP and FAIRE techniques to study how transcription factors affect chromatin structure to regulate the expression of target genes in response to changes in environmental conditions in *Chlamydomonas*. We focused our analysis on five genes of the heat shock and copper response pathways that in *Chlamydomonas* are regulated by the HSF1 and CRR1 transcription factors, respectively. Our results, summarized in Figure 10, reveal that both transcription factors regulate the expression of these genes via conserved mechanisms involving histone acetylation, histone methylation, nucleosome eviction, and polymerase loading/activation. However, at each target promoter, these means are employed quite individually to establish a characteristic chromatin state, presumably to allow for a fine-tuning of gene expression that meets the requirements of the respective environmental condition.

Preloading of Transcription Factors

ChIP assays using antibodies against HSF1 revealed that HSF1 constitutively binds the *HSP70A* promoter and that the association increased ~ 4 -fold after heat shock (Figures 3 and 10; see Supplemental Figure 2D online). This finding is in line with previous findings showing that constitutive hypersensitive sites exist at the HSE1/TATA box and HSE4 within the *HSP70A*

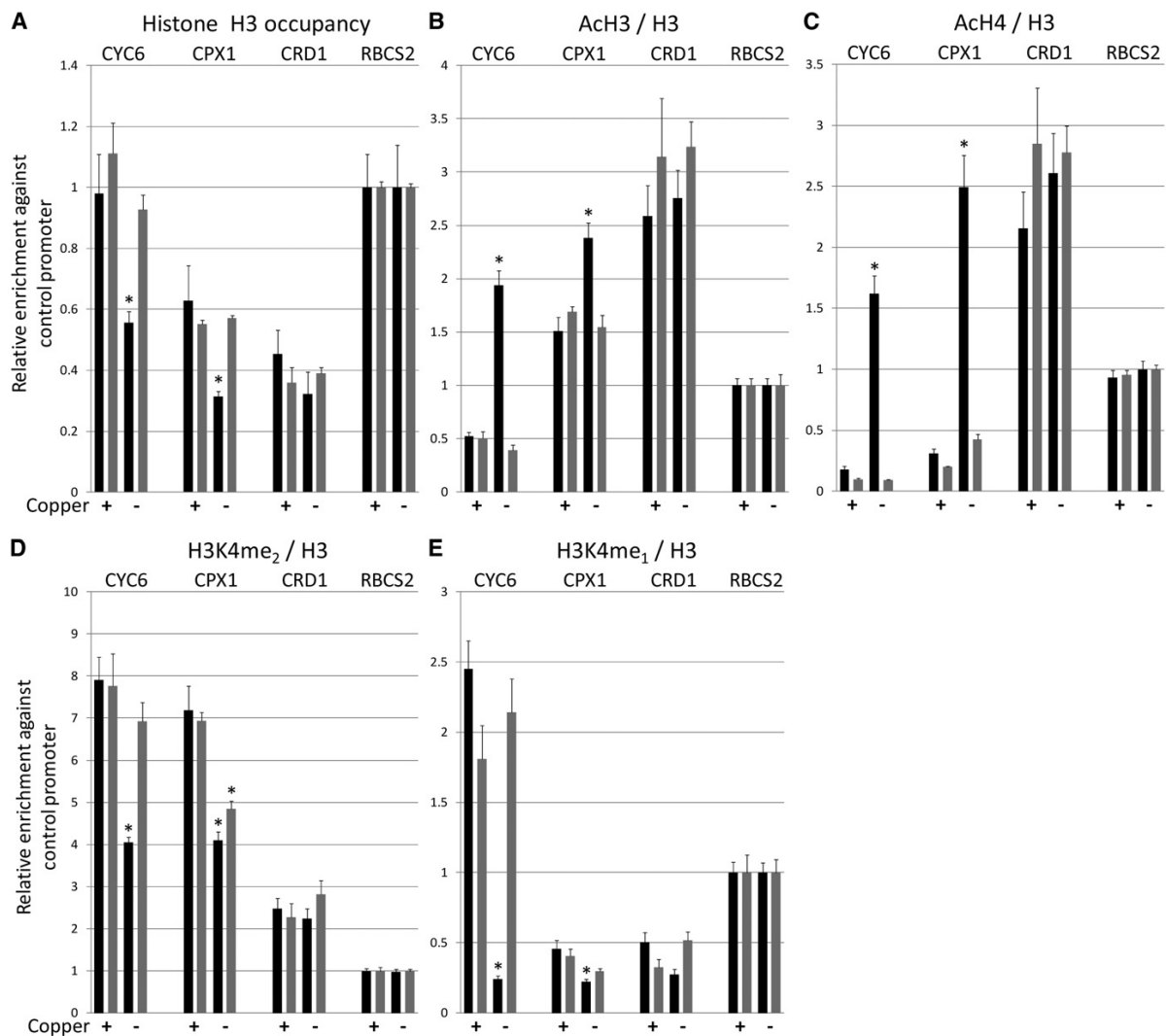


Figure 7. Analysis of Nucleosome Occupancy and Histone Modifications at Copper-Responsive and Control Promoters.

(A) Nucleosome occupancy declines at copper-responsive gene promoters under copper depletion. ChIP was done on control (black bars) and *crr1* knockout cells (gray bars) grown under copper-replete or copper deprivation conditions. From DNA fragments precipitated with antibodies against the unmodified C terminus of histone H3, the promoter regions shown in Figure 2 were amplified by qPCR. The enrichment relative to 10% input DNA was calculated and normalized to the values obtained for the *RBCS2* promoter. Error bars indicate standard errors of two biological replicates, each analyzed in triplicate.

(B) CRR1 promotes histone H3 acetylation at the *CYC6* and *CPX1* promoters after copper depletion. ChIP was done using antibodies against acetylated Lys-9 and -14 of histone H3.

(C) CRR1 promotes histone H4 acetylation at the *CYC6* and *CPX1* promoters after copper depletion. ChIP was done using antibodies against acetylated Lys-5, -8, -12, and -16 of histone H4.

(D) CRR1 promotes reduction of H3K4 dimethylation at promoters *CYC6* and *CPX1* after copper depletion. ChIP was done using antibodies against dimethylation of Lys-4 at histone H3 (H3K4).

(E) CRR1 promotes reduction of H3K4 monomethylation at promoters *CYC6* and *CPX1* after copper depletion. ChIP was done using antibodies against monomethylation of Lys-4 at histone H3 (H3K4).

qPCR data from the experiments in **(B)** to **(E)** are given relative to the nucleosome occupancy at the respective promoter region (data from **(A)**). Asterisks indicate the significance of change at the respective promoter compared with control cells under copper replete conditions (*t* test, *P* value \leq 0.01).

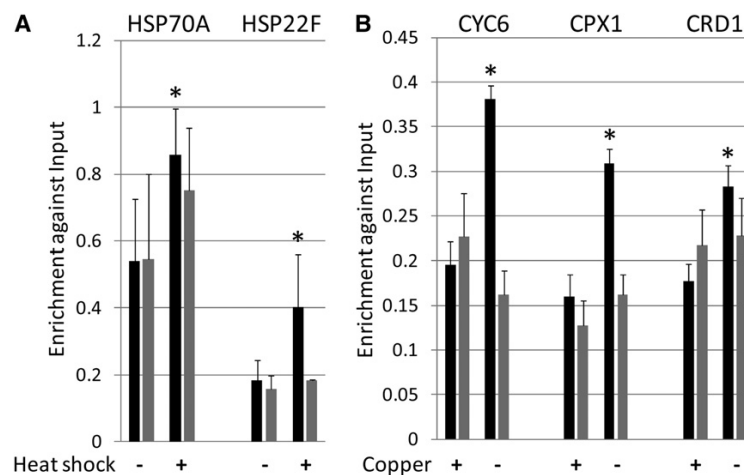


Figure 8. FAIRE Indicates Chromatin Remodeling after Transcriptional Activation.

(A) Nucleosome occupancy declines at heat shock gene promoters after heat shock. FAIRE was performed with control (black bars) and HSF1-underexpressing cells (gray bars) grown under nonstress conditions or subjected to a 30-min heat shock. DNA fragments present in the supernatant after phenol/chloroform extraction of formaldehyde-cross-linked chromatin were precipitated, and the promoter regions of *HSP70A* and *HSP22F* (Figure 2) were amplified by qPCR. The enrichment relative to input DNA, after reversion of the cross-link, was calculated. Error bars indicate standard errors from two biological replicates, each analyzed in duplicate. Asterisks indicate the significance of change at the respective promoter compared with control cells under nonstress conditions (t test, P value ≤ 0.05).

(B) Nucleosome occupancy declines at the *CYC6* promoter after copper depletion. FAIRE was performed with control and *crr1* knockout cells grown in the presence or absence of copper. qPCR analyses were done as in **(A)**. Asterisks indicate the significance of change at the respective promoter compared with control cells under copper replete conditions (t test, P value ≤ 0.01).

promoter (Lodha and Schroda, 2005). Constitutive binding to heat shock gene promoters was reported for yeast HSF1, but not for human, fly, or plant HSFs (Sorger et al., 1987; Zhang et al., 2003; Erkina and Erkine, 2006; Kodama et al., 2007). This discrepancy is presumably related to the fact that like yeast HSF1, *Chlamydomonas* HSF1 is constitutively trimeric, but HSF1 trimerization is induced only under stress conditions in higher plants, flies, and humans (Sorger and Nelson, 1989; Rabindran et al., 1993; Lee et al., 1995; Schulz-Raffelt et al., 2007). While HSF1 preloading was evident at the *HSP70A* promoter, little or none was observed at the *HSP22F* promoter (Figures 3, 5, and 10; see Supplemental Figure 2D online). Similar observations were made in yeast, where preloading was observed at the *HSP82* and *SSA4* promoters but not at the *HSP12* promoter (Erkina and Erkine, 2006; Erkina et al., 2010). Apparently, it may be a widespread phenomenon that HSFs occupy small heat shock gene promoters only after stress (Erkina and Erkine, 2006; Kodama et al., 2007), and this generalization correlates well with the expression of many *sHSP* genes only under stress conditions (Haslbeck, 2002).

In the absence of a functional antibody against CRR1, we could not perform ChIP experiments to analyze whether CRR1 binds to its target promoters also in the presence of copper. However, as ChIP and FAIRE analyses revealed no striking differences between the chromatin states of noninduced control and *crr1* mutant strains (Figures 7 and 8), it appears more likely that CRR1 is not preloaded to its target promoters in the presence of copper.

Constitutive versus Inducible Histone Modification

We observed constitutively high levels of histone H3 and H4 acetylation at the *HSP70A* and *CRD1* promoters (Figures 4B, 4C, 7B, 7C, and 10). In HSF1-underexpressing strains, constitutive H3 acetylation at the *HSP70A* promoter was lower and therefore appears to be mediated by preloaded HSF1. On the contrary, as H3/4 acetylation levels at the *CRD1* promoter were constitutively high in control and *crr1* mutant cells, they must be mediated by an activator distinct from CRR1. In contrast with the *HSP70A* and *CRD1* promoters, the *HSP22F*, *CYC6*, and *CPX1* promoters had low levels of H3 and particularly H4 acetylation under noninducing conditions. However, levels of acetylation increased under heat shock (*HSP22F*) or copper deprivation (*CYC6* and *CPX1*) conditions. Inducible H3/4 acetylation at these promoters appears to be mediated by HSF1 and CRR1, as it was reduced or abolished in the respective mutant strains (Figures 4B, 4C, 7B, 7C, and 10; see Supplemental Figure 6B online). A direct role for HSF1 in mediating histone acetylation at target promoters has also been demonstrated in yeast by the use of strains carrying a mutated HSE (Zhao et al., 2005) or expressing an HSF1 variant without transactivation domain (Erkina and Erkine, 2006). Good candidates for coactivators of *Chlamydomonas* HSF1 with histone acetylase activity are homologs of the yeast NuA4 and SAGA complexes that, following heat shock, have been shown to rapidly enrich at HSF1-dependent heat shock gene promoters (Reid et al., 2000; Robert et al., 2004; Kremer and Gross, 2009). In contrast with *Chlamydomonas*, it is not clear whether preloaded HSF1 also drives constitutive histone acetylation in yeast.

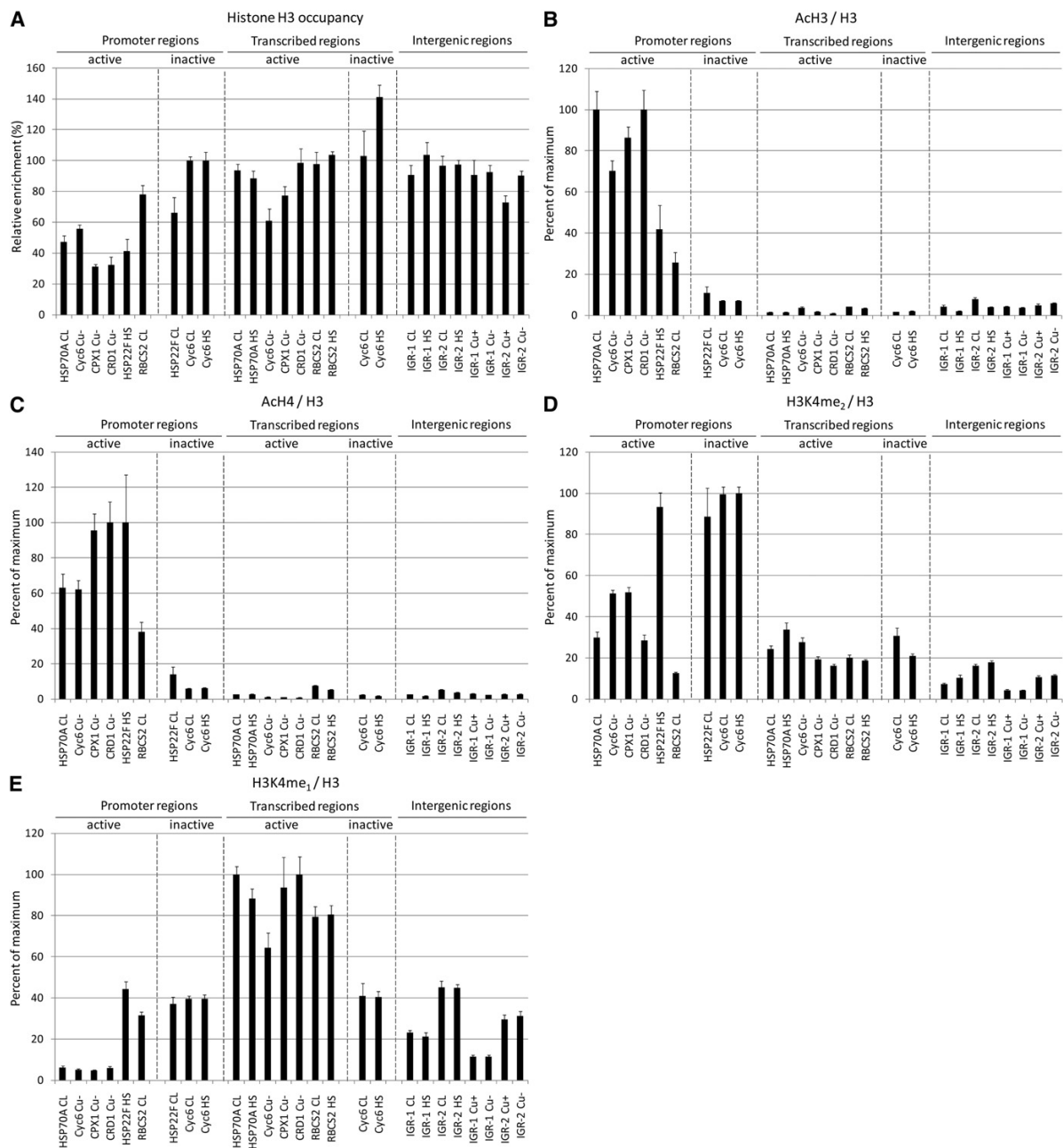


Figure 9. Gene-Wide Overview of the Relative Abundance of Histone Occupancy and Modifications.

ChIP was done on control cells grown under the following conditions: nonstress in copper-replete medium (CL or Cu+), 30 min heat shock (HS), and medium depleted from copper (Cu-). ChIP was done using antibodies against the unmodified C terminus of histone H3 (A), acetylated Lys-9 and -14 of histone H3 (B), acetylated Lys-5, -8, -12, and -16 of histone H4 (C), dimethylation of Lys-4 at histone H3 (H3K4me₂) (D), and monomethylation of Lys-4 at histone H3 (H3K4me₁) (E). Fragments corresponding to transcribed regions shown in Figure 2 and intergenic regions separating genes *au5.g14265_t1/P23* (IGR-1) and *RBCS2/au5.g9204_t1* (IGR-2) were amplified by qPCR. The enrichment relative to 10% input DNA was calculated and normalized to the values obtained for the *CYC6* promoter (heat stress experiments) or the *RBCS2* promoter (copper depletion experiments). The data on the promoter regions correspond to that shown in Figures 4 and 7. In case of ChIP analysis with antibodies against modified histones, an additional

A remarkable property of the *HSP70A* promoter is that in a transgene setting it strongly increases the likelihood that a promoter fused downstream becomes active (Schroda et al., 2000, 2002). This effect is dependent on the presence of HSEs within the *HSP70A* promoter, suggesting that it is mediated by HSFs (Lodha et al., 2008). As the constitutively high acetylation levels at the *HSP70A* promoter depend on HSF1, it is tempting to speculate that in the transgene setting the activation of downstream promoters is mediated by histone acetyltransferase activities recruited by HSF1. In turn, the constitutively high acetylation levels at the *CRD1* promoter suggest that like the *HSP70A* promoter it may also be capable of activating neighboring transgenic promoters.

Levels of H3K4 mono- and dimethylation declined in a CRR1-dependent manner at the *CYC6*, *CPX1*, and *CRD1* promoters (Figures 7D, 7E, and 10). Hence, CRR1 appears to recruit histone demethylase activities to its target promoters. Alternatively, CRR1 may recruit histone methyltransferase activities that convert mono- and dimethylated H3 to the trimethylated state. As H3K4 monomethylation in *Chlamydomonas* was shown to be linked to inactive chromatin (van Dijk et al., 2005) and H3K4 trimethylation is widely accepted as a typical mark of active euchromatin (Lachner and Jenuwein, 2002; Santos-Rosa et al., 2002), we favor the latter scenario. In contrast with the copper-responsive promoters, induction of the *HSP22F* promoter was not accompanied with a decline of H3K4 mono- and dimethylation levels (because of the low nucleosome occupancy at the *HSP70A* promoter after heat shock, we cannot draw any conclusions on the methylation state of nucleosomes at that promoter) (Figures 4D, 4E, and 10). In contrast with growth under copper-deficient conditions, cells experienced heat shock only for 30 min. Hence, it is possible that remodeling of the H3K4 methylation state proceeds more slowly than that of the H3/4 acetylation state. In consequence, the acetylation state of a nucleosome appears to be directly connected with promoter activation, while the H3K4 methylation state, as suggested previously (Ng et al., 2003), may serve a memory function to mark promoters that have been active for a certain time. Accordingly, yeast mutants defective in the Set1 and Set2 methyltransferases, catalyzing methylation of histones H3K4 and H3K36, respectively, were hardly impaired in the transcriptional output of the *HSP82* gene (Kremer and Gross, 2009).

Nucleosome Displacement by Activated HSF1 and CRR1 Transcription Factors

Both ChIP and FAIRE analyses revealed that during copper starvation and heat shock, histone occupancy at the copper-responsive promoters and at the *HSP22F* promoter declined in a CRR1- and HSF1-dependent manner, respectively (Figures 4A, 7A, 8, and 10; see Supplemental Figure 6 online). As there is a

good correlation between high levels of histone H3/4 acetylation and histone loss at these promoters, it appears that binding of activated CRR1 or HSF1 mediates histone acetylation, thus facilitating histone eviction. This conclusion is supported by a time-course experiment, where HSF1 binding, nucleosome occupancy, H3/4 acetylation, and transcription from the *HSP22F* promoter were monitored within the first 10 min after exposure of cells to heat stress (Figure 5; see Supplemental Figure 6A online). The results indicate the following sequence of events: within the first 30 s after onset of heat stress, HSF1 is activated, binds to the *HSP22F* promoter, and already mediates acetylation of histone H4. Within 60 s after temperature shift, acetylation of H3 and H4 strongly increases, which coincides with nucleosome eviction. Higher levels of *HSP22F* transcripts are detected only 2 min after onset of heat stress, thus indicating that chromatin remodeling at the *HSP22F* promoter most likely is a prerequisite and not a consequence of transcription. Our data agree very well with observations made at the yeast *HSP82* promoter: there, nucleosome occupancy declines drastically within the first 60 s after onset of heat stress and is preceded by a burst of acetylation of histones H2A, H3, and H4 (Zhao et al., 2005). A correlation between histone acetylation and nucleosome loss was demonstrated previously also at the yeast *PHO5*, *SSA4*, and *HSP12* promoters (Reinke and Hörz, 2003; Erkina and Erkinen, 2006), at the viral *HTLV-1* promoter in human cells (Sharma and Nyborg, 2008), or at the *Arabidopsis thaliana HSP18.2* promoter (Kodama et al., 2007).

However, we observed that high levels of histone acetylation do not necessarily always correlate with low histone occupancy. For example, H3/4 acetylation levels under nonstress conditions were higher at the *RBCS2* promoter than at the *HSP22F* promoter, but nucleosome occupancy at *HSP22F* was lower than at *RBCS2* (Figures 4A to 4C). Moreover, levels of H3 acetylation at the *HSP70A* promoter were lower in HSF1-underexpressing strains than in the control strain, but these lower acetylation levels were not accompanied by reduced nucleosome occupancy.

Interestingly, the most dramatic nucleosome loss among the promoters studied here, as detected by ChIP and FAIRE, was observed at the *HSP70A* promoter during heat shock (Figures 4A, 8A, and 10). This loss appeared to be HSF1 independent but also may have been mediated by residual HSF1 in HSF1-underexpressing cells (Figure 3). The evidence for strong chromatin remodeling at the *HSP70A* promoter during heat shock, which was obtained by both ChIP and FAIRE experiments, corroborates previous results obtained from micrococcal nuclease digestion studies (Lodha and Schroda, 2005). In that set of experiments, the *HSP70A* promoter under nonstress conditions was found to be embedded into a nucleosome array, which was strongly perturbed by heat shock.

Figure 9. (continued).

normalization was necessary due to different levels of modification within control promoters (*RBCS2* and *CYC6*) that lead to different absolute values between the copper starvation response data set and the heat shock data set. Therefore, the maximum value of each data set was set to 100%. Error bars indicate standard errors of the mean of two biological replicates, each analyzed in triplicate.

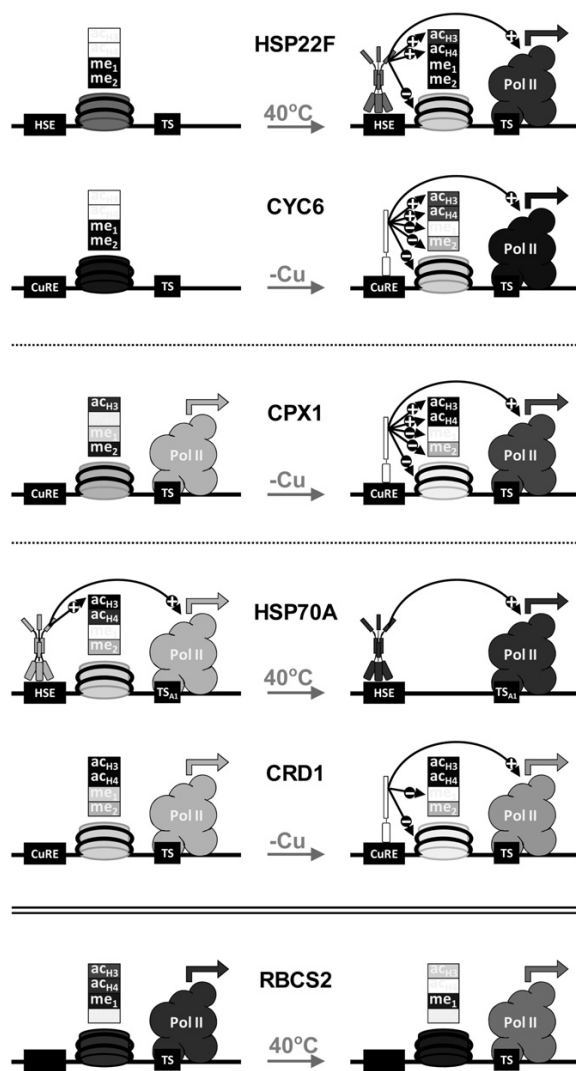


Figure 10. Schematic Description of How Transcription Factors Affect Chromatin State and Activity of the Promoters Studied.

Promoters are schematically depicted by a transcription factor binding site, one nucleosome, and the transcriptional start site (TS). Histone modifications are given on top of the nucleosome, where ac_{H3} stands for acetylation at H3K9 and H3K14; ac_{H4} for acetylation at H4K5, H4K8, H4K12, and H4K16; me₁ for H3K4 monomethylation; and me₂ for H3K4 dimethylation. HSF1 is shown as constitutive trimer, CRR1 as monomer, and polymerase II as multiprotein complex. The darker the symbols for proteins and modifications are drawn, the higher their levels under the respective condition. As we have no data on the occupancy of the CuREs by CRR1, the latter is drawn in white.

Chlamydomonas Promoter Categories Based on Their Chromatin State

Based on their activation by chromatin remodeling, we may place the six promoters analyzed here into four categories (Figure 10): the *CYC6* and *HSP22F* promoters belong to the first category. Under nonstress or copper-replete conditions, these promoters are inactive. The inactive state is mediated by a closed chromatin structure as judged from high nucleosome occupancy, low levels of histone H3/4 acetylation, and high levels of histone H3K4 mono- and dimethylation. HSF1 and CRR1 transcription factors that are activated by heat stress and copper deprivation, respectively, mediate an opening of the chromatin structure at the promoters that is characterized by reduced nucleosome occupancy, high levels of histone H3/4 acetylation, and, presumably only after prolonged activation, reduced levels of histone H3K4 mono- and dimethylation. Moreover, activated HSF1 and CRR1 transcription factors mediate transcription initiation/elongation and, thus, high level transcription of the *HSP22F* and *CYC6* genes.

The *HSP70A* and *CRD1* promoters belong to the second category. They are constitutively in an open chromatin state, as judged from low nucleosome occupancy, high levels of histone H3/4 acetylation, and low levels of histone H3/K4 mono- and dimethylation. Although the chromatin state of the noninduced *HSP70A* and *CRD1* promoters resembles that of the induced *CYC6* promoter, the *HSP70A* and *CRD1* genes under nonstress and copper-replete conditions are only weakly expressed (von Gromoff et al., 1989; Moseley et al., 2000). Apparently, high-level expression under heat stress and copper deprivation conditions requires that the activated HSF1 and CRR1 transcription factors enhance transcription initiation/elongation. At least activated CRR1 also mediates further reduction of nucleosome occupancy. In case of the *HSP70A* promoter, the open chromatin state and basal expression is mediated to a large part by preloaded HSF1, whereas at the *CRD1* promoter it is mediated by an unknown activator.

The *CPX1* promoter belongs to a third category that represents an intermediate between the *HSP22F/CYC6* and *HSP70A/CRD1* promoter categories in that it has a partially open chromatin structure under noninducing conditions. The latter is characterized by intermediate levels of nucleosome occupancy, high levels of histone H3 acetylation and H3K4 dimethylation, but low levels of histone H4 acetylation and H3K4 monomethylation. Similar to the fully opened *HSP70A* and *CRD1* promoters, the partially opened chromatin state at the *CPX1* promoter allows for low level expression of the *CPX1* gene (Quinn et al., 1999). Thus, *HSP70A*, *CRD1*, and *CPX1* promoters are poised for full transcriptional activation. The fully opened chromatin state at the *CPX1* promoter, mediated by activated CRR1 under copper-deprived conditions and leading to high level expression of the *CPX1* gene, resembles exactly that observed at the *CYC6* promoter.

A fourth category is represented by the *RBCS2* promoter, which is constitutively active and drives constitutive high-level expression of the *RBCS2* gene (Goldschmidt-Clermont and Rahire, 1986). A constitutively active chromatin state at the *RBCS2* promoter is suggested by high levels of histone H3/4 acetylation and low levels of H3K4 dimethylation. However, the *RBCS2* promoter also exhibits high levels of nucleosome

occupancy and H3K4 monomethylation, which rather are characteristic for inactive chromatin. Heat shock leads to a closed chromatin structure, as levels of histone H3/4 acetylation strongly decrease and nucleosome occupancy increases. These results suggested reduced activity of the *RBCS2* promoter under heat stress conditions, which indeed was observed previously for *RBCS2* promoter driven transgenes that are much more weakly expressed than the endogenous *RBCS2* gene (Schroda et al., 2002). Expression levels also of other *Chlamydomonas* genes were observed to decline during heat stress (Dorn et al., 2010). This response might be part of a global, heat shock-induced loss of histone acetylation, which was first observed long ago in *Drosophila melanogaster* (Arrigo, 1983). In contrast with what was reported from a recent study in mammalian cell cultures (Fritah et al., 2009), this effect appears not to depend on HSF1 in *Chlamydomonas*.

In summary, *Chlamydomonas* adjusts gene expression levels in response to changes in environmental conditions by specific transcription factors, such as HSF1 and CRR1 that individually remodel chromatin structure at their target genes, but also by yet unknown factors that appear to generally remodel the chromatin state of many promoters. The most important mark indicative of open chromatin and transcriptionally active promoters appears to be histone acetylation: basal activity of promoters was observed only when at least histone H3 carried high acetylation levels and strong activity was observed only when both histones H3 and H4 were acetylated at high levels. Moreover, histone acetylation preceded nucleosome eviction. By contrast, levels of nucleosome occupancy, H3K4 monomethylation, or H3K4 dimethylation appeared not to have a crucial influence on promoter activity.

The Gene-Wide Distribution of Histone Marks in *Chlamydomonas* versus Yeast

Nucleosome occupancy and histone modifications were determined at a genome-wide scale in yeast by ChIP-on-chip assays (Bernstein et al., 2004; Lee et al., 2004, 2007; Pokholok et al., 2005). When compared with these yeast studies, the glimpse we obtained here by examining selected regions in the *Chlamydomonas* genome suggests similar, but also distinct, features. Similar to yeast, nucleosome occupancy in *Chlamydomonas* in general was low at active promoters and high in transcribed regions (Figures 9 and 10). Moreover, histone H3/4 acetylation was high at promoters of active genes and low at inactive promoters and transcribed and intergenic regions. Furthermore, H3K4 monomethylation was generally low at active promoters and high toward the 3' end of transcribed regions. Finally, H3K4 dimethylation appeared to be higher at 5' regions of inactive/weakly transcribed genes compared with actively transcribed genes, which correlated with the notion derived from studies on metazoans that H3K4 dimethylation may mark regions of poised, inactive genes (Schneider et al., 2004; Bernstein et al., 2005; Sims and Reinberg, 2006).

In contrast with what has been observed for yeast, where nucleosome occupancy is low at intergenic regions, we observed high nucleosome occupancy at two intergenic regions (Figure 9). Also, in human cells, nucleosome occupancy appears to be more or less evenly distributed, but contrary to what has been observed for yeast and now *Chlamydomonas*, histones are not particularly

depleted at promoter regions (Bernstein et al., 2005). Hence, there appear to be organism-specific differences in histone occupancy and modifications, which can only be elucidated in depth by ChIP-on-chip or ChIP-seq approaches. As the chromatin structure of *Chlamydomonas* appears to be of particularly repressive nature in that nucleosomes exhibit overall low levels of acetylation and high levels of H3K4 monomethylation (Waterborg et al., 1995; van Dijk et al., 2005), it will be of special interest to investigate chromatin structure at a genome-wide level in *Chlamydomonas*.

METHODS

Strains and Cultivation Conditions

To generate strains for investigating the heat shock response, *Chlamydomonas reinhardtii* strain cw15-325 (cw_d, mt⁺, arg7⁻; kindly provided by R. Matagne, University of Liège, Belgium) was transformed with pCB412 (containing only the wild-type *ARG7* gene; control strain), pMS418 (containing *ARG7* and an *HSF1*-RNAi construct), and pMS540 (containing *ARG7* and an *HSF1*-amiRNA construct) as described previously (Schulz-Raffelt et al., 2007; Schmollinger et al., 2010). Arg prototrophic transformants were screened for thermosensitivity by exposing cells on agar plates three times within 48 h to a 1-h heat shock by floating plates in a water bath prewarmed to 40°C. To generate strains for investigating the copper response, strain CC3960 (*cr1-2*, *arg7*⁻; kindly provided by S. Merchant, UCLA, CA) was transformed with plasmid pARG7.8 (Debuchy et al., 1989) or cotransformed with pARG7.8 and pCRR1F1B6 (*CRR1*⁺ control strain) as described previously (Kropat et al., 2005). Strains were grown mixotrophically to a density of 4 to 7 × 10⁶ cells/mL in Tris-acetate-phosphate medium (Harris, 2008) on a rotary shaker at 24°C and ~30 μE m⁻² s⁻¹. For heat shock experiments, cells were pelleted by a 4-min centrifugation at 24°C and 2704g, resuspended in Tris-acetate-phosphate medium prewarmed to 40°C, and incubated under agitation in a water bath at 40°C and ~30 μE m⁻² s⁻¹ for 30 min. Prior to harvest, ice was added to the cells. Copper depletion experiments were performed as described previously (Quinn and Merchant, 1998).

Protein Extraction, Immunodetection, RNA Extraction, and qRT-PCR

Protein extraction and immunoblot analyses were done as described previously (Liu et al., 2005). RNA was isolated from ~10⁸ cells with the TRIzol reagent (Invitrogen) using the manufacturer's protocol except for the last steps: before RNA precipitation, two additional chloroform/isoamyl alcohol (24:1) extractions were performed. A DNase digest was done using RNase-free Turbo DNase (Ambion). The quality of the RNA preparations was estimated by agarose gel electrophoresis, and RNA concentration and purity were determined spectrophotometrically (NanoDrop-1000). cDNA synthesis was performed using the MULV reverse transcriptase (Promega), deoxynucleotide triphosphate, and oligo-d(T)18 primers. Primers for qRT-PCRs were selected based on ≥90% primer efficiency, a single melt curve, a single band on a 1.5% agarose gel, and on the correct sequence of the amplicon. They are listed in Supplemental Table 1 online. qRT-PCR was performed using the StepOnePlus RT-PCR system (Applied Biosystems) and the Maxima SYBR Green kit from Fermentas. Each reaction contained the vendor's master mix, 200 nM of each primer, and cDNA corresponding to 10 ng input RNA in the reverse transcriptase reaction. The reaction conditions were as follows: 95°C for 10 min, followed by cycles of 95°C for 15 s and 65°C for 60 s, up to a total of 40 cycles. Primer efficiencies and amplicon sizes for all eight targets are listed in Supplemental Figure 3B online. Controls without template or reverse transcriptase were always included.

ChIP

A total of 10^9 cells that were grown under nonstress conditions and heat shocked for 30 min or grown under copper-replete and copper deprivation conditions were harvested by a 2-min centrifugation at 4°C and 3220g. To cross-link protein–DNA interactions, cells were resuspended in 10 mL freshly prepared cross-linking buffer (20 mM HEPES-KOH, pH 7.6, 80 mM KCl, and 0.35% formaldehyde) and incubated for 10 min at 24°C. Cross-linking was quenched by the addition of Gly at a final concentration of 125 mM and further incubation for 5 min at 24°C. Cells were collected by a 2-min centrifugation at 4°C and 3220g, washed twice with 1 mL 20 mM HEPES-KOH, pH 7.6, and 80 mM KCl, and lysed by the addition of 400 μ L lysis buffer (1% SDS, 10 mM EDTA, 50 mM Tris-HCl, pH 8.0, and 0.25 \times protease inhibitor cocktail [Roche]). Cells were sonicated on ice using a BANDELIN Sonopuls HD 2070 sonicator with sonication tip MS 73 (55% output control and 60% duty cycle) to gain an average DNA fragment size of \sim 200 bp. Sonication efficiency was verified for each sample by agarose gel electrophoresis. ChIP was performed with aliquots corresponding to \sim 2 \times 10⁷ cells that were diluted 1/10 with ChIP buffer (1.1% Triton X-100, 1.2 mM EDTA, 167 mM NaCl, and 16.7 mM Tris-HCl, pH 8) and supplemented with BSA and sonicated λ -DNA at final concentrations of 100 and 1 μ g/mL, respectively. Antibodies specific for the following epitopes were used: histone H3 (5 μ L; Abcam ab1791); diacetyl H3K9 and H3K14 (10 μ L; Upstate 06-599); tetra-acetyl H4K5, H4K8, H4K12, and H4K16 (10 μ L; Upstate 06-866); monomethylated H3K4 (5 μ L; Abcam ab8895); dimethylated H3K4 (10 μ L; Upstate 07-030); HSF1 (40 μ L; affinity purified from rabbit antiserum; Schulz-Raffelt et al., 2007); vesicle-inducing protein in plastids 2 (VIPP2) (40 μ L; affinity purified from rabbit antiserum, used as mock control). Affinity purification was done as described previously (Willmund and Schroda, 2005). Antibody-protein/DNA complexes were allowed to form during a 1-h incubation at 4°C, were complexed with 6 mg preswollen protein A Sepharose beads (Sigma-Aldrich) during a 2-h incubation at 4°C, and precipitated by a 20-s centrifugation at 16,000g. Sepharose beads were washed once with washing buffer 1 (0.1% SDS, 1% Triton X-100, and 2 mM EDTA, pH 8) containing 150 mM NaCl, once with washing buffer 1 containing 500 mM NaCl, once with washing buffer 2 (250 mM LiCl, 1% Nonidet P-40, 1% Na-deoxycholate, 1 mM EDTA, and 10 mM Tris-HCl, pH 8), and twice with TE (1 mM EDTA and 10 mM Tris-HCl, pH 8). Protein-DNA complexes were eluted by incubating twice for 15 min at 65°C in elution buffer (1% SDS and 0.1 M NaHCO₃), and cross-links were reverted by an overnight incubation at 65°C after addition of NaCl to a final concentration of 0.5 M. Proteins were digested by incubating for 1 h at 55°C after the addition of proteinase K (3.5 μ g/mL), EDTA (8 mM), and Tris-HCl, pH 8.0 (32 mM). DNA was extracted once with phenol/chloroform/isoamyl alcohol (25:24:1), once with chloroform/isoamyl alcohol (24:1), and precipitated by incubation with 2 volumes of ethanol after addition of 0.3 M Na-acetate, pH 5.2, and 10 μ g/mL glycogen for 3 h at -20° C. Precipitated DNA was collected by a 20-min centrifugation at 4°C and 16,000g, washed with 70% ethanol, and air-dried and resuspended in TE; 1/40th of the precipitated DNA was used for qPCR using the same settings as for qRT-PCR (see above). Controls where template was omitted or derived from ChIP using an affinity-purified antibody against VIPP2 (mock control) were always included. Signals for individual gene regions were normalized against 10% input DNA and then to the corresponding signal derived from the *CYC6* promoter (heat shock) or from the *RBCS2* promoter (copper depletion), which showed no changes after the respective treatment (see Supplemental Figure 5 online). Primers used for qPCR are listed in Supplemental Table 2 online.

FAIRE

A total of 10^9 cells that were grown under nonstress conditions and heat shocked for 30 min or grown under copper-replete and copper deprivation

conditions were harvested by a 2-min centrifugation at 4°C and 3220g. Cross-linking of DNA–protein interactions was performed exactly as described above for the ChIP Protocol. Cells were sonicated on ice using a BANDELIN Sonopuls HD 2070 sonicator with sonication tip MS 73 (55% output control and 60% duty cycle) to give an average DNA fragment size of \sim 200 bp. Sonication efficiency was verified for each sample by agarose gel electrophoresis. FAIRE was performed with aliquots corresponding to \sim 2 \times 10⁷ cells. DNA was extracted once with phenol/chloroform/isoamyl alcohol (25:24:1) and twice with chloroform/isoamyl alcohol (24:1) and precipitated by incubation with 2 volumes of ethanol after addition of 0.3 M Na-acetate, pH 5.2, for 4 h at -20° C. Precipitated DNA was collected by a 20-min centrifugation at 4°C and 16,000g, washed with 70% ethanol, air-dried, and resuspended in TE, pH 8. Resuspended DNA was incubated at 65°C for 10 min; 1/40th of 10% of the precipitated DNA was used for qPCR using the same primer pairs as for ChIP (see above).

Accession Numbers

Accession numbers for all genes investigated in this study are given in Supplemental Tables 1 and 2 online.

Supplemental Data

The following materials are available in the online version of this article.

Supplemental Figure 1. Analysis of HSF1 Target Gene Expression in Different *HSF1*-RNAi and *HSF1*-amiRNA Strains.

Supplemental Figure 2. Test of the Specificity of Affinity-Purified HSF1 Antibodies.

Supplemental Figure 3. Experimental Parameters Underlying Transcript Quantification by qRT-PCR.

Supplemental Figure 4. PCR End Products Amplified on Selected Chromatin Precipitates.

Supplemental Figure 5. Nucleosome Occupancy and Histone Modifications at Promoters *CYC6* and *RBCS2* Remain Unaltered after Heat Shock and Copper Depletion, Respectively.

Supplemental Figure 6. Different Amplicons within the *HSP22F* and *CYC6* Promoters Confirm Results.

Supplemental Table 1. Primers Used for qRT-PCR.

Supplemental Table 2. Primers Used for qPCR on Chromatin Precipitates.

ACKNOWLEDGMENTS

We thank Stephen M. Miller (University of Maryland, Baltimore, MD) and Sabeeha Merchant (University of California, Los Angeles, CA) for stimulating discussions and critical comments on the manuscript. We also thank Francis-André Wollman (Institut de Biologie Physico-Chimique, Paris, France) for the antiserum against CF1 β . This work was supported by the Max Planck Society and grants from the Deutsche Forschungsgemeinschaft (Schr 617/4-3) and the Bundesministerium für Bildung und Forschung (Systems Biology Initiative FORSYS, Project GoFORSYS).

AUTHOR CONTRIBUTIONS

M.S. and D.S. conceived the project and designed the experiments. D.S. performed and analyzed all qRT-PCR, ChIP, and FAIRE experiments. D.S. and S.S. performed the immunoblotting experiments and the statistical analyses. F.S. contributed to setting up copper starvation

2300 The Plant Cell

experiments and M.S.R. to setting up the ChIP protocol. M.S. and D.S. wrote the manuscript. All authors contributed to the interpretation of results and edited the manuscript.

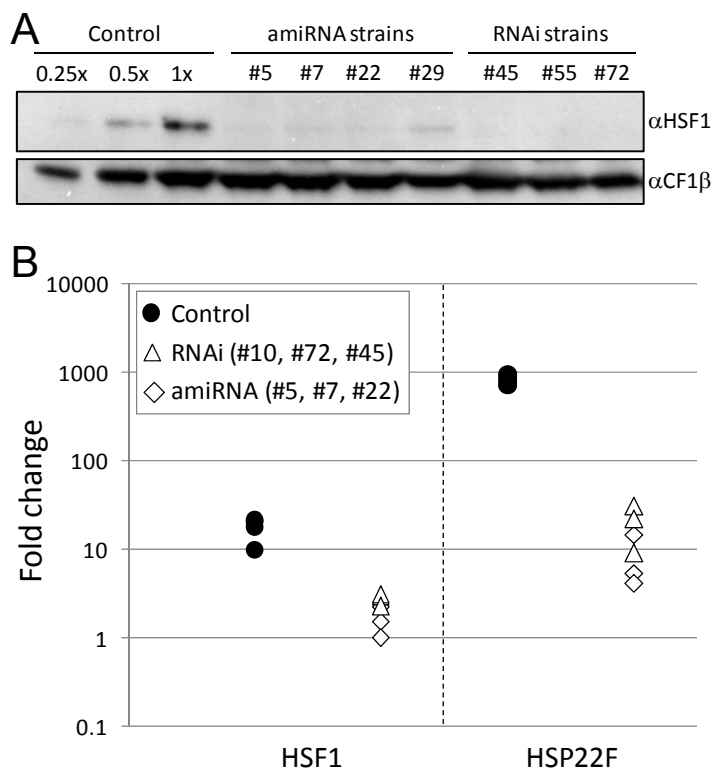
Received March 15, 2011; revised May 9, 2011; accepted June 7, 2011; published June 24, 2011.

REFERENCES

- Aalfs, J.D., and Kingston, R.E. (2000). What does 'chromatin remodeling' mean? *Trends Biochem. Sci.* **25**: 548–555.
- Arrigo, A.P. (1983). Acetylation and methylation patterns of core histones are modified after heat or arsenite treatment of *Drosophila* tissue culture cells. *Nucleic Acids Res.* **11**: 1389–1404.
- Bernstein, B.E., Kamal, M., Lindblad-Toh, K., Bekiranov, S., Bailey, D.K., Huebert, D.J., McMahon, S., Karlsson, E.K., Kulbokas III, E.J., Gingeras, T.R., Schreiber, S.L., and Lander, E.S. (2005). Genomic maps and comparative analysis of histone modifications in human and mouse. *Cell* **120**: 169–181.
- Bernstein, B.E., Liu, C.L., Humphrey, E.L., Perlstein, E.O., and Schreiber, S.L. (2004). Global nucleosome occupancy in yeast. *Genome Biol.* **5**: R62.
- Couture, J.F., Collazo, E., and Trievel, R.C. (2006). Molecular recognition of histone H3 by the WD40 protein WDR5. *Nat. Struct. Mol. Biol.* **13**: 698–703.
- Debuchy, R., Purton, S., and Rochaix, J.D. (1989). The argininosuccinate lyase gene of *Chlamydomonas reinhardtii*: An important tool for nuclear transformation and for correlating the genetic and molecular maps of the ARG7 locus. *EMBO J.* **8**: 2803–2809.
- de la Cruz, X., Lois, S., Sánchez-Molina, S., and Martínez-Balbás, M.A. (2005). Do protein motifs read the histone code? *Bioessays* **27**: 164–175.
- Dorn, K.V., Willmund, F., Schwarz, C., Henselmann, C., Pohl, T., Hess, B., Veyel, D., Usadel, B., Friedrich, T., Nickelsen, J., and Schroda, M. (2010). Chloroplast DnaJ-like proteins 3 and 4 (CDJ3/4) from *Chlamydomonas reinhardtii* contain redox-active Fe-S clusters and interact with stromal HSP70B. *Biochem. J.* **427**: 205–215.
- Eriksson, M., Moseley, J.L., Tottey, S., Del Campo, J.A., Quinn, J., Kim, Y., and Merchant, S. (2004). Genetic dissection of nutritional copper signaling in *Chlamydomonas* distinguishes regulatory and target genes. *Genetics* **168**: 795–807.
- Erkina, T.Y., and Erkin, A.M. (2006). Displacement of histones at promoters of *Saccharomyces cerevisiae* heat shock genes is differentially associated with histone H3 acetylation. *Mol. Cell. Biol.* **26**: 7587–7600.
- Erkina, T.Y., Zou, Y., Freeling, S., Vorobyev, V.I., and Erkin, A.M. (2010). Functional interplay between chromatin remodeling complexes RSC, SWI/SNF and ISWI in regulation of yeast heat shock genes. *Nucleic Acids Res.* **38**: 1441–1449.
- Fritah, S., Col, E., Boyault, C., Govin, J., Sadoul, K., Chiocca, S., Christians, E., Khochbin, S., Jolly, C., and Vourc'h, C. (2009). Heat shock factor 1 controls genome-wide acetylation in heat-shocked cells. *Mol. Biol. Cell* **20**: 4976–4984.
- Giresi, P.G., Kim, J., McDaniel, R.M., Iyer, V.R., and Lieb, J.D. (2007). FAIRE (Formaldehyde-Assisted Isolation of Regulatory Elements) isolates active regulatory elements from human chromatin. *Genome Res.* **17**: 877–885.
- Goldschmidt-Clermont, M., and Rahire, M. (1986). Sequence, evolution and differential expression of the two genes encoding variant small subunits of ribulose biphosphate carboxylase/oxygenase in *Chlamydomonas reinhardtii*. *J. Mol. Biol.* **191**: 421–432.
- Harris, E.H. (2008). *The Chlamydomonas Sourcebook: Introduction to Chlamydomonas and Its Laboratory Use.* (San Diego, CA: Elsevier/Academic Press).
- Haslbeck, M. (2002). sHsps and their role in the chaperone network. *Cell. Mol. Life Sci.* **59**: 1649–1657.
- Kodama, Y., Nagaya, S., Shinmyo, A., and Kato, K. (2007). Mapping and characterization of DNase I hypersensitive sites in *Arabidopsis* chromatin. *Plant Cell Physiol.* **48**: 459–470.
- Kouzarides, T. (2007). Chromatin modifications and their function. *Cell* **128**: 693–705.
- Kremer, S.B., and Gross, D.S. (2009). SAGA and Rpd3 chromatin modification complexes dynamically regulate heat shock gene structure and expression. *J. Biol. Chem.* **284**: 32914–32931.
- Krogan, N.J., Dover, J., Wood, A., Schneider, J., Heidt, J., Boateng, M.A., Dean, K., Ryan, O.W., Golshani, A., Johnston, M., Greenblatt, J.F., and Shilatifard, A. (2003). The Paf1 complex is required for histone H3 methylation by COMPASS and Dot1p: Linking transcriptional elongation to histone methylation. *Mol. Cell* **11**: 721–729.
- Kropat, J., Tottey, S., Birkenbihl, R.P., Depège, N., Huijser, P., and Merchant, S. (2005). A regulator of nutritional copper signaling in *Chlamydomonas* is an SBP domain protein that recognizes the GTAC core of copper response element. *Proc. Natl. Acad. Sci. USA* **102**: 18730–18735.
- Lachner, M., and Jenuwein, T. (2002). The many faces of histone lysine methylation. *Curr. Opin. Cell Biol.* **14**: 286–298.
- Lee, C.K., Shibata, Y., Rao, B., Strahl, B.D., and Lieb, J.D. (2004). Evidence for nucleosome depletion at active regulatory regions genome-wide. *Nat. Genet.* **36**: 900–905.
- Lee, J.H., Hübel, A., and Schöffl, F. (1995). Derepression of the activity of genetically engineered heat shock factor causes constitutive synthesis of heat shock proteins and increased thermotolerance in transgenic *Arabidopsis*. *Plant J.* **8**: 603–612.
- Lee, W., Tillo, D., Bray, N., Morse, R.H., Davis, R.W., Hughes, T.R., and Nislow, C. (2007). A high-resolution atlas of nucleosome occupancy in yeast. *Nat. Genet.* **39**: 1235–1244.
- Li, B., Carey, M., and Workman, J.L. (2007). The role of chromatin during transcription. *Cell* **128**: 707–719.
- Li, H., Ilin, S., Wang, W., Duncan, E.M., Wysocka, J., Allis, C.D., and Patel, D.J. (2006). Molecular basis for site-specific read-out of histone H3K4me3 by the BPTF PHD finger of NURF. *Nature* **442**: 91–95.
- Liu, C., Willmund, F., Whitelegge, J.P., Hawat, S., Knapp, B., Lodha, M., and Schroda, M. (2005). J-domain protein CDJ2 and HSP70B are a plastidic chaperone pair that interacts with vesicle-inducing protein in plastids 1. *Mol. Biol. Cell* **16**: 1165–1177.
- Lodha, M., and Schroda, M. (2005). Analysis of chromatin structure in the control regions of the *Chlamydomonas* HSP70A and RBCS2 genes. *Plant Mol. Biol.* **59**: 501–513.
- Lodha, M., Schulz-Raffelt, M., and Schroda, M. (2008). A new assay for promoter analysis in *Chlamydomonas* reveals roles for heat shock elements and the TATA box in HSP70A promoter-mediated activation of transgene expression. *Eukaryot. Cell* **7**: 172–176.
- Luger, K. (2003). Structure and dynamic behavior of nucleosomes. *Curr. Opin. Genet. Dev.* **13**: 127–135.
- Merchant, S., and Bogorad, L. (1986). Regulation by copper of the expression of plastocyanin and cytochrome c552 in *Chlamydomonas reinhardtii*. *Mol. Cell. Biol.* **6**: 462–469.
- Merchant, S., and Bogorad, L. (1987). Metal ion regulated gene expression: Use of a plastocyanin-less mutant of *Chlamydomonas reinhardtii* to study the Cu(II)-dependent expression of cytochrome c-552. *EMBO J.* **6**: 2531–2535.
- Merchant, S.S., Allen, M.D., Kropat, J., Moseley, J.L., Long, J.C., Tottey, S., and Terauchi, A.M. (2006). Between a rock and a hard place: Trace element nutrition in *Chlamydomonas*. *Biochim. Biophys. Acta* **1763**: 578–594.
- Moseley, J., Quinn, J., Eriksson, M., and Merchant, S. (2000). The *Crd1* gene encodes a putative di-iron enzyme required for photosystem I

- accumulation in copper deficiency and hypoxia in *Chlamydomonas reinhardtii*. *EMBO J.* **19**: 2139–2151.
- Müller, F.W., Igloi, G.L., and Beck, C.F. (1992). Structure of a gene encoding heat-shock protein HSP70 from the unicellular alga *Chlamydomonas reinhardtii*. *Gene* **111**: 165–173.
- Ng, H.H., Robert, F., Young, R.A., and Struhl, K. (2003). Targeted recruitment of Set1 histone methylase by elongating Pol II provides a localized mark and memory of recent transcriptional activity. *Mol. Cell* **11**: 709–719.
- Owen, D.J., Ornaghi, P., Yang, J.C., Lowe, N., Evans, P.R., Ballario, P., Neuhaus, D., Filetici, P., and Travers, A.A. (2000). The structural basis for the recognition of acetylated histone H4 by the bromodomain of histone acetyltransferase gcn5p. *EMBO J.* **19**: 6141–6149.
- Pelham, H.R. (1982). A regulatory upstream promoter element in the *Drosophila hsp 70* heat-shock gene. *Cell* **30**: 517–528.
- Peña, P.V., Davrazou, F., Shi, X., Walter, K.L., Verkhusha, V.V., Gozani, O., Zhao, R., and Kutateladze, T.G. (2006). Molecular mechanism of histone H3K4me3 recognition by plant homeodomain of ING2. *Nature* **442**: 100–103.
- Pokholok, D.K., et al. (2005). Genome-wide map of nucleosome acetylation and methylation in yeast. *Cell* **122**: 517–527.
- Quinn, J.M., and Merchant, S. (1995). Two copper-responsive elements associated with the *Chlamydomonas* *Cyc6* gene function as targets for transcriptional activators. *Plant Cell* **7**: 623–628.
- Quinn, J.M., and Merchant, S. (1998). Copper-responsive gene expression during adaptation to copper deficiency. *Methods Enzymol.* **297**: 263–279.
- Quinn, J.M., Nakamoto, S.S., and Merchant, S. (1999). Induction of coproporphyrinogen oxidase in *Chlamydomonas* chloroplasts occurs via transcriptional regulation of *Cpx1* mediated by copper response elements and increased translation from a copper deficiency-specific form of the transcript. *J. Biol. Chem.* **274**: 14444–14454.
- Rabindran, S.K., Haroun, R.I., Clos, J., Wisniewski, J., and Wu, C. (1993). Regulation of heat shock factor trimer formation: Role of a conserved leucine zipper. *Science* **259**: 230–234.
- Reid, J.L., Iyer, V.R., Brown, P.O., and Struhl, K. (2000). Coordinate regulation of yeast ribosomal protein genes is associated with targeted recruitment of Esa1 histone acetylase. *Mol. Cell* **6**: 1297–1307.
- Reinke, H., and Hörz, W. (2003). Histones are first hyperacetylated and then lose contact with the activated PHO5 promoter. *Mol. Cell* **11**: 1599–1607.
- Robert, F., Pokholok, D.K., Hannett, N.M., Rinaldi, N.J., Chandy, M., Rolfe, A., Workman, J.L., Gifford, D.K., and Young, R.A. (2004). Global position and recruitment of HATs and HDACs in the yeast genome. *Mol. Cell* **16**: 199–209.
- Ruthenburg, A.J., Wang, W., Graybosch, D.M., Li, H., Allis, C.D., Patel, D.J., and Verdine, G.L. (2006). Histone H3 recognition and presentation by the WDR5 module of the MLL1 complex. *Nat. Struct. Mol. Biol.* **13**: 704–712.
- Santos-Rosa, H., Schneider, R., Bannister, A.J., Sherriff, J., Bernstein, B.E., Emre, N.C., Schreiber, S.L., Mellor, J., and Kouzarides, T. (2002). Active genes are tri-methylated at K4 of histone H3. *Nature* **419**: 407–411.
- Schmollinger, S., Strenkert, D., and Schroda, M. (2010). An inducible artificial microRNA system for *Chlamydomonas reinhardtii* confirms a key role for heat shock factor 1 in regulating thermotolerance. *Curr. Genet.* **56**: 383–389.
- Schneider, R., Bannister, A.J., Myers, F.A., Thorne, A.W., Crane-Robinson, C., and Kouzarides, T. (2004). Histone H3 lysine 4 methylation patterns in higher eukaryotic genes. *Nat. Cell Biol.* **6**: 73–77.
- Schroda, M., Beck, C.F., and Vallon, O. (2002). Sequence elements within an *HSP70* promoter counteract transcriptional transgene silencing in *Chlamydomonas*. *Plant J.* **31**: 445–455.
- Schroda, M., Blöcker, D., and Beck, C.F. (2000). The *HSP70A* promoter as a tool for the improved expression of transgenes in *Chlamydomonas*. *Plant J.* **21**: 121–131.
- Schroda, M., and Vallon, O. (2008). Chaperones and proteases. In *The Chlamydomonas Sourcebook: Organellar and Metabolic Processes*, 2nd ed, Vol. 2, D.B. Stern, ed (San Diego, CA: Academic Press), pp. 671–729.
- Schulz-Raffelt, M., Lodha, M., and Schroda, M. (2007). Heat shock factor 1 is a key regulator of the stress response in *Chlamydomonas*. *Plant J.* **52**: 286–295.
- Sharma, N., and Nyborg, J.K. (2008). The coactivators CBP/p300 and the histone chaperone NAP1 promote transcription-independent nucleosome eviction at the HTLV-1 promoter. *Proc. Natl. Acad. Sci. USA* **105**: 7959–7963.
- Shi, X., et al. (2006). ING2 PHD domain links histone H3 lysine 4 methylation to active gene repression. *Nature* **442**: 96–99.
- Sims III, R.J., and Reinberg, D. (2006). Histone H3 Lys 4 methylation: Caught in a bind? *Genes Dev.* **20**: 2779–2786.
- Sommer, F., Kropat, J., Malasarn, D., Grosseohme, N.E., Chen, X., Giedroc, D.P., and Merchant, S.S. (2010). The CRR1 nutritional copper sensor in *Chlamydomonas* contains two distinct metal-responsive domains. *Plant Cell* **22**: 4098–4113.
- Sorger, P.K., Lewis, M.J., and Pelham, H.R. (1987). Heat shock factor is regulated differently in yeast and HeLa cells. *Nature* **329**: 81–84.
- Sorger, P.K., and Nelson, H.C. (1989). Trimerization of a yeast transcriptional activator via a coiled-coil motif. *Cell* **59**: 807–813.
- Sorger, P.K., and Pelham, H.R. (1988). Yeast heat shock factor is an essential DNA-binding protein that exhibits temperature-dependent phosphorylation. *Cell* **54**: 855–864.
- Tottey, S., Block, M.A., Allen, M., Westergren, T., Albrieux, C., Scheller, H.V., Merchant, S., and Jensen, P.E. (2003). *Arabidopsis* CHL27, located in both envelope and thylakoid membranes, is required for the synthesis of protochlorophyllide. *Proc. Natl. Acad. Sci. USA* **100**: 16119–16124.
- van Dijk, K., Marley, K.E., Jeong, B.R., Xu, J., Hesson, J., Cerny, R.L., Waterborg, J.H., and Cerutti, H. (2005). Monomethyl histone H3 lysine 4 as an epigenetic mark for silenced euchromatin in *Chlamydomonas*. *Plant Cell* **17**: 2439–2453.
- von Gromoff, E.D., Schroda, M., Oster, U., and Beck, C.F. (2006). Identification of a plastid response element that acts as an enhancer within the *Chlamydomonas HSP70A* promoter. *Nucleic Acids Res.* **34**: 4767–4779.
- von Gromoff, E.D., Treier, U., and Beck, C.F. (1989). Three light-inducible heat shock genes of *Chlamydomonas reinhardtii*. *Mol. Cell. Biol.* **9**: 3911–3918.
- Waterborg, J.H., Robertson, A.J., Tatar, D.L., Borza, C.M., and Davie, J.R. (1995). Histones of *Chlamydomonas reinhardtii*. Synthesis, acetylation, and methylation. *Plant Physiol.* **109**: 393–407.
- Willmund, F., and Schroda, M. (2005). HEAT SHOCK PROTEIN 90C is a bona fide Hsp90 that interacts with plastidic HSP70B in *Chlamydomonas reinhardtii*. *Plant Physiol.* **138**: 2310–2322.
- Wood, P.M. (1978). Interchangeable copper and iron proteins in algal photosynthesis. Studies on plastocyanin and cytochrome c-552 in *Chlamydomonas*. *Eur. J. Biochem.* **87**: 9–19.
- Zeng, L., Zhang, Q., Li, S., Plotnikov, A.N., Walsh, M.J., and Zhou, M.M. (2010). Mechanism and regulation of acetylated histone binding by the tandem PHD finger of DPF3b. *Nature* **466**: 258–262.
- Zhang, L., Lohmann, C., Prändl, R., and Schöffl, F. (2003). Heat stress-dependent DNA binding of *Arabidopsis* heat shock transcription factor HSF1 to heat shock gene promoters in *Arabidopsis* suspension culture cells *in vivo*. *Biol. Chem.* **384**: 959–963.
- Zhao, J., Herrera-Diaz, J., and Gross, D.S. (2005). Domain-wide displacement of histones by activated heat shock factor occurs independently of Swi/Snf and is not correlated with RNA polymerase II density. *Mol. Cell. Biol.* **25**: 8985–8999.

Supplemental Data. Strenkert et al. (2011) Plant Cell 10.1105/tpc.111.085266

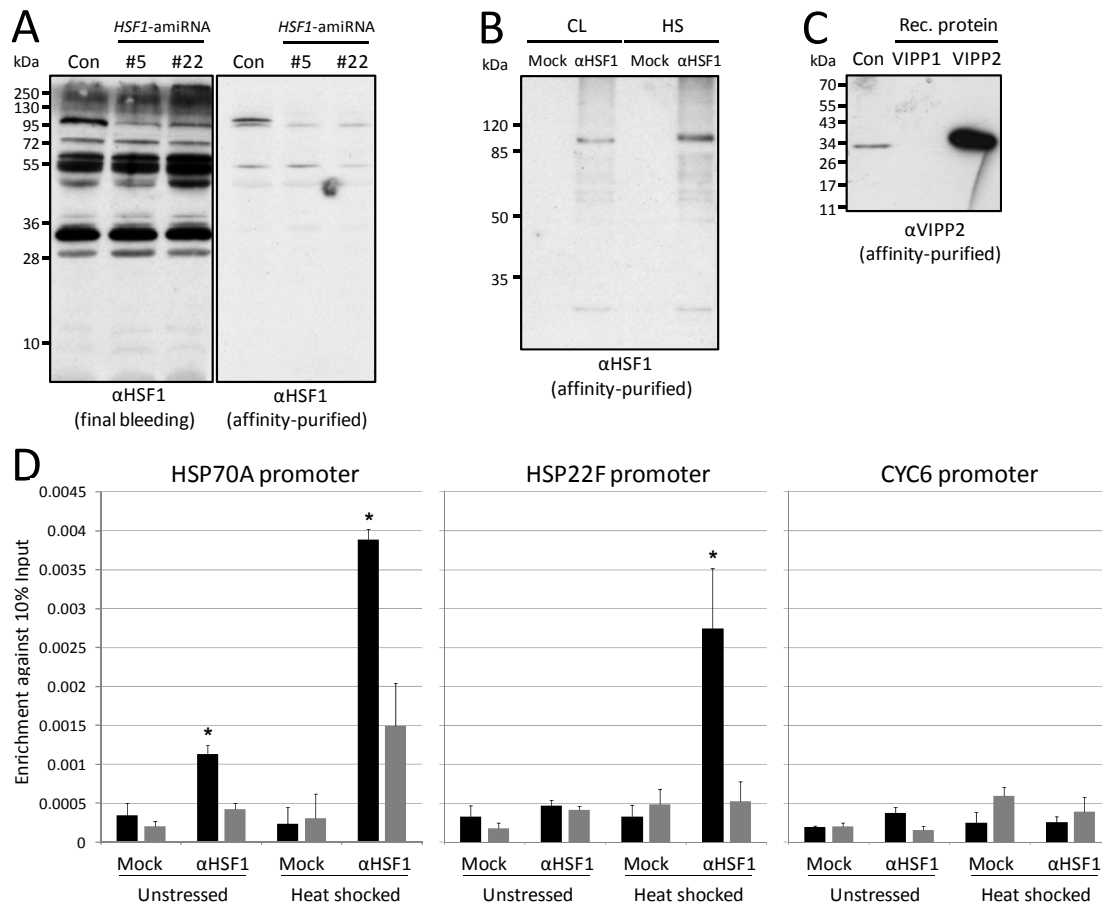


Supplemental Figure 1. Analysis of HSF1 target gene expression in different *HSF1*-RNAi and *HSF1*-amiRNA strains.

(A) *HSF1*-amiRNA and RNAi strains selected for thermosensitivity accumulate comparably low levels of residual HSF1 protein. Whole-cell proteins were extracted from non-stressed control, *HSF1*-amiRNA, and *HSF1*-RNAi strains and proteins corresponding to 2 μ g chlorophyll (1x in control) were separated on a 10% SDS-polyacrylamide gel and analyzed by immunoblotting using antisera against HSF1 and CF1 β (as loading control).

(B) Residual target gene expression is comparable between *HSF1*-amiRNA and *HSF1*-RNAi strains selected for thermosensitivity. RNA was extracted from non-stressed control, *HSF1*-amiRNA, and *HSF1*-RNAi strains and accumulation of *HSF1* and *HSP22F* transcripts was analyzed by qRT-PCR using the comparative CT method with *CBLP2* as control gene. Shown are fold changes in transcript accumulation between stressed (30 min heat shock) versus non-stressed strains.

Supplemental Data. Strenkert et al. (2011) Plant Cell 10.1105/tpc.111.085266

**Supplemental Figure 2. Test of the specificity of affinity-purified HSF1 antibodies.**

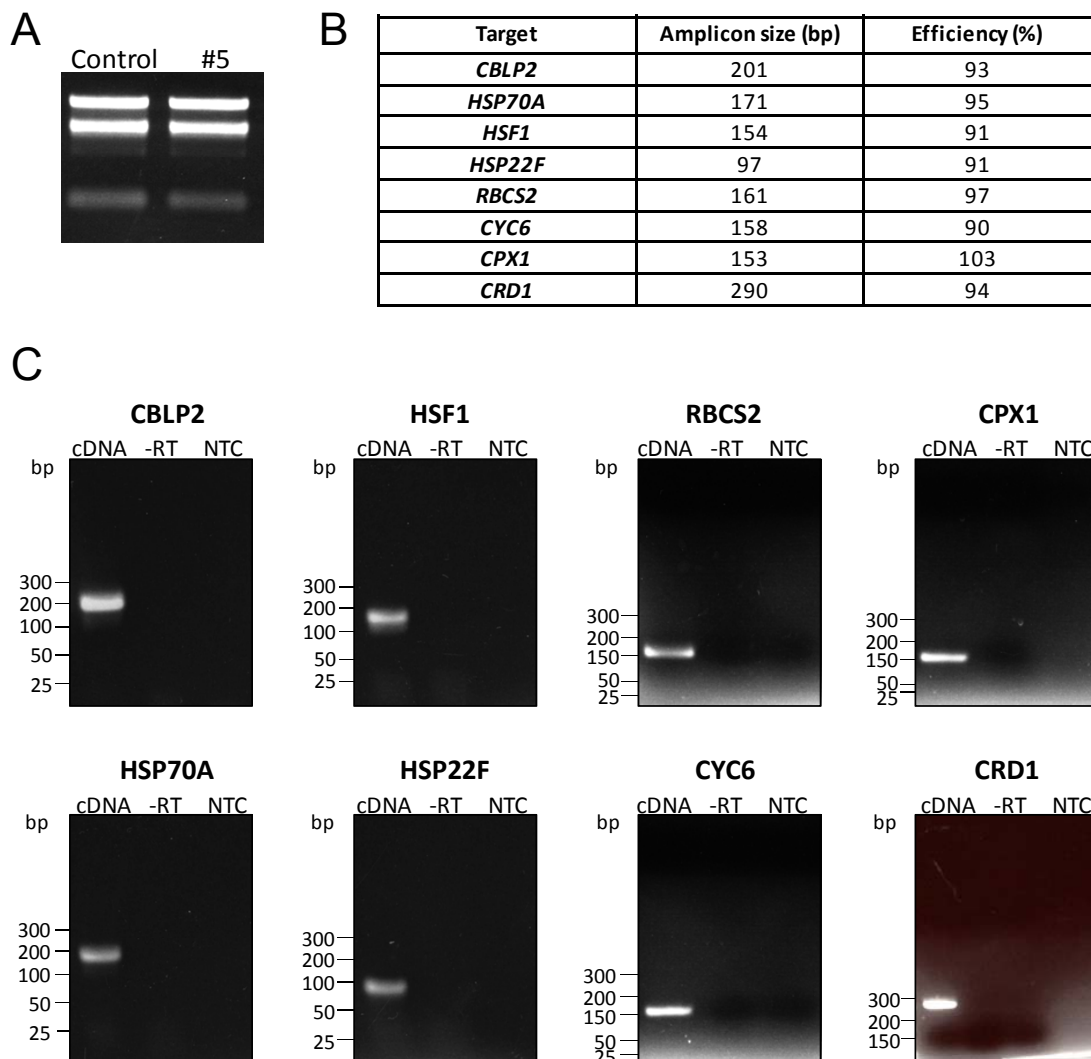
(A) Comparison of HSF1 antibodies from the final bleeding and after affinity purification. Whole-cell proteins of cells from control and *HSF1*-amiRNA lines grown under non-stress conditions were extracted and proteins corresponding to 2 μ g chlorophyll were separated by SDS-PAGE and analyzed by immunoblotting using antibodies against HSF1 of the final bleeding or after affinity purification.

(B) Analysis of α HSF1 immunoprecipitates. ChIP without formaldehyde treatment was done using an antibody against VIPP2 (mock) or affinity-purified antibodies against HSF1 on non-stressed (CL) or heat-shocked (HS) control cells. 10% of the immunoprecipitates were separated by SDS-PAGE and analyzed by immunoblotting using affinity-purified antibodies against HSF1.

(C) Specificity of affinity-purified VIPP2 antibodies. Whole-cell proteins from unstressed control cells corresponding to 2 μ g chlorophyll and 15 ng each of recombinant VIPP1 and VIPP2 were separated by SDS-PAGE and analyzed by immunoblotting using affinity-purified antibodies against VIPP2.

(D) Comparison of ChIP results done with antibodies against VIPP2 and HSF1. ChIP was done on control (black bars) and HSF1-underexpressing strains (grey bars) grown under non-stress conditions or subjected to a 30-min heat shock using affinity-purified antibodies against VIPP2 (mock) or HSF1. From precipitated DNA fragments the regions of the *HSP70A*, *HSP22F* and *CYC6* promoters shown in Figure 2 were amplified by qPCR and the enrichment relative to 10% input DNA was calculated. PCRs were done in triplicate, error bars indicate standard errors. Asterisks indicate the significance of change at the respective promoter with p values ≤ 0.001 calculated by the all pairwise multiple comparison procedure (Holm-Sidak method).

Supplemental Data. Strenkert et al. (2011) Plant Cell 10.1105/tpc.111.085266



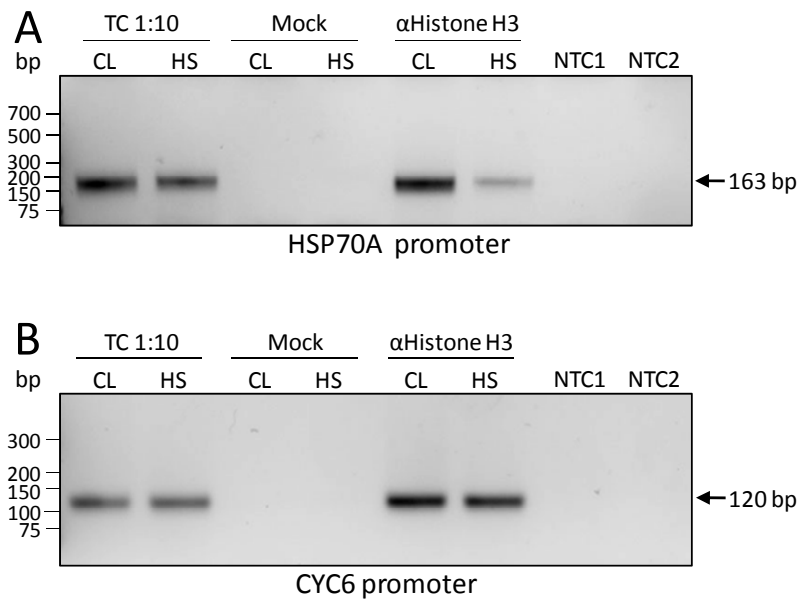
Supplemental Figure 3. Experimental parameters underlying transcript quantification by qRT-PCR.

(A) Exemplary mRNA preparation from control and *HSF1*-amiRNA strain #5. RNA was extracted from non-stressed cells and separated on a 1.5% agarose gel and stained with GelRed.

(B) Amplicon sizes and primer efficiencies for the 8 target transcripts analyzed. Primer efficiencies were calculated from serial dilutions of cDNA prepared from RNA extracted from cells subjected to a 30-min heat shock (*HSP70A*, *HSP22F*, *HSF1*, *CBLP2*), or RNA extracted from cells grown under copper deficiency (*CYC6*, *CRD1*, *CPX1* and *RBCS2*).

(C) PCR end products obtained in a representative qRT-PCR experiment for the 8 target transcripts analyzed. 1/10th of a real-time PCR reaction on cDNA prepared as described in (B) was separated on a 1.5% agarose gel and stained with GelRed. The reactions were carried out without template (non-template control, NTC) or on 10 ng RNA which was subjected to reverse transcription (cDNA) or where the reverse transcription step was omitted (-RT).

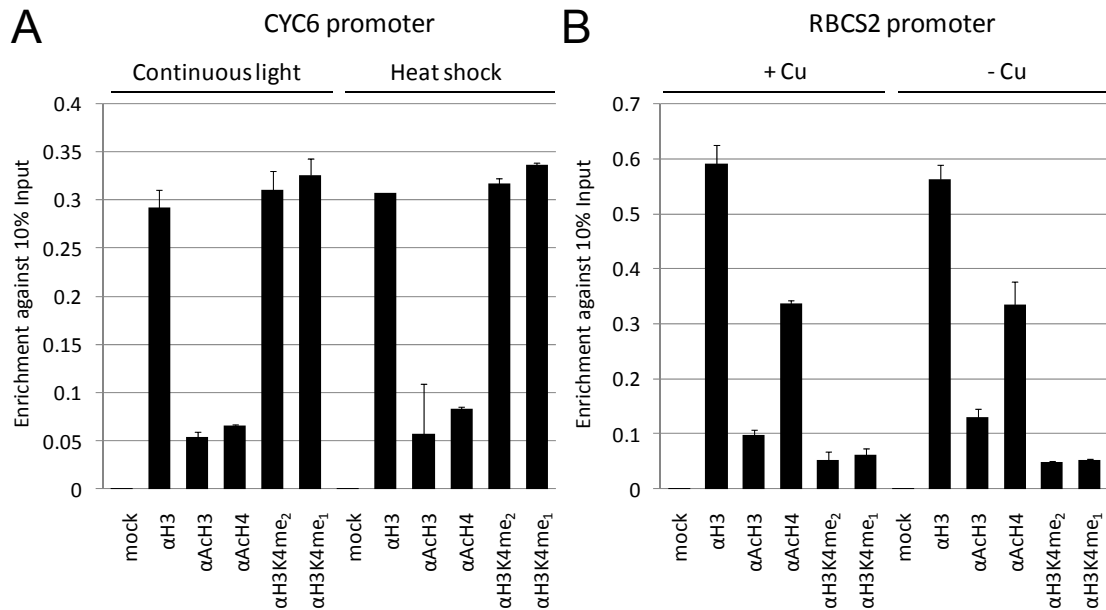
Supplemental Data. Strenkert et al. (2011) Plant Cell 10.1105/tpc.111.085266

**Supplemental Figure 4. PCR end products amplified on selected chromatin precipitates.****(A) Heat shock results in a strong reduction of histone H3 occupancy at the *HSP70A* promoter.**

ChIP was done on control strains grown under non-stress conditions (CL) or subjected to a 30-min heat shock (HS). From DNA fragments precipitated with antibodies against VIPP2 (mock) and histone H3, the promoter region of the *HSP70A* promoter (see Figure 2) was amplified by PCR. As controls, the PCR was also done on 10% of ChIP input DNA (template control, TC) and without template (non-template control, NTC). After 26 amplification cycles, the entire reactions were separated on a 1.5%-agarose gel and stained with GelRed.

(B) Histone H3 occupancy at the *CYC6* promoter is unaffected by heat stress. PCR was done as described in (A), but region I of the *CYC6* promoter (see Figure 2) was amplified.

Supplemental Data. Strenkert et al. (2011) Plant Cell 10.1105/tpc.111.085266

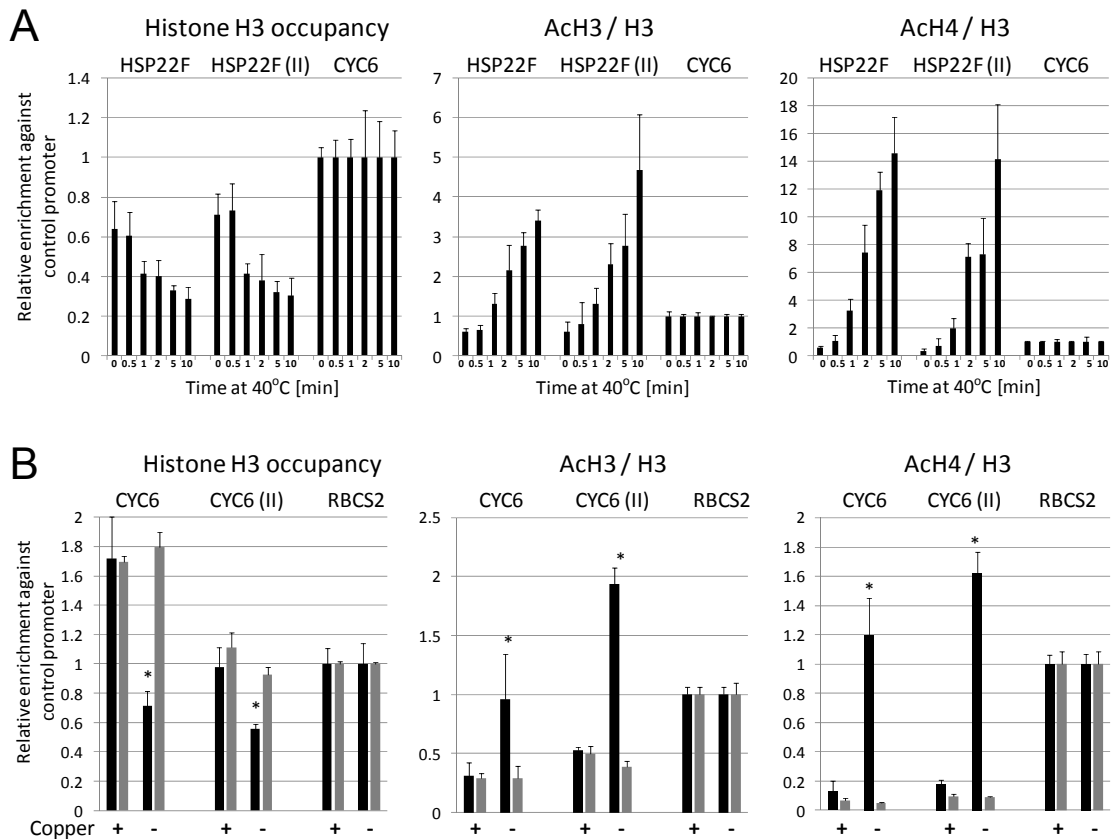


Supplemental Figure 5. Nucleosome occupancy and histone modifications at promoters *CYC6* and *RBCS2* remain unaltered after heat shock and copper depletion, respectively.

(A) ChIP was done on control cells grown under non-stress conditions or subjected to a 30-min heat shock. DNA fragments were precipitated with antibodies against the unmodified C-terminus of histone H3, acetylated lysines 9 and 14 of histone H3, acetylated lysines 5, 8, 12 and 16 of histone H4, dimethylation of lysine 4 at histone H3 (H3K4me₂), monomethylation of lysine 4 at histone H3 (H3K4me₁), and VIPP2 (mock). DNA fragments from the *CYC6* promoter as shown in Figure 2 were amplified by qPCR and the enrichment relative to 10% input DNA was calculated. Error bars indicate standard errors from three technical replicates.

(B) ChIP was done as in (A) but using cells grown under copper replete (+Cu) and copper deprivation (-Cu) conditions and qPCR primers hybridizing to the *RBCS2* promoter.

Supplemental Data. Strenkert et al. (2011) Plant Cell 10.1105/tpc.111.085266



Supplemental Figure 6. Different amplicons within the *HSP22F* and *CYC6* promoters confirm results.

(A) Rapidly increasing levels of histone acetylation and reduced histone occupancy during heat stress are observed at different regions of the *HSP22F* promoter. ChIP was done on control cells grown under non-stress conditions or subjected to heat shock at 40°C for 10 min. DNA fragments were precipitated with antibodies against the unmodified C-terminus of histone H3, acetylated lysines 9 and 14 of histone H3 (AcH3), and acetylated lysines 5, 8, 12 and 16 of histone H4 (AcH4). DNA fragments were amplified by qPCR and the enrichment relative to 10% input DNA was calculated and normalized against values obtained for the *CYC6* promoter. Amplicons are from regions I (same values as shown in Figure 5A) and II of the *HSP22F* promoter, as illustrated in Figure 2. Error bars indicate standard errors from two biological replicates, each analyzed in triplicate.

(B) *CRR1*-dependent increase in histone acetylation and drop in histone occupancy under copper-deplete conditions are observed at different regions of the *CYC6* promoter. ChIP was done on control (black bars) and *crr1* knock-out cells (grey bars) grown under copper replete or copper deprivation conditions. DNA fragments were precipitated with antibodies against the unmodified C-terminus of histone H3, acetylated lysines 9 and 14 of histone H3 (AcH3), and acetylated lysines 5, 8, 12 and 16 of histone H4 (AcH4). DNA fragments were amplified by qPCR and the enrichment relative to 10% input DNA was calculated and normalized against values obtained for the *RBCS2* promoter. Amplicons are from regions I (same values as shown for *CYC6* in Figure 7) and II of the *CYC6* promoter, as illustrated in Figure 2. Error bars indicate standard errors from two biological replicates, each analyzed in triplicate.

Supplemental Data. Strenkert et al. (2011) Plant Cell 10.1105/tpc.111.085266

Supplemental Table 1. Primers used for qRT-PCR.

Target transcript	Protein ID Augustus 5	GeneBank accession	Primers (5' to 3')
<i>CBLP2</i>	514942	EDO99650	Fwd: GCCACACCGAGTGGGTGTCGTGCG Rev: CCTTGCCGCCCGAGGCGCACAGCG
<i>RBCS2</i>	519413	EDO96903	Fwd: GCCCAGGTCGACTACATTGTC Rev: AACATGGGCAGCTTCCACA
<i>HSP70A</i>	525480	EDO97621	Fwd: GATCGAGCGCATGGTGC Rev: TCCATCGACTCCTTGTCGG
<i>HSP22F</i>	515453	EDP10019	Fwd: TGCACCCACGCCGTG Rev: TGATCTCAACGCTGATGTCCTC
<i>CYC6</i>	516039	EDO99527	Fwd: CAGGTCTTCAACGGCAACTGT Rev: ATCGCCCCCTTGCCAT
<i>CPX1</i>	518660	EDP06704	Fwd: CCAGACCTCCAAGCGTGTGT Rev: GCGTTGCGGATCACCTTCTC
<i>CRD1</i>	524896	EDP04035	Fwd: CGTAGGTAGGCTGACTGCGTTG Rev: GTCATTTATGCGCAGCCCTTG
<i>HSF1</i>	525816	ABL74450	Fwd: TCCTTATCAAGACGTATGACCTCGT Rev: AAGCTGGAGAAATTGTTGTGCTT

3.3. ARTICLE 3: A PROTOCOL FOR THE IDENTIFICATION OF PROTEIN-PROTEIN INTERACTIONS BASED ON ¹⁵N METABOLIC LABELING, IMMUNOPRECIPITATION, QUANTITATIVE MASS SPECTROMETRY AND AFFINITY MODULATION.

Authors:

Stefan Schmollinger, Daniela Strenkert, Vittoria Offeddu, André Nordhues, Frederik Sommer and Michael Schroda

Journal:

Journal of Visualized Experiments,67, e4083

Date:

2012, September

Contribution to:

Figure 1

Figure 2

Figure 3

Video Article

A Protocol for the Identification of Protein-protein Interactions Based on ¹⁵N Metabolic Labeling, Immunoprecipitation, Quantitative Mass Spectrometry and Affinity Modulation

Stefan Schmollinger^{1,2}, Daniela Strenkert^{1,2}, Vittoria Offeddu^{1,2}, André Nordhues^{1,2}, Frederik Sommer^{1,2}, Michael Schroda^{1,2}

¹Max Planck Institute of Molecular Plant Physiology

²University of Kaiserslautern

Correspondence to: Michael Schroda at Schroda@biologie.uni-kl.de

URL: <http://www.jove.com/video/4083/>

DOI: 10.3791/4083

Keywords: Genetics, Issue 67, Molecular Biology, Physiology, Plant Biology, ¹⁵N metabolic labeling, QUICK, protein cross-linking, *Chlamydomonas*, co-immunoprecipitation, molecular chaperones, HSP70

Date Published: 9/24/2012

This is an open-access article distributed under the terms of the Creative Commons Attribution-NonCommercial License, which permits non-commercial use, distribution, and reproduction, provided the original work is properly cited.

Citation: Schmollinger, S., Strenkert, D., Offeddu, V., Nordhues, A., Sommer, F., Schroda, M. A Protocol for the Identification of Protein-protein Interactions Based on ¹⁵N Metabolic Labeling, Immunoprecipitation, Quantitative Mass Spectrometry and Affinity Modulation. *J. Vis. Exp.* (67), e4083 10.3791/4083, DOI : 10.3791/4083 (2012).

Abstract

Protein-protein interactions are fundamental for many biological processes in the cell. Therefore, their characterization plays an important role in current research and a plethora of methods for their investigation is available¹. Protein-protein interactions often are highly dynamic and may depend on subcellular localization, post-translational modifications and the local protein environment². Therefore, they should be investigated in their natural environment, for which co-immunoprecipitation approaches are the method of choice³. Co-precipitated interaction partners are identified either by immunoblotting in a targeted approach, or by mass spectrometry (LC-MS/MS) in an untargeted way. The latter strategy often is adversely affected by a large number of false positive discoveries, mainly derived from the high sensitivity of modern mass spectrometers that confidently detect traces of unspecifically precipitating proteins. A recent approach to overcome this problem is based on the idea that reduced amounts of specific interaction partners will co-precipitate with a given target protein whose cellular concentration is reduced by RNAi, while the amounts of unspecifically precipitating proteins should be unaffected. This approach, termed QUICK for QUantitative Immunoprecipitation Combined with Knockdown⁴, employs Stable Isotope Labeling of Amino acids in Cell culture (SILAC)⁵ and MS to quantify the amounts of proteins immunoprecipitated from wild-type and knock-down strains. Proteins found in a 1:1 ratio can be considered as contaminants, those enriched in precipitates from the wild type as specific interaction partners of the target protein. Although innovative, QUICK bears some limitations: first, SILAC is cost-intensive and limited to organisms that ideally are auxotrophic for arginine and/or lysine. Moreover, when heavy arginine is fed, arginine-to-proline interconversion results in additional mass shifts for each proline in a peptide and slightly dilutes heavy with light arginine, which makes quantification more tedious and less accurate^{5,6}. Second, QUICK requires that antibodies are titrated such that they do not become saturated with target protein in extracts from knock-down mutants.

Here we introduce a modified QUICK protocol which overcomes the abovementioned limitations of QUICK by replacing SILAC for ¹⁵N metabolic labeling and by replacing RNAi-mediated knock-down for affinity modulation of protein-protein interactions. We demonstrate the applicability of this protocol using the unicellular green alga *Chlamydomonas reinhardtii* as model organism and the chloroplast HSP70B chaperone as target protein⁷ (Figure 1). HSP70s are known to interact with specific co-chaperones and substrates only in the ADP state⁸. We exploit this property as a means to verify the specific interaction of HSP70B with its nucleotide exchange factor CGE1⁹.

Video Link

The video component of this article can be found at <http://www.jove.com/video/4083/>

Protocol

1. Antibody Adsorption

1. Weigh out 120 mg of Protein A Sepharose in a 15-ml conical tube (Falcon). As 15 mg Protein A sepharose is needed for each immunoprecipitation (IP) this amount is sufficient for 8 IPs. Add 5 ml 0.1 M phosphate buffer (pH 7.4) and let the Protein A Sepharose swell for 30 min at 4 °C.

(Note that all steps from this point on need to be carried out with gloves to avoid contamination with keratin and on ice to avoid protein degradation/complex dissociation.)

2. Centrifuge for 60 sec at 1,000 x g and 4 °C to pellet the swollen Protein A Sepharose. Carefully remove the supernatant and resuspend the beads in 5 ml 0.1 M phosphate buffer (pH 7.4). Repeat this step three times to wash the beads thoroughly.
3. After the last centrifugation step, remove supernatant and leave approximately 0.5 ml of phosphate buffer. Add 0.9 ml 0.5 M phosphate buffer (pH 7.4), 400 µl affinity purified primary antibodies (50 µl per IP) against the target protein (here HSP70B), and 16 µl antibodies against a control protein (here CF1β). Fill up with ddH₂O to a total volume of 5 ml.

(Note that affinity-purified antibodies should be used to reduce contamination by unspecific IgGs, which interfere with nano-LC-MS analysis - for a protocol see Willmund et al. (2005)¹⁰. CF1β is precipitated as a loading control and was chosen because it is abundant and, after cell lysis, present in soluble and membrane fractions. Alternatively, levels of contaminating proteins may be used to normalize for unequal loading.)

4. Allow Protein A Sepharose beads to adsorb IgGs during a 1-hr incubation at 25 °C on a tube roller (CAT RM5W, 36 rpm).
5. Centrifuge for 60 sec at 1,000 x g and 4 °C to pellet the Protein A Sepharose beads. Carefully remove the supernatant and resuspend the beads in 5 ml 0.1 M sodium borate buffer (pH 9.0). Repeat this step three times to thoroughly remove amines that would quench the crosslinker.
6. Weigh out 25.9 mg of fresh, solid dimethylpimelimidate and resuspend it in 5 ml 0.1 M sodium borate buffer (pH 9.0) to obtain a final concentration of 20 mM. Add this solution to the Protein A Sepharose beads.
7. Allow IgGs to cross-link to Protein A for 30 min at 25 °C on a tube roller.
8. Centrifuge for 60 sec at 1,000 x g and 4 °C to pellet the beads. Carefully remove the supernatant and resuspend the beads in 5 ml 1 M Tris-HCl (pH 7.5) to quench free crosslinker. Repeat this step once and incubate for 2 hr at 25 °C or 12-24 hr at 4 °C on a tube roller.
9. Optional: if Protein A Sepharose beads coupled to IgGs are not directly used for IP, storage for up to one week is possible. For this, centrifuge for 60 sec at 1,000 x g and 4 °C to pellet the beads, carefully remove the supernatant and resuspend beads in 5 ml 0.1 M phosphate buffer (pH 7.5) containing 0.02% sodium azide and store at 4 °C until further use.

2. Cell Lysis, Crosslinking and Sample Preparation

1. Grow two *Chlamydomonas* cultures in medium containing 7.5 mM ¹⁴NH₄Cl or ¹⁵NH₄Cl as nitrogen source to a density of ~5 x 10⁶ cells/ml. Cells need to pass through at least ten generations for full labeling. Here, cells were grown photomixotrophically in TAP medium¹¹ on a rotatory shaker at 25 °C under continuous irradiation with white light (30 µE m⁻² s⁻¹).
2. Transfer two aliquots each of ¹⁴N- and ¹⁵N-labeled cells to four GSA tubes and harvest cells by a 4-min centrifugation at 4,000 x g and 4 °C *(The cell number harvested for each aliquot depends on the cellular concentration of the target protein and needs to be determined empirically in advance to ensure that sufficient target protein is precipitated. A good starting point is 10⁹ cells per aliquot, i.e., 200 ml of a culture with 5 x 10⁶ cells/ml.)*

For crosslinking only: in case protein complexes will be crosslinked prior to IP, cells need to be washed to remove amines present in the medium. For this, resuspend cells in 40 ml pre-cooled KH buffer (20 mM HEPES-KOH (pH 7.2), 80 mM KCl) and transfer them to 50-ml Falcon tubes. Centrifuge for 60 sec at 1,000 x g and 4 °C. Repeat this step once.

3. Resuspend cells in 2 ml Lysis buffer (20 mM HEPES-KOH (pH 7.2), 1 mM MgCl₂, 10 mM KCl, 154 mM NaCl) pre-cooled to 4 °C and transfer them to 15-ml Falcon tubes. Collect remaining cells in GSA tubes with an additional 1 ml Lysis buffer each. Add 50 µl 25 x protease inhibitor and 12.5 µl 1 M MgCl₂ (to a final concentration of 3.5 mM) to each aliquot.
4. Add 150 µl Lysis buffer, 12.5 µl 1 M ATP, 833 µl 270 mM creatine phosphate and 7 µl 5 µg/µl creatine phosphokinase (the final concentration is 2.5 mM ATP, 45 mM creatine phosphate, and 7 µg/ml creatine phosphokinase) to one of the aliquots containing ¹⁴N- and ¹⁵N-labeled cells (these are the +ATP aliquots).
5. Add 930 µl Lysis buffer and 70 µl 1 U/µl apyrase to the other aliquots containing ¹⁴N- and ¹⁵N-labeled cells (these are the -ATP aliquots).
6. Incubate for 2 min at 25 °C on a tube roller to establish ATP-deplete and ATP-replete states. If the crosslinking step is omitted, add another 1 ml of Lysis buffer.

For crosslinking only: in case the investigated protein-protein interactions are transient it is advisable to capture them by a crosslinking step. For this, add 500 µl 20 mM dithio-bis(succinimidyl propionate) (DSP) dissolved in DMSO (final concentration is 2 mM) to each tube directly before sonication.

7. Sonicate four times 20 sec on ice to break cells with 20-sec breaks in between for cooling. *(We use the Bandelin Sonoplus HD2070 with a KE76 tip at output control of 75% and duty cycle of 60%. The necessary settings for other machines/devices/tips need to be determined in advance to ensure complete cell lysis and to avoid spilling.)*

For crosslinking only: allow protein complexes to cross-link by incubating for 1 hr at 4 °C on a tube roller. After crosslinking, supplement each tube with 500 µl 1 M glycine and incubate on a tube roller for another 15 min at 4 °C to quench free crosslinker.

8. Prepare four 6-ml sucrose cushions (20 mM HEPES-KOH (pH 7.2), 0.6 M sucrose) in SW41 Ti thin wall tubes (Beckman Coulter Item No: 344059), carefully lay the entire ~5.5 ml of cell lysates onto the sucrose cushions (balance with Lysis buffer) and centrifuge for 30 min at 200,000 x g and 4 °C in a SW41 Ti rotor.
9. Transfer the top of the gradient containing soluble protein complexes into four 15-ml Falcon tubes (avoid transferring parts of the sucrose cushion), add 350 µl 10% Triton X-100 to a final concentration of 0.5% to each of them, mix carefully and add Lysis buffer to a total volume of 7 ml each.

(Transfer 70 µl of each soluble cell extract to fresh 1.5-ml conical tubes (Eppendorf tubes) and add 70 µl 2 x SDS-sample buffer (4% SDS, 125 mM Tris-HCl (pH 6.8), 20% glycerol, 10% 2-mercaptoethanol) to each for SDS-PAGE and immunoblot analyses.)

10. Discard the sucrose cushions and resuspend the membrane pellets in 3 ml Lysis buffer each. Add to each 1 ml 10% Triton X-100 to a final concentration of 2%, sonicate on ice to dissolve pellets, and add Lysis buffer to a total volume of 5 ml each.
11. Prepare another four 6-ml sucrose cushions in SW41 Ti thin wall tubes, lay the ~5 ml of solubilized membranes from step 2.10 carefully onto the sucrose cushions, and centrifuge for 30 min at 200,000 x g and 4 °C in a SW41 Ti rotor.
12. Transfer the top of the gradient containing membrane protein complexes into four 15-ml Falcon tubes and add Lysis buffer (containing 2% Triton X-100) to a final volume of 7 ml each. *(Transfer 70 µl of each soluble cell extract to fresh Eppendorf tubes and add 70 µl 2 x SDS-sample to each for SDS-PAGE and immunoblot analyses.)*

3. Immunoprecipitation

1. Pellet the Protein A Sepharose beads containing coupled antibodies (from steps 1.8 or 1.9) by a 60-sec centrifugation at 1,000 x g and 4 °C, carefully remove the supernatant and resuspend beads in 4 ml Lysis buffer. Repeat this step twice to equilibrate beads in Lysis buffer.
2. Fill up to 8 ml with Lysis buffer and transfer 1 ml of the suspension to each of the eight 15-ml Falcon tubes containing soluble or membrane protein complexes from ATP-replete and ATP-deplete ¹⁴N- and ¹⁵N-labeled cells (from step 2.9 and 2.12).
3. Incubate for 2 hr at 4 °C on a tube roller to precipitate protein complexes.
4. Pellet the beads by a 60-sec centrifugation at 1,000 x g and 4 °C and discard the supernatants. Leave a small volume of liquid on top of the beads to facilitate transfer.
5. Transfer the beads from each Falcon tube to 1.5-ml conical tubes (Eppendorf tubes). To collect all remaining beads in the Falcon tubes, add another 0.8 ml Lysis buffer containing 0.1% Triton to each, vortex gently, centrifuge for 60 sec at 1,000 x g and 4 °C and transfer the buffer with residual beads to the Eppendorf tubes. Tube exchange is necessary to prevent contaminations from proteins adhering to the plastic walls.
6. Pellet the beads by a 15-sec centrifugation at 16,100 x g and 4 °C, carefully remove the supernatants and resuspend beads in 1.3 ml Lysis buffer containing 0.1% Triton. Repeat this step twice with lysis buffer containing Triton and twice with Lysis buffer lacking Triton to thoroughly wash the beads. Leave a small volume of liquid on top of the beads to facilitate transfer.
7. Again transfer the beads to fresh 1.5-ml Eppendorf tubes to remove proteins adhering to the plastic walls. Wash the old tubes with 1 ml Lysis buffer lacking Triton and transfer all residual beads to the fresh tubes.
8. Centrifuge for 15 sec at 16,100 x g and 4 °C, remove the supernatants first with a normal pipette, then remove any remaining supernatant completely with a 50-µl Hamilton syringe.

4. Sample Preparation for nano-LC-MS/MS

1. Add 100 µl freshly prepared Elution buffer (8 M urea, 25 mM NH₄HCO₃) to each tube, use the 100 µl Elution buffer to wash off beads sticking to the Hamilton syringe and incubate for 10 min in a thermomixer at 800 rpm and 65 °C, and for another 20 min at 30 °C. *(A much more complete elution of bound proteins is achieved by elution with 2% SDS and subsequent precipitation with 80% acetone.)*
2. Centrifuge for 15 sec at 16,100 x g and 25 °C. Transfer supernatants to fresh tubes with a 50-µl Hamilton syringe.
3. Add 50 µl Elution buffer to the beads, use the 50 µl Elution buffer to wash off beads sticking to Hamilton syringe and repeat incubation and centrifugation steps 4.1 and 4.2, respectively. Pool the respective eluates.

(Transfer 30 µl of the eluates to fresh Eppendorf tubes, add 30 µl 2 x SDS-sample buffer to each for SDS-PAGE and immunoblot analyses.)

4. Combine the eluted precipitates from +/-ATP-treated, ¹⁴N- and ¹⁵N-labeled soluble and membrane proteins as follows:

120 µl ¹⁵N/+ATP and 120 µl ¹⁴N/-ATP

120 µl ¹⁴N/+ATP and 120 µl ¹⁵N/-ATP

120 µl ¹⁵N/+ATP and 120 µl ¹⁴N/-ATP

120 µl ¹⁴N/+ATP and 120 µl ¹⁵N/-ATP

5. Add 1.5 µl freshly prepared 1 M DTT to a final concentration of 6.5 mM to each of the four combinations to reduce disulfide bonds (including those in the crosslinker) and incubate for 30 min at 25 °C.
6. Add 10.5 µl freshly prepared 0.6 M iodoacetamide to a final concentration of 25 mM to carboxymethylate the reduced thiols and incubate for 20 min at 25 °C in the dark.
7. Add 256 µl 40 mM NH₄HCO₃ and 4 µl Lys-C (0.1 µg/µl), seal tubes with parafilm, and incubate for at least 16 hr overnight on a rotation wheel at 37 °C.
8. Add 470 µl 20 mM NH₄HCO₃, 10 µl 100 % acetonitrile (to a final concentration of 1%) and 8 µl trypsin beads, and incubate on a rotation wheel for at least 16 hr at 37 °C.
9. Centrifuge for 5 min at 16,100 x g and 4 °C, and transfer supernatants to fresh 2-ml Eppendorf tubes. Wash the old tubes with 50 µl 20 mM NH₄HCO₃, 0.5% acetic acid, and pool with first supernatants.
10. For desalting, prepare homemade C₁₈-StageTips by cutting out two discs from Empore C₁₈ material with a syringe needle and placing them in a 200-µl pipette tip. In this way prepare four 200-µl tips. Punch holes into the lids of four 2-ml Eppendorf tubes and insert tips.
11. Precondition the C₁₈-StageTips with 50 µl Solution B (80% acetonitrile, 0.5% acetic acid). Centrifuge for 3 min at 800 g and 25 °C.
12. Equilibrate the C₁₈-StageTips with 100 µl Solution A (0.5% acetic acid, 2% acetonitrile). Centrifuge for 3 min at 800 g and 25 °C. Repeat this step once.
13. Load 100 µl of the supernatants from the tryptic digestions (4.9) on the C₁₈-StageTips and centrifuge for 3 min at 800 g and 25 °C. Repeat this step until the complete supernatants were applied to the columns.
14. Wash the C₁₈-StageTips with 100 µl Solution A. Centrifuge for 3 min at 800 g and 25 °C. Repeat this step twice.

15. Elute tryptic peptides into a fresh 1.5-ml Eppendorf tube with 50 μ l Solution B. Centrifuge for 3 min at 800 g and 25 $^{\circ}$ C. Repeat this step once. Dry peptides to completion in a speed vac.
16. Optional: seal Eppendorf tubes with parafilm and store at -80 $^{\circ}$ C until further use.
17. Resuspend the dried peptides with 20 μ l Solution A and incubate for at least 1 hr on ice, interrupted by two 15-min incubations in a sonicator bath. Centrifuge for 20 min at 16,100 x g and 4 $^{\circ}$ C, and apply supernatant to nano-LC-MS/MS.

5. Representative Results

As shown exemplarily for the 14 N-labeled cell extracts in **Figure 2A**, HSP70B and CGE1 are almost exclusively localized to the soluble fraction, independent of the ATP state. In contrast, CF1 β is localized to soluble and membrane-enriched fractions, as sonication shears part of it from membrane-located CF $_{60}$, and therefore serves as loading control for both fractions. As shown in **Figure 2B**, similar amounts of HSP70B were precipitated with the anti-HSP70B antibodies from 14 N- and 15 N-labeled soluble extracts, independent of the ATP state. In contrast, only little HSP70B was precipitated from membrane fractions with slightly larger amounts originating from ATP-depleted membrane fractions as compared to ATP replete fractions, hence corroborating earlier results⁹. No CGE1 was co-precipitated with HSP70B in ATP-replete soluble or membrane fractions, while large amounts of CGE1 were co-precipitated with HSP70B from ATP-depleted soluble fractions, and little from ATP-depleted membrane fractions.

The interaction of CGE1 with HSP70B only in the ADP state is also observed in the MS analysis: in **Figure 3**, representative MS1 spectra of HSP70B and CGE1 peptides from precipitates generated with the HSP70B antiserum from soluble cell extracts are shown. In the experiment shown in **Figure 3A**, precipitates were from mixtures of 14 N-labeled extracts lacking ATP and 15 N-labeled extracts containing ATP. While the heavy and light labeled form of the HSP70B peptide were detected at equal intensities, only the light labeled form of the CGE1 peptide (from -ATP extracts) was found. In **Figure 3B** the same peptides from the anti-HSP70B precipitate derived from mixtures of reciprocally labeled soluble cell extracts are shown. Accordingly, this time only the heavy labeled form of the CGE1 peptide (from -ATP extracts) was detected, while this was again the case for both, light and heavy labeled HSP70B peptides.

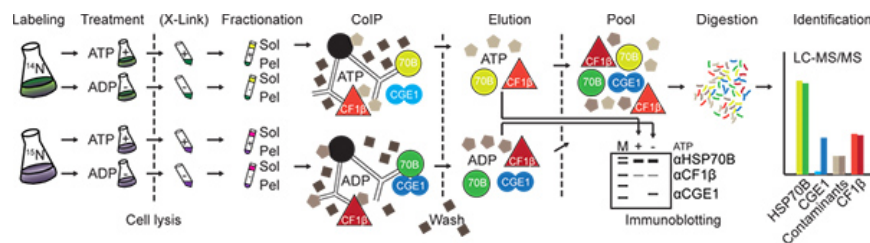


Figure 1. Experimental workflow. Cells are metabolically labeled with 14 N and 15 N for at least 10 generations, harvested and supplied with or depleted from ATP. After cell lysis protein complexes optionally may be crosslinked (X-link) with DSP. Lysed cells are then separated in soluble (Sol) and membrane enriched (Pel) fractions. Target proteins (here HSP70B) and a control protein (here CF1 β) are immunoprecipitated with specific antibodies coupled to protein A sepharose beads (black). After washing, precipitated proteins are eluted and either directly analyzed by immunoblotting, or the respective 14 N- and 15 N-labeled fractions in +ATP and -ATP states are pooled, digested and analyzed by nano-LC-MS/MS. In the example case shown here the 15 N-labeled fraction was depleted from ATP. Accordingly, the ratio of intensities of heavy labeled (dark colors) to light labeled (light colors) peptides from the control protein (CF1 β), the target protein (HSP70B) and non-specifically bound contaminants should be around one, while this ratio is expected to be very high for proteins specifically interacting with the target protein (CGE1). [Click here to view larger figure.](#)

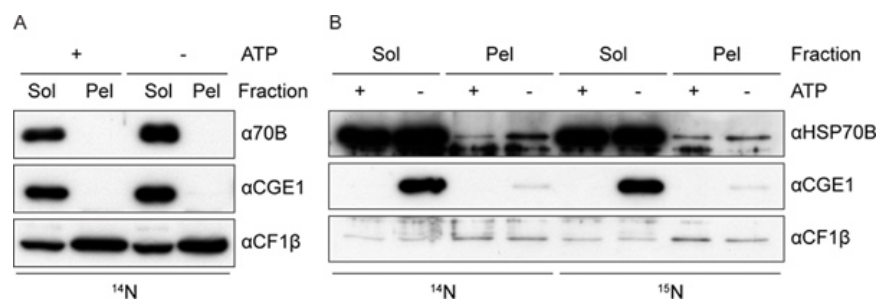


Figure 2. A Analysis of the input for HSP70B immunoprecipitation. Total protein was extracted from soluble (Sol) and membrane enriched (Pel) fractions either depleted from ATP (-ATP) or supplemented with ATP and an ATP regenerating system (+ATP). 0.01% of the protein extracts were separated on a 10% SDS-polyacrylamide gel, and levels of HSP70B and CGE1 protein relative to loading control CF1 β were analyzed by immunoblotting. **B Analysis of immunoprecipitates.** HSP70B was immunoprecipitated from 14 N- and 15 N-labeled soluble and membrane-enriched cell extracts containing or lacking ATP. Proteins corresponding to 3.3% of the immunoprecipitates were separated on a 10% SDS-

polyacrylamide gel and levels of HSP70B and CGE1 relative to loading control CF1 β were analyzed by immunoblotting. [Click here to view larger figure.](#)

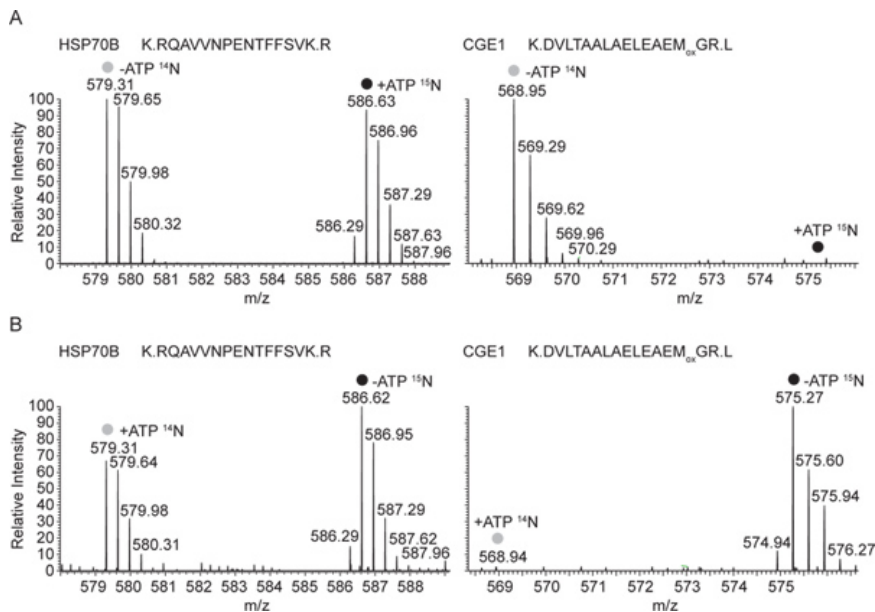


Figure 3. A Representative mass spectra of HSP70B and CGE1 peptides from anti-HSP70B immunoprecipitates performed on mixed soluble fractions (^{14}N -ATP/ ^{15}N +ATP). Full MS spectra of ^{14}N and ^{15}N labeled peptides, corresponding to the -ATP and +ATP states, respectively, from HSP70B and co-immunoprecipitated CGE1 are shown. Both peptides are triply charged, the HSP70B peptide contains 22 nitrogen atoms, the CGE1 peptide 19, corresponding to a mass shift of 7.33 and 6.33 m/z, respectively. **B Representative mass spectra from the reciprocal experiment (^{14}N +ATP/ ^{15}N -ATP).** Full MS spectra of the same ^{14}N and ^{15}N labeled peptides, here corresponding to the +ATP and -ATP states, respectively, from HSP70B and co-immunoprecipitated CGE1 are shown. [Click here to view larger figure.](#)

Discussion

We have recently introduced two improvements to the QUICK approach: a crosslinking step for capturing transient protein-protein interactions (QUICK-X), and a control precipitation to normalize for unequal precipitation efficiencies⁶. Here we present a protocol containing two more improvements of QUICK: first, we replace SILAC⁵ for ^{15}N metabolic labeling. The advantages are that ^{15}N metabolic labeling is much cheaper than SILAC, if ^{15}N is provided as simple inorganic salt. Furthermore, with ^{15}N metabolic labeling QUICK can be applied to organisms prototrophic for all amino acids, like most plants, fungi and bacteria. And finally, arginine-to-proline interconversion inherent to SILAC^{5,6} does not present a problem for quantification of ^{15}N labeled peptides. Examples for suitable tools for the quantitative evaluation of ^{15}N proteomics data are MSQUANT¹² or IOMIQS¹³.

Second, we introduce affinity modulation as a means for specifically reducing the amount of proteins interacting with a given target protein in one sample versus another. The advantages of this approach are that it circumvents the construction of knockdown mutants, which for some model systems are difficult to generate or cannot be generated at all in case of essential target proteins. Moreover, it avoids misinterpretations caused by differential protein expression potentially occurring as a response of the cell to knocking-down a target protein: if other proteins are down-regulated as well and cross-react with the antiserum used for immunoprecipitation, they would be interpreted as true interaction partners of the target protein. At last, affinity modulation abolishes the need of finding a proper antibody-to-antigen ratio.

Although we apply our protocol to *Chlamydomonas reinhardtii* as model organism, it can easily be adapted to any other organism that can be grown in cell culture and is able to use ammonium or nitrate as nitrogen source. Affinity modulation of protein complexes by ATP/ADP may directly be applied to other chaperones whose interaction with substrates and cohort proteins depends on the ATP state, like the GroEL/HSP60/Cpn60 or HSP90 chaperone systems^{14,15}, or to any other system where binding affinities are modulated by ATP. Affinity modulation should also work for cases where affinities between protein interactions are altered by specific drugs, like radicicol or geldanamycin in the case of HSP90 systems¹⁵.

A clear limitation of our protocol is that it requires affinity-purified antibodies against a target protein known to be sensitive to a specific treatment/drug that modulates its affinity for partner proteins. Therefore, it is no high-throughput method.

Disclosures

No conflicts of interest declared.

Acknowledgements

We thank Olivier Vallon for the antiserum against CF1 β . This work was supported by the Max Planck Society and grants from the Deutsche Forschungsgemeinschaft (Schr 617/5-1) and the Bundesministerium für Bildung und Forschung (Systems Biology Initiative FORSYS, project GoFORSYS).

References

1. Perrakis, A., Musacchio, A., Cusack, S., & Petosa, C. Investigating a macromolecular complex: the toolkit of methods. *J. Struct. Biol.* **175**, 106-112 (2011).
2. Gavin, A.C., Maeda, K., & Kuhner, S. Recent advances in charting protein-protein interaction: mass spectrometry-based approaches. *Curr. Opin. Biotechnol.* **22**, 42-49 (2011).
3. Markham, K., Bai, Y., & Schmitt-Ulms, G. Co-immunoprecipitations revisited: an update on experimental concepts and their implementation for sensitive interactome investigations of endogenous proteins. *Anal. Bioanal. Chem.* **389**, 461-473 (2007).
4. Selbach, M. & Mann, M. Protein interaction screening by quantitative immunoprecipitation combined with knockdown (QUICK). *Nat Methods.* **3**, 981-983 (2006).
5. Ong, S.E. & Mann, M. A practical recipe for stable isotope labeling by amino acids in cell culture (SILAC). *Nat Protoc.* **1**, 2650-2660 (2006).
6. Heide, H., et al. Application of quantitative immunoprecipitation combined with knockdown and cross-linking to *Chlamydomonas* reveals the presence of vesicle-inducing protein in plastids 1 in a common complex with chloroplast HSP90C. *Proteomics.* **9**, 3079-3089 (2009).
7. Nordhues, A., Miller, S.M., Muhlhaus, T., & Schroda, M. New insights into the roles of molecular chaperones in *Chlamydomonas* and *Volvox*. *International review of cell and molecular biology.* **285**, 75-113 (2010).
8. Mayer, M.P. & Bukau, B. Hsp70 chaperones: cellular functions and molecular mechanism. *Cell Mol. Life Sci.* **62**, 670-684 (2005).
9. Schroda, M., Vallon, O., Whitelegge, J.P., Beck, C.F., & Wollman, F.A. The chloroplastic GrpE homolog of *Chlamydomonas*: two isoforms generated by differential splicing. *The Plant Cell.* **13**, 2823-2839 (2001).
10. Willmund, F. & Schroda, M. HEAT SHOCK PROTEIN 90C is a bona fide Hsp90 that interacts with plastidic HSP70B in *Chlamydomonas reinhardtii*. *Plant Physiol.* **138**, 2310-2322 (2005).
11. Harris, E.H. The *Chlamydomonas* Sourcebook: Introduction to *Chlamydomonas* and Its Laboratory Use., Elsevier, Academic Press, San Diego, CA, (2008).
12. Mortensen, P., et al. MSQuant, an open source platform for mass spectrometry-based quantitative proteomics. *J. Proteome Res.* **9**, 393-403 (2010).
13. Muhlhaus, T., Weiss, J., Hemme, D., Sommer, F., & Schroda, M. Quantitative Shotgun Proteomics Using a Uniform ¹⁵N-Labeled Standard to Monitor Proteome Dynamics in Time Course Experiments Reveals New Insights into the Heat Stress Response of *Chlamydomonas reinhardtii*. *Mol. Cell Proteomics.* **10**, M110 004739 (2011).
14. Bukau, B. & Horwich, A.L. The Hsp70 and Hsp60 chaperone machines. *Cell.* **92**, 351-366 (1998).
15. Wandinger, S.K., Richter, K., & Buchner, J. The Hsp90 chaperone machinery. *J. Biol. Chem.* **283**, 18473-18477 (2008).

3.4. MANUSCRIPT 1: DISSECTION OF THE HEAT STRESS RESPONSE IN CHLAMYDOMONAS REVEALS A ROLE FOR CHLOROPLAST HSP70B IN STRESS SIGNALING.

Authors:

Stefan Schmollinger*, Miriam Schulz-Raffelt*, Daniela Strenkert, Daniel Veyel, Olivier Vallon and Michael Schroda

Manuscript currently submitted for publication

Contribution to:

Figure 5

Figure 6

Figure 7

Dissection of the heat stress response in *Chlamydomonas* reveals a role for chloroplast HSP70B in stress signaling

Stefan Schmollinger^{1,2*}, Miriam Schulz-Raffelt^{3*}, Daniela Strenkert^{1,2}, Daniel Veyel², Olivier Vallon⁴ and Michael Schroda^{1,2}

*equal contribution

¹ Molekulare Biotechnologie & Systembiologie, TU Kaiserslautern, Paul-Ehrlich-Str. 23, D-67663 Kaiserslautern, Germany

² Max-Planck-Institut für Molekulare Pflanzenphysiologie, Am Mühlenberg 1, D-14476 Potsdam-Golm, Germany

³ CEA–CNRS–Université Aix Marseille, Institut de Biologie Environnementale et Biotechnologie – UMR 6191 CEA Cadarache – 13108 Saint-Paul-lez-Durance, France

⁴ Institut de Biologie Physico-Chimique, UMR 7141 CNRS/Université Pierre et Marie Curie, F-75005 Paris, France

Corresponding author: Michael Schroda

Tel.: + 49 (0)631 205-2697

Fax: + 49 (0)631 205-2999

e-mail: schroda@biologie.uni-kl.de

Running title: Regulation of the *Chlamydomonas* stress response

Key words: heat shock factor; calcium; unfolded proteins; stress response; inhibitor feeding; *Chlamydomonas reinhardtii*; HSP90; HSP70; protein folding

Word count:

Summary	243
Introduction	335
Results	2497
Discussion	1600
Experimental Procedures	803
Acknowledgments	39
Figure Legends	1462
Total	6979

Summary

To understand fundamental concepts of the heat stress response (HSR) in plants, we applied pharmaceutical and antisense/amiRNA approaches to the unicellular green alga *Chlamydomonas reinhardtii*. Feeding with the protein kinase inhibitor staurosporine strongly retarded the HSR. Activation of stress kinase(s) appears to be triggered by the accumulation of unfolded proteins, as demonstrated by the induction of the stress response after feeding cells with the arginine analog canavanine. Feeding with cycloheximide, an inhibitor of cytosolic protein synthesis, abolished the attenuation of the HSR. Feeding with HSP90 inhibitors induced a stress response under ambient conditions and retarded attenuation of the HSR at elevated temperatures. We detected a direct physical interaction between cytosolic HSP90A/HSP70A and HSF1, but surprisingly this interaction persisted after the onset of stress. Of the calcium chelators EGTA and BAPTA, only the addition of BAPTA to washed cells retarded the HSR and impaired thermotolerance. Finally, the expression of antisense constructs targeting chloroplast HSP70B resulted in a pleiotropic disturbance of the cell's HSR. We propose the following hypothetical model to integrate these results: heat stress is sensed at a calcium channel in the cytoplasmic membrane by changes of membrane fluidity, or by sequestration of HSP90/70 from this channel to unfolded proteins accumulating during heat stress or after feeding with canavanine or HSP90 inhibitors. Calcium inflow results in the activation of calcium dependent kinases phosphorylating HSF1, at which also stress signals from the chloroplast are integrated. Attenuation of the HSR is mediated by chaperone-assisted phosphatase(s).

Introduction

The engineering of crop plants that are resistant to heat, drought and salinity stress is essential for guaranteeing crop yield safety, which is jeopardized by the changing climate. To this end a thorough understanding of the mechanisms underlying stress response pathways in plants is imperative. The heat stress response (HSR), which results in the induction of heat shock proteins (HSPs), is regulated at the transcriptional level by the activity of heat shock factors (HSFs) (Akerfelt *et al.* 2010, Anckar and Sistonen 2011, Kotak *et al.* 2007, Mittler *et al.* 2012, Voellmy and Boellmann 2007). This highly conserved cellular response is elicited by diverse environmental and physiological stressors including elevated temperatures, heavy metals, oxidants, toxic chemicals or bacterial and viral infection. These stressors disturb membrane integrity and/or lead to the accumulation of misfolded/aggregated proteins. In mammals, HSFs are activated in a multistep process that includes trimerization, phosphorylation and translocation to the nucleus, where HSF binds to heat shock elements (HSEs) at the promoters of *HSP* genes in a cooperative manner (Morimoto 1998). Hyperphosphorylation at multiple serine residues typically characterizes the transcriptionally competent state of HSFs (Cotto *et al.* 1996). The induction of HSPs allows the cell to restore protein homeostasis, at which time HSF is inactivated and the response is attenuated (Shi *et al.* 1998).

The high complexity of the HSF family in higher plants with at least 21 members (Nover *et al.* 2001) has complicated the dissection of the HSR in plants (Hahn *et al.* 2011, von Koskull-Doring *et al.* 2007). In contrast, the presence of only one canonical HSF in *Chlamydomonas reinhardtii* that exhibits all characteristic features of plant class A HSFs and that was shown to be a key regulator of the HSR (Schmollinger *et al.* 2010, Schulz-Raffelt *et al.* 2007), makes this alga an attractive model for studying fundamental principles of the plant HSR. To this end, we combined pharmaceutical and antisense/artificial micro-RNA approaches which have enabled us to gain new insights of how the HSR is regulated in this model alga.

Results

Kinase-mediated hyperphosphorylation of HSF1 is essential for transcriptional activation of HSF1

Hyperphosphorylation of HSFs has been recognized as an essential step for their activation (Cotto *et al.* 1996, Liu *et al.* 2008). That this was the case also in *Chlamydomonas* was suggested by our previous finding that during heat shock HSF1 hyperphosphorylation correlated with the accumulation of stress gene expression (Schulz-Raffelt *et al.* 2007). To substantiate this notion, we fed *Chlamydomonas* cells immediately before applying heat stress with different concentrations of the protein kinase inhibitor staurosporine. Staurosporine competes with ATP for binding to the ATP-binding sites of a broad spectrum of kinases (Karaman *et al.* 2008). We monitored the accumulation of stress gene transcripts over time and for this chose the *HSF1* gene itself because it displayed a very fast response to stress (Schulz-Raffelt *et al.* 2007) and, more arbitrary, the *HSP90A* and *HSP90C* genes encoding cytosolic and chloroplast-targeted chaperones (Willmund and Schroda 2005).

As shown in Figures 1a and 1b, staurosporine feeding resulted in a concentration-dependent delay of the HSR of all three genes analyzed. At high staurosporine concentrations also the amplitude of the response was reduced. The delayed accumulation of stress gene transcripts correlated well with delayed hyperphosphorylation of HSF1, which is reflected by its shifting to forms of higher apparent molecular mass (Schulz-Raffelt *et al.* 2007) and became evident particularly at higher concentrations of the drug (Figure 1c). Under these conditions also no increase in HSP90C protein levels was observed and after 2 h heat shock cells tended to lyse.

Preexisting HSF1 is sufficient to mediate a stress response but newly synthesized, cytosolic proteins are required for attenuation

We next asked whether cytosolic or organellar protein biosynthesis is required for regulating any steps in the HSR of *Chlamydomonas*. To address this question we fed cells prior to heat shock with cycloheximide and chloramphenicol, potent inhibitors of cytosolic and organellar translation elongation, respectively, that are effective in *Chlamydomonas* (Hooper and Blobel 1969). As shown in Figures 2a and 2b, feeding with chloramphenicol had no significant effect on transcript accumulation kinetics of the three stress genes analyzed. Feeding with cycloheximide had no effect on the initial kinetics of stress gene transcript accumulation, but abolished the attenuation phase of the HSR, as transcripts continued to accumulate. At the protein level, feeding with chloramphenicol prior to heat stress application hardly had an effect on the kinetics of HSF1 hyperphosphorylation and accumulation of HSF1 and HSP90C proteins. Feeding with cycloheximide had no effect on HSF1 hyperphosphorylation. However, hyperphosphorylation persisted throughout the stress treatment and, as expected for an inhibitor of cytosolic protein synthesis, protein levels neither of HSF1 nor of HSP90C increased.

The stress response in *Chlamydomonas* is elicited by unfolded proteins

The observation that a stress response was elicited by the injection of denatured proteins into *Xenopus laevis* oocytes founded the concept that unfolded proteins accumulating *e.g.* during thermal stress may serve as trigger for the HSR (Ananthan *et al.* 1986). To test whether also in *Chlamydomonas* a stress response is elicited by the accumulation of unfolded proteins, we fed an arginine auxotrophic *Chlamydomonas* mutant with the amino acid analog canavanine or with arginine as control. Canavanine is incorporated into newly synthesized proteins in place of arginine, but it contains an oxygen atom instead of the third methylene group within the side chain of arginine, which perturbs secondary structure formation. Canavanine feeding has been shown previously to elicit stress responses in mammalian cells (Hightower and White 1981, Watowich and Morimoto 1988) and in *Arabidopsis* (Kurepa *et al.* 2003). As shown in Figures 3a and 3b, the feeding of canavanine at ambient temperatures indeed elicited a stress response, albeit with slower kinetics than heat shock. Most likely, heat shock leads to the rapid accumulation of unfolded proteins, whereas the accumulation of unfolded proteins after canavanine feeding depends on the translation rate. The canavanine-induced stress response did not attenuate, as judged from the observation that stress gene transcripts remained high or even increased further after 2 h at elevated temperatures. Combining heat stress and canavanine feeding induced the stress response with the same initial kinetics as heat shock alone but attenuation of the response did not take place. At the protein level, incorporation of canavanine into newly synthesized HSP90C became evident from its shifting to an increased apparent molecular mass over time, in particular during heat shock (Figure 3c).

Inhibition of HSP90 activity results in an increased and prolonged stress response

It was observed previously that compromising HSP90 function impaired the refolding of heat-denatured proteins in mammalian cells (Schneider *et al.* 1996). To test whether this was the case also in *Chlamydomonas*, we employed the HSP90 inhibitors radicicol and geldanamycin. These mimic the kinked conformation of ATP that is required for its binding to the ATP-binding sites of HSP90s (Roe *et al.* 1999). We first used radicicol, as radicicol efficiently inhibited the ATPase activity of *Chlamydomonas* chloroplast HSP90C *in vitro* (Willmund and Schroda 2005). As presented in Figures 4a and 4b, feeding of radicicol prior to heat shock resulted in increased amplitude and delayed attenuation of the accumulation of all stress transcripts studied. Both effects were augmented with increasing concentrations of radicicol (100 μ M *versus* 10 μ M). Increased amplitude and delayed attenuation of stress gene transcript accumulation were also observed when geldanamycin (3.6 μ M) was fed to the cells prior to stress (Figures 4c and 4d).

Feeding cells with high concentrations of geldanamycin elicits a transient stress response at ambient temperatures

Feeding mammalian cells at ambient temperatures with geldanamycin was shown to elicit a stress response (Ali *et al.* 1998, Zou *et al.* 1998). Interestingly, when we fed *Chlamydomonas* cells with the same geldanamycin concentrations (3.6 μ M) that apparently were sufficient to

compromise HSP90 function during stress, we did not observe a stress response (Figure S1a). However, higher geldanamycin concentrations (10-20 μM) and high radicicol concentrations (100 μM) did induce a stress response at ambient temperatures (Figures 5a and 5b; Figure S1b). The induced stress response appeared to be general, as judged from the induction of genes encoding HSF1, cytosolic HSP90A and plastidic HSP70B, and also resulted in elevated HSF1 and HSP90C protein levels (Figure 5c). Note that the drug-induced stress response was weaker and less rapid than that induced by heat shock (compare Figures 4a and 5a). While the response was attenuated for genes *HSF1* and *HSP70B*, it appeared to persist for *HSP90A*.

In mammals it was found that a complex between HSF1 and HSP90 was disrupted by heat stress, an important finding for the suggestion that HSP90 controls HSF1 activity (Zou *et al.* 1998). To test whether also in *Chlamydomonas* a physical interaction between HSP90A and HSF1 exists that is disrupted by heat stress, we immunoprecipitated HSF1 from wild-type and an *HSF1*-amiRNA strain that were unstressed or subjected to heat shock for 30 min. HSP90A and HSP70A were then detected in the precipitates by immunoblotting (Figure 6). HSP90A and HSP70A were clearly detected in precipitates from control cells, but to a much lesser extent in precipitates from *HSF1*-amiRNA strains, indicating that both chaperones specifically interact with HSF1. Surprisingly, the interaction between HSF1 and the chaperones was observed both under heat stress and under control conditions. Interestingly, in contrast to HSP70A, levels of HSP90A in the *HSF1*-amiRNAi strain were slightly lower than in the control strain, presumably because HSF1 also plays a role in controlling basic transcription of the *HSP90A* gene.

Chlamydomonas cells induce a HSR also in the presence of calcium chelators

It was previously reported that removal of extracellular Ca^{2+} by washing and application of Ca^{2+} -chelators EGTA or BAPTA completely abolished the HSR in *Physcomitrella patens* (Saidi *et al.* 2009). These results indicate a crucial role for the influx of extracellular Ca^{2+} in stress signalling in moss. To test whether a similar mechanism is also present in *Chlamydomonas*, we removed extracellular Ca^{2+} by extensive washing in distilled water and resuspended cells in distilled water supplemented with high concentrations of EGTA or BAPTA prior to applying heat stress. As shown in Figures 7a and 7b, kinetics and amplitude of the heat stress-induced expression of genes *HSF1*, *HSP90A* and *HSP90C* appeared unaffected in washed cells resuspended in 20 mM EGTA. Moreover, the presence of EGTA at concentrations of 10 or 20 mM neither affected the heat stress-induced accumulation of HSF1 protein (Figure 7c), nor the ability of cells to survive a 2-h heat shock at 40°C (Figure 7d). In contrast, the addition of BAPTA to washed cells prior to heat shock did affect the HSR: as shown in Figures 7a and 7b, the presence of 7.5 mM BAPTA led to delayed kinetics and reduced amplitude of heat shock-induced stress gene expression. Moreover, the presence of BAPTA at 1 and 7.5 mM final concentrations delayed and reduced the stress-induced accumulation of HSF1 protein (Figure 7c) and resulted in reduced survival of heat-stressed cells (Figure 7d).

The expression of *HSP70B* antisense constructs pleiotropically affects the general stress response

To test, whether a mechanism for stress detection/stress signal relay to the nucleus might exist in chloroplasts, we generated antisense constructs that target *HSP70B* transcripts encoding the major HSP70 homolog in the *Chlamydomonas* chloroplast (Schroda and Vallon 2008). As a complete loss of function of chloroplast HSP70 was shown to be lethal (Su and Li 2008), we chose an antisense approach, which in *Chlamydomonas* produces only weak underexpression phenotypes (Schroda 2006, Schroda *et al.* 1999). As a vehicle for antisense expression we used the *ble* gene driven by the strong *HSP70A-RBCS2* promoter fusion (Schroda *et al.* 2002) and inserted the *HSP70B* antisense part between the *ble* coding region and the 3' UTR of *RBCS2* (Figure 8a). To avoid off-target effects, we used for the antisense part only 253 nt of the extreme 5' region of the *HSP70B* transcript, comprising the 5' UTR and the sequence encoding the chloroplast transit peptide. The antisense construct and a control construct lacking the antisense part were transformed into *Chlamydomonas* and transformants were directly selected for zeocin resistance. *HSP70B* and *ble* transcript accumulation were then monitored under non-stress and heat-shock conditions in ten randomly picked transformants carrying the antisense construct and in three containing the control construct.

Four types of *ble* transcripts were detected (Figure 8b): those originating from the *RBCS2* promoter at 25°C from control (T4) and antisense constructs (T2); and those originating from the *HSP70A* promoter after heat shock from control (T3) and antisense constructs (T1). As judged from the signal intensities observed after hybridization with a probe detecting the extreme 253 nt of the *HSP70B* transcript, the antisense construct was expressed at levels similar to those of the endogenous *HSP70B* gene under both, non-stress and heat-shock conditions (Figure 8b). Despite these high levels of *HSP70B* antisense RNA, the effects on the expression of endogenous *HSP70B* appeared to be rather modest: *HSP70B* mRNA levels were only slightly decreased in transformant 9-13 under non-stress conditions, but strongly decreased in transformants 9-5 and 9-13 after heat shock (Figure 8b). In these two transformants the normally observed ~2.4-fold increase in HSP70B protein levels after heat shock (Mühlhaus *et al.* 2011) was also abolished (Figure 8c).

Interestingly, in Coomassie-stained gels we noticed that transformants 9-5 and 9-13 also exhibited impaired accumulation of a ~20-kD heat shock-inducible protein (Figure 8d), presumably HSP22A, C, or E/F which were found previously to be strongly induced by heat stress (Mühlhaus *et al.* 2011). To test whether the *HSP70B*-antisense strains were impaired also in the expression of other proteins, we performed [¹⁴C]-acetate pulse-labeling experiments with *HSP70B*-antisense strains 9-5 and 9-13, and strain 1-2 containing the control construct. At 25°C, protein labeling was about identical in all three strains, suggesting that expression of the *HSP70B*-antisense construct had no visible effect under non-stress conditions (Figure 9). During heat stress, the labelling pattern changed drastically, with very few protein bands common with the control condition. This suggests a complete reorientation of the protein translation landscape under heat stress. In *HSP70B*-antisense strains, the expression of several

heat shock proteins was impaired during heat shock, including that of small HSPs in the 20 kDa range.

While the downregulation of HSF1 affected virtually all HSPs (Schulz-Raffelt *et al.* 2007), that of HSP70B was expected to affect only chloroplast protein biogenesis and folding. We were thus surprised to see this general effect on all HSPs, and wondered whether it was manifested at the transcriptional or translational level. We therefore monitored the kinetics of transcript accumulation during heat shock of four different heat shock genes in two *HSP70B*-antisense and one control strain (Figure 10). The genes selected encode HSP70B, its co-chaperone CGE1, cytosolic HSP70A and mitochondrial HSP70C, *i.e.*, chaperones from different cell compartments. Since the two *HSP70B*-antisense strains 9-5 and 9-13 became silenced in the meantime - a frequently observed phenomenon in *Chlamydomonas* (Schroda 2006) - we used two newly generated *HSP70B*-antisense strains termed 9-31 and 9-32. Compared to control strain 1-2, expression kinetics of all four heat shock genes analyzed were delayed, especially in strain 9-32 where also no attenuation was observed over the 60 min of the experiment. Larger differences in the initial expression kinetics were observed for *CGE1* and *HSP70A* as compared to *HSP70B* and *HSP70C*. Hence, translation rates of HSP70A and HSP70B in the *HSP70B*-antisense strains would be expected to be close to those of the control strain at an early stage of the heat shock, whereas those of CGE1 and HSP70C should be slower. Over all we can conclude that the expression of *HSP70B*-antisense constructs leads to a pleiotropic delay of the general stress response in *Chlamydomonas*.

Discussion

Stress signaling in *Chlamydomonas* is relayed via kinases to HSF1

The following evidence indicates that like in *Arabidopsis* (Liu *et al.* 2008), heat stress signals are propagated via kinases and relayed to HSF1 also in *Chlamydomonas*: (i) Heat stress-induced HSF1 hyperphosphorylation correlates with the accumulation of heat shock gene transcripts (Schulz-Raffelt *et al.* 2007). (ii) Inhibition of protein kinases by staurosporine delays the heat stress response (HSR) in a dose-dependent manner, correlating with delayed HSF1 hyperphosphorylation (Figure 1) (iii) Feeding with the cytosolic protein synthesis inhibitor cycloheximide blocks HSF1 in the hyperphosphorylated state, resulting in continuous expression of *HSP* genes (Figure 2). As HSF1 is a constitutive trimer (Schulz-Raffelt *et al.* 2007), its activation appears to depend solely on its hyperphosphorylation. Because staurosporine displays little selectivity, we can draw conclusions neither on the nature of the stress kinase(s) involved nor on their position within the signaling cascade.

An unfolded protein response in the chloroplast?

Challenging the function of chloroplast HSP70B by the expression of antisense constructs resulted in a pleiotropic disturbance of the entire cell's HSR (Figures 8-10). This finding suggests that like in the ER (Parmar and Schroder 2012) and in mitochondria (Pellegrino *et al.* 2012) the stress state of the chloroplast is sensed and transmitted to the nucleus. The apparent generality of the effect suggests that the chloroplast-derived signal is integrated at the level of HSF1. This is supported by the complete lack of transcription of the *HSP90C* gene, encoding a chloroplast chaperone, in *HSF1*-RNAi strains (Schulz-Raffelt *et al.* 2007). If stress-induced expression of chloroplast-targeted chaperones was realized by an *HSF1*-independent pathway, like the UPR in mitochondria and the ER, heat shock in *HSF1*-RNAi strains would be expected to induce transcription of *HSP90C*. As the effect exerted by expression of *HSP70B* antisense constructs resembles that of staurosporine feeding (compare Figures 1b and 10b), we speculate that constitutive employment of the chloroplast-to-nucleus stress signaling pathway in *HSP70B*-antisense strains might lead to a desensitizing of kinase-mediated HSF1 activation.

How does *Chlamydomonas* sense heat/proteotoxic stress?

The issue of how plants sense heat stress is still controversial (Mittler *et al.* 2012). The most popular view lend from data on mammalian cells (Morimoto 1998, Voellmy and Boellmann 2007) is that proteotoxic stress occurring under several stress conditions is sensed at the level of HSP90-HSF complexes. According to this hypothesis, HSP90 acts as a repressor by preventing activation of HSF. Once HSF is activated it mediates the expression of heat stress genes. Accumulating chaperones restore protein homeostasis and a surplus of newly synthesized HSP70 interacts with the transactivation domain of DNA-bound HSF to inactivate it, eventually leading to the attenuation of the stress response (Shi *et al.* 1998). This view was challenged recently by the work of Goloubinoff and co-workers on moss, who proposed that heat stress

is sensed by the inflow of extracellular Ca^{2+} through a Ca^{2+} -permeable channel in the plasma membrane (Saidi *et al.* 2009). According to this hypothesis, changes in membrane fluidity caused by elevated temperatures or chemicals open the channel and Ca^{2+} influx activates a calmodulin-dependent kinase (Liu *et al.* 2008). From the results presented in this study, can we draw any conclusions on the mechanism by which stress sensing is realized in *Chlamydomonas*? In favour of a role for extracellular Ca^{2+} , we observe that the addition of the Ca^{2+} chelator BAPTA to washed cells results in a delayed and less pronounced accumulation of stress gene transcripts, correlating with reduced thermotolerance (Figure 7). Surprisingly, however, EGTA had no effect, while both chelators were shown to completely abolish the HSR in moss (Saidi *et al.* 2009). As BAPTA is not membrane permeable, it appears unlikely that BAPTA affects intracellular Ca^{2+} levels. However, our data may be explained by the presence of two different pools of extracellular Ca^{2+} contributing to the stress response, one of which would be accessible to BAPTA, but neither to EGTA. However, as BAPTA and its derivatives are known to exert effects that are independent of their Ca^{2+} -binding properties (Lancaster and Batchelor 2000, Saoudi *et al.* 2004), we cannot rule out that BAPTA interferes with another process involved in stress sensing, *e.g.* by compromising the function of a stress sensor on the membrane surface. The notion of a direct control of HSF1 activity by an interaction with HSP70A/HSP90A also has its problems. We have found that in *Chlamydomonas* HSF1 interacts with these chaperones, both before and 30 min after the onset of heat stress, with similar efficiency (Schulz-Raffelt *et al.*, 2007; Figure 6). After 30 min heat shock, HSF1 binding to *HSP* gene promoters is strong and accumulation of *HSP* gene transcripts is at its peak (Schulz-Raffelt *et al.* 2007, Strenkert *et al.* 2011). If HSP90A was repressing HSF1 activity, its interaction with HSF1 would be expected to be disrupted soon after the onset of stress (Zou *et al.* 1998). Perhaps the constitutive interaction of HSF1 with HSP90A/HSP70A is required for nucleosome removal during transactivation, or for the maximal activation of paused polymerase II, as suggested previously (Floer *et al.* 2008, Sawarkar *et al.* 2012)?

Apparently in favour of a role for HSP90A in controlling HSF1 activity, however, is the observation that feeding of HSP90 inhibitors geldanamycin and radicicol elicited a stress response (Figure 5; Figure S1b). This is a common phenomenon in eukaryotic cells ranging from yeast (Duina *et al.* 1998), *Xenopus* (Ali *et al.* 1998), mammals (Zou *et al.* 1998), moss (Saidi *et al.* 2009) to *Arabidopsis* (Yamada *et al.* 2007), and is fundamental for the hypothesis that HSP90 is a suppressor of HSF activation (Voellmy and Boellmann 2007). However, the kinetics of the effect is not consistent with the hypothesis of a release from HSP90 inhibition: stress gene transcripts were detectable only 30 min after feeding cells even with high concentrations of geldanamycin (Figure 5; Figure S1b), instead of the immediate response expected. Radicicol exerted its effect faster, yet not faster than heat shock. Rather than a delayed uptake of the inhibitors by the cell, we speculate that they activate HSF1 transcription indirectly, by promoting a proteotoxic response, as detailed below. Note that radicicol could also trigger a stress response directly, independent of HSP90 inactivation. This scenario is supported by the finding that exposing *Arabidopsis* to radicicol led to the up-regulation of 8.5 x more genes than

did feeding with geldanamycin and even of 2.6 x more genes than did heat stress (Yamada *et al.* 2007).

How can the relatively slow induction of the stress response by geldanamycin feeding be explained? As HSP70A and HSP90A are the only abundant and constitutively expressed molecular chaperones in the *Chlamydomonas* cytosol (Mühlhaus *et al.* 2011), they are both likely to be important for maintaining protein homeostasis. That this is true for HSP90s is indicated by the observation that geldanamycin increased the amplitude and duration of the HSR even at low concentrations (3.6 μ M) that do not elicit a stress response (Figure 4 and Figure S1a). Cytosolic HSP90 was shown not to be required for general protein folding, but to play an important role in the maturation of a select group of proteins whose folding is inherently problematic, among them many proteins involved in signal transduction (Nathan *et al.* 1997, Pratt and Toft 2003). During heat stress, HSP90 might stabilize partially unfolded protein conformations, prevent further unfolding, and thereby facilitate a more rapid recovery (Nathan *et al.* 1997). Compromising the function of HSP90A by high concentrations of geldanamycin or radicicol is likely to result in the accumulation of unfolded HSP90 clients (Rutherford and Lindquist 1998). HSP70A might be able to bind these clients, but not to fold them as they depend on a specific interaction with HSP90. Such a buffering effect by a chaperone like HSP70A appears supported by (i) the inability of low concentrations of geldanamycin to trigger a stress response (Supplemental Figure 1a); (ii) the observation that the geldanamycin/radicicol-induced stress response is attenuated for HSF1 and HSP70A (albeit not for HSP90A) after \sim 120 min, presumably when levels of alternative chaperone systems have increased (Figure 5; Figure S1b).

Taken together, we hypothesize that the slow induction of the stress response upon feeding high concentrations of geldanamycin is triggered by the accumulation of unfolded/aggregated HSP90 clients, but only after they have exhausted the buffering capacity of other chaperones. The relatively slow induction of the stress response by feeding cells with the arginine analog canavanine (Figure 4) might be explained similarly with an exhaustion of chaperone buffering capacity when unfolded/aggregated proteins accumulate.

If indeed unfolded/aggregated proteins trigger the stress response, how are they sensed and how does this result in activation of HSF1 if not by sequestration of HSP90A from HSF1 to unfolded protein substrates? As unfolded/aggregated proteins accumulating *e.g.* during canavanine feeding trigger a stress response at ambient temperatures, it is difficult to imagine how they could increase membrane fluidity to activate a Ca^{2+} channel in the cytoplasmic membrane. However, as geldanamycin feeding resulted in Ca^{2+} inflow in moss (Saidi *et al.* 2009), it is tempting to speculate that HSP90/HSP70 chaperones might interact with the Ca^{2+} channel, which is activated upon sequestration of the chaperones to unfolded protein substrates.

Attenuation of the HSR is also physiologically important, as it allows return to a normal gene expression pattern and growth. The constitutive binding of HSP70A to HSF1 is not in favour of a role in mediating attenuation, but what are other possible mechanisms? As we

found a strict correlation between HSF1 hyperphosphorylation and the accumulation of stress gene transcripts, it appears straight forward to postulate a metastable phosphatase requiring chaperone-assisted folding to acquire the native, active state. Phosphatase activity would then be coupled to the state of cellular protein homeostasis.

Experimental procedures

Strains and Culture Conditions

Chlamydomonas reinhardtii strain cw15-302 (cw_d mt+ arg7 nit-), kindly provided by R. Matagne (University of Liège, Belgium), was used for the arginine/canavanine feeding experiment (Figure 3). CF185, which is cw15-302 transformed with pCB412 containing the wild-type ARG7 gene (Schroda *et al.* 1999), was used as recipient strain for *ble* transformation (Figure 8) and inhibitor feeding experiments. Strain cw15-325 (cw_d mt+ arg7 nit+), also kindly provided by R. Matagne, was used as recipient strain for transformation with pCB412 (control) and HSF1-amiRNA construct pMS550 (Schmollinger *et al.* 2010). Strains were grown mixotrophically in TAP medium (Harris 1989) on a rotatory shaker at 25°C and ~30 μE m⁻² s⁻¹. To remove extracellular calcium from cells grown in TAP medium, *Chlamydomonas* cells were pelleted by centrifugation for 4 min at 4000 g and 25°C and resuspended in 150 ml distilled water. This was repeated twice before cells were resuspended in 70 ml pre-warmed distilled water +/- Ca²⁺ chelators.

Vector construction

For the construction of the *HSP70B* antisense vector, a 303-bp fragment containing the *HSP70B* 5' UTR and transit peptide coding region was PCR-amplified using *HSP70B* cDNA clone pCB611 as template and primers 5'-CGCTCTAGAACTAGTGGATC-3' and 5'-TTTGCTAGCAGATCCCGGGCGGCCA-3'. The 303-bp fragment was digested with Sall and BamHI and ligated in antisense orientation into Sall-BamHI-digested pSP108, between *ble* coding region and 3' UTR of *RBCS2* (Stevens *et al.* 1996), yielding pMS172. pMS172 was then digested with FseI and KpnI and the resulting 625-bp fragment was ligated into FseI-KpnI-digested pMS171 (Schroda *et al.* 2002), giving pMS179. pMS171 and pMS179 were linearized with KpnI and transformed into CF185 by agitation with glass beads (Kindle 1990). Transformants were selected on TAP-agar plates containing 1.1 μg/ml zeocine (InvivoGen).

Inhibitor feeding experiments

For feeding experiments the following inhibitors were used: staurosporine (LC Laboratories) was dissolved as a 4 mM stock solution in DMSO and 1 x PhosStop (Roche) was added to cells after harvest to inhibit dephosphorylation of HSF1 during protein extraction. Chloramphenicol (Sigma-Aldrich) was dissolved in ethanol as a 310 mM stock solution and cycloheximide (Sigma-Aldrich) was dissolved in water as a 35 mM stock solution. Arginine (Merck) and canavanine (Sigma-Aldrich) were dissolved as 100 mg/ml stock solutions in water. Radicol (Roth) was

dissolved in ethanol as a 5 mg/ml stock solution and geldanamycin (InvivoGen) as a 10 mM stock solution in DMSO. EGTA (Roth) was dissolved as a 500 mM stock solution in distilled water (pH 8 with NaOH). BAPTA (Sigma-Aldrich) was directly dissolved as 1 or 7.5 mM stock solution in distilled water. Splitting of cultures for control and inhibitor feeding and addition of the inhibitors occurred immediately before the experiment was started.

RNA analyses

Heat shock kinetics, RNA extraction, hybridization and quantification were performed as described previously (Liu *et al.* 2005, Willmund and Schroda 2005). Probes used were a ~3.8-kb *Sall* fragment from pCB353 (*HSP70A* cDNA in pUC18), a ~1.5-kb *NcoI* fragment from pCB611 (*HSP70B* cDNA in pBS SK+), and those described in Schulz-Raffelt *et al.* (2007).

Protein analyses

Protein extractions, SDS-PAGE, and immunodetections were carried out as described before (Liu *et al.* 2005, Schulz-Raffelt *et al.* 2007). Antisera described previously were against HSF1 and HSP90A (Schulz-Raffelt *et al.*, 2007), HSP90C (Willmund and Schroda 2005), HSP70B (Schroda *et al.* 1999), and CF1b (Lemaire and Wollman 1989). [¹⁴C]-acetate labeling of cellular proteins was done as described previously (Schulz-Raffelt *et al.* 2007).

Immunoprecipitation from soluble cell extracts

Chlamydomonas wild-type and *HSF1*-amiRNAi strains were grown in 1 L TAP medium to a density of about 3-5 x 10⁶ cells/ml. 1 x 10⁹ cells were harvested by centrifugation, resuspended in 200 ml TAP medium preheated to 40°C (HS) or left at 25°C (CL) and harvested after 30 min incubation at the respective temperature. Each pellet was washed twice in 20 mM HEPES-KOH, pH 7.2, 80 mM KCl before resuspending in 18 ml lysis buffer (20 mM HEPES-KOH, pH 7.2, 10 mM KCl, 2.5 mM MgCl₂, 154 mM NaCl, 0.25 x protease inhibitor cocktail (Roche)). Cells were sonicated on ice for 90 s before the addition of 2 mM DSP crosslinker. Complexes were crosslinked for 1 h at 4°C. Lysates were then loaded onto sucrose cushions (20 mM HEPES-KOH pH 7.2, 0.6 M sucrose) and centrifuged in a TI50 rotor (Beckman, Palo Alto, CA) for 30 min at 152,000 g and 4°C. Antibody coupling and immunoprecipitations were carried out as described previously (Liu *et al.* 2005, Schroda *et al.* 2001).

Acknowledgements

We wish to thank Kaiyao Huang (Yale University, New Haven, CT) for the antibody against HSP70A. This work was supported by the Deutsche Forschungsgemeinschaft (Schr 617/2-3) and the Bundesministerium für Bildung und Forschung (Systems Biology Initiative FORSYS, project GoFORSYS).

References

- Akerfelt, M., Morimoto, R.I. and Sistonen, L. (2010) Heat shock factors: integrators of cell stress, development and lifespan. *Nature reviews*, **11**, 545-555.
- Ali, A., Bharadwaj, S., O'Carroll, R. and Ovsenek, N. (1998) HSP90 interacts with and regulates the activity of heat shock factor 1 in *Xenopus* oocytes. *Molecular and cellular biology*, **18**, 4949-4960.
- Ananthan, J., Goldberg, A.L. and Voellmy, R. (1986) Abnormal proteins serve as eukaryotic stress signals and trigger the activation of heat shock genes. *Science (New York, N.Y.)*, **232**, 522-524.
- Anckar, J. and Sistonen, L. (2011) Regulation of HSF1 function in the heat stress response: implications in aging and disease. *Annual review of biochemistry*, **80**, 1089-1115.
- Cotto, J.J., Kline, M. and Morimoto, R.I. (1996) Activation of heat shock factor 1 DNA binding precedes stress-induced serine phosphorylation. Evidence for a multistep pathway of regulation. *The Journal of biological chemistry*, **271**, 3355-3358.
- Duina, A.A., Kalton, H.M. and Gaber, R.F. (1998) Requirement for Hsp90 and a CyP-40-type cyclophilin in negative regulation of the heat shock response. *The Journal of biological chemistry*, **273**, 18974-18978.
- Floer, M., Bryant, G.O. and Ptashne, M. (2008) HSP90/70 chaperones are required for rapid nucleosome removal upon induction of the GAL genes of yeast. *Proceedings of the National Academy of Sciences of the United States of America*, **105**, 2975-2980.
- Hahn, A., Bublak, D., Schleiff, E. and Scharf, K.D. (2011) Crosstalk between Hsp90 and Hsp70 chaperones and heat stress transcription factors in tomato. *The Plant cell*, **23**, 741-755.
- Harris, E.H. (1989) *The Chlamydomonas sourcebook: A comprehensive guide to biology and laboratory use* San Diego, CA: Academic Press Inc.
- Hightower, L.E. and White, F.P. (1981) Cellular responses to stress: comparison of a family of 71--73-kilodalton proteins rapidly synthesized in rat tissue slices and canavanine-treated cells in culture. *Journal of cellular physiology*, **108**, 261-275.
- Hooper, J.K. and Blobel, G. (1969) Characterization of the chloroplastic and cytoplasmic ribosomes of *Chlamydomonas reinhardi*. *J Mol Biol*, **41**, 121-138.
- Karaman, M.W., Herrgard, S., Treiber, D.K., Gallant, P., Atteridge, C.E., Campbell, B.T., Chan, K.W., Ciceri, P., Davis, M.I., Edeen, P.T., Faraoni, R., Floyd, M., Hunt, J.P., Lockhart, D.J., Milanov, Z.V., Morrison, M.J., Pallares, G., Patel, H.K., Pritchard, S., Wodicka, L.M. and Zarrinkar, P.P. (2008) A quantitative analysis of kinase inhibitor selectivity. *Nature biotechnology*, **26**, 127-132.
- Kindle, K.L. (1990) High-frequency nuclear transformation of *Chlamydomonas reinhardtii*. *Proceedings of the National Academy of Sciences of the United States of America*, **87**, 1228-1232.
- Kotak, S., Larkindale, J., Lee, U., von Koskull-Doring, P., Vierling, E. and Scharf, K.D. (2007) Complexity of the heat stress response in plants. *Current opinion in plant biology*, **10**, 310-316.
- Kurepa, J., Walker, J.M., Smalle, J., Gosink, M.M., Davis, S.J., Durham, T.L., Sung, D.Y. and Vierstra, R.D. (2003) The small ubiquitin-like modifier (SUMO) protein modification system in Arabidopsis. Accumulation of SUMO1 and -2 conjugates is increased by stress. *The Journal of biological chemistry*, **278**, 6862-6872.
- Lancaster, B. and Batchelor, A.M. (2000) Novel action of BAPTA series chelators on intrinsic K⁺ currents in rat hippocampal neurones. *The Journal of physiology*, **522 Pt 2**, 231-246.
- Lemaire, C. and Wollman, F.A. (1989) The chloroplast ATP synthase in *Chlamydomonas reinhardtii*. I. Characterization of its nine constitutive subunits. *The Journal of biological chemistry*, **264**, 10228-10234.

- Liu, C., Willmund, F., Whitelegge, J.P., Hawat, S., Knapp, B., Lodha, M. and Schroda, M. (2005) J-domain protein CDJ2 and HSP70B are a plastidic chaperone pair that interacts with vesicle-inducing protein in plastids 1. *Molecular biology of the cell*, **16**, 1165-1177.
- Liu, H.T., Gao, F., Li, G.L., Han, J.L., Liu, D.L., Sun, D.Y. and Zhou, R.G. (2008) The calmodulin-binding protein kinase 3 is part of heat-shock signal transduction in *Arabidopsis thaliana*. *Plant J*, **55**, 760-773.
- Mittler, R., Finka, A. and Goloubinoff, P. (2012) How do plants feel the heat? *Trends in biochemical sciences*, **37**, 118-125.
- Morimoto, R.I. (1998) Regulation of the heat shock transcriptional response: cross talk between a family of heat shock factors, molecular chaperones, and negative regulators. *Genes & development*, **12**, 3788-3796.
- Mühlhaus, T., Weiss, J., Hemme, D., Sommer, F. and Schroda, M. (2011) Quantitative Shotgun Proteomics Using a Uniform ¹⁵N-Labeled Standard to Monitor Proteome Dynamics in Time Course Experiments Reveals New Insights into the Heat Stress Response of *Chlamydomonas reinhardtii*. *Mol Cell Proteomics*, **10**, M110 004739.
- Nathan, D.F., Vos, M.H. and Lindquist, S. (1997) In vivo functions of the *Saccharomyces cerevisiae* Hsp90 chaperone. *Proceedings of the National Academy of Sciences of the United States of America*, **94**, 12949-12956.
- Nover, L., Bharti, K., Doring, P., Mishra, S.K., Ganguli, A. and Scharf, K.D. (2001) Arabidopsis and the heat stress transcription factor world: how many heat stress transcription factors do we need? *Cell stress & chaperones*, **6**, 177-189.
- Parmar, V.M. and Schroder, M. (2012) Sensing endoplasmic reticulum stress. *Adv Exp Med Biol*, **738**, 153-168.
- Pellegrino, M.W., Nargund, A.M. and Haynes, C.M. (2012) Signaling the mitochondrial unfolded protein response. *Biochimica et biophysica acta*.
- Pratt, W.B. and Toft, D.O. (2003) Regulation of signaling protein function and trafficking by the hsp90/hsp70-based chaperone machinery. *Exp Biol Med (Maywood)*, **228**, 111-133.
- Roe, S.M., Prodromou, C., O'Brien, R., Ladbury, J.E., Piper, P.W. and Pearl, L.H. (1999) Structural basis for inhibition of the Hsp90 molecular chaperone by the antitumor antibiotics radicicol and geldanamycin. *Journal of medicinal chemistry*, **42**, 260-266.
- Rutherford, S.L. and Lindquist, S. (1998) Hsp90 as a capacitor for morphological evolution. *Nature*, **396**, 336-342.
- Saidi, Y., Finka, A., Muriset, M., Bromberg, Z., Weiss, Y.G., Maathuis, F.J. and Goloubinoff, P. (2009) The heat shock response in moss plants is regulated by specific calcium-permeable channels in the plasma membrane. *The Plant cell*, **21**, 2829-2843.
- Saoudi, Y., Rousseau, B., Doussiere, J., Charrasse, S., Gauthier-Rouviere, C., Morin, N., Sautet-Laugier, C., Denarier, E., Scaife, R., Mioskowski, C. and Job, D. (2004) Calcium-independent cytoskeleton disassembly induced by BAPTA. *European journal of biochemistry / FEBS*, **271**, 3255-3264.
- Sawarkar, R., Sievers, C. and Paro, R. (2012) Hsp90 globally targets paused RNA polymerase to regulate gene expression in response to environmental stimuli. *Cell*, **149**, 807-818.
- Schmollinger, S., Strenkert, D. and Schroda, M. (2010) An inducible artificial microRNA system for *Chlamydomonas reinhardtii* confirms a key role for heat shock factor 1 in regulating thermotolerance. *Current genetics*, **56**, 383-389.
- Schneider, C., Sepp-Lorenzino, L., Nimmegern, E., Ouerfelli, O., Danishefsky, S., Rosen, N. and Hartl, F.U. (1996) Pharmacologic shifting of a balance between protein refolding and degradation mediated by Hsp90. *Proceedings of the National Academy of Sciences of the United States of America*, **93**, 14536-14541.
- Schroda, M. (2006) RNA silencing in *Chlamydomonas*: mechanisms and tools. *Current genetics*, **49**, 69-84.
- Schroda, M., Beck, C.F. and Vallon, O. (2002) Sequence elements within an HSP70 promoter

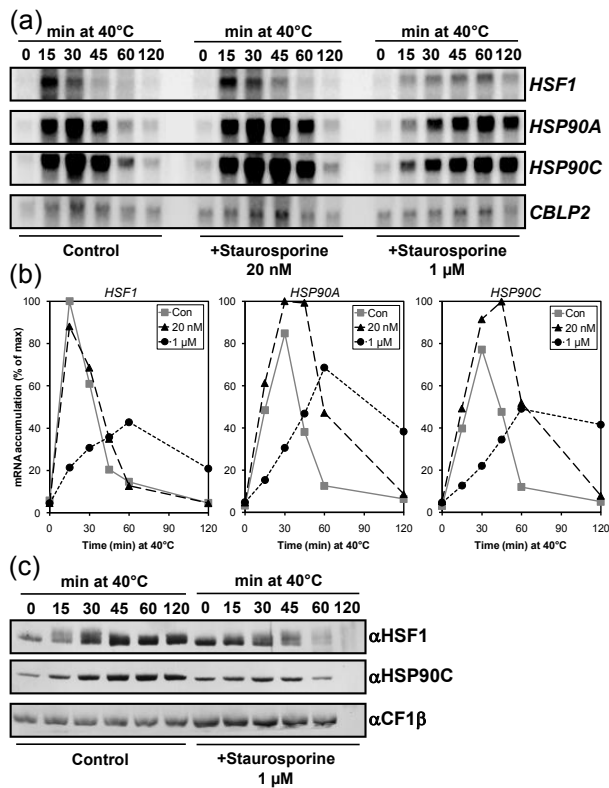
- counteract transcriptional transgene silencing in *Chlamydomonas*. *Plant J*, **31**, 445-455.
- Schroda, M. and Vallon, O.** (2008) *Chaperones and Proteases*. In: *The Chlamydomonas Sourcebook, Second Edition* San Diego, CA: Elsevier / Academic Press.
- Schroda, M., Vallon, O., Whitelegge, J.P., Beck, C.F. and Wollman, F.A.** (2001) The chloroplastic GrpE homolog of *Chlamydomonas*: two isoforms generated by differential splicing. *The Plant cell*, **13**, 2823-2839.
- Schroda, M., Vallon, O., Wollman, F.A. and Beck, C.F.** (1999) A chloroplast-targeted heat shock protein 70 (HSP70) contributes to the photoprotection and repair of photosystem II during and after photoinhibition. *The Plant cell*, **11**, 1165-1178.
- Schulz-Raffelt, M., Lodha, M. and Schroda, M.** (2007) Heat shock factor 1 is a key regulator of the stress response in *Chlamydomonas*. *Plant J*, **52**, 286-295.
- Shi, Y., Mosser, D.D. and Morimoto, R.I.** (1998) Molecular chaperones as HSF1-specific transcriptional repressors. *Genes & development*, **12**, 654-666.
- Stevens, D.R., Rochaix, J.D. and Purton, S.** (1996) The bacterial phleomycin resistance gene ble as a dominant selectable marker in *Chlamydomonas*. *Mol Gen Genet*, **251**, 23-30.
- Strenkert, D., Schmollinger, S., Sommer, F., Schulz-Raffelt, M. and Schroda, M.** (2011) Transcription factor dependent chromatin remodeling at heat shock and copper responsive promoters in *Chlamydomonas reinhardtii*. *Plant Cell*, **23**, 2285-2301.
- Su, P.H. and Li, H.M.** (2008) Arabidopsis stromal 70-kD heat shock proteins are essential for plant development and important for thermotolerance of germinating seeds. *Plant physiology*, **146**, 1231-1241.
- Voellmy, R. and Boellmann, F.** (2007) Chaperone regulation of the heat shock protein response. *Adv Exp Med Biol*, **594**, 89-99.
- von Koskull-Doring, P., Scharf, K.D. and Nover, L.** (2007) The diversity of plant heat stress transcription factors. *Trends in plant science*, **12**, 452-457.
- Watowich, S.S. and Morimoto, R.I.** (1988) Complex regulation of heat shock- and glucose-responsive genes in human cells. *Molecular and cellular biology*, **8**, 393-405.
- Willmund, F. and Schroda, M.** (2005) HEAT SHOCK PROTEIN 90C is a bona fide Hsp90 that interacts with plastidic HSP70B in *Chlamydomonas reinhardtii*. *Plant physiology*, **138**, 2310-2322.
- Yamada, K., Fukao, Y., Hayashi, M., Fukazawa, M., Suzuki, I. and Nishimura, M.** (2007) Cytosolic HSP90 regulates the heat shock response that is responsible for heat acclimation in *Arabidopsis thaliana*. *The Journal of biological chemistry*, **282**, 37794-37804.
- Zou, J., Guo, Y., Guettouche, T., Smith, D.F. and Voellmy, R.** (1998) Repression of heat shock transcription factor HSF1 activation by HSP90 (HSP90 complex) that forms a stress-sensitive complex with HSF1. *Cell*, **94**, 471-480.

Short legends for Supporting Information

Figure S1. Analysis of the effect of low concentrations of geldanamycin in triggering a stress response

RNA gel blot analysis of transcript accumulation of selected genes in unstressed *Chlamydomonas* cells in the absence (Control) or presence of 3.6 μ M (a) and 10 μ M (b) of HSP90 inhibitor geldanamycin.

Figure 1

**Figure 1. Analysis of the effect of staurosporine on the HSR.**

(a) RNA gel blot analysis of transcript accumulation of selected genes after exposing *Chlamydomonas* cells to heat stress in the absence (Control) and presence of 20 nM and 1 μM protein kinase inhibitor staurosporine.

(b) Quantification of hybridization signals from RNA blots shown in (a). Values were corrected for unequal loading based on *CBLP2* signals and plotted as percentage of the maximal signal intensity measured for the respective stress gene. Grey lines depict the response in mock treated control, black lines that in drug treated cells. Note that we observed variations in amplitude and kinetics of stress gene expression from experiment to experiment, presumably because of slight variations in the physiological states of the cultured cells and experimental conditions. We therefore show only a single representative experiment of at least three that were performed.

(c) Protein gel blot analysis of selected proteins after exposing *Chlamydomonas* cells to heat stress in the absence (Control) and presence of 1 μM staurosporine. CF1b serves as loading control.

Figure 2

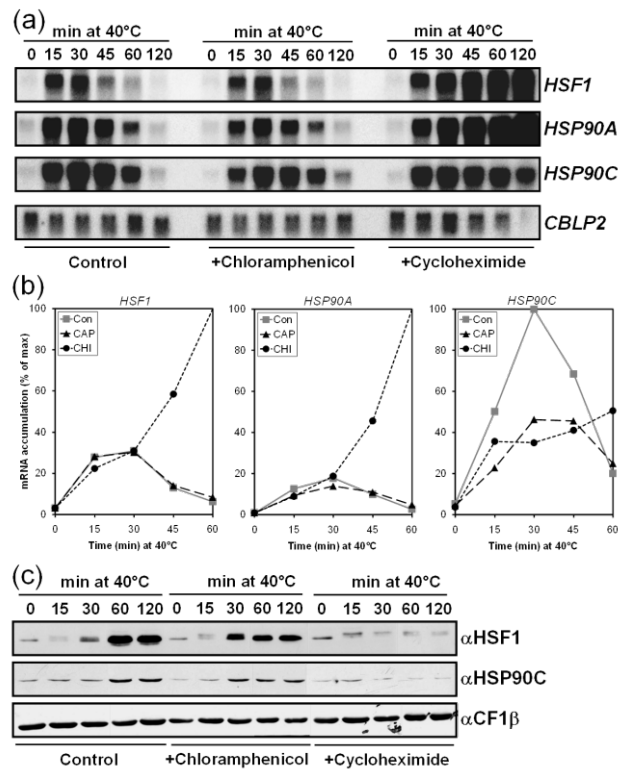


Figure 2. Analysis of the effect of chloramphenicol and cycloheximide on the HSR.

(a) RNA gel blot analysis of transcript accumulation of selected genes after exposing Chlamydomonas cells to heat stress in the absence (Control) and presence of inhibitors of organellar translation (chloramphenicol, 310 μ M) and cytosolic translation (cycloheximide, 35 μ M).

(b) Quantification of hybridization signals from RNA gel blots shown in (a) were done as described in Figure 1b. Grey lines depict the response in mock treated control, black lines that in drug treated cells (CAP – chloramphenicol; CHI – cycloheximide).

(c) Protein gel blot analysis of selected proteins after exposing Chlamydomonas cells to heat stress in the absence (Control) and presence of the translation inhibitors at the same concentrations as in (a).

Figure 3

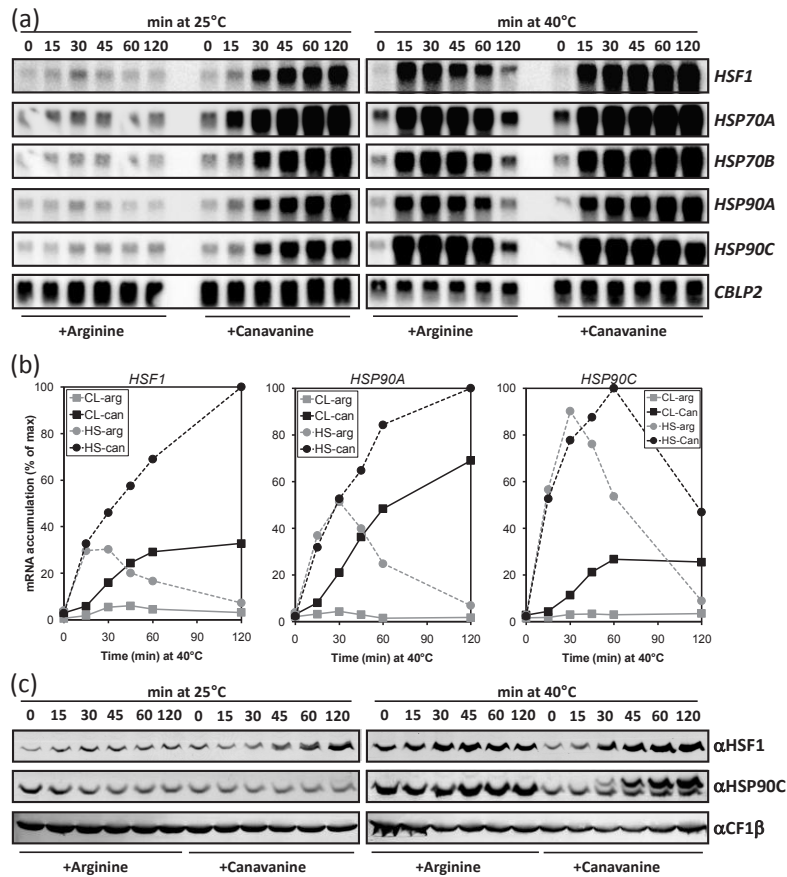


Figure 3. Analysis of the effect of canavanine on the HSR.

(a) RNA gel blot analysis of transcript accumulation of selected genes in unstressed and heat-stressed *Chlamydomonas* cells fed with 50 $\mu\text{g/ml}$ arginine (Control) or with 50 $\mu\text{g/ml}$ canavanine.

(b) Quantification of hybridization signals from RNA blots shown in (a) were done as described in Figure 1b. Grey lines indicate transcript levels from cells fed with arginine (arg), black lines those from cells fed with canavanine (can). Solid lines represent transcript levels from cells kept at 25°C, dotted lines indicate transcript levels from cells subjected to heat shock. For simplicity quantification was restricted to *HSF1*, *HSP90A*, and *HSP90C* transcript levels.

(c) Protein gel blot analysis of selected proteins in unstressed and heat-stressed *Chlamydomonas* cells fed with arginine or canavanine. Note that *HSF1* phosphorylation was not resolved in this gel.

Figure 4

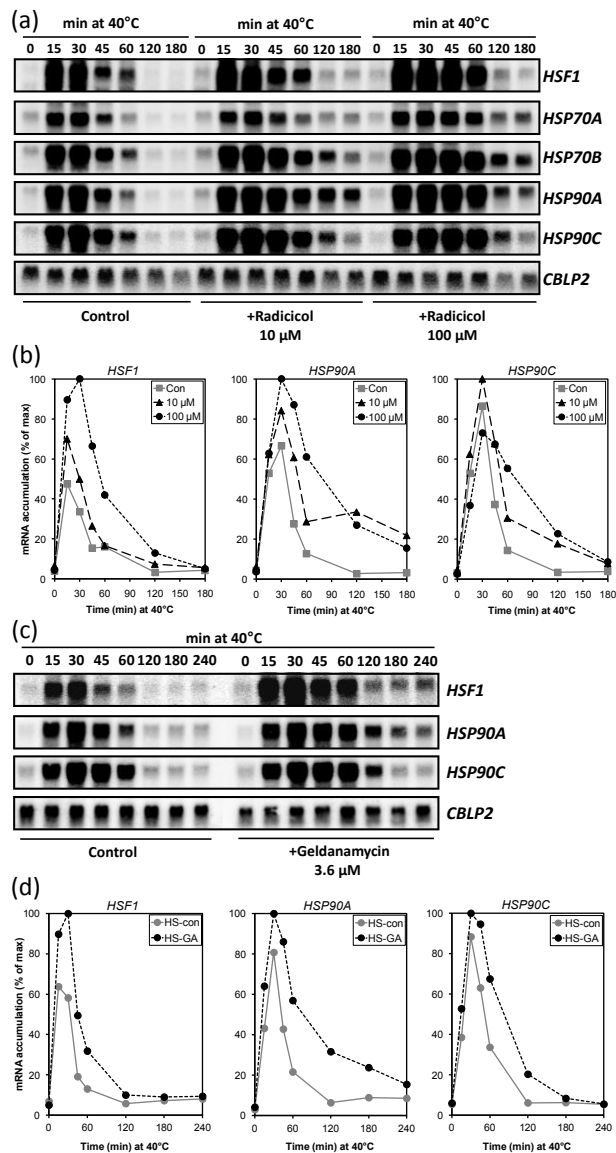


Figure 4. Analysis of the effect of HSP90 inhibitors on the HSR.

(a) RNA gel blot analysis of transcript accumulation of selected genes after exposing *Chlamydomonas* cells to heat stress in the absence (Control) and presence of HSP90 inhibitor radicicol.

(b) Quantification of hybridization signals from RNA blots shown in (a) were done as described in Figure 1b. Grey lines depict the response in mock treated control, black lines that in drug treated cells. For simplicity quantification was restricted to *HSF1*, *HSP90A*, and *HSP90C* transcript levels.

(c) RNA gel blot analysis of transcript accumulation of selected genes after exposing *Chlamydomonas* cells to heat stress in the absence (Control) and presence of 3.6 µM HSP90 inhibitor geldanamycin.

(d) Quantification of hybridization signals from RNA blots shown in (c) was done as described in Figure 1b. Grey lines depict the response in mock treated control, black lines that in geldanamycin (GA) treated cells.

Figure 5

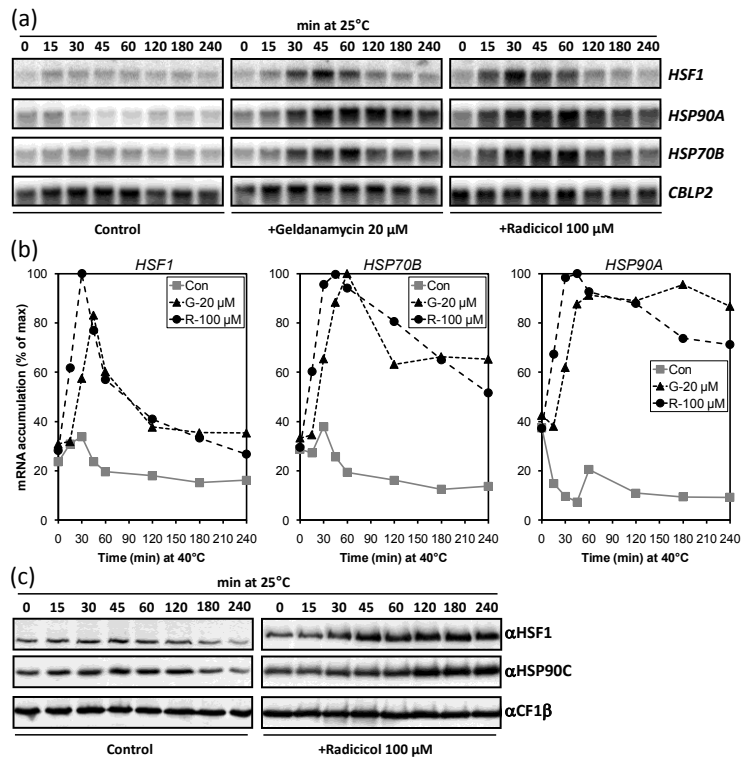


Figure 5. Analysis of HSP90 inhibitors as stress response triggers.

(a) RNA gel blot analysis of transcript accumulation of selected genes in unstressed *Chlamydomonas* cells in the absence (Control) or presence of HSP90 inhibitors geldanamycin and radicicol.

(b) Quantification of hybridization signals from RNA blots shown in (a) were done as described in Figure 1b. Grey lines indicate transcript levels from mock treated control, black lines those from cells fed with 20 μM geldanamycin (G-20 μM) or 100 μM radicicol (R-100 μM).

(c) Protein gel blot analysis of selected proteins in unstressed *Chlamydomonas* cells that were mock treated or fed with 100 μM radicicol.

Figure 6

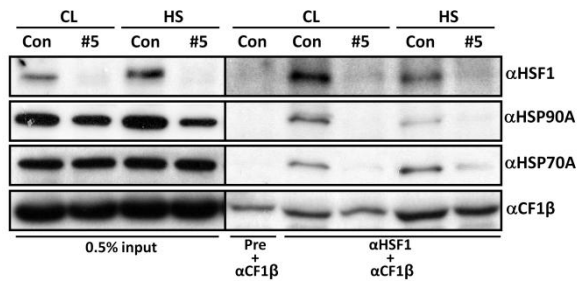


Figure 6. Analysis of the interaction between HSF1 and HSP90A.

Total soluble proteins were isolated from control (Con) or *HSF1*-amiRNA strain #5 that were grown for 24 h on TAP medium containing nitrate to induce expression of the *HSF1*-amiRNA construct and either kept at 25°C (CL) or exposed to a 30-min heat shock at 40°C (HS). 0.5 % of total soluble proteins (input for immunoprecipitation) and 10 % of the precipitates generated with mixtures of an antiserum against CF1b and preimmune serum (pre) or affinity-purified antibodies against HSF1 were separated on a 10% SDS-polyacrylamide gel and analysed by immunoblotting..

Figure 7

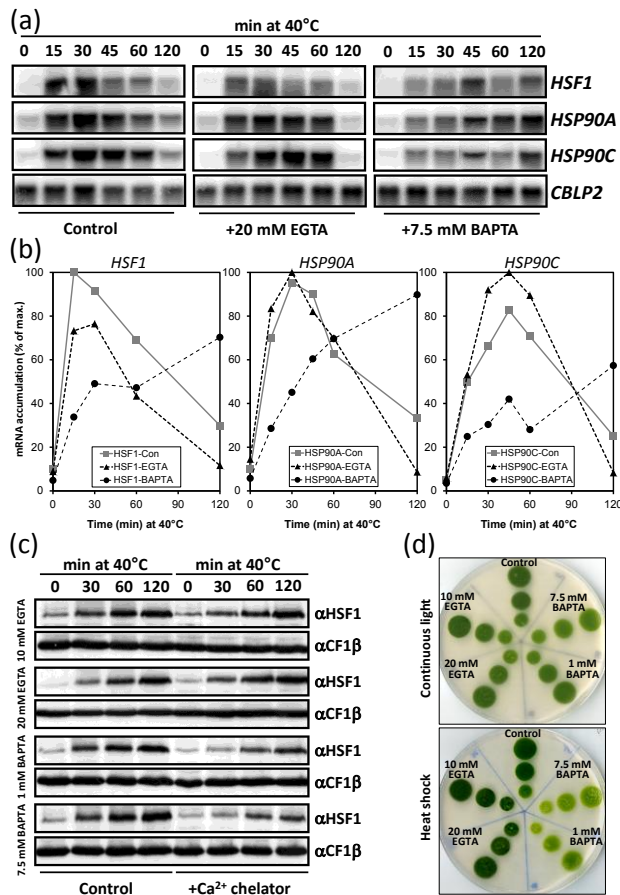


Figure 7. Analysis of the effect of calcium chelators on the HSR.

(a) RNA gel blot analysis of transcript accumulation of selected genes after exposing *Chlamydomonas* cells to heat stress in the absence (Control) and presence of calcium chelators EGTA and BAPTA.

(b) Quantification of hybridization signals from RNA blots shown in (a) were done as described in Figure 1b. Grey lines depict the response in untreated control, black lines that in washed cells supplemented with the calcium chelators.

(c) Protein gel blot analysis of HSF1 protein levels in heat stressed *Chlamydomonas* cells that were untreated or fed with 10 or 20 mM EGTA and 1 or 7.5 mM BAPTA. CF1b served as loading control.

(d) Growth assay of *Chlamydomonas* cells that were left untreated or, after washing, were supplemented with the indicated concentrations of calcium chelators. 2.5 , 5 and 7.5×10^5 cells were spotted directly onto TAP agar plates after a 2-h incubation on a rotary shaker at 25°C (continuous light) or after a 2-h heat shock at 40°C (heat shock). Plates were incubated for 3 days at light of $\sim 30 \mu\text{E m}^{-2} \text{s}^{-1}$.

Figure 8

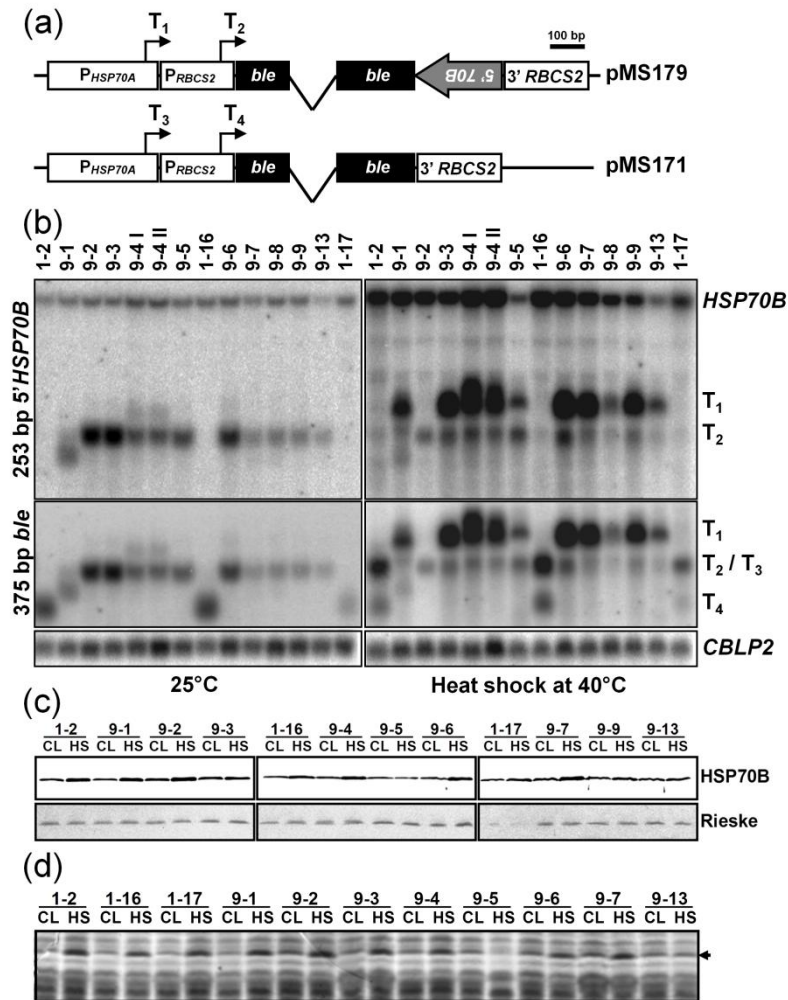


Figure 8. Expression of HSP70B antisense constructs in *Chlamydomonas*.

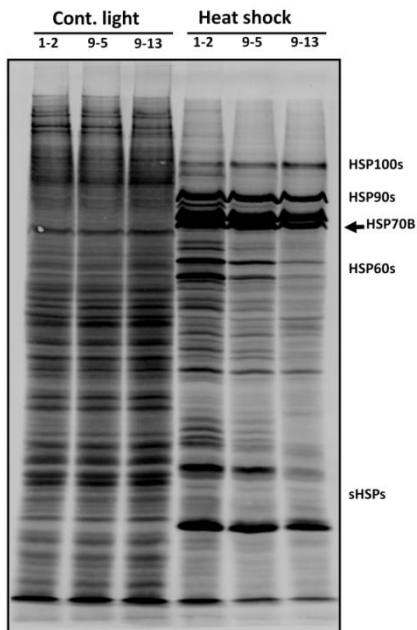
(a) Control construct (pMS171) and the construct used for the expression of *HSP70B* antisense transcripts (pMS179). Expression is driven by the *HSP70A-RBCS2* fusion promoter. The *ble* ORF, conferring resistance to zeocin, is interrupted by the first intron of the *RBCS2* gene and followed by its 3' UTR. In pMS179, a fragment containing 253 nt of *HSP70B* 5' UTR and transit peptide coding region is inserted in antisense orientation between *ble* and the *RBCS2* 3' UTR. Transcription initiation sites of the *HSP70A* and *RBCS2* promoters are designated T₁ and T₂, respectively, in pMS179 and T₃ and T₄, respectively, in pMS171.

(b) RNA gel blot analysis of transcript accumulation of the endogenous *HSP70B* gene and of transgenes in *Chlamydomonas* transformants containing pMS171 (strains 1-X) and pMS179 (strains 9-X). Roman numerals designate two independent cultures of transformant 9-4. Transformant cultures were kept at 25°C or heat shocked at 40°C for 40 min. Transcripts were detected with probes against 272 nt of the *HSP70B* 5' region, the *ble* gene, and *CBLP2* as loading control. The transcriptional start sites of the detected transcripts are indicated.

(c) Protein gel blot analysis of HSP70B levels in selected transformants. Transformant cultures were grown at 25°C (CL) or heat-shocked for 60 min at 40°C (HS). The Rieske protein served as loading control.

(d) Analysis of heat shock-inducible proteins in selected transformants. Transformant cultures were grown at 25°C (CL) or heat-shocked for 60 min at 40°C (HS). Total proteins were separated on a 10% SDS-polyacrylamide gel and stained with Coomassie brilliant blue. For simplicity, only the region containing proteins of low molecular weight is shown and the heat-inducible ~20 kD protein is indicated by an arrowhead.

Figure 9

**Figure 9.**

[¹⁴C]-acetate labeling of nuclear-encoded proteins in transformants containing pMS171 and pMS179. [¹⁴C]-acetate labeling was carried out for 40 min at 25°C (Cont. light) or between 30 and 40 min after transfer from 25°C to 40°C (heat shock). Proteins corresponding to 12 µg chlorophyll were separated on a 7.5 to 15% polyacrylamide-SDS-gel, transferred to nitrocellulose, and exposed to a phosphorimager plate for four weeks. The membrane was subsequently immunodecorated with an antiserum against HSP70B and the HSP70B signal was used as orientation to deduce the positions of the other chaperones.

Figure 10

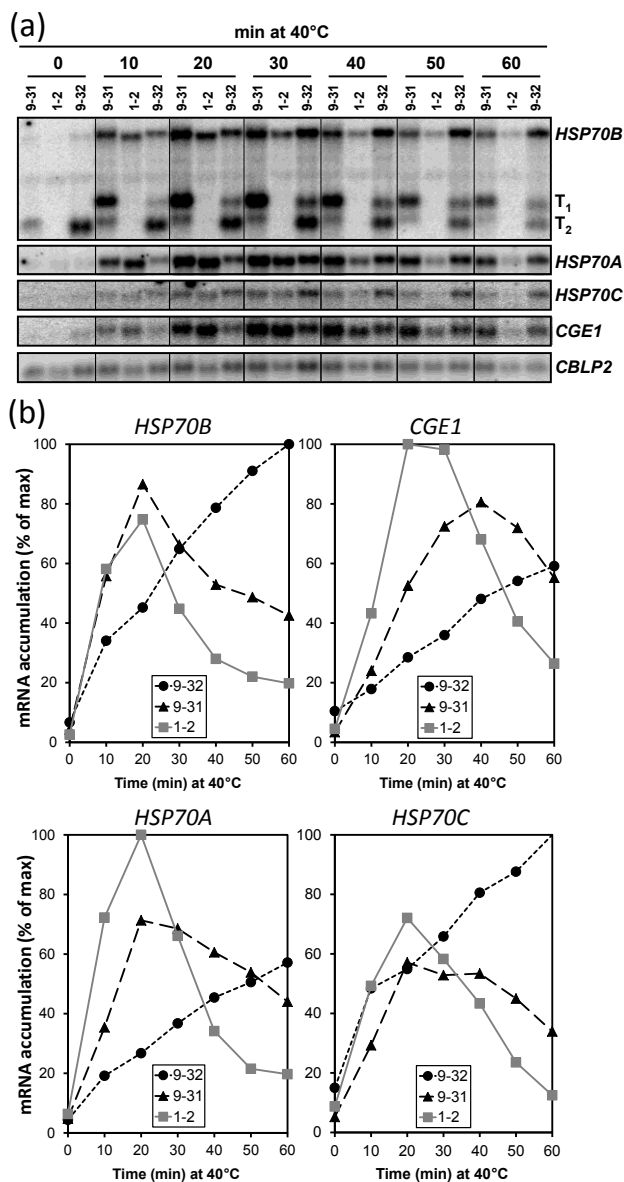
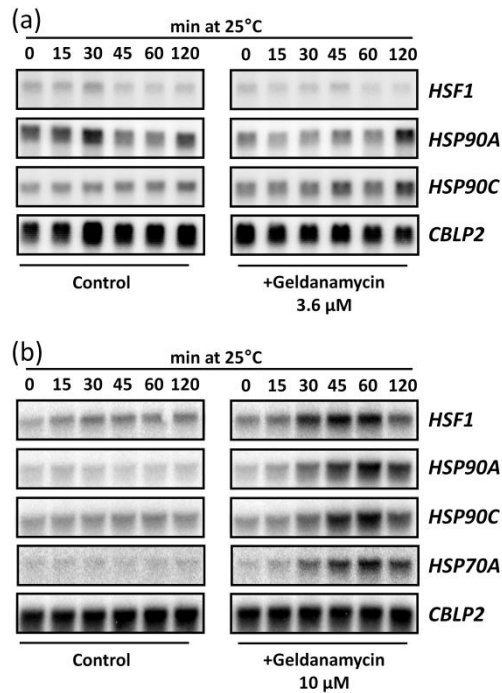


Figure 10. Analysis of heat stress kinetics of selected stress genes in transformants containing control and *HSP70B* antisense constructs.

(a) RNA gel blot analysis of transcript accumulation of selected genes after exposing *Chlamydomonas* transformants containing pMS171 (1-2) and pMS179 (9-31 and 9-32) to heat stress. *ble-HSP70B*-antisense transcripts initiated from the *HSP70A* promoter and from the *RBCS2* promoter are designated as T_1 and T_2 , respectively.

(b) Quantification of hybridization signals from RNA blots shown in (a) were done as described in Figure 1b. Grey solid lines indicate transcript levels from control transformant 1-2. Black dashed lines and black dotted lines represent transcript levels from *HSP70B* antisense transformants 9-31 and 9-32, respectively.

Figure S1

**Figure S1. Analysis of the effect of low concentrations of geldanamycin in triggering a stress response**

RNA gel blot analysis of transcript accumulation of selected genes in unstressed *Chlamydomonas* cells in the absence (Control) or presence of 3.6 μ M (a) and 10 μ M (b) of HSP90 inhibitor geldanamycin.

3.5. MANUSCRIPT 2: THE HSF1-DEPENDENT HEAT SHOCK RESPONSE IN *CHLAMYDOMONAS REINHARDTII*.

Authors:

Stefan Schmollinger, Timo Mühlhaus, Daniela Strenkert, Miriam Schulz-Raffelt, Corinna Gruber, Stefanie Schönfelder, Sebastian Klie, Björn Voss, Thorsten Kurz, Wolfgang Hess and Michael Schroda

Draft manuscript

Contribution to:

Figure 1

Figure 2

Figure 3

Figure 4

Figure 5

Figure 6

Figure 7

Supplemental Figure 1

Supplemental Figure 2

The *HSF1*-dependent heat shock response in *Chlamydomonas reinhardtii*

Stefan Schmollinger^{1,2}, Timo Mühlhaus^{1,2}, Daniela Strenkert^{1,2}, Miriam Schulz-Raffelt³, Corinna Gruber^{1,2}, Stefanie Schönfelder², Sebastian Klie², Björn Voss⁴, Thorsten Kurz⁴, Wolfgang Hess⁴ and Michael Schroda^{1,2}

¹ Molekulare Biotechnologie & Systembiologie, TU Kaiserslautern, Paul-Ehrlich-Str. 23, D-67663 Kaiserslautern, Germany

² Max-Planck-Institut für Molekulare Pflanzenphysiologie, Am Mühlenberg 1, D-14476 Potsdam-Golm, Germany

³ CEA–CNRS–Université Aix Marseille, Institut de Biologie Environnementale et Biotechnologie – UMR 6191 CEA Cadarache – 13108 Saint-Paul-lez-Durance, France

⁴ Institute of Biology II, Universität Freiburg, Schänzlestraße 1, D-79104 Freiburg, Germany

Corresponding author: Michael Schroda

Tel.: + 49 (0)631 205-2697

Fax: + 49 (0)631 205-2999

e-mail: schroda@biologie.uni-kl.de

Running titel: The HSF1-dependent heat shock response in *Chlamydomonas reinhardtii*

Keywords: HSF1, HSF, Chlamydomonas, Chlorophyll biosynthesis, MPA1,

Word count:

Summary	282
Introduction	1023
Results and Discussion	5109
Experimental procedures	732
Acknowledgements	48
Figure legends	2593
Total	10420

Summary

Facing climate change, acclimation to higher temperatures is one of the upcoming challenges for plants and therefore is also of interest in plant sciences and biotechnology. When exposed to elevated temperatures cells activate a highly conserved genetic program, the heat shock response (HSR) which is regulated by a conserved class of transcription factors, so called heat shock factors (HSFs). In order to understand acclimation strategies in photosynthetic organisms we used the model alga *Chlamydomonas reinhardtii* with its single plant type HSF (HSF1) and monitored transcriptome dynamics upon heat stress using microarrays in wild-type and *HSF1* RNAi lines. At ambient conditions, we identified 31 differentially expressed genes, whereas 977 transcript levels were altered at 40°C between wild-type and *HSF1* knock-down strains, indicating the importance of HSF1 for gene expression for acclimation to temperature changes. The observed changes in mRNA abundance also caused similar alterations of corresponding proteins. Beside genes involved in chaperoning and redox regulation we also identified plant specific processes to be regulated by HSF1 i.e. genes from the chloroplast import machinery and tetrapyrrole biosynthetic pathway. We further analyzed exemplary promoter regions for the existence of HSF1 binding sites and directly probed for transcription factor binding using chromatin immunoprecipitation (ChIP). Thereby, promoter regions of CLPB3 (a chloroplast chaperone of the HSP100 class), MPA1 (phosphatase) and HSF1 itself showed HSF1 binding upon heat shock. Direct binding of a HSF gene by the transcription factor itself was not observed before in any organism and was necessary for full activation of stress-related genes in *Chlamydomonas*. Furthermore, in contrast to model systems like *Drosophila melanogaster*, HSF1 binding to promoter HSEs was not dependent on a specific epigenetic profile in the promoter regions.

Introduction

In order to maintain homeostasis and survive changing environmental conditions all living organisms developed cellular mechanisms to cope with various stresses. One of them, the heat shock response (HSR), is a highly ordered genetic response upon proteotoxic conditions like the eponymous heat shock, oxidative stress, elevated heavy metal concentrations or toxin levels and pathogen attacks (Akerfelt *et al.* 2010, Morimoto 1998). The major target of the HSR is a specific set of proteins, so called heat shock proteins (HSP), mainly molecular chaperones and proteases. They are subdivided in six major HSP families, according to their molecular weight, the small HSP, HSP40s, HSP60s, HSP70s, HSP90s and HSP100s. Whereas some of these proteins are exclusively present under stress conditions, many of them have essential proofreading function in protein biogenesis and protein homeostasis under normal growth conditions (Bukau *et al.* 2006, Hartl *et al.* 2011).

The HSR is mainly regulated at the transcriptional level by a well characterized class of transcription factors, the heat shock factors (HSF). The basic HSF domain architecture was highly conserved throughout eukaryotic evolution. HSFs consist of an N-terminal DNA binding domain (DBD) of the “winged” helix-turn-helix type, an adjacent oligomerization domain containing two hydrophobic heptad repeats (HR-A/B) and a C-terminal transactivation domain (CTAD) containing aromatic, large hydrophobic and acidic (AHA) amino acid motifs necessary for transactivation (Damberger *et al.* 1994, Doring *et al.* 2000, Littlefield and Nelson 1999, Peteranderl and Nelson 1992, Treuter *et al.* 1993). Upon stress, HSFs become activated in a multistep process, including the resolving of repressing protein-protein interactions, trimerization, post-translational modifications and translocation into the nucleus (Cotto *et al.* 1996, Goldenberg *et al.* 1988, Sorger and Pelham 1988, Zimarino and Wu 1987). Fully activated HSFs then bind with high affinity to *cis*-acting sequences in promoter regions, so called heat shock elements (HSEs), leading to the activation of gene expression. These HSEs consist of multiple inverted repeats of the pentameric sequence nGAAn (Amin *et al.* 1988, Guertin and Lis 2010, Pelham 1982, Trinklein *et al.* 2004, Wu 1995, Xiao and Lis 1988).

In the green lineage the heat shock factor family is quite complex with 21 members in *Arabidopsis thaliana*, 25 members in rice (*Oryza sativa*) and maize (*Zea mays*) compared to only four HSFs in mammals and a single HSF in *Saccharomyces cerevisiae*, *Drosophila melanogaster* and *Caenorhabditis elegans* (Akerfelt *et al.* 2007, Guo *et al.* 2008, Lin *et al.* 2011, Nover *et al.* 2001). Spacing between the HR-A and HR-B region and the presence (A) or absence (B, C) of the AHA motifs in the transactivation domain was used to classify HSFs in three distinct classes (A, B and C) (Nover *et al.* 2001). Members of plant class A HSFs have been identified as activators of HSP expression increasing thermotolerance, whereas HSFs of class B, for example tomato HSF1, are not able to activate HSP expression alone but act as co-activators of class A HSFs. One example, *Arabidopsis* AtHsf1, even acts as a repressor of class A HSF promoted transcription, lacking a short histone like motif in the CTAD, present in a tomato HSF (HSF1) which was shown to be necessary for its co-activating function (Bharti *et al.* 2004, Czarnecka-

Verner *et al.* 2000, Lee *et al.* 1995, Prandl *et al.* 1998). In addition to the interplay between different HSFs in modulating HSP transcription, some HSFs of class A, as demonstrated for tomato HSFA1a and HSFA2, assemble into hetero-oligomeric supercomplexes resulting in an further enhanced expression of target genes (Chan-Schaminet *et al.* 2009, Scharf *et al.* 1998). The composition of the HSF pool in plants is furthermore altered in different tissues and upon occurrence of different environmental stresses, thus enabling further specialized acclimation and fine-tuning of the HSR (von Koskull-Doring *et al.* 2007).

Knock-out approaches and expression profiling was used to characterize subsets of genes regulated by individual HSFs in plants. Double knock-out of HSFA1a/b in Arabidopsis resulted in differential expression of 112 genes, most of them less expressed in the mutants (Busch *et al.* 2005). A limited number of genes with functions in stress related pathways among them members of the small HSP family, HSFs (class A and B) and co-chaperones of HSP70s were identified to be HSF regulated. More interestingly, a specific trait of carbohydrate metabolism (the Raffinose family oligosaccharide (RFO) pathway, i.e. AtGolS1) was newly identified to be regulated by HSFA1. RFOs have been identified before as potential osmoprotective substances playing an important role during drought stress (Taji *et al.* 2002). Knock-out of HSFA2 in Arabidopsis resulted in differential expression of 720 genes, among them genes already identified in the HSFA1a/b double knock-out (sHSPs, HSP101.3 and AtGolS1) exemplifying redundancy between different members of the HSF family. HSFA2 specific targets like members of HSP70 family and APX2 (a protein involved in ROS scavenging) were also identified (Schramm *et al.* 2006). In contrast, the transcriptome analysis of a knock-out strain of heat stress induced class B HSFs (HSFB1/HSFB2b double knock out) showed no overlap with those HSFA studies at all (Kumar *et al.* 2009). Furthermore, no member of any stress related gene family were affected in their expression levels pointing to a completely different role for these specific class B HSFs, in this case as repressor of genes in pathogen defense.

To learn more about the complete plant-specific target set of the HSF-dependent stress response we used RNAi mediated knock-down of *HSF1* in *Chlamydomonas reinhardtii* and analyzed the transcriptome upon stress treatment using microarrays (Eberhard *et al.* 2006, Voss *et al.* 2011). This single-celled green algae at the origin of the green lineage, harbors only a single canonical HSF. *Chlamydomonas* HSF1 shows high similarity with plant class A HSFs and shares the same domain architecture, namely a 21 amino acid insertion between the HR-A and B region and AHA motifs in the CTAD (Schulz-Raffelt *et al.* 2007). Other typical plant HSF features like the heat shock inducibility are also valid for *Chlamydomonas* *HSF1*, which allows its use to understand fundamental mechanisms of the plant heat shock response in a less complex background. Furthermore, *Chlamydomonas* HSF1 is a key regulator of the *Chlamydomonas* heat stress response and essential for thermotolerance (Schmollinger *et al.* 2010, Schulz-Raffelt *et al.* 2007).

Results and Discussion

Knock-down of *HSF1* results in differential gene expression specifically upon heat shock

In order to specifically assess *HSF1*-dependent processes we generated knock-down strains of *HSF1* and therefore transformed *Chlamydomonas reinhardtii* with a constitutive RNAi construct (pMS418) targeting the region of exon 7-9. Two independent lines were selected that showed reduced thermotolerance in a 2-h heat shock treatment, as already reported previously (Schulz-Raffelt *et al.* 2007). We confirmed underexpression of *HSF1* within a 30-minutes heat shock experiment and ensured that previously reported underexpression of *HSP90C*, a potential target of HSF1, is still realized in the two *HSF1* knock-down strains (Figure 1A). Time-course experiments showed that mRNA induction peaked for fast responding genes (*HSF1*) approximately 15 minutes after shifting the cells from ambient to elevated temperatures whereas *HSP90A* and *HSP90C* induction peaked 30-45 minutes after the switch (Schulz-Raffelt *et al.* 2007).

Two *HSF1* knock-down (#42 and #46) and two empty vector control strains (Con1 and 2) were therefore subjected to a 30-minute 40°C heat shock treatment (HS) or were kept at ambient temperature for the same time (CL). RNA was subsequently extracted and analyzed each in technical duplicates on recently improved Agilent custom microarrays (Figure 1B) to cover a broad range of genes in an unbiased manner (Voss *et al.* 2011). The probeset of the microarrays for *Chlamydomonas* was initially developed on version 2.0 of the *Chlamydomonas* genome so we remapped the probes on the most current version 4.0 (Augustus 5 gene models) and identified 7408 of the 16709 genes in version 4 (44.3 % coverage) (Eberhard *et al.* 2006). We then combined the results from the two technical and two biological replicates of each of the four different conditions (Con CL/HS and *hsf1* CL/HS) for differential gene expression analysis (Figure 1C).

First, we analyzed the heat shock response in *Chlamydomonas* in general by comparing CL and HS in the control strains (HS_{Con}, Figure 1C). Here transcripts of 3090 genes were significantly differentially expressed (41.7 %), almost half of them were upregulated (1535), 1555 genes downregulated (Figure 1D). Previously identified fast, *HSF1* (\log_2 fold change of 4.3), and also more slowly activated genes, *HSP90A* (\log_2 fold change of 4.2) and *HSP90C* (\log_2 fold change of 7.0), were both induced in the control strains upon heat shock, demonstrating that both responses were covered within the microarray experiment. In *HSF1* knock-down strains 4271 genes were differentially expressed in CL and HS samples (HS_{*hsf1*}, 58%), again almost half of them up- and downregulated (2058/2213). The magnitude of up/downregulation in both comparisons is quite equally distributed around 0 showing no distinct tendencies (Figure 1D).

On the other hand we directly analyzed *HSF1*-dependent changes of transcript levels either at ambient temperature (*hsf1*_{CL}) or upon heat shock (*hsf1*_{HS}) by comparing *HSF1* knock-down strains with the control strains at the respective condition. Thereby, transcripts from *HSF1* itself were significantly decreased in the knock-down strains compared to control

strains under non-stress conditions as well as after heat-shock treatment, confirming the underexpression of HSF1 in the knock-down strains during the microarray experiment. Additionally, 30 differentially expressed genes were identified at ambient temperature (0.4 %, 16 up/15 down) and 976 upon heat shock (13.2 %, 445 up/532 down, Figure 1C). *HSF1*-dependent expression is more or less equally distributed at ambient temperatures (around 0), while upon heat shock there are more genes *HSF1*-dependently underexpressed (Figure 1D) consistent with a role of HSF1 as a transcriptional activator upon heat-shock treatment.

qRT-PCR validation confirms significant changes in the Microarray dataset

To ensure the quality of the obtained microarray data, we first analyzed the behavior of selected housekeeping genes directly within the microarray dataset. In total, we chose 5 genes on the microarray covering a broad range of signal intensities that should not be affected by heat treatment. First, *CBLP2*, a gene used frequently in *Chlamydomonas* as loading control in several RNA analysis also in heat shock experiments. *CBLP* is known from northern blot analysis not to be heat regulated (Schulz-Raffelt *et al.* 2007). Furthermore two genes involved in cell structure, Actin from the *IDA5* locus and *TUB1* were analysed. To cover also low abundant mRNAs we chose *WRK1* a plant specific transcription factor not known to be affected by heat regulation and the eukaryotic initiation factor *EIF1A*. We analyzed the distribution of the microarray signal intensities after normalization for all of these genes in all 16 microarrays (Figure 2A) and with exception for *EIF1A*, the least abundant mRNA, we found the intensities in a narrow range. We conclude that, with respect to the technical limitations of a microarray, we were able to display a wide range of signal intensities correctly throughout the experiment.

Furthermore we conducted qRT-PCR analyses in two *HSF1* underexpressing strains, to validate the identified *HSF1*-regulated genes. Again we chose genes that change over a wide range of \log_2 fold changes to probe the whole dataset. At this time, inducible amiRNAs targeting the *HSF1* mRNA were used, underexpressing the transcription factor exclusively on nitrate containing media (Schmollinger *et al.* 2010). In contrast to the RNAi construct which is targeting the distal part of the *HSF1* mRNA encoding the transactivation domain, the amiRNAs target a ~20 bp region close to the 5' encoding for the DNA binding domain. Using these two independent systems we can additionally probe for off-targeting effects of the RNAi construct. In total, we compared the expression of 19 selected genes at ambient and elevated temperatures in *hsf1* and control strains. The \log_2 fold changes of transcripts levels were compared to those determined in the microarray experiment and good overall correlation was found (Figure 2B). 13 out of the 19 genes we tested were significantly *HSF1*-dependently regulated and in all cases we reproduced the *HSF1*-dependent regulation within the amiRNA strains (Figure 2C).

Protein levels are altered accordingly

To assess the impact of the transcriptional changes on protein abundance we compared the microarray dataset with a recently published high-throughput proteomics study, where the

adaptation of the *Chlamydomonas* soluble proteome to a 3h heat stress treatment was analyzed (Muhlhaus *et al.* 2011). In this study 244 proteins were identified to change significantly (38 increasing/206 decreasing). 100 corresponding transcript levels were determined after 30 minutes of heat shock within the present microarray experiment (41.0 %) which is slightly less than expected with microarrays having a 44.3 % coverage. The microarray datasets shows a quite good overall correlation when compared to the maximum protein accumulation in the soluble proteome analysis (Figure 3B). In more detail, 22 transcripts of the 38 upregulated proteins were covered in the microarray dataset (57.9%), 20 of them (90.9%) showed a strong induction on the mRNA level upon stress treatment (Figure 3A).

Unexpectedly two proteins accumulate (ULP1 and LHCA3) while the mRNA is less expressed. Light harvesting complex protein 3 (LHCA3) is, as a part of the antenna from photosystem I, a membrane bound protein in thylakoids (Stauber *et al.* 2009). As the proteomics study focused on soluble proteins the increase of LHCA3 protein could be due to an accumulation of precursor protein or due to an altered protein extractability of mature protein from membranes at higher temperatures in our preparations. The first hypothesis is supported by the observation that transcripts of *FFC* (chloroplast *SRP54*) are significantly *HSF1*-dependently increased upon heat stress treatment. LHCs are mainly integrated via the chloroplast signal recognition particle pathway. The second protein, ULP1 (Unknown Luminal Protein 1), is an uncharacterized protein with similarities to PSBS in the region responsible for trafficking. Therefore ULP1 is predicted to target the chloroplast lumen. In order to understand the unexpected protein accumulation on RNA loss, we raised antibodies specific for ULP1 and tested protein accumulation upon heat shock treatment in soluble and total protein extracts (Figure 3C). Within whole cell protein extracts ULP1 protein is not increasing upon heat shock treatment, the overall protein levels are not changed at all, if not slightly decreased. In contrast, heat shock resulted in strong accumulation of soluble ULP1 protein. We conclude that ULP1 either re-localizes at elevated temperatures or might also be affected from the effects on the translocation machinery (see below).

From the 206 significantly less abundant proteins upon heat stress treatment 78 transcripts were measured within the microarray dataset (37.8%). 62 of them showed corresponding underexpression of transcripts (79.5 %). However, 16 proteins decreased while their transcripts accumulate (summarized in Figure 3A). In this case induction of transcription might be used to counteract depletion of thermo-labile proteins. Four genes among the set of 16 showed additionally significant *HSF1*-dependency (*TIC40*, *TIC110*, *PRPL1* and *PRPL9*). Interestingly, TIC and PRPL proteins are both part of larger protein complexes (Translocon over the chloroplast inner envelope membrane and large ribosomal subunit in the chloroplast, respectively). Especially the TIC proteins showed a quite strong *HSF1*-dependent transcript accumulation upon heat stress treatment. In pea, it was already shown that heat stress leads to an impaired import into the chloroplast (Dutta *et al.* 2009). Here we observed that *HSF1* is involved in regulation of TIC proteins upon heat shock (Dutta *et al.* 2009). Taken together, *HSF1* might be necessary to counteract transport problems upon heat shock in photosynthetic

organisms.

While the TIC proteins are less expressed when HSF1 is missing, expression of the plastid ribosomal proteins is increased in HSF1 knock-down strains. In wild-type strains there is no altered expression upon stress treatment, therefore the increased expression in *HSF1* knock-down strains might be a consequence of *HSF1*-dependent loss of chloroplast chaperoning capacity at elevated temperatures, that might be required for proper translation.

Chlorophyll biosynthesis is *HSF1*-dependently repressed upon heat shock treatment

To analyze the *HSF1*-dependent HS response in more detail we conducted a bin enrichment analysis among the differentially expressed genes in control and *hsf1* strains after HS (*hsf1*_{HS}). We used the MapMan ontology for Chlamydomonas for this purpose in its most recent version (May *et al.* 2008). The results are summarized in Figure 4A. We found four bins of the highest level to be significantly enriched (P-value ≤ 0.05 , ≥ 5 members): tetrapyrrole biosynthesis (19), stress (20), redox regulation (21) and protein (29). Though, their behavior upon heat stress treatment (HS_{Con}) and *HSF1* depletion (*hsf1*_{HS}) is quite different, and therefore the distribution is summarized in Figure 4B for all significantly enriched bins. Most transcripts from the stress/redox regulation/protein category are, as expected, increased after stress treatment and *HSF1*-dependent induction is diminished in *HSF1*-RNAi strains (bin 20/21/29 in Figure 4B).

In contrast, most significantly enriched genes in tetrapyrrole biosynthesis are repressed upon stress treatment and *HSF1*-dependently de-repressed in *HSF1* knock-down strains (bin 19 in Figure 4B). In more detail, all significantly changed enzymes required for the conversion from glutamate to heme are *HSF1*-dependent de-repressed (downregulated after heat shock, less pronounced downregulation in *hsf1* strains), with the exception of *UROS* which is indeed increasingly expressed upon *HSF1* depletion but not repressed upon stress treatment (Figure 4D) (Tanaka and Tanaka 2007). From Protoporphyrin IX towards the chlorophylls four significantly changing transcripts (*CHLI1*, *CHLD*, *CTH1A* and *CAO1*) are de-repressed as well (Figure 4D). Two genes (*CRD1* and *POR*) are *HSF1*-dependently less expressed after heat shock treatment. Interestingly, *CTH1A* and *CRD1* catalyze the same reaction, the formation of the isocyclic ring (Mg-protoporphyrin IX monomethyl ester cyclase or aerobic oxidative cyclase). In copper replete conditions, like in this experiment, *CTH1A*, the *HSF1*-dependent isoform, is the dominating isoform for the formation of the isocyclic ring (Moseley *et al.* 2002). Beside the light-dependent nuclear-encoded *POR* (NADPH:protochlorophyllide oxidoreductase) isoform identified less expressed upon *HSF1* depletion, Chlamydomonas harbors also a second, chloroplast encoded light independent *POR* contributing to the total catalytic capacity. In addition, previous studies of wildtype Chlamydomonas proteome dynamics upon heat stress treatment are in line with these findings, showing significantly decreased protein levels for 5 out of 14 measured enzymes involved in chlorophyll/heme biosynthesis (Muhlhaus *et al.* 2011).

Repression of chlorophyll biosynthesis to different environmental conditions including heat stress was quite frequently observed in higher plants and is widely believed to reflect a

reduction of potential ROS generating intermediates during ongoing stress (Kumar Tewari and Charan Tripathy 1998, Phung *et al.* 2011, Reinbothe and Reinbothe 1996). So far, involved transcriptional regulators in the nucleus have not been identified. Analysis of the promoter regions of several of the genes involved in tetrapyrrole biogenesis did not reveal HSEs. It is tempting to speculate what is the role of HSF1 in repressing the expression of these genes upon heat shock. HSF1 might directly control the expression of a repressor in tetrapyrrole biosynthesis or a *HSF1*-regulated gene is necessary for the retrograde signaling from the chloroplast to the nucleus at heat shock conditions.

Chaperones of all classes and compartments are strongly increased *HSF1*-dependently

Several members from different chaperone families are found within the significant protein.folding (29.6) and stress.abiotic (20.2) bins of the MapMan ontology (Schroda 2004). Not surprisingly, they showed the strongest induction upon heat shock and strongest reduction upon *HSF1* depletion (Figure 4B). In contrast to the studies carried out in *Arabidopsis* members of all chaperone families (sHSPs, HSP60s, HSP70s, HSP90s, HSP100s) have been identified *HSF1*-dependent regulated and all of the bins containing chaperones showed up significantly in the bin enrichment analysis (summarized within Table 1). With the goal to understand general acclimation strategies in photosynthetic organisms to heat stress this nicely demonstrates the advantages of a simplified system. Chaperones and co-chaperones from all different compartments were identified to depend on *HSF1*, including the chloroplast, indicating a role for *HSF1* also in the adaptation of the chloroplast to proteotoxic stress conditions.

Trafficking between the compartments is *HSF1*-dependently modulated

Beside the protein.folding bin (29.6) there is a second subtree significantly *HSF1*-dependently enriched: protein.targeting (29.3). Most of the transcripts increase upon heat stress treatment, but upon *HSF1* depletion there is no obvious tendency. A closer look in this group reveals two subsets of genes (Summarized in Table 2). Proteins involved in organellar targeting show a distinct different expression pattern than those involved in targeting towards the secretory pathway.

With exception of *TOM40* all transcripts of the organellar group are strongly underexpressed upon *HSF1* depletion. Upon stress treatment most of the transcripts within this group, with exception of the outer membrane translocons *TOM40* and *TOC75*, are increased. Beside the translocons of the inner/outer chloroplast/mitochondria membranes there are two proteins involved in inner chloroplast targeting significantly increased upon stress and decreased upon *HSF1* depletion: *FFC* (Fifty-Four-Chloroplast Homologue), a subunit of chloroplast signal recognition particle involved in LHC integration in thylakoids and *TATA α* , a subunit of the Sec independent twin-arginine translocon in the thylakoid membrane (Li *et al.* 1995).

The major difference of the secretory pathway group is the increased expression of nearly all transcripts in *hsf1* strains compared to control strains whereas in the organellar

group the transcripts are less expressed when HSF1 is missing. The only exception is *SRRA1* which is significantly less expressed upon HSF1 depletion. Upon stress treatment most of the members of this group are strongly increased as well. Single exception: *COG3* is significantly less expressed upon stress treatment.

Heat shock acclimation: Protein degradation, protein modification and plastid ribosomes

Beside the chaperones and the trafficking, there are several other proteins *HSF1*-dependently regulated within the, quite general, protein bin (29). Among them several ribosomal proteins of chloroplast ribosomes (*PSRP1*, *PRPL1*, *PRPL4*, *PRPL9* and *PRP1L9*), the respective bin (29.2.1.1.1) is also significantly enriched (Figure 4A). This group of genes is not induced upon heat shock in control cells, but significantly in *hsf1* strains. Furthermore significantly regulated, not unexpected, is the protein.degradation.ubiquitin bin (29.5.11). Most of the genes within this group are strongly induced upon heat stress treatment, even more pronounced in *hsf1* strains. The highest diversity is found within the E3 ligase subgroup, also not unexpected. Several genes from the protein.modification bin (29.4) are found as well *HSF1*-dependently regulated, even though not significantly enriched. There's no conserved response within this subgroup, there is more or less individual adaptation of the different members upon HSF1 depletion. Among them are several protein kinases and also phosphatases. As activation of the HSR involves phosphorylation and HSF1 is a constitutive trimer and not regulated on the level of oligomerization in *Chlamydomonas*, both phosphatases and kinases are of special interest for activation and attenuation of the HSR. Among these genes the strongest *HSF1*-dependent expressed gene is found, *MPA1*. The expression of *MPA1* is strongly increased upon heat shock treatment (fold change in Con_{HS} is 304.4), whereas no induced expression upon heat shock is found in *hsf1* strains (fold change in $hsf1_{HS}$ is 0.7). A close homolog of *MPA1* is the yeast DCR2 protein, a phosphatase involved in signaling/attenuating of the unfolded protein response (Guo and Polymenis 2006). It's closest homolog however, *AtPAP29* in *Arabidopsis*, is not further analyzed so far. There is evidence that *MPA1* is strongly induced in other limiting conditions, phosphate depleted cells harboring no PSR1, the transcription factor necessary for the adaptation to those conditions (Moseley *et al.* 2002).

Redox regulation and ROS protection

Protection from reactive oxygen species (ROS) and redox regulation are especially interesting in photosynthetic organisms because of the second potent ROS source with the proteins along the photosynthetic electron transport chain and many redox regulated enzymes within photosynthesis, especially in the dark reaction. We found the redox.regulation bin (21) to be one of the significantly *HSF1*-dependent regulated bins upon heat shock. In total, most genes in this bin are upregulated upon heat shock and less strong expressed when *HSF1* is underexpressed (Figure 4B).

The thioredoxin superfamily consists of thioredoxins (TRX), glutaredoxins (GRX), protein disulfide isomerase (PDI), glutathione peroxidase (GPX) and glutathione-S-transferase

(GST). While the GPXs and GSTs are involved in ROS scavenging the others facilitate redox regulation of various proteins. Especially the genes in the TRX subgroup (21.1) showed a strong HSF1-dependent transcript increase (Figure 4B). Within this subgroup *TRXx*, a plant specific TRX in the chloroplast, is the only gene less expressed upon heat shock and HSF1-dependently de-repressed. The strongest increase upon heat shock and decrease upon HSF1 depletion was found in *NTR3*, a NADPH-thioredoxin-reductase most probably located in the cytosol (Lemaire and Miginiac-Maslow 2004). Consistently transcripts of the *FTR* (catalytic subunit, beta chain), the chloroplast counterpart of the NTRs in the cytosol/mitochondria responsible for reduction of TRX/GRX proteins, and *GSH1*, the Gamma-glutamylcysteine synthetase which is the rate limiting enzyme in the biosynthesis pathway of glutathione, were also found to be increased upon heat shock and HSF1-dependently less expressed (Griffith and Mulcahy 1999). In total two glutaredoxins (GRX) were found to be upregulated upon heat shock in a HSF1-dependent manner, *GRX3* and *GRX4*, both of the CGFS type involved in deglutathionylation (Lemaire 2004). *GRX3* is the major glutaredoxin in the chloroplast, whereas *GRX4* is probably located in the cytosol (Zaffagnini *et al.* 2008).

ROS protection is facilitated by a number of mechanisms including enzymatic protection by superoxide dismutase, catalase, glutathione peroxidase (GPX) and ascorbate peroxidase (APX). *Chlamydomonas* has, compared to other algae, a weak resistance to ROS (Tanaka *et al.* 2011). We found three manganese superoxide dismutases (*MSD1-3*) to be regulated significantly by HSF1. *MSD1* and *MSD2* were slightly less expressed in HSF1 knock-down strains, whereas *MSD3* is strongly overexpressed when HSF1 is missing. *MSD1* and *MSD3* are predicted to be localized in the cytosol, whereas *MSD2* is probably located in mitochondria. Two members of glutathione-S-transferase (GST) genes were as well found to be upregulated upon heat shock (*GSTS1* stronger than *GSTS2*), HSF1-dependently less pronounced. Both were recently identified induced upon several different oxidative stress conditions (Ledford *et al.* 2007). Within the protein bin there is an additional HSF1-dependent upregulated gene involved in ROS protection (*MSRA3*) which is involved in reactivation of oxidized methionine upon ROS exposure (Brot and Weissbach 1991).

Another way to decrease ROS is to directly adapt the photosynthetic electron transport chain to elevated temperatures and therefore avoid the production of ROS at this site. Heat stress in control cells is not significantly inducing *LHCSR1*, only in *hsf1* strains we found a very strong induction, thus resulting in the strongest HSF1-dependent upregulation. The *LHCSR1* is a gene induced upon several photo-oxidative stress conditions (Im *et al.* 2003, Ledford *et al.* 2004, Miura *et al.* 2004, Peers *et al.* 2009, Richard *et al.* 2000). This might imply that necessary remodeling of the photosynthetic electron transport chain cannot take place in HSF1 knock-down strains. The most prominent change we found was the *LHCBM9* gene, one of the strongest upregulated genes in control cells upon heat shock treatment, but much less induced in HSF1 knock-down strains. *LHCBM9* is also induced at several stress conditions and is probably the least abundant of the major LHCII proteins at ambient conditions (Elrad *et al.* 2002). The second gene directly involved in the photosynthetic electron transport is *FDX6*,

one of six ferredoxins in *Chlamydomonas*. *FDX6* is downregulated to a large extent upon heat shock in control cells, less pronounced in *hsf1* strains. *PETF* is the most abundant ferredoxin in standard growth conditions (98% of the total *FDX* mRNA pool), whereas *FDX6* is expressed to a significant level only in iron limiting condition (Terauchi *et al.* 2009).

Identification of direct HSF1 regulated genes

After characterization of the *HSF1*-dependent heat shock response we aimed to identify candidates for direct targets. HSFs are widely recognized as transcription factors activating transcription of their direct targets, so knock-down should result in less pronounced expression of strongly upregulated genes upon heat stress. Our approach so far aimed for the identification of all *HSF1* regulated genes, also those stronger expressed in *HSF1* mutants, exemplified also in the regulation of tetrapyrrole biosynthesis. Additionally, high affinity target regions might be able to bind residual *HSF1* and will not express significantly different. Indeed we identified three regions in previous studies with chromatin immunoprecipitation to be directly occupied by *HSF1*, namely *HSP70A*, *HSP90A* and *HSP22F* (Strenkert *et al.* 2011b). Only *HSP22F* was identified significantly *HSF1*-dependent in this microarray study (Figure 5D). We therefore used a hierarchical clustering approach to identify similar expressing genes (Figure 5A). When dividing the dataset top-down in three clusters we identified a cluster of 581 genes strongly co-regulated. All genes within the cluster showed strong induction upon stress treatment that is less pronounced upon *HSF1* depletion (Figure 5B). Within this cluster we also found a strong enrichment of significantly *HSF1*-dependent genes (295/581, 50.7 %) compared to the other clusters (Figure 5C). Furthermore, all of the so far known direct *HSF1* targets are located within this cluster (Figure 5D). We therefore propose that among these 581 candidate genes it is very likely to identify new targets of *HSF1*.

HSF1 binds to the promoter region of *HSF1*, *MPA1*, *CLPB3* and *HSP70G*

To characterize these candidates further, we selected a number of candidates to assess *HSF1* binding. We were looking for a set of genes covering most of the aspects raised by this study to be *HSF1*-dependent but still feasible for in depth analysis. We choose genes of potential heat labile proteins (*HSP70G*, *TIC110* and *TIC40*), proteins involved in chloroplast targeting (*TIC110*, *TIC40* and *FFC*), chloroplast proteins in general (*CLPB3*, *CDJ1*, *FFC* and *LHCBM9*), the plant specific stress response (*HSF1*, *LHCBM9*, *CLPB3* and *CDJ1*) and also signaling (*MPA1*).

First, we analyzed the promoter region of these genes for the presence of heat shock elements (HSE). None of the promoters contained perfect HSEs. This is not unexpected, the *HSP70A* promoter in *Chlamydomonas* harbors not a single perfect HSE and is constitutively occupied with *HSF1* even under non-stress conditions (Lodha and Schroda 2005, Strenkert *et al.* 2011a, Strenkert *et al.* 2011b). When allowing one mismatch in the nGAAn consensus we identified potential HSEs within all of the promoter regions (Figure 6A, B). With the exception of *LHCBM9* there is at least one potential HSE within the first 250 bp upstream of the transcriptional start site (TSS). The highest density of HSEs is found in the *MPA1* promoter

where 4 HSEs are found within the first 150 bp.

We next directly monitored HSF1 binding to the promoters (Figure 6C). We identified the *HSP70G* promoter occupied by HSF1 under non-stress and heat shock conditions as well as the *HSF1*, *CLPB3* and *MPA1* promoter bound by HSF1 exclusively after heat shock treatment. All of the described interactions are significantly reduced in *HSF1* knock-down strains.

The promoter regions of *CDJ1*, *TIC40*, *TIC110*, *FFC* and *LHCBM9* showed no direct interaction of HSF1 at the given time and temperature of the experiment. As all of them harbor comparable HSEs to those genes found interacting, we wondered what could be the reason for this discrimination. Possible explanations include other factors necessary for HSF1 binding in the promoter regions and also the chromatin structure surrounding the HSE might be different. It was shown recently in *Drosophila*, that specific active chromatin marks, especially acetylation of lysines in histone 3 and 4, are enriched in HSE already before HSF1 binding (Guertin and Lis 2010). We therefore performed ChIP with antibodies against histone H3, as well as acetylated histone H3 and acetylated histone 4 (Figure 6D, see also Supplemental Figure 2). We combined HSF1-bound HSEs and compared them to those not bound by HSF1. We could not observe a difference in histone occupancy or acetylation level at ambient conditions. However, we found that HSF1-binding induces a conserved response on the chromatin level that includes nucleosome remodelling and acetylation of H3 and H4 (Strenkert *et al.* 2011b). This response was not observed HSF1-unbound promoters (Figure 6D), indicating that indeed a different mechanism is used for the activation of these genes upon heat shock.

In case of the *LHCBM9* promoter we found a very high occupancy of histone H3 and almost no acetylation of histone H3 and H4. This might be due to the fact that the potential HSEs in this promoter are found further away from the TSS, where there is also a less active chromatin setting.

Feedback mechanism: Additional HSF1 is required for further enhanced gene expression

A unique feature of the HSR in plants is the heat shock inducibility of the *HSF* mRNA. We directly observed binding of HSF1 to its own promoter region responsible for this induction during our ChIP experiments. In order to understand the function of this feedback mechanism, we made use of inducible amiRNA strains targeting HSF1. The amiRNA in these strains is controlled by the *NIT1* promoter, which is carefully repressed in ammonia containing media and strongly induced when nitrate is the single nitrogen source (Schmollinger *et al.* 2010). While *HSF1* mRNA and protein level in these strains is unaltered compared to control strains in ammonia containing media, both mRNA and protein is depleted when the amiRNA is induced (Figure 7A/B). Depletion of mRNA is thereby preceding the depletion of HSF1 protein which is mainly dependent on cell division (Schmollinger *et al.* 2010). Already two hours after the switch on nitrate containing media mRNA levels of *HSF1* are readily declining (Figure 7A) while protein levels four hours after the switch are still unaltered (Figure 7B). We made use of this mechanism and performed a heat shock experiment within this time-frame, two hours after the switch of the nitrogen source (Figure 7C). Additional mRNA of *HSF1* is rapidly degraded

via the RNAi pathway (Data not shown) that no further HSF1 protein is synthesized (Figure 7D). Thereby, the initial level of HSF1 is unaltered compared to the control strain (Figure D/E). As there is still HSP90A protein accumulating, the initial HSF1 protein is able to still induce expression of its target genes (Figure 7D). HSF1 protein, both in control and HSF1 amiRNA strains, is also migrating slower in SDS-PAGE experiments after 15 minutes of heat shock (Figure 7E), indicating that phosphorylation, which is part of the activation process of HSF1, is readily performed in both strains (Schulz-Raffelt *et al.* 2007). When comparing the expression of several target genes of *HSF1* (*HSP22F*, *HSP70A*, *HSP70B*, *HSP90A*, *HSP90C*, *CLPB3*) 60 minutes after the onset of heat stress between control and inducible amiRNA strains, heat shock induction is slightly lower in *HSF1* amiRNA strains (Figure 7F). We therefore performed time course experiments to closer inspect the differences between control and amiRNA lines. 30 minutes after onset of the stress there are virtually no differences between control and amiRNA strain (Figure 7G), all three genes are induced to the same amount in all the lines. 60 minutes after the switch to elevated temperatures no additional mRNA is made in the amiRNA lines while the RNA levels still increase in control lines (Figure 7G). The attenuation of the HSR is not affected and also faster in the amiRNA lines, probably due to less pronounced induction in these strains. We therefore conclude that the additional HSF1 protein is necessary to further enhance the transcription of target genes and the feedback loop is necessary to reach the full amplitude of the stress response. It might also be possible that the additional protein is also necessary to induce a second set of targets with lower affinity binding sites. While several HSFs in higher plants are also able to induce induction of other HSFs and thereby modulate the HSR, in *Chlamydomonas* with only a single HSF present this might be the initial evolutionary event in enabling a more fine scaled heat shock response.

Experimental procedures

Strains and Culture Conditions

Chlamydomonas reinhardtii strain cw15-325 (*cwd mt+ arg7*), kindly provided by R. Matagne (University of Liège, Belgium), was used as recipient strain for transformation with control construct pCB412 (Schroda *et al.* 1999), *HSF1*-RNAi construct pMS418 (Schulz-Raffelt *et al.* 2007) and *HSF1*-amiRNA construct pMS540 (Schmollinger *et al.* 2010). Linearized pCB412, pMS418 and pMS540 were transformed into cw15-325 by agitation with glass beads (Kindle 1990). For all experiments strains were grown mixotrophically in TAP medium on a rotatory shaker at 25°C at $\sim 30 \mu\text{E m}^{-2} \text{s}^{-1}$ (Harris 1989). For heat shock experiments, *Chlamydomonas* cells were grown in 120 ml of TAP medium to a cell density of 4×10^6 cells/ml and harvested at 3100 g at room temperature. Cells were immediately resuspended to a cell density of 1×10^7 cells/ml in 40°C prewarmed TAP medium. The culture was incubated in a 40°C water bath under agitation in the light. Samples were taken at the indicated timepoints.

RNA extraction and analysis

Northern experiments: RNA extraction, RNA gels, Northern transfer and hybridization were done as described previously (Liu *et al.* 2005). RNA concentration was determined using a NanoDrop ND-1000 spectrophotometer (NanoDrop Technologies). Probes used were a 2.36-kb *NheI*-*XbaI* fragment from the *HSF1* cDNA clone AV627029 (Asamizu *et al.* 2000), a 3.6-kb *Sall* fragment from the *HSP90C* cDNA (Willmund and Schroda 2005) and the 1-kb cDNA of *CBLP2* (Vonkampen *et al.* 1994). Radioactive signals were detected with BAS-IP MS 2040 phosphorimager plates (Raytest, Straubenhardt, Germany), scanned with a Molecular Imager FX phosphorimager (BioRad, München, Germany).

qRT-PCR analysis: RNA extraction was realized with a modified protocol using the TRIzol reagent (Invitrogen) described previously (Strenkert *et al.* 2011b). Following DNase treatment, reverse transcription and qPCR analysis was performed accordingly. RNA concentration was determined using a NanoDrop ND-1000 spectrophotometer (NanoDrop Technologies). Primers for qRT-PCRs were selected based on a single melt curve, a single band on a 1.5% agarose gel at the calculated amplicon size and maximal efficiency. Primer sequences and amplicon position are illustrated in Supplemental Figure 1 online. qRT-PCR was performed using the StepOnePlus RT-PCR system (Applied Biosystems) with the Maxima SYBR Green kit from Fermentas. Each reaction contained the vendor's master mix, 100 nM of each primer and 10 ng cDNA. A 10 min 95°C denaturation step was followed by 40 cycles of 95°C for 15 s and 65°C for 60 s. Template depleted controls were always included.

Microarray analysis: RNA was analyzed as described previously (Voss *et al.* 2011). RNA concentration was determined using a NanoDrop ND-1000 spectrophotometer (NanoDrop Technologies), integrity/quality was determined on an Agilent 2100 Bioanalyzer (Agilent Technologies). The Agilent 2100 Expert software was used for RNA integrity number index calculation. 0.5 mg of total RNA was reverse transcribed into cDNA, labeled with Cy3 using the

one-color Quick Amp Labeling Kit (Agilent) and hybridized at a temperature of 65°C overnight, according to the manufacturers protocol. The Agilent G2565CA DNA microarray scanner was used to scan the arrays at a resolution of 5 µm and the Feature Extraction Software 9.5.3.1 to process and analyze array images.

Protein analysis

SDS-PAGE for heat shock kinetics and screening for *HSF1* underexpressing strains was performed as described before (Liu *et al.* 2005). Immunodetection was realized using enhanced chemiluminescence (ECL) detected with Hyperfilm-ECL (Amersham, UK).

Chromatin Immunoprecipitation (ChIP)

A total of 10⁹ cells grown under nonstress conditions or 40°C heat shock for 30 min were harvested and prepared for ChIP analysis as described previously (Strenkert *et al.* 2011a). ChIP was performed with aliquots of the initial material corresponding to 2x10⁷ cells and antibodies specific for: histone H3 (5 µL, ab1791 (Abcam)), diacetyl H3K9 and H3K14 (10 µL, 06-599 (Upstate)), tetra-acetyl H4K5, H4K8, H4K12, and H4K16 (10 µL; 06-866 (Upstate)); HSF1 (40µl, affinity purified from rabbit antiserum (Schulz-Raffelt *et al.* 2007, Strenkert *et al.* 2011b)), vesicle-inducing protein in plastids 2 (VIPP2) (40 µL; affinity purified from rabbit antiserum, used as mock control (Strenkert *et al.* 2011a)). Affinity purification was done as described previously (Willmund and Schroda 2005). Precipitated DNA was used for qPCR using the same settings as for qRT-PCR (see above). Primers, selected on single melt curve and a single band on a 1.5% agarose gel at the calculated amplicon size, are summarized in Supplemental Figure 1. Signals for individual gene regions, illustrated in Figure 6C, were normalized against 10% input DNA and then to the corresponding signal derived from the *CYC6* promoter (heat shock).

Acknowledgments

We thank Björn Usadel for providing the most recent MapMan annotations, Olivier Vallon for the antiserum against CF1β. This work was supported by the Max Planck Society and grants from the Deutsche Forschungsgemeinschaft (Schr 617/5-1) and the Bundesministerium für Bildung und Forschung (Systems Biology Initiative FORSYS, project GoFORSYS).

References

- Akerfelt, M., Morimoto, R.I. and Sistonen, L.** (2010) Heat shock factors: integrators of cell stress, development and lifespan. *Nature reviews*, **11**, 545-555.
- Akerfelt, M., Trouillet, D., Mezger, V. and Sistonen, L.** (2007) Heat shock factors at a crossroad between stress and development. *Annals of the New York Academy of Sciences*, **1113**, 15-27.
- Amin, J., Ananthan, J. and Voellmy, R.** (1988) Key features of heat shock regulatory elements. *Molecular and cellular biology*, **8**, 3761-3769.
- Asamizu, E., Miura, K., Kucho, K., Inoue, Y., Fukuzawa, H., Ohyama, K., Nakamura, Y. and Tabata, S.** (2000) Generation of expressed sequence tags from low-CO₂ and high-CO₂ adapted cells of *Chlamydomonas reinhardtii*. *DNA research : an international journal for rapid publication of reports on genes and genomes*, **7**, 305-307.
- Bharti, K., Von Koskull-Doring, P., Bharti, S., Kumar, P., Tintschl-Korbitzer, A., Treuter, E. and Nover, L.** (2004) Tomato heat stress transcription factor HsfB1 represents a novel type of general transcription coactivator with a histone-like motif interacting with the plant CREB binding protein ortholog HAC1. *The Plant cell*, **16**, 1521-1535.
- Brot, N. and Weissbach, H.** (1991) Biochemistry of methionine sulfoxide residues in proteins. *Biofactors*, **3**, 91-96.
- Bukau, B., Weissman, J. and Horwich, A.** (2006) Molecular chaperones and protein quality control. *Cell*, **125**, 443-451.
- Busch, W., Wunderlich, M. and Schoffl, F.** (2005) Identification of novel heat shock factor-dependent genes and biochemical pathways in *Arabidopsis thaliana*. *Plant J*, **41**, 1-14.
- Chan-Schaminet, K.Y., Baniwal, S.K., Bublak, D., Nover, L. and Scharf, K.D.** (2009) Specific interaction between tomato HsfA1 and HsfA2 creates hetero-oligomeric superactivator complexes for synergistic activation of heat stress gene expression. *The Journal of biological chemistry*, **284**, 20848-20857.
- Cotto, J.J., Kline, M. and Morimoto, R.I.** (1996) Activation of heat shock factor 1 DNA binding precedes stress-induced serine phosphorylation. Evidence for a multistep pathway of regulation. *The Journal of biological chemistry*, **271**, 3355-3358.
- Czarnecka-Verner, E., Yuan, C.X., Scharf, K.D., English, G. and Gurley, W.B.** (2000) Plants contain a novel multi-member class of heat shock factors without transcriptional activator potential. *Plant molecular biology*, **43**, 459-471.
- Damberger, F.F., Pelton, J.G., Harrison, C.J., Nelson, H.C. and Wemmer, D.E.** (1994) Solution structure of the DNA-binding domain of the heat shock transcription factor determined by multidimensional heteronuclear magnetic resonance spectroscopy. *Protein Sci*, **3**, 1806-1821.
- Doring, P., Treuter, E., Kistner, C., Lyck, R., Chen, A. and Nover, L.** (2000) The role of AHA motifs in the activator function of tomato heat stress transcription factors HsfA1 and HsfA2. *The Plant cell*, **12**, 265-278.
- Dutta, S., Mohanty, S. and Tripathy, B.C.** (2009) Role of temperature stress on chloroplast biogenesis and protein import in pea. *Plant physiology*, **150**, 1050-1061.
- Eberhard, S., Jain, M., Im, C.S., Pollock, S., Shrager, J., Lin, Y., Peek, A.S. and Grossman, A.R.** (2006) Generation of an oligonucleotide array for analysis of gene expression in *Chlamydomonas reinhardtii*. *Current genetics*, **49**, 106-124.
- Elrad, D., Niyogi, K.K. and Grossman, A.R.** (2002) A major light-harvesting polypeptide of photosystem II functions in thermal dissipation. *The Plant cell*, **14**, 1801-1816.
- Goldenberg, C.J., Luo, Y., Fenna, M., Baler, R., Weinmann, R. and Voellmy, R.** (1988) Purified human factor activates heat shock promoter in a HeLa cell-free transcription system. *The Journal of biological chemistry*, **263**, 19734-19739.

- Griffith, O.W. and Mulcahy, R.T.** (1999) The enzymes of glutathione synthesis: gamma-glutamylcysteine synthetase. *Adv Enzymol Relat Areas Mol Biol*, **73**, 209-267, xii.
- Guertin, M.J. and Lis, J.T.** (2010) Chromatin landscape dictates HSF binding to target DNA elements. *PLoS genetics*, **6**.
- Guo, J. and Polymenis, M.** (2006) Dcr2 targets Ire1 and downregulates the unfolded protein response in *Saccharomyces cerevisiae*. *EMBO reports*, **7**, 1124-1127.
- Guo, J., Wu, J., Ji, Q., Wang, C., Luo, L., Yuan, Y., Wang, Y. and Wang, J.** (2008) Genome-wide analysis of heat shock transcription factor families in rice and Arabidopsis. *Journal of genetics and genomics = Yi chuan xue bao*, **35**, 105-118.
- Harris, E.H.** (1989) The Chlamydomonas Sourcebook. A Comprehensive Guide to Biology and Laboratory Use. Elizabeth H. Harris. Academic Press, San Diego, CA, 1989. xiv, 780 pp., illus. \$145. *Science (New York, N.Y.)*, **246**, 1503-1504.
- Hartl, F.U., Bracher, A. and Hayer-Hartl, M.** (2011) Molecular chaperones in protein folding and proteostasis. *Nature*, **475**, 324-332.
- Im, C.S., Zhang, Z., Shrager, J., Chang, C.W. and Grossman, A.R.** (2003) Analysis of light and CO(2) regulation in *Chlamydomonas reinhardtii* using genome-wide approaches. *Photosynthesis research*, **75**, 111-125.
- Kindle, K.L.** (1990) High-frequency nuclear transformation of *Chlamydomonas reinhardtii*. *Proceedings of the National Academy of Sciences of the United States of America*, **87**, 1228-1232.
- Kumar, M., Busch, W., Birke, H., Kemmerling, B., Nurnberger, T. and Schoffl, F.** (2009) Heat shock factors HsfB1 and HsfB2b are involved in the regulation of Pdf1.2 expression and pathogen resistance in Arabidopsis. *Mol Plant*, **2**, 152-165.
- Kumar Tewari, A. and Charan Tripathy, B.** (1998) Temperature-stress-induced impairment of chlorophyll biosynthetic reactions in cucumber and wheat. *Plant physiology*, **117**, 851-858.
- Ledford, H.K., Baroli, I., Shin, J.W., Fischer, B.B., Eggen, R.I. and Niyogi, K.K.** (2004) Comparative profiling of lipid-soluble antioxidants and transcripts reveals two phases of photo-oxidative stress in a xanthophyll-deficient mutant of *Chlamydomonas reinhardtii*. *Molecular genetics and genomics : MGG*, **272**, 470-479.
- Ledford, H.K., Chin, B.L. and Niyogi, K.K.** (2007) Acclimation to singlet oxygen stress in *Chlamydomonas reinhardtii*. *Eukaryotic cell*, **6**, 919-930.
- Lee, J.H., Hubel, A. and Schoffl, F.** (1995) Derepression of the activity of genetically engineered heat shock factor causes constitutive synthesis of heat shock proteins and increased thermotolerance in transgenic Arabidopsis. *Plant J*, **8**, 603-612.
- Lemaire, S.D.** (2004) The glutaredoxin family in oxygenic photosynthetic organisms. *Photosynthesis research*, **79**, 305-318.
- Lemaire, S.D. and Miginiac-Maslow, M.** (2004) The thioredoxin superfamily in *Chlamydomonas reinhardtii*. *Photosynthesis research*, **82**, 203-220.
- Li, X., Henry, R., Yuan, J., Cline, K. and Hoffman, N.E.** (1995) A chloroplast homologue of the signal recognition particle subunit SRP54 is involved in the posttranslational integration of a protein into thylakoid membranes. *Proceedings of the National Academy of Sciences of the United States of America*, **92**, 3789-3793.
- Lin, Y.X., Jiang, H.Y., Chu, Z.X., Tang, X.L., Zhu, S.W. and Cheng, B.J.** (2011) Genome-wide identification, classification and analysis of heat shock transcription factor family in maize. *BMC genomics*, **12**, 76.
- Littlefield, O. and Nelson, H.C.** (1999) A new use for the 'wing' of the 'winged' helix-turn-helix motif in the HSF-DNA cocrystal. *Nat Struct Biol*, **6**, 464-470.
- Liu, C., Willmund, F., Whitelegge, J.P., Hawat, S., Knapp, B., Lodha, M. and Schroda, M.** (2005) J-domain protein CDJ2 and HSP70B are a plastidic chaperone pair that interacts with vesicle-inducing protein in plastids 1. *Molecular biology of the cell*, **16**, 1165-1177.

- Lodha, M. and Schroda, M.** (2005) Analysis of chromatin structure in the control regions of the chlamydomonas HSP70A and RBCS2 genes. *Plant molecular biology*, **59**, 501-513.
- May, P., Wienkoop, S., Kempa, S., Usadel, B., Christian, N., Rupprecht, J., Weiss, J., Recuenco-Munoz, L., Ebenhoh, O., Weckwerth, W. and Walther, D.** (2008) Metabolomics- and proteomics-assisted genome annotation and analysis of the draft metabolic network of *Chlamydomonas reinhardtii*. *Genetics*, **179**, 157-166.
- Miura, K., Yamano, T., Yoshioka, S., Kohinata, T., Inoue, Y., Taniguchi, F., Asamizu, E., Nakamura, Y., Tabata, S., Yamato, K.T., Ohyama, K. and Fukuzawa, H.** (2004) Expression profiling-based identification of CO₂-responsive genes regulated by CCM1 controlling a carbon-concentrating mechanism in *Chlamydomonas reinhardtii*. *Plant physiology*, **135**, 1595-1607.
- Morimoto, R.I.** (1998) Regulation of the heat shock transcriptional response: cross talk between a family of heat shock factors, molecular chaperones, and negative regulators. *Genes & development*, **12**, 3788-3796.
- Moseley, J.L., Page, M.D., Alder, N.P., Eriksson, M., Quinn, J., Soto, F., Theg, S.M., Hippler, M. and Merchant, S.** (2002) Reciprocal expression of two candidate di-iron enzymes affecting photosystem I and light-harvesting complex accumulation. *The Plant cell*, **14**, 673-688.
- Muhlhaus, T., Weiss, J., Hemme, D., Sommer, F. and Schroda, M.** (2011) Quantitative shotgun proteomics using a uniform (1)N-labeled standard to monitor proteome dynamics in time course experiments reveals new insights into the heat stress response of *Chlamydomonas reinhardtii*. *Mol Cell Proteomics*, **10**, M110 004739.
- Nover, L., Bharti, K., Doring, P., Mishra, S.K., Ganguli, A. and Scharf, K.D.** (2001) Arabidopsis and the heat stress transcription factor world: how many heat stress transcription factors do we need? *Cell stress & chaperones*, **6**, 177-189.
- Peers, G., Truong, T.B., Ostendorf, E., Busch, A., Elrad, D., Grossman, A.R., Hippler, M. and Niyogi, K.K.** (2009) An ancient light-harvesting protein is critical for the regulation of algal photosynthesis. *Nature*, **462**, 518-521.
- Pelham, H.R.** (1982) A regulatory upstream promoter element in the *Drosophila* hsp 70 heat-shock gene. *Cell*, **30**, 517-528.
- Peteranderl, R. and Nelson, H.C.** (1992) Trimerization of the heat shock transcription factor by a triple-stranded alpha-helical coiled-coil. *Biochemistry*, **31**, 12272-12276.
- Phung, T.H., Jung, H.I., Park, J.H., Kim, J.G., Back, K. and Jung, S.** (2011) Porphyrin biosynthesis control under water stress: sustained porphyrin status correlates with drought tolerance in transgenic rice. *Plant physiology*, **157**, 1746-1764.
- Prandl, R., Hinderhofer, K., Eggers-Schumacher, G. and Schoffl, F.** (1998) HSF3, a new heat shock factor from *Arabidopsis thaliana*, derepresses the heat shock response and confers thermotolerance when overexpressed in transgenic plants. *Mol Gen Genet*, **258**, 269-278.
- Reinbothe, S. and Reinbothe, C.** (1996) The regulation of enzymes involved in chlorophyll biosynthesis. *European journal of biochemistry / FEBS*, **237**, 323-343.
- Richard, C., Ouellet, H. and Guertin, M.** (2000) Characterization of the LI818 polypeptide from the green unicellular alga *Chlamydomonas reinhardtii*. *Plant molecular biology*, **42**, 303-316.
- Scharf, K.D., Heider, H., Hohfeld, I., Lyck, R., Schmidt, E. and Nover, L.** (1998) The tomato Hsf system: HsfA2 needs interaction with HsfA1 for efficient nuclear import and may be localized in cytoplasmic heat stress granules. *Molecular and cellular biology*, **18**, 2240-2251.
- Schmollinger, S., Strenkert, D. and Schroda, M.** (2010) An inducible artificial microRNA system for *Chlamydomonas reinhardtii* confirms a key role for heat shock factor 1 in regulating thermotolerance. *Current genetics*, **56**, 383-389.

- Schramm, F., Ganguli, A., Kiehlmann, E., English, G., Walch, D. and von Koskull-Doring, P.** (2006) The heat stress transcription factor HsfA2 serves as a regulatory amplifier of a subset of genes in the heat stress response in Arabidopsis. *Plant molecular biology*, **60**, 759-772.
- Schroda, M.** (2004) The Chlamydomonas genome reveals its secrets: chaperone genes and the potential roles of their gene products in the chloroplast. *Photosynthesis research*, **82**, 221-240.
- Schroda, M., Vallon, O., Wollman, F.A. and Beck, C.F.** (1999) A chloroplast-targeted heat shock protein 70 (HSP70) contributes to the photoprotection and repair of photosystem II during and after photoinhibition. *The Plant cell*, **11**, 1165-1178.
- Schulz-Raffelt, M., Lodha, M. and Schroda, M.** (2007) Heat shock factor 1 is a key regulator of the stress response in Chlamydomonas. *Plant J*, **52**, 286-295.
- Sorger, P.K. and Pelham, H.R.** (1988) Yeast heat shock factor is an essential DNA-binding protein that exhibits temperature-dependent phosphorylation. *Cell*, **54**, 855-864.
- Stauber, E.J., Busch, A., Naumann, B., Svatos, A. and Hippler, M.** (2009) Proteotypic profiling of LHCI from Chlamydomonas reinhardtii provides new insights into structure and function of the complex. *Proteomics*, **9**, 398-408.
- Strenkert, D., Schmollinger, S. and Schroda, M.** (2011a) Protocol: methodology for chromatin immunoprecipitation (ChIP) in Chlamydomonas reinhardtii. *Plant Methods*, **7**, 35.
- Strenkert, D., Schmollinger, S., Sommer, F., Schulz-Raffelt, M. and Schroda, M.** (2011b) Transcription factor-dependent chromatin remodeling at heat shock and copper-responsive promoters in Chlamydomonas reinhardtii. *The Plant cell*, **23**, 2285-2301.
- Taji, T., Ohsumi, C., Iuchi, S., Seki, M., Kasuga, M., Kobayashi, M., Yamaguchi-Shinozaki, K. and Shinozaki, K.** (2002) Important roles of drought- and cold-inducible genes for galactinol synthase in stress tolerance in Arabidopsis thaliana. *Plant J*, **29**, 417-426.
- Tanaka, R. and Tanaka, A.** (2007) Tetrapyrrole biosynthesis in higher plants. *Annu Rev Plant Biol*, **58**, 321-346.
- Tanaka, S., Ikeda, K., Miyasaka, H., Shioi, Y., Suzuki, Y., Tamoi, M., Takeda, T., Shigeoka, S., Harada, K. and Hirata, K.** (2011) Comparison of three Chlamydomonas strains which show distinctive oxidative stress tolerance. *J Biosci Bioeng*, **112**, 462-468.
- Terauchi, A.M., Lu, S.F., Zaffagnini, M., Tappa, S., Hirasawa, M., Tripathy, J.N., Knaff, D.B., Farmer, P.J., Lemaire, S.D., Hase, T. and Merchant, S.S.** (2009) Pattern of expression and substrate specificity of chloroplast ferredoxins from Chlamydomonas reinhardtii. *The Journal of biological chemistry*, **284**, 25867-25878.
- Thimm, O., Blasing, O., Gibon, Y., Nagel, A., Meyer, S., Kruger, P., Selbig, J., Muller, L.A., Rhee, S.Y. and Stitt, M.** (2004) MAPMAN: a user-driven tool to display genomics data sets onto diagrams of metabolic pathways and other biological processes. *Plant J*, **37**, 914-939.
- Treuter, E., Nover, L., Ohme, K. and Scharf, K.D.** (1993) Promoter specificity and deletion analysis of three heat stress transcription factors of tomato. *Mol Gen Genet*, **240**, 113-125.
- Trinklein, N.D., Murray, J.I., Hartman, S.J., Botstein, D. and Myers, R.M.** (2004) The role of heat shock transcription factor 1 in the genome-wide regulation of the mammalian heat shock response. *Molecular biology of the cell*, **15**, 1254-1261.
- von Koskull-Doring, P., Scharf, K.D. and Nover, L.** (2007) The diversity of plant heat stress transcription factors. *Trends in plant science*, **12**, 452-457.
- Vonkampen, J., Nielander, U. and Wetter, M.** (1994) Stress-Dependent Transcription of a Gene Encoding a G-Beta-Like Polypeptide from Chlamydomonas-Reinhardtii. *J Plant Physiol*, **143**, 756-758.
- Voss, B., Meinecke, L., Kurz, T., Al-Babili, S., Beck, C.F. and Hess, W.R.** (2011) Hemin and magnesium-protoporphyrin IX induce global changes in gene expression in

- Chlamydomonas reinhardtii*. *Plant physiology*, **155**, 892-905.
- Willmund, F. and Schroda, M.** (2005) HEAT SHOCK PROTEIN 90C is a bona fide Hsp90 that interacts with plastidic HSP70B in *Chlamydomonas reinhardtii*. *Plant physiology*, **138**, 2310-2322.
- Wu, C.** (1995) Heat shock transcription factors: structure and regulation. *Annual review of cell and developmental biology*, **11**, 441-469.
- Xiao, H. and Lis, J.T.** (1988) Germline transformation used to define key features of heat-shock response elements. *Science (New York, N.Y.)*, **239**, 1139-1142.
- Zaffagnini, M., Michelet, L., Massot, V., Trost, P. and Lemaire, S.D.** (2008) Biochemical characterization of glutaredoxins from *Chlamydomonas reinhardtii* reveals the unique properties of a chloroplastic CGFS-type glutaredoxin. *The Journal of biological chemistry*, **283**, 8868-8876.
- Zimarino, V. and Wu, C.** (1987) Induction of sequence-specific binding of *Drosophila* heat shock activator protein without protein synthesis. *Nature*, **327**, 727-730.

Short legends for Supporting Information

Figure S1: Individual analyzed genes, qRT-PCR and CHIP primers, gene models

Figure S2: HSE sequence information, individual promoter regions in CHIP experiments (Nucleosome occupancy, acetylation of H3 and H4 histones)

Supplemental table 1: Differential HSF1-dependent expressed genes at ambient temperature (*hsf1_{CL}*)

Supplemental table 2: Differential HSF1-dependent expressed genes upon heat shock (*hsf1_{HS}*)

Supplemental table 3: Potential direct HSF1 targets from hierarchical clustering (Cluster 2)

Figures and tables

Table 1: Differential expressed chaperones and co-chaperones upon heat shock treatment

Name	Au5 ID	MapMan	microarray		qRT-PCR		Protein
			HS _{Con}	<i>hsf1</i> _{HS}	HS _{Con}	<i>hsf1</i> _{HS}	HS _{Con}
Heat shock factor							
HSF1	525816	20.2.1	4.33	-2.45	4.50	-3.35	-
sHSPs							
HSP22A	524323	29.6.2.1.1	10.33	(-2.73)	-	-	4.42
HSP22B	524324	29.6.2.1.1	-1.73	(0.31)	-	-	-
HSP22C	511863	29.6.2.1.1	9.40	(-2.72)	-	-	4.70
HSP22F	515324	29.6.2.1.1	8.53	-4.83	11.91	-8.84	-
HSP60s							
CPN60B1	517973	29.6.2.2.2.1	2.87	-4.15	-	-	1.07
CPN60A	521778	29.6.2.2.2.1	3.72	-3.44	5.13	-3.05	2.04
CPN60B2	524751	29.6.2.2.2.1	2.25	-2.29	-	-	2.00
CCT5	520572	29.6.2.2.1.1	0.81	-3.15	-	-	-
CCT7	511155	29.6.2.2.1.1	1.80	-2.35	-	-	-
HSP60 co-chaperones							
CPN20	520331	29.6.2.2.2.2	2.25	-3.45	-	-	1.32
CPN23	512968	29.6.2.2.2.2	5.50	-4.40	-	-	1.32
HSP70s							
HSP70A	525480	20.2.5	3.85	(-0.55)	5.71	-0.77	1.54
HSP70B	522821	29.6.2.3.1	2.77	-1.87	3.83	-2.82	1.26
HSP70C	525943	29.6.2.3.1	4.13	-3.70	2.25	-2.35	0.38
HSP70E	516599	29.6.2.3.1	4.39	(-1.11)	-	-	1.00
HSP70G	510023	29.6.2.3.1	3.56	(-0.37)	1.75	-3.13	-
BIP1	518564	29.6.2.3.1	3.36	(-0.81)	-	-	-
HSP70 co-chaperones							
CGE1.a	524803	20.2.1	3.04	-2.74	-	-	-
CDJ1	513011	20.2.1	4.34	-3.13	1.86	-0.61	-
CDJ3	510809	20.2.1	-4.65	(-0.06)	-	-	-
CDJ5	524356	20.2.1	-3.48	(-1.21)	-	-	-
DNJ1	517115	29.6.2.3.2.2	3.28	-2.36	-	-	1.20
DNJ6	523046	29.6.2.3.2.2	2.40	(0.37)	-	-	-
DNJ8	511277	20.2.1	2.25	-3.09	-	-	-
DNJ21	512133	20.2.1	6.61	-3.27	-	-	-
DNJ26	519172	29.6.2.3.2.2	1.54	(0.36)	-	-	-
DNJ34	524507	29.6.2.3.2.2	-2.21	1.42	-	-	-
ERJ1	524350	20.2.1	2.32	-1.20	-	-	-
HSP90s							
HSP90A	525808	20.2.1	4.16	(-0.67)	5.04	-0.49	2.38
HSP90B	518563	20.2.1	5.82	(-0.86)	-	-	0.49
HSP90C	513163	20.2.1	7.03	-5.75	5.48	-4.77	1.77
HSP100s							
CLPB1	518085	20.2.1	7.31	(-0.91)	-	-	4.47
CLPB3	518776	20.2.1	4.49	-2.26	6.76	-5.40	2.51

CLPB4	518155	20.2.1	1.73	-1.86	-	-	2.63
CLPD1	510564	29.6.2.5.1	-2.57	(1.47)	-	-	-
Misc							
CGL57	516970	20.2.1	-1.42	-1.28	-	-	-
HOP1	521280	20.2.1	5.98	-3.63	-	-	1.38
CDI1	514067	20.2.1	1.74	-1.06	-	-	-
	513811	20.2.1	-2.24	-2.92	-	-	-
ERM9	510452	20.2.3	-2.91	(0.21)	-	-	-
DDB1	509864	20.2.5	1.94	(1.42)	-	-	-
HSLU1	513078	29.6.2.5.1	-1.64	(-0.71)	-	-	-
FKB42	518811	29.6.3.1	3.98	-4.23	-	-	-
FKB16-8	512268	29.6.3.1	-1.50	(-0.98)	-	-	-
FKB12	514667	29.6.3.1	-2.39	(0.73)	-	-	-0.28
CYN26	520960	29.6.3.2	1.67	(0.27)	-	-	-
CYN20-1	523573	29.6.3.2	-0.67	(0.16)	-	-	-0.14

Values in brackets () are not significantly changing upon treatment

Table 2: Differential HSF1-dependent expressed genes involved in protein targeting (29.3)

Name	Au5 ID	MapMan	microarray		qRT-PCR		Protein <i>hsf1</i> _{HS}
			HS _{Con}	<i>hsf1</i> _{HS}	HS _{Con}	HS _{Con}	
Chloroplast/mitochondria							
TOM40	509712	29.3.2	(-0.67)	1.56	-	-	-
TIM14	519682	20.2.1	2.50	-1.14	-	-	-
TIM17	510295	29.3.2	1.83	-2.35	-	-	-
TIM22B	521131	29.3.2	1.04	-1.52	-	-	-
TOC75	520970	29.3.3	-2.20	-1.33	-	-	-
TIC40	513018	29.3.3	2.26	-3.28	0.80	-2.45	-0.91
TIC110	510291	29.3.3	1.82	-2.50	0.55	-4.46	-
FFC	512407	29.3.3	3.63	-3.26	1.42	-2.17	-
TATA	509998	29.3.3	1.04	-2.86	-	-	-
ER/Golgi/Secretory pathway							
SRRA1	516748	29.3.4.1	2.27	-0.98	-	-	-
SRRB1	517472	29.3.4.99	1.40	0.94	-	-	-
SEC13	517414	29.3.4.4	1.52	1.06	-	-	-
SEC31	513315	29.3.4.99	(0.37)	1.63	-	-	-
SEC61B	524314	29.3.4.99	1.85	1.39	-	-	-
SEC61G	512035	29.3.4.99	2.34	1.08	-	-	-
CGL49	512584	29.3.4.99	1.82	1.34	-	-	-
AP2M2	512082	29.3.4.99	2.34	1.64	-	-	-
RER1	514016	29.3.4.1	(0.95)	1.76	-	-	-
COG3	521578	29.3.4.2	-2.32	1.53	-	-	-
VPS28	516622	29.3.4.3	2.12	1.08	-	-	-

Values in brackets () are not significantly changing upon treatment

Figure 1

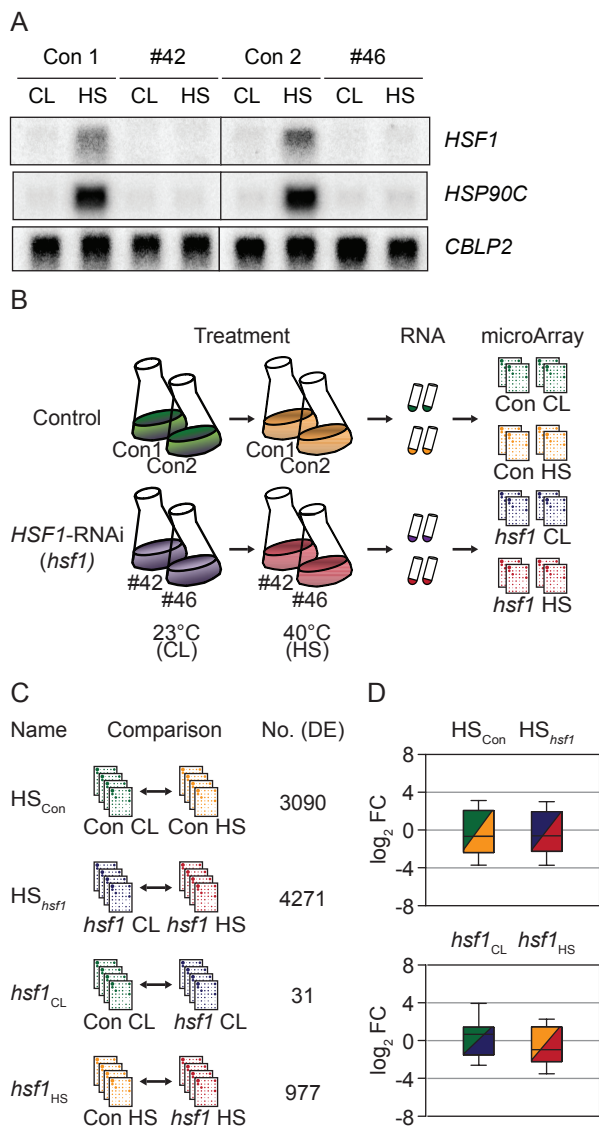


Figure 1: Experiment overview

A: *HSF1* expression in the used *HSF1* knockdown lines: RNA gel blot analysis of transcript accumulation in two control (Con1 and 2) and two independent *HSF1*-RNAi *Chlamydomonas* strains (#42 and #46). Cells were subjected to a 30-minutes heat shock treatment at 40°C in the light (HS) or kept at 23°C in the light (CL). Total RNA was extracted, separated on formaldehyde-containing agarose gels, transferred to nylon membranes and hybridized with radioactive probes against *HSF1*, *HSP90C* and *CBLP2* as loading control.

B: Experimental setup for the microarray experiment: Two independent *HSF1* knockdown lines (*HSF1*-RNAi) and two empty vector control strains (Control) were subjected to a 30 minutes heat shock treatment at 40°C in the light (HS) or kept at 23°C for 30 minutes in the light (CL). RNA was subsequently extracted and analyzed in duplicates on Agilent single color Custom Arrays (Eberhard *et al.* 2006, Voss *et al.* 2011)

C: Microarray analysis overview: The response to heat shock treatment was analyzed in control (HS_{Con}) and *HSF1* knockdown strains (HS_{hsf1}). The influence of *HSF1* knockdown on gene expression was analyzed at ambient temperatures ($hsf1_{CL}$) and after 30 minutes heat shock ($hsf1_{HS}$). The number of significantly differential expressed genes (No.(DE)) in each comparison was determined.

D: Differential gene expression overview: The distribution of \log_2 fold changes (\log_2 FC) of all transcripts due to heat shock treatment or *HSF1* knockdown (HS_{Con} , HS_{hsf1} , $hsf1_{CL}$, $hsf1_{HS}$) is illustrated with boxplots. From bottom to top plotted lines correspond to the 10th, 25th (Q_1), 50th (median), 75th (Q_3), and 90th percentiles.

Figure 2

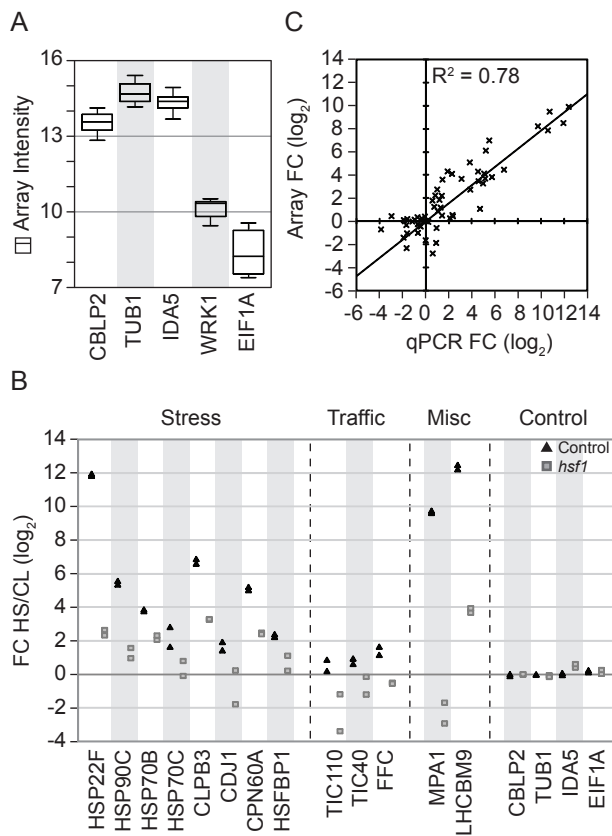


Figure 2: Microarray quality control

A: Variation of housekeeping genes: The raw signal intensity after normalization (Array intensity) of selected housekeeping transcripts in all 16 microarrays is illustrated with boxplots, from bottom to top plotted lines correspond to the 10th, 25th (Q₁), 50th (median), 75th (Q₃), and 90th percentiles.

B: Comparison of qRT-PCR and microarray measured transcript accumulation: For 19 selected genes the transcript log₂ fold change (log₂ FC) upon heat stress treatment and *HSF1* depletion was compared to the control group under non stress conditions (57 datapoints in total). Transcript accumulation derived from microarray analysis (y-axis) is plotted against corresponding qRT-PCR derived accumulation (x-axis). The linear regression line through the origin with the coefficient of determination (R²) is added to the plot. Experimental conditions and RNA extraction as described in Figure 1B for the microarray data and Figure 2C for the qRT-PCR data.

C: Selected significant *HSF1*-dependent underexpressing genes (*hsf1*_{HS}): Two independent inducible *HSF1* amiRNA knockdown lines (grey square) and two empty vector control strains (black triangle) were subjected to a 30 minutes heat shock treatment at 40°C in the light (HS) or kept at ambient temperatures (23°C) for 30 minutes in the light (CL). RNA was subsequently extracted for qRT-PCR analysis performed in three technical replicates using the comparative CT method with *CBLP2* as control gene (except for *CBLP2*, where *TUB1* served as control gene). Transcript accumulation (log₂) of 13 selected significantly *HSF1*-dependent underexpressing genes and 4 housekeeping genes upon heat shock treatment (HS/CL) was analyzed.

Figure 3

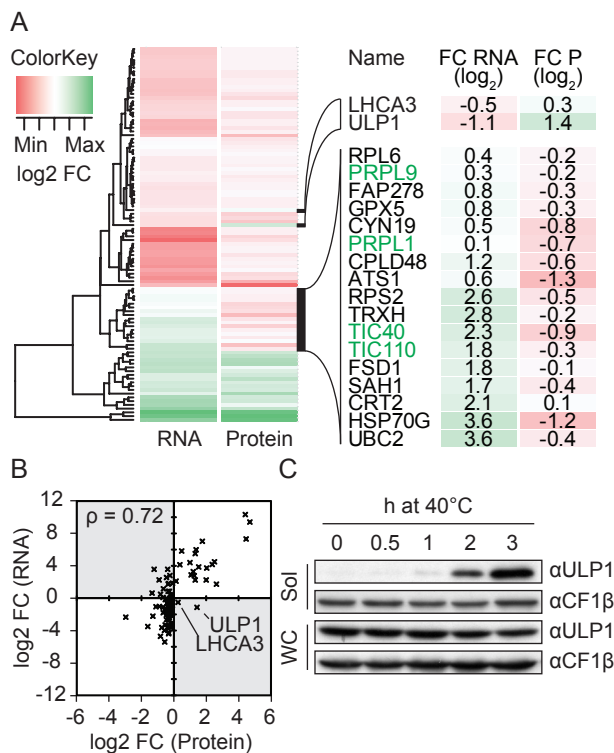


Figure 3: Comparison of transcript and protein accumulation upon heat shock treatment

A: Transcript and protein accumulation overview: Hierarchical clustering tree (Manhattan distances, Average linkage, using the hclust function in R) based on transcript accumulation (log₂) upon 30 minutes heat shock treatment in control cells (RNA) and the maximal protein accumulation (log₂) within a 3 hours heat shock treatment (Protein)(Muhlhaus *et al.* 2011). Underexpressed genes or proteins are colored in red, accumulated transcripts/proteins in green. Non-conforming gene/protein pairs are highlighted and their log₂ transformed accumulation of transcripts/protein upon heat shock (FC RNA/FC P) is given. Additionally, significantly *HSF1*-dependently transcribed genes are written in green letters.

B: Correlation between RNA and protein accumulation: For 100 genes and their encoded significantly changing proteins the transcript log₂ fold change (log₂ FC) upon stress treatment derived from microarray analysis (y-axis) is plotted against corresponding protein maximal log₂ fold change (FC) within a 3 hours heat shock treatment (x-axis). The Pearson Product Moment Correlation Coefficient (ρ) as calculated with SigmaPlot is added to the graph. Non correlating protein/RNA areas are shaded in grey.

C: Analysis of the heat shock induction of ULP1: Total (WC) and soluble proteins (Sol) of 30 minutes 40°C heat shock treated *Chlamydomonas* wildtype cells were extracted, loaded corresponding to 2 μ g Chlorophyll and separated on a 10% SDS-polyacrylamide gel. Levels of ULP1 relative to loading control CF1 β were analyzed by immunoblotting.

Figure 4

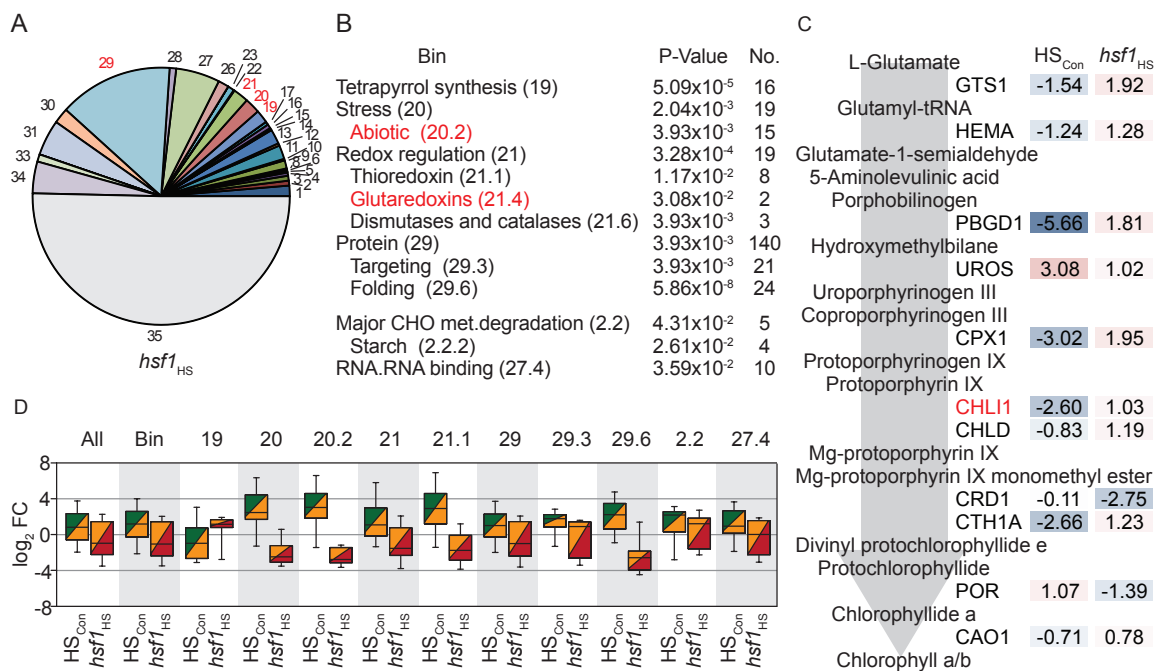


Figure 4: *HSF1*-dependent genes upon heat shock treatment (*hsf1*_{HS})

A: Functional category overview: All *HSF1*-dependent differentially expressed genes after heat shock were grouped according to their assigned functional category in MapMan (Bin) (Thimm *et al.* 2004). The number of differentially expressed genes within a certain bin corresponds to the size of the pie slice. Significantly enriched categories are colored in red.

B: Significantly enriched functional categories: Significantly enriched MapMan functional categories (P-Value ≤ 0.05 , ≥ 5 significantly differential expressed genes (No.)) of the highest order and significant subcategories are summarized. Significant *HSF*-dependent bins previously identified in *Arabidopsis thaliana* microarray studies are colored in red (20.2 and 21.4).

C: Tetrapyrrole biosynthesis pathway: Scheme of the chlorophyll a/b and heme biosynthesis pathway in *Chlamydomonas*. Included are significantly *HSF1*-dependent expressed genes, the log₂ fold change of their transcripts upon stress treatment (HS_{Con}) and upon *HSF1* depletion after heat shock (*hsf1*_{HS}). Genes whose corresponding protein levels have been identified to be significantly depleted upon heat shock (CHL11) in a recently performed proteomic study are colored in red (Muhlhaus *et al.* 2011).

D: Differential gene expression in significantly enriched functional categories: The distribution of log₂ fold changes of transcripts (log₂ FC) to heat shock treatment in the control strains or *HSF1* knockdown upon heat shock (HS_{Con}, *hsf1*_{HS}) of all 977 differentially expressed genes (All), those present in any significantly enriched MapMan functional category (Bin) and those present in the individual bins (i.e. 29.3) is illustrated with boxplots. From bottom to top plotted lines correspond to the 10th, 25th (Q₁), 50th (median), 75th (Q₃), and 90th percentiles.

Figure 5

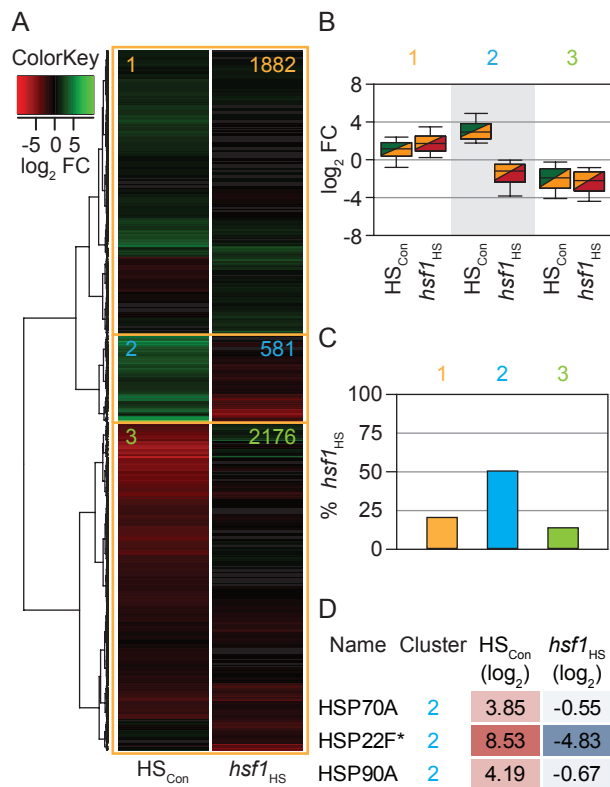


Figure 5: Potential direct HSF1 targets

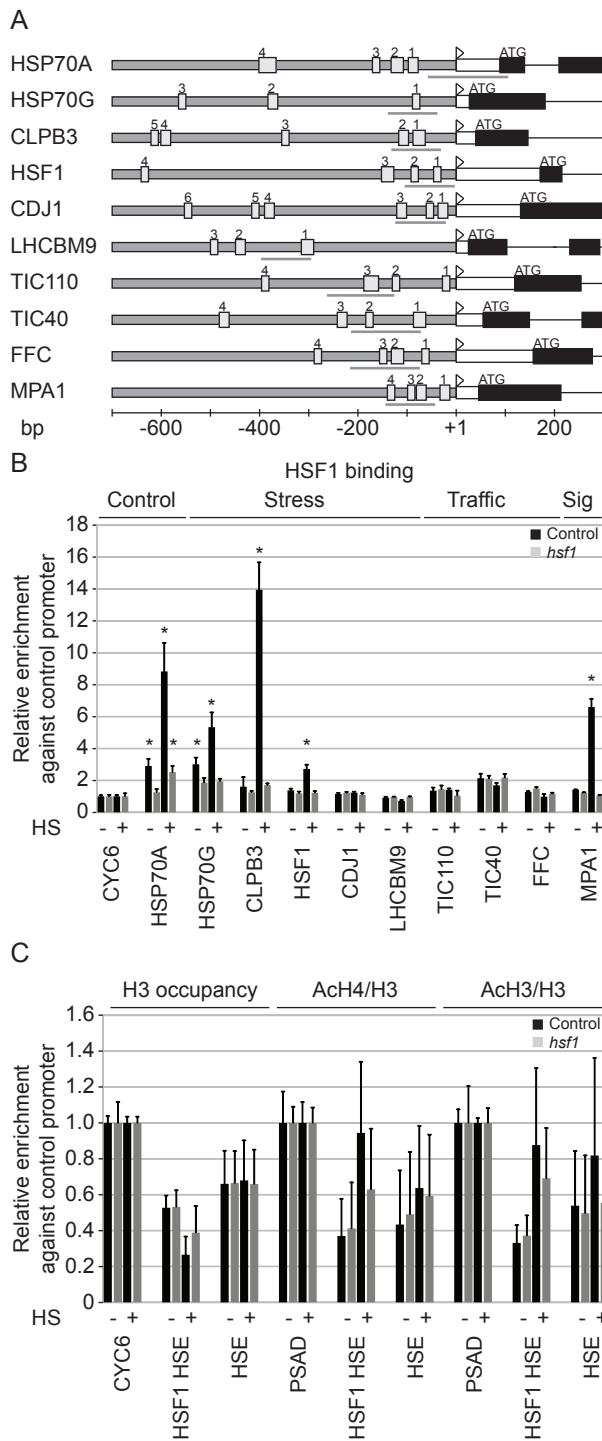
A: HSF1-dependent activated genes during stress treatment: Hierarchical clustering tree (Manhattan distances, Ward's linkage, using the hclust function in R) based on transcript accumulation (\log_2 fold change) upon heat shock treatment and *HSF1* knockdown (HS_{con}, hsf1_{HS}). Strong underexpressed genes upon heat shock or *HSF1* depletion are colored in red, overexpressed genes in green. Clusters, derived in a top-down manner, are labeled from top to bottom (1, 2, 3/orange, blue, green respectively) and the respective number of genes in the cluster is given in the figure.

B: Differential gene expression in top three clusters: The \log_2 fold change of transcripts (\log_2 FC) to heat shock treatment in the control strains or *HSF1* knockdown after heat shock (HS_{con}, hsf1_{HS}) of the three clusters (from Figure 5A) is illustrated with boxplots. From bottom to top plotted lines correspond to the 10th, 25th (Q₁), 50th (median), 75th (Q₃), and 90th percentiles.

C: Significantly HSF1-dependent transcripts in top three clusters: The percentage of significant *HSF1*-dependent genes after heat shock (% hsf1_{HS}) in each of the three clusters (from Figure 5A) is analyzed.

D: Known direct targets of HSF1: Summary of so far known direct *HSF1* targets, the cluster (from Figure 5 A) they belong to, the transcript \log_2 fold change to heat shock treatment in the control strains or *HSF1* knockdown after heat shock (HS_{con}, hsf1_{HS}) within the present study (Strenkert *et al.* 2011b).

Figure 6

**Figure 6: Direct interaction analysis**

A: Promoter regions of selected potential direct targets of HSF1: Shown is the region (from -700 to +300) around the predicted transcriptional start sites (+1, white triangle) of the ten genes investigated in this study. The translational start site (ATG) is denoted at the first exon (black boxes), introns are indicated with thin black lines. The promoter box is shaded in gray, the 5'UTR region is drawn as white box. Putative HSEs (light grey boxes) in the promoter region are labeled from 1 up to 6 according to their position to the transcriptional start sites (closer corresponds to lower numbers). The sequence of the HSEs is summarized in Supplemental Figure 2A. Gray lines below the gene model designate the regions amplified with qPCR in Chromatin Immunoprecipitation (ChIP) experiments.

B: HSF1 binding in selected promoter regions: ChIP with affinity purified HSF1 antibodies was done on control (black bars) and *HSF1* knockdown strains (gray bars) subjected to a 30 minutes heat shock (HS) treatment at 40°C in the light (+) or kept at ambient temperatures (23°C) for 30 minutes in the light (-). The enrichment relative to 10% input DNA was calculated and normalized to the values obtained for the *CYC6* promoter. Error bars indicate standard errors of two biological replicates, each analyzed in technical triplicate. Asterisks indicate the significance of change compared to the *CYC6* promoter in control cells (ANOVA, P -value ≤ 0.01).

C: Nucleosome occupancy and acetylation of H3 and H4 histones: ChIP was performed as described in Figure 6 C with antibodies against the unmodified C-terminal region of histone H3 (H3 occupancy), acetylated Lys-5, -8, -12, and -16 of histone H4 (AcH4/H3) and acetylated Lys-9 and -14 of histone H3 (AcH3/H3). qPCR data from the experiments with modified histones are given relative to the nucleosome occupancy at the respective promoter region. Error bars indicate standard errors of two biological replicates, each analyzed in technical triplicate for the control genes (*CYC6*/*PSAD*) and standard error of the mean between the five *HSF1* bound (*HSF1* HSE) and five unbound (HSE) loci, each analyzed with two biological replicates and technical triplicate.

Figure 7

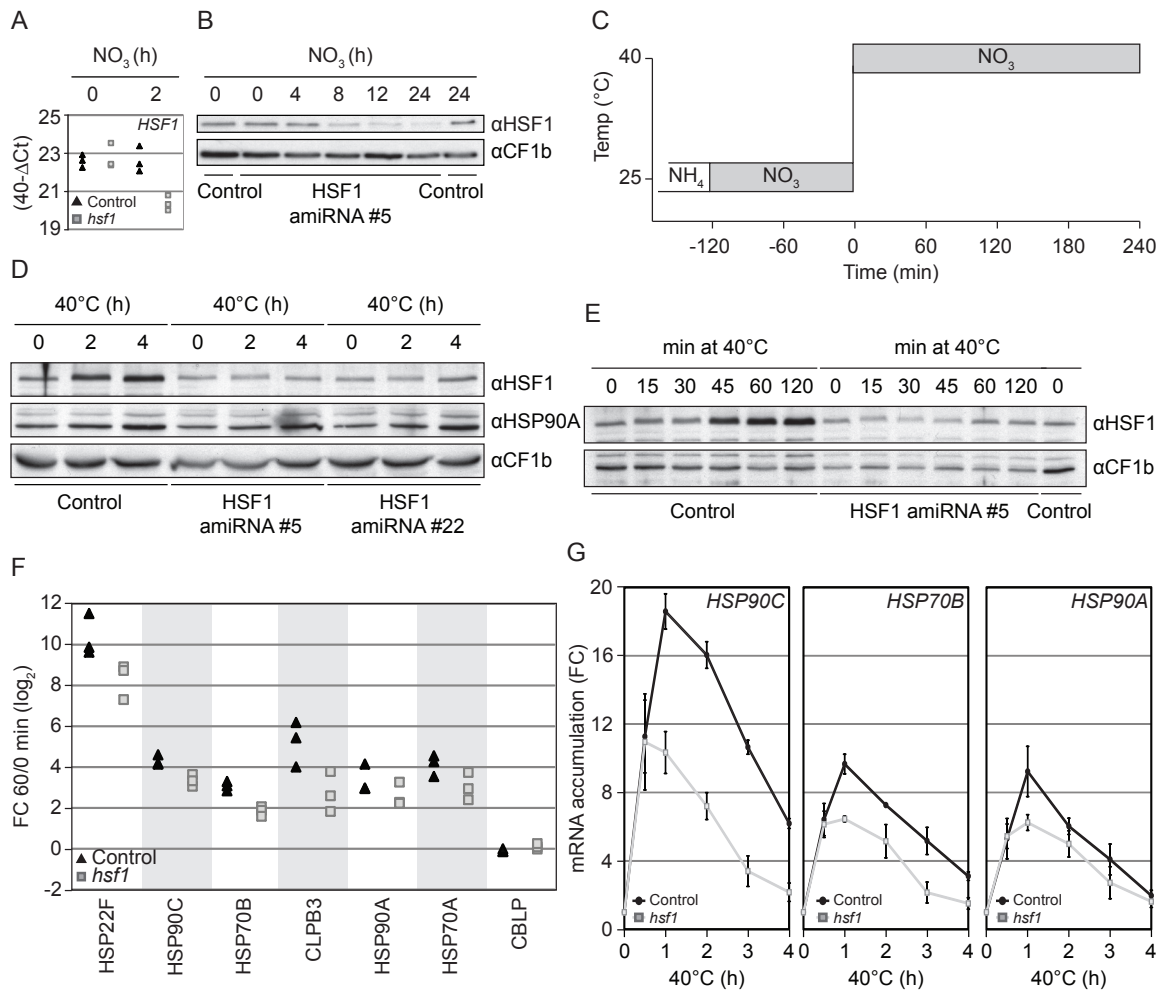


Figure 7: Feedback mechanism

A: *HSF1* expression in inducible *HSF1* amiRNA lines: Accumulation of transcripts from *HSF1* in three control and three independent inducible *HSF1* amiRNA strains (#5, #7 and #22) directly after switching the nitrogen source from ammonia to nitrate and 2 h after the switch. (Schmollinger *et al.* 2010)). *HSF1* targeting amiRNA is induced only on nitrate containing media. RNA was subsequently extracted for qRT-PCR analysis which is performed in three technical replicates using the comparative CT method with *CBLP2* as control gene.

B: Depletion of *HSF1* after induction of the amiRNA: Total protein of a control and *HSF1* amiRNA strain was extracted, loaded corresponding to 2µg Chlorophyll and separated on a 10% SDS-polyacrylamide gel. Levels of *HSF1* relative to loading control CF1β were analyzed by immunoblotting at different times after the switch from ammonia to nitrate containing media.

C: Experimental setup of the feedback mechanism experiment: Cells were inoculated in ammonia containing media and switched to nitrate containing media to induce the *HSF1* targeting amiRNA. Two hours after the switch the temperature is increased to 40°C (heat shock conditions). While the mRNA of *HSF1* is already degraded, protein levels are still at the level of the control cells.

D: Induction of *HSF1* after heat shock on nitrate containing media: Total protein of a control and two *HSF1* amiRNA strains (#5 and #22) was extracted, loaded corresponding to 2µg Chlorophyll and separated on a 10% SDS-polyacrylamide gel. Levels of *HSF1* and *HSP90A* relative to loading control CF1β were analyzed by immunoblotting at different times after the switch from ambient (23°C) to elevated temperatures (40°C), two hours after the switch to nitrate containing media.

E: Phosphorylation dependent size shift: Total protein was extracted from a control and *HSF1* amiRNA strain (#5) at different time points after the switch from ambient (23°C) to elevated temperatures (40°C) on nitrate containing media. Protein was loaded corresponding to 2µg Chlorophyll and separated on a 7.5-15% gradient SDS-polyacrylamide gel. Levels of *HSF1* relative to loading control CF1β were analyzed by immunoblotting.

F: Gene expression in inducible *HSF1* amiRNA lines F: 60-minute heat shock induced accumulation of transcripts of directly *HSF1* regulated genes in three control and three independent inducible *HSF1* amiRNA strains (#5, #7 and #22) two hours after switching the nitrogen source. RNA was subsequently extracted for qRT-PCR analysis which is performed in three technical replicates using the comparative CT method with *CBLP2* as control gene.

G: *HSF1*-dependent expression of target genes when no additional *HSF1* protein is synthesized: A control and two independent inducible *HSF1* amiRNA strains (#5 and #22) were subjected to a 4-hour heat shock treatment at 40°C in the light, two hours after switching the nitrogen source to nitrate containing media. Total RNA was extracted, separated on formaldehyde-containing agarose gels, transferred to nylon membranes and hybridized with radioactive probes against *HSP70B*, *HSP90C*, *HSP90A* and *CBLP* as loading control. Signals relative to *CBLP* were quantified from two independent experiments using the Quantity One Software (Biorad) and fold induction was calculated. Error bars indicate standard error from two control and four *HSF1* knockdown strains.

Figure S1

Name	Au5 protein ID	Gene location	Probe	Forward primer (5'->3')	Reverse primer (5'->3')	Amplicon and probe location
HSP1	525816	chromosome_9:247570-224054	7829.D	TCCTTATCAAGACGATGACCTCGT	AAGCTGGAGAAATTGTTGTGCTT	
HSEBP1	524556	chromosome_7:2227957-2229985	3822.C	ATGGCCGACCAAGTACGCTG	TGTTGGCTCCAGATTGTCA	
HSP22F	515324	chromosome_14:1393775-1395593	9317.E	TGCACCACGCCGTG	TGATCTCAACCGCTGATGTCCTC	
CPNB0A	521778	scaffold_32:146456-154390	342.A	GCCATGACATCAAGAACGTTGCG	TCGGTGTGTTCCGAGGCTC	
HSP70A	525480	chromosome_8:2072040-2075978	291.A	GATCGAGCGCATGGTGC	TCATCGACTCCTTGTCCCG	
HSP70B	522821	chromosome_6:137607-142355		GACAAAGCCATCGTGGACT	GGCAGGTTGATGAGGCTCTG	
HSP70C	525943	chromosome_9:1155566-1164520	8957.E	CCTCATCGCCGGTGTACGACCT	TCAAAGTCCCTCCCTCCAG	
HSP70G	510023	chromosome_10:2836080-2846274		GACCTGGGCTGGAGTACTTG	GGCCGTTCAACAACCCAC	
HSP90A	525808	chromosome_9:203030-207524	8824.D	CGGCTCAAAGAAATGGGCTACG	CGCTTCTCTCCTCCTCGCTC	
HSP90C	513163	chromosome_12:3588442-3593816	8031.D	AGGGCCCGCAAGATTATGGAG	GGCCGCTCTCTGACAGCAG	
CLPB3	518776	chromosome_2:2232473-2240687	5371.C	TACAGCAAGGACCCCATGCCGG	ACGTGCCCACTGCTGAAC	
CDJ1	513011	chromosome_12:2735325-2740029	1539.C	TCCTCGCACTGCCGATTAAGA	CAGCACCTATACGCCCTCG	
BAG6	520480	chromosome_3:649438-654282	4877.C	GGCGGAGGTGAACGAGCT	GGCCTAACGAGGTTTGCG	
TIC110	510291	chromosome_10:4542762-4554530		GCAACGCCCGTTCGAGAA	CGCATGTTGAGGTTGAAAGT	
TIC40	513018	chromosome_12:2803756-2807924	5608.C	GGCGCTCCTTGGTGGATTT	AGCCCATAGCGCCAGACAT	
FFC	512407	chromosome_11:2160245-2170119	475.A	ACGTGTCCGTCGCTGTGT	AGCTCATTGACACCGGCTTG	
MPA1	511883	chromosome_1:8441331-8445305	6942.C	GCCTTCCGCGTCTACGTGAT	CCTTCTCCAGCGCCATCGA	
LHCBM9	523559	chromosome_6:4095556-4097814	350.A	CCTTCCGACCAAGTACACTC	AAACATTCAAGCACAGCCGT	
LHCSR1	525343	chromosome_8:1257473-1259901	251.A	GTTGCTATGCTTGGCCGCTCTGG	TGGCCGATCTGCTGGAAGTGT	
ARG7	511047	chromosome_1:3160809-3168803	46.A	GTCGTGTGGAAGGCAACCT	CGTGTCAAACAGCAGCTCC	
CBLP	514942	chromosome_13:5097466-5099700	116.A	GCCACACCCAGTGGGTGTCTGCG	CCTTGGCCGCCGAGGCGCACAGCG	
TUB1	513735	chromosome_12:6949067-6951785	9225.E	CCCCCGCCTGCACCTTCTC	GTCGGCGCGCACATCAT	
IDA5	515031	chromosome_13:5927390-5931804	95.A	CTGACTCTGCCITACCCCAT	CCTCAGTCAACGACACGGG	
EIF1A	519056	chromosome_2:4003530-4005798	9729.E	GACATCGTGGTGGTCTT	TACGAATGTGCTCCGGCAG	
Name	Au5 protein ID	Amplicon location	Probe	Forward primer (5'->3')	Reverse primer (5'->3')	
HSP1	525816	chromosome_9 : 247702 - 247803	7829.D	CGGCTTTTCCAGTTTTCCC	CAACGCATTTCTTTCGAGTGA	
HSP70A	525480	chromosome_8 : 2075850 - 2076012	291.A	CGGTATATAAAGCCCGCGAC	GTGCCAGGTCATAIACCAGATAG	
HSP70G	510023	chromosome_10 : 2835952 - 2836052		CCCGGTGGGAAAAAGGAGT	TAAGGCCAGCAGGGTGGCAA	
CLPB3	518776	chromosome_2 : 2232349 - 2232449	5371.C	GCGTACACATAGCCGAGTTCG	GGTTGAAAAAGTTTTCGAGTGTG	
CDJ1	513011	chromosome_12 : 2735193 - 2735295	1539.C	GGCTGAATATGACATGCGTGT	GTCTCGCGAATTTCCGCC	
LHCBM9	523559	chromosome_6 : 4098149 - 4098291	350.A	GCCGAAGGCTTTGGCAGTGTG	GCATGCCAGGTTCTCAACCC	
TIC110	510291	chromosome_10 : 4554657 - 4554793		GCCTTCCGGTTTACCACATCT	ACGTGAATTACTGAGCCCCG	
TIC40	513018	chromosome_12 : 2807997 - 2808138	5608.C	GGCGTGCAGGTGAAGTACG	TTCTGGCTTTTAAAGCGC	
FFC	512407	chromosome_11 : 2160466 - 2160607	475.A	GGGAGCCTAGGAGCAGTGTATG	ACCGATGGCAGACCCAGAT	
MPA1	511883	chromosome_1 : 8441449 - 8441550	6942.C	CTGTTCTTGATCCAACGGGA	GGCGGAGTAGTGAAGTCTGT	
CYC6	516039	chromosome_16 : 437128 - 437248	261.A	ACACGCCCTCATTCACACAGA	GCAACGAGACACTCCGAGC	

1000 bp

Figure S1: qRT-PCR amplicons and primers

A: Overview over the genes studied with qRT-PCR: Summary of the qRT-PCR analyzed genes, their user defined names (Name), the Augustus 5 protein ID (Au5 protein ID) specifying the assumed gene model, the genomic coordinates (Gene location) according to the improved assembly v4 of the Chlamydomonas genome, the corresponding microarray v2 probe ID (Probe) and the sequence of the forward and reverse primer (5' to 3'). The qRT-PCR amplicon and microarray v2 probe location (Amplicon and probe location) is illustrated as follows: Shown is the complete transcribed region of the analyzed genes (5' to 3') according to the gene model prediction. The 5'UTR and 3'UTR regions are drawn as white box, the exons as black boxes and introns with thin black lines. Black lines above the model designate the regions amplified by qRT-PCR, grey lines indicate introns spanned by the primers. Black lines below indicate the corresponding microarray probe.

B: Overview over the genes studied with ChIP: Summary of the genes whose promoters were studied with ChIP, their user defined names (Name), the Augustus 5 protein ID (Au5 protein ID) of the gene model, the genomic coordinates of the amplicon (Amplicon location) according to the improved assembly v4 of the Chlamydomonas genome, the corresponding microarray v2 probe ID (Probe) and the sequence of the forward and reverse primer (5' to 3').

Figure S2

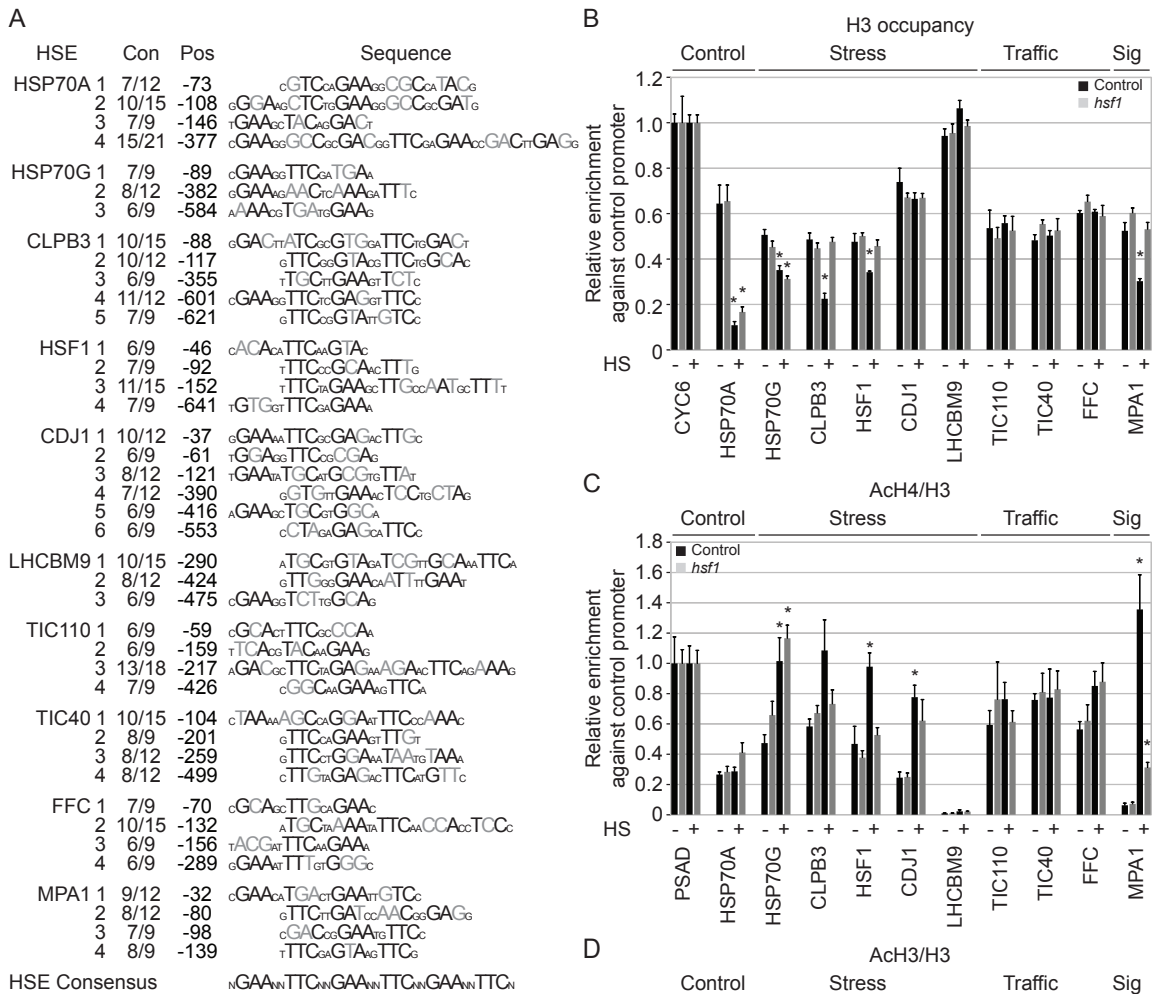


Figure S2: Individual promoter regions in ChIP experiments for nucleosome occupancy and acetylation of H3 and H4 histones

A: Potential heat shock elements within the promoter region: The sequence, the relative position of the first nucleotide of each potential heat shock element (HSE) to the transcriptional start sites (Pos) and the number of matches to the HSE consensus (Con) is summarized for each potential HSE.

B: H3 occupancy in individual promoters: ChIP with antibodies against the unmodified C-terminal region of histone H3 was done on control (black bars) and *HSF1* knockdown strains (gray bars) subjected to a 30 minutes heat shock (HS) treatment at 40°C in the light (+) or kept at ambient temperatures (23°C) for 30 minutes in the light (-). The enrichment relative to 10% input DNA was calculated and normalized to the values obtained for the *CYC6* promoter. Error bars indicate standard errors of two biological replicates, each analyzed in technical triplicate. Asterisks indicate the significance of change compared to the promoter in control cells under ambient conditions (T-Test, P-value ≤ 0.01).

C: Acetylation of histone H4 in individual promoters: ChIP was done as described in Figure S2 A using antibodies against acetylated Lys-5, -8, -12, and -16 of histone H4. ChIP signals for acetylated histone H4 are given relative to the observed histone H3 occupancy at the individual promoters (AcH4/H3).

D: Acetylation of histone H4 in individual promoters: ChIP was done as described in Figure S2 A using antibodies against acetylated Lys-9 and -14 of histone H3. ChIP signals for acetylated histone H3 are given relative to the observed histone H3 occupancy at the individual promoters (AcH3/H3).

3.6. MANUSCRIPT 3: STROMAL HSP70B IS AN ESSENTIAL PROTEIN FOR CELL GROWTH WITH FUNCTIONS IN THYLAKOID ASSEMBLY AND AMINO ACID METABOLISM.

Authors:

Stefan Schmollinger, Corinna Gruber, Daniela Strenkert, Daniel Veyel, Timo Mühlhaus, Frederik Sommer, Dorothea Hemme and Michael Schroda

Draft manuscript

Contribution to:

Figure 1

Figure 2

Figure 3

Figure 4

Figure 6

Figure 7

Supplemental Figure 1

Supplemental Figure 2

Supplemental Figure 4

Supplemental Figure 5

Supplemental Figure 6

Supplemental Figure 7

Stromal HSP70B in *Chlamydomonas* is an essential protein for cell growth with functions in thylakoid biogenesis and amino acid metabolism.

Stefan Schmollinger^{1,2}, Corinna Gruber^{1,2}, Daniela Strenkert^{1,2}, Ann-Katrin Unger³, Stefan Geimer³, Daniel Veyel^{1,2}, Timo Mühlhaus^{1,2}, Dorothea Hemme^{1,2}, Frederik Sommer^{1,2}, and Michael Schroda^{1,2}

¹Molekulare Biotechnologie & Systembiologie, TU Kaiserslautern, Paul-Ehrlich-Str. 23, D-67663 Kaiserslautern, Germany

²Max-Planck-Institut für Molekulare Pflanzenphysiologie, Am Mühlenberg 1, D-14476 Potsdam-Golm, Germany

³Zellbiologie/Elektronenmikroskopie, Universität Bayreuth, D-95440 Bayreuth, Germany

Corresponding author: Michael Schroda

Tel.: + 49 (0)631 205-2697

Fax: + 49 (0)631 205-2999

e-mail: schroda@biologie.uni-kl.de

Running title: Functional characterization of HSP70B

Keywords: HSP70B, HSP70, *Chlamydomonas*, Chloroplast, Stroma, VIPP1, Stroma, thylakoid

Word count:

Summary	185
Introduction	712
Results	2798
Discussion	1625
Experimental procedures	1182
Acknowledgements	37
Figure legends	2151
Total	8609

Summary

Chaperones of the HSP70 class have essential functions in all compartments of the cell, also in the chloroplast. However, only little emphasis was put on investigations regarding the functions of HSP70s in this compartment. We therefore used an inducible knock-down approach to characterize the functions of the essential stromal HSP70B in *Chlamydomonas reinhardtii*. Inducible underexpression of HSP70B allowed to decrease protein levels to ~20 % wild-type levels before cells displayed a growth-arrest, failed to divide and accumulated starch. Time-resolved analysis during the depletion process showed that HSP70B depletion results in overexpression of a client protein, VIPP1, and specific co-chaperones. Despite its overexpression, phenotypes are found in HSP70B-depleted cells comparable to VIPP1 mutant strains, especially the aberrant structures at the origin of thylakoid membranes. Especially the distribution between oligomeric and monomeric VIPP1 isoforms is distorted in HSP70B knock-down cells. In addition, we observed the induction of organism-wide stress responses upon depletion of HSP70B, especially the HSF1-dependent heat shock response and ATG8-mediated autophagy. Addition of arginine was able to partially rescue the growth-arrest phenotype, indicating that the growth arrest results from HSP70B functions in anabolic pathways.

Introduction

In general, chaperones of the HSP70 class provide the cell a diverse set of functions connected to protein quality control. They assist in folding of newly synthesized proteins, especially those containing more than 100 amino acids (Hartl and Hayer-Hartl 2009), refold misfolded or aggregated proteins upon proteotoxic stress conditions (Bukau *et al.* 2006, Sharma *et al.* 2009), translocate proteins across cell membranes (Sousa and Lafer 2006) and assemble, disassemble or modify protein complexes. HSP70s consist of two conserved functional domains, an N-terminal ATPase domain and a C-terminal substrate-binding domain, and know two functional distinct states, dependent on the bound nucleotide ATP or ADP. In the ATP state, the substrate binding domain is in an open conformation with little affinity for substrates (Zhu *et al.* 1996). ATP hydrolysis is used to transfer the substrate binding domain to a closed conformation that promotes a tight binding of the substrate. Substrate release is then achieved by exchanging the bound ADP with ATP, returning HSP70s back into the low-affinity ATP-state. Thereby HSP70s work in concert with a number of co-chaperones (Mayer and Bukau 2005) most important nucleotide exchange factors (GrpE, BAG1), increasing the rate for replacing the used up ADP by ATP (Harrison 2003) and substrate delivering J-domain proteins, managing the substrate pool and stimulating ATPase activity to achieve a more tight binding (Kampinga and Craig 2010). Substrates are recognized by a hydrophobic stretch, consisting of 4-5 amino acids, that is flanked by 4-5 residues on either side enriched in basic amino acids (Rudiger *et al.* 1997). Hydrophobic amino acids exposed to the aqueous phase are generally believed to indicate misfolded proteins and potential consensus regions are found in virtually any protein every 36 amino acids (Rudiger *et al.* 1997).

HSP70s are found in all compartments of the cell, also in the chloroplast. While mitochondrial and cytosolic systems are quite well understood only little is known about plastidic, especially stromal HSP70s. So far, the best characterized plastidic HSP70 system is the one from *Chlamydomonas reinhardtii*, a unicellular green alga (Nordhues *et al.* 2010, Schroda 2004). Several co-chaperones of the stromal HSP70B (Drzymalla *et al.* 1996, Schroda *et al.* 1999) have been identified so far, including the nucleotide exchange factor CGE1 (Chloroplast GrpE homolog 1) (Schroda *et al.* 2001, Willmund *et al.* 2007), five different J-domain proteins, termed Chloroplast DnaJ homologs (CDJ) one to five (Dorn *et al.* 2010, Liu *et al.* 2005, Willmund *et al.* 2008a) and an escort protein required for initial folding of HSP70B upon chloroplast import, termed HEP2 (HSP70 Escort Protein 2) (Willmund *et al.* 2008b). Contacts to other plastidic chaperones systems, i.e. the HSP90C system could be demonstrated as well (Heide *et al.* 2009, Willmund and Schroda 2005). So far the only, but as judged from abundance in co-immunoprecipitations the most prominent, substrate identified is the VIPP1 protein (Liu *et al.* 2005). The HSP70B-CDJ2 chaperone system was shown to be indispensable for assembly and disassembly of VIPP1 oligomeric structures (Liu *et al.* 2007). Beside defining the chaperone network, functional characterization has proven difficult. Mutants could not be obtained, and constitutive knock-down approaches failed to reduce protein levels beyond 80% wild-

type levels (Schroda *et al.* 1999). Therefore, so far, addressed functions were restricted to conditions where protein levels of HSP70B are adjusted within a short time frame to higher levels, like during photoinhibition. Here knock-down approaches were successful in reducing this accumulation and revealed a role of HSP70B during photoprotection and in repair of PSII (Schroda *et al.* 1999). In addition, stromal HSP70 proteins from higher plants (*Physcomitrella patens* and *Arabidopsis thaliana*) were found to participate in translocation of nuclear encoded proteins into the chloroplast, (Shi and Theg 2010, Su and Li 2010).

Here we present the conditional down-regulation of the essential *HSP70B* in *Chlamydomonas*. HSP70 underexpression results in accumulation of misfolded proteins that do not only lose their biological functionality but also disturb protein homeostasis in the whole cell, damages thylakoid membranes and finally induces autophagy emphasizing their biological importance at ambient conditions. More specifically, we demonstrate that underexpression of *HSP70B* results in alteration of the stoichiometry between VIPP1 oligomers and monomers, finally leading to phenotypes similar to *VIPP1* knock-down strains. Furthermore, we found indications that stromal HSP70 is linked to biosynthetic pathways in the chloroplast especially producing amino acids, including arginine, which is one growth limiting process.

Results

Inducible underexpression of *HSP70B* results in a growth arrest and increased cell diameters

In *Chlamydomonas*, constitutive underexpression of *HSP70B* reduced protein levels to ~80 % of wild type protein amounts and resulted only in slightly reduced growth rates (Schroda *et al.* 1999). Knock-down strains with further reduced protein levels have not been obtained so far. These findings together indicated an essential role for stromal HSP70s hampering mutant generation and consequently further functional characterization. In order to further decrease protein levels of *HSP70B* in *Chlamydomonas* we therefore made use of a recently developed inducible amiRNA system (Schmollinger *et al.* 2010). In contrast to constitutive knock-down systems, this system should allow for time-resolved analysis of essential target genes, dependent on the presence of the nitrogen sources in the media. We therefore equipped the inducible amiRNA vector (pMS539) (Schmollinger *et al.* 2010) with sequences targeting a region in exon 3 of the *HSP70B* mRNA (pMS542), encoding a part of the N-terminal ATPase domain (Figure 1).

Among the transformants selected for arginine prototrophy, we indeed identified knock-down strains specifically underexpressing *HSP70B* in the presence of nitrate as single nitrogen source (Figure 2A). The amount of *HSP70B* in these strains was reduced to about ~20% of wild type levels about 24 hours after induction of the amiRNA. With ammonium as nitrogen source the *HSP70B* protein amounts are unaltered compared to strains harboring one of the empty vectors pMS539 or pCB412 (Figure 2A, Supplemental Figure 1 online).

Underexpression of *HSP70B* indeed had severe consequences on cell growth. Strains inducibly underexpressing *HSP70B* were not viable on TAP media containing nitrate as single nitrogen source while control strains are unaffected (Figure 2B). In more detail, after a short lag period (~3h) upon the exchange of the nitrogen sources (Figure 1C), control and *HSP70B* underexpressing strains exhibited the same growth rate within the first 24 hours after induction of the amiRNA. After 24 hours, cells stopped to divide exponentially when *HSP70B* protein levels are reduced and finally completely stopped to divide (Figure 1C). When *HSP70B* underexpressing strains are transferred back to ammonium containing media after a 24-hour period of induction, cells do not show this growth arrest (Figure 2B). Underexpression of *HSP70B* furthermore results in an increase of cell diameter (Figure 2D). While control cells are not increasing in size upon exchange of the nitrogen source (Supplemental Figure 1 online), *HSP70B*-depleted cells grow in size already 24 hours after the induction of the amiRNA, while the cell size increase is even more pronounced at later time points (Figure 2D).

Inducible knock-down strains of *HSP70B* were stable on TAP plates (NH_4) for about 9-12 months. We therefore had to replace the strains from time to time during our studies. In total we were using seven independent strains identified in three independent rounds of transformation. All of them showed arrested growth and an increase in cell diameter on nitrate containing media (Supplemental Figure 1 online).

Consequences of HSP70B depletion on the expression of co-chaperones and the target protein VIPP1

To evaluate the molecular consequences of HSP70B depletion we first focused on known co-chaperones and targets of the HSP70B chaperone system in the chloroplast. We therefore monitored time-dependently the abundance of these proteins upon HSP70B depletion (Figure 3). In general, co-chaperone and target protein abundance is increased upon HSP70B depletion, if altered at all. Protein levels of CGE1, the major nucleotide exchange factor, increased about 24 h after the induction of the amiRNA, and even more pronounced after 36 h specifically in inducible *HSP70B* knock-down strains. Interestingly, the composition of the J-domain protein pool in the chloroplast is altered upon HSP70B depletion and upon switch to nitrate. While CDJ2 levels are unchanged, protein levels of CDJ4 are increased upon switch to nitrate in control and HSP70B amiRNA strains. CDJ1 was strongly increasing specifically in *HSP70B* underexpressing strains, comparable to CGE1, about 24 h after induction of the amiRNA and more severe after 36 h. CDJ1 is a type I J-domain protein generally involved in recruiting unfolded or misfolded substrates to HSP70s (Cheetham and Caplan 1998, Willmund *et al.* 2008a), while CDJ2 has a more specific function and is involved in recruiting the VIPP1 protein to HSP70B in *Chlamydomonas* (Liu *et al.* 2005). We conclude, that the J-domain pool is altered towards recruiting more unfolded/misfolded proteins to HSP70B instead of supplying specific functions.

The CDJ2 substrate VIPP1 was also strongly accumulating, starting already about 12 h after the switch of the nitrogen source, and therefore earlier than CGE1 and CDJ1. The second VIPP homolog in *Chlamydomonas* (VIPP2), is also increasingly expressed in inducible HSP70B underexpressing strains. VIPP2 showed a similar expression pattern than VIPP1, appearing already 12 h after the induction of the amiRNA (Figure 3A). VIPP2 is almost not expressed in NH⁴ -containing media in control and HSP70B amiRNA strains (Figure 3A). Previously, VIPP2 was observed to strongly increase in VIPP1 knock-down strains and upon shift to higher light intensities (Nordhues *et al.* 2012).

HSP70B was found in complex with HSP90C, a chaperone of the HSP90 class in the *Chlamydomonas* chloroplast (Willmund and Schroda 2005). Upon HSP70B depletion the 90kD chaperone is slightly increased, late (36 h) after induction of the amiRNA.

Accumulation of target proteins, co-chaperones and interaction chaperones coincided with the growth arrest of inducible HSP70B underexpressing strains ~24 hours after the switch of the nitrogen source. We therefore examined mRNA levels to find out if increased protein amounts result from transcriptional regulation or simply accumulate in no longer dividing cells. The mRNA levels of *VIPP1/2* and *HSP90C* were strongly increased, compared to control strains where the mRNAs were unaltered upon exchange of the nitrogen sources. The mRNA of *HSP70B* was found to be less abundant, consistent with the view that amiRNA-mediated mRNA cleavage is involved in knock-down of target genes in *Chlamydomonas*, at least for cre-miR1157 and cre-miR1162 based amiRNA constructs (Molnar *et al.* 2009, Schmollinger *et al.* 2010, Zhao *et al.* 2008). We therefore conclude that accumulation of VIPP1/2, HSP90C, CGE1

is not a consequence of the growth arrest, but rather a specific response on HSP70B depletion.

Assembly/disassembly of VIPP1 oligomers and localization is altered upon HSP70B underexpression

Depletion of HSP70B resulted in specifically increasing amounts of its substrate VIPP1 (Figure 3A). In a previous work, we found the HSP70B chaperone system to be involved in the assembly and disassembly of VIPP1 oligomers (Liu *et al.* 2007). Accordingly, we analyzed the distribution of VIPP1 between monomers and oligomers, using sucrose density gradient centrifugations that were established for that purpose previously (Liu *et al.* 2007). The distribution of VIPP1 between monomers and oligomers was not altered compared to control strains on ammonium containing media (Figure 4A). Upon HSP70B depletion, and even though the total amount of VIPP1 is increasing, less VIPP1 was found in the triton-solubilized supernatant (Figure 4A). Consequently, the amount of higher molecular weight isoforms of VIPP1 is strongly increased (Figure 4A and Supplemental Figure 2D online). The VIPP2 protein, which is completely removed from membranes with triton in control cells (Data not shown), is also found in the pellet upon HSP70B depletion. HSP70B and the integral membrane protein CYTF, used to control the efficiency of triton-mediated membrane solubilization, were found only in the supernatant fraction. CF1 β , part of the ATPase located in the thylakoid membrane, was also mainly found in the supernatant and running only partially into the first fraction of the sucrose gradient. We therefore propose that depleting HSP70B results in reduced disassembly of high molecular weight VIPP1/2 oligomers. This is consistent with our previous findings, that increasing amounts of HSP70B and co-chaperones in the presence of ATP resulted in increasing amounts of low molecular weight isoforms of VIPP1.

Only about ~50% of VIPP1 is associated to membranes (thylakoids and low-density membranes) in *Chlamydomonas*. But, in contrast to other organisms (*Arabidopsis thaliana*, *Pisum sativum* and cyanobacteria) where VIPP1 was found only attached to membranes (Kroll *et al.* 2001, Li *et al.* 1994, Westphal *et al.* 2001), also soluble VIPP1 isoforms were found (Liu *et al.* 2005). To determine the location of VIPP1 and to avoid precipitation of high molecular weight complexes, we used only low g-forces (30 min at 16100g) to separate soluble from membrane bound proteins (Supplemental Figure 2C online), a method previously established for high-throughput analysis (Muhlhaus *et al.* 2011). Again CYTF was used as a control to ensure complete pelleting of membranes with the modified method. We found soluble VIPP1 complexes to be strongly reduced in inducible HSP70B knock-down strains while membrane association was strongly increasing. Taken together, we conclude that the increasing number of VIPP1 oligomers is rather attached to membranes than found in large soluble complexes.

Phenotypes of VIPP1 knock-down strains are also displayed upon HSP70B depletion

The exact molecular function of VIPP1 in *Chlamydomonas* is still a mystery. Recent work demonstrated that the early hypothesis for VIPP1 function as a protein inducing vesicle trafficking in the chloroplast is rather wrong. More likely, VIPP1 is involved in the structural

organization of the large thylakoid protein complexes, and therefore probably located in thylakoid centers (Nordhues *et al.* 2012). The loss of VIPP1 function in respective knock-down strains resulted in cells more sensitive to higher light intensities and led to the occurrence of aberrant structures at the thylakoid centers.

We wondered if similar phenotypes are also observed in *HSP70B* knock-down strains, where total VIPP1 amounts are increased but localization and oligomerization are distorted. We therefore transferred cells 24 hours after induction of the amiRNA from standard growth light intensities ($\sim 30 \mu\text{E m}^{-2} \text{s}^{-1}$) to high light intensities ($\sim 1000 \mu\text{E m}^{-2} \text{s}^{-1}$). While control strains were unaffected from these changes inducible *HSP70B* knock-down strains failed to acclimate and bleached (Figure 4B). High light induced bleaching in *VIPP1* knock-down strains occurred in a similar time frame on TAP-NO₃ media (Nordhues *et al.* 2012). In addition, we examined electron micrographs of inducible *HSP70B* underexpressing strains for the presence of aberrant structures at the origin of thylakoid membranes. Indeed, about 24 hours after induction of the amiRNA targeting *HSP70B* we first observed similar structures in the proximity of the pyrenoid, but also in other areas of the chloroplast (Figure 5A). Serial sections were carried out to closer inspect the aberrant structures (Figure 5B, Supplemental Figure 3 online). The bulky structures contain several distinct white areas of variable size, maybe starch or lipids. Several thylakoid membranes emerge from the structure, which seems to be more detached (looser stacked) in the proximity of the aberrant structures compared to the close-ups of control thylakoid membranes or membranes of the same strains on ammonium containing media (Figure 5A).

When inspecting the electron microscopy pictures we found that chloroplasts in *HSP70B* mutants strongly accumulate starch upon *HSP70B* depletion, beginning already 24 hours upon exchange of the nitrogen source. Even more severe the starch accumulation was observed at later time-points, indicating that growth-arrested cells further accumulate starch (Figure 5A, Supplemental Figure 6 online). Starch accumulation is a frequently observed phenomenon in nutrient limited, especially growth-arrested *Chlamydomonas* cells (Ball *et al.* 1990).

***HSP70B* underexpressing strains induce an organism-wide stress response via the *HSF1*-dependent pathway**

We found that underexpression of *HSP70B* resulted in accumulation of a chaperone of the HSP90 class in the chloroplast, *HSP90C* (Figure 3A). We were interested if also other chaperones and stress-related proteins are affected from *HSP70B* depletion, or accumulation of *HSP90C* is a specific result from depletion of *HSP70B* from shared complexes. We therefore monitored protein levels of the two cytosolic chaperones *HSP70A* and *HSP90A* upon shift to inducing conditions. Both proteins accumulated upon depletion of *HSP70B*, about 26 hours after exchange of the nitrogen source (Figure 6A). Another interesting class of chaperones is the HSP100 (CLP proteins) class, involved in resolving protein aggregates, while especially CLPB proteins target their substrates to HSP70s for refolding instead of supplying proteolytic pathways (Glover and Lindquist 1998, Goloubinoff *et al.* 1999). In absence of antibodies against *Chlamydomonas*

CLPB proteins we used antibodies generated against bacterial CLPB also in order to target preferentially proteins from organelles (Weibezahn *et al.* 2003). Upon depletion of HSP70B an additional band appeared, migrating at higher molecular weight, indicating either a modified isoform of an already present protein or the expression of another CLPB protein not present at ambient conditions. This response is specific for *HSP70B* underexpressing strains (Figure 6A, Supplemental Figure 6 online).

In addition, we tested protein levels of HSF1, a key regulator of the heat shock response in *Chlamydomonas*, previously shown to induce levels of several chaperones (including HSP90A/C) upon proteotoxic stress conditions (Schulz-Raffelt *et al.* 2007). Protein levels of HSF1 were also found to be increased specifically in inducible *HSP70B* underexpressing strains. HSF1 protein levels itself are also increased upon heat stress in *Chlamydomonas*, in a *HSF1*-dependent manner, indicating that depletion of *HSP70B* might have induced a HSF1-dependent HSR to increase chaperoning capacity in general (Schulz-Raffelt *et al.* 2007). The HSR is regulated on the transcript level, accordingly we found several transcripts of chaperones to be increased in *HSP70B* knock-down strains 24 hours upon induction of the amiRNA targeting *HSP70B* (Figure 6B). Among the CLPB proteins, the *CLPB3* gene showed induced expression upon *HSP70B* depletion. *CLPB3* is probably located in the chloroplast. Increased amounts of chaperones might therefore be a consequence of an induction of a general HSR.

In addition to chaperones we were also probing other stress-related proteins, several were found upregulated. The DEG1C protease is upregulated, specifically in inducible *HSP70B* knock-down strains about 24 hours after the exchange of the nitrogen source (Supplemental Figure 6 online). According to predictions, this protease is located in the thylakoid membrane. There is also a slight upregulation of LHCSR3 and a strong accumulation of the ATG8 protein (Supplemental Figure 6 online). The ATG8 protein is a marker protein for autophagy, a process that is used during stress conditions or special developmental stages to recycle nutrients from molecules separated in a double-membrane compartment called autophagosome (Nakatogawa *et al.* 2009). Two bands were observed for ATG8 on 15% SDS-polyacrylamide gels (Supplemental Figure 6B online), indicating that ATG8 modification was induced in inducible *HSP70B* underexpressing strains in order to activate autophagy (Perez-Perez *et al.* 2010). LHCSR3 is a stress-related protein, somehow similar to light harvesting complex proteins, that is involved in photoprotection, specifically thermal dissipation of excess light (qE) (Peers *et al.* 2009). This indicates that at normal light conditions energy transfer is not as effective in the photosynthetic electron transport chain in *HSP70B* knock-down strains.

Taken together, depletion of *HSP70B* results in induction of several stress-related proteins, that is not restricted to plastidic proteins. HSF1 is involved in regulation, judged from upregulation of both, mRNA and protein level of the transcription factor.

Amino acid metabolism is an essential process potentially responsible for the *HSP70B*-depletion-induced growth arrest

Photosynthesis seems to be only slightly affected within the first 36 hours, judged from only

minor effects on the abundance of proteins from the photosynthetic electron transport chain (Supplemental Figure 5 online). Only PETO levels are dramatically altered upon HSP70B depletion (Supplemental Figure 5 online). Taken together, the phenotype upon shift to high light (Figure 4B), induction of LHCSR3 (Supplemental Figure 6 online), depletion of PETO from HSP70B mutant strains and a slight reduction (less than 10%) of photosynthetic proteins (Supplemental Figure 5 online) indicates that HSP70B supports the already addressed function either in assembly or repair of photosynthetic proteins. Similar phenotypes were already observed previously in strains expressing constitutively an antisense construct targeting the *HSP70B* mRNA when transferred to photoinhibitory conditions (Schroda *et al.* 1999).

On the other hand, photosynthesis is a dispensable process in *Chlamydomonas* (Harris 1989). The essential nature of the chloroplast to the cell probably depends on its function in assimilating nutrients (C, N, S) and its capacity to build key metabolites (i.e. amino acids, fatty acids and nucleotides) for cell growth (Rolland *et al.* 2012). Starch accumulation and ATG8-mediated autophagy often occurs in response to nutrient limitation (Ball *et al.* 1990, Bassham 2007). We therefore wondered which synthesis effort of the chloroplast is affected in inducible *HSP70B* knock down strains. For example, ten amino acids are exclusively produced in the chloroplast: Arg, Lys, Thr, Leu, Ile, Val, Trp, Phe, Tyr and His. We therefore tested if limitation from essential amino acids is affecting cell growth in HSP70B underexpressing strains. When resupplied with 7.5 mM arginine in TAP-NO₃ inducible *HSP70B* knock-down strains indeed resumed growth (Figure 7A). Growth rate was still reduced (~24 h per division) compared to control strains (~10 h per division) (Figure 7B). Other amino acids were not successful in increasing the growth rate of inducibly HSP70B-depleted cells (Supplemental Figure 7 online). Arginine can be used as an alternative nitrogen source and thereby perturb our knockdown approach using different nitrogen sources (NH₄ and NO₃). We therefore analyzed in 24-hour NO₃-induced *HSP70B* knock-down strains if HSP70B protein levels are still reduced. Indeed levels of HSP70B are reduced to similar levels compared to strains that were grown without additional arginine or supplied with several other amino acids (Figure 7C). In addition, the VIPP2 protein is also induced to similar levels independent of the addition of arginine, indicating that the missing action of HSP70B on VIPP1 is comparable in arginine supplied *HSP70B* knock-down strains (Figure 7C). *VIPP1/2* and *HSP22F* mRNA were also still upregulated when arginine is fed (Figure 7D). The ARG7 gene surprisingly, is less strong expressed on NO₃ containing media, compared to standard TAP media.

Discussion

The essential nature of stromal HSP70s is not found in photosynthetic or import functions, but rather in assimilating nutrients and it's biosynthetic portfolio

We show here in detail that depletion of the main, if not unique, stromal HSP70 in *Chlamydomonas* results in a growth arrest, when protein levels are reduced to approximately 20% wild type levels (Figure 2). In addition, in a previous study where HSP70B levels were challenged with a constitutively expressed antisense construct, slightly reduced growth rates were observed (Schroda et al. 1999). In these strains, reduction of growth rate was less severe as protein levels were not reduced to the same extent than in the inducible amiRNA lines (80% wild-type levels in constitutive compared to 20% in inducible mutant lines). Knock-down strains with further reduced protein levels could not be obtained with the constitutive construct. Accordingly, knock-out of a stromal HSP70 (Hsp70-2) was lethal to the moss *Physcomitrella patens* (Shi and Theg 2010) and simultaneous knock-down of the two stromal Hsp70s from *Arabidopsis* (cpHsc70-1 and cpHsc70-2, 91% identity) has not produced viable progeny (Su and Li 2008), indicating that essential functions inherent to stromal HSP70s are conserved within the green lineage.

Several observations led us to the conclusion that, for a certain time frame, cells are only reversibly arrested in growth and not irreversibly damaged: (1) when ammonium is added to the medium to repress the expression of the amiRNA in already HSP70B-depleted cells, growth rates recover to comparable levels between inducible HSP70B knock-down and control strains (Figure 2) (2) metabolism is still active and generates energy for sugar synthesis and storage when cells are already arrested in growth, as judged from the accumulation of large amounts of starch, and also proteins, in HSP70B knock-down strains at later time points (Figure 4 and S2) (3) two stress responses are induced at late time-points (Figure 6) when cells already stopped to divide, the heat stress response and autophagy, both programs (Muhlhaus et al. 2011) (4) microscopy images demonstrate that cells are indeed viable but cell diameters are increased, indicating that cells stopped to divide but fail to divide and are arrested in late stages of the cell cycle (Figure 2).

Given the wealth of processes in the chloroplast of *Chlamydomonas* HSP70B as the only HSP70 might contribute to, only speculations can be made on the impact of individual functions to the growth arrest phenotype (Schroda and Vallon 2008). It's rather unlikely, that the two functions previously described for HSP70B, VIPP1 oligomer assembly/disassembly and photoprotection of PSII (Liu et al. 2007, Schroda et al. 1999) contribute to the growth arrest. VIPP1 knock-down did not result in growth defects at ambient conditions (Nordhues et al. 2012) and we could not observe significant changes in protein levels from the photosynthetic electron transport chain within the first 36 hours of HSP70B depletion (Figure S5). Additionally, *Chlamydomonas* is able to generate energy from various sources, making energy generation via photosynthesis a dispensable process (Harris 1989). From the data gathered in this work, we therefore rather propose two other processes contributing more to the growth-arrest::

nutrient-limitation and stress responses. Especially starch accumulation and ATG8-mediated autophagy is frequently observed in nutrient-limited *Chlamydomonas* cells (Figure 5, 6 and S6) (Ball et al. 1990, Bassham 2007). Indeed, the addition of arginine, in concentrations similar to those provided to auxotrophic strains, partially covered the growth arrest phenotype in HSP70B knock-down strains (Figure 7 and S7). HSP70B proteins levels were still reduced in arginine-supplied *Chlamydomonas* cells, to similar levels than in unsupplied HSP70B knock-down strains. This clearly indicates that *NIT1* is still induced and nitrogen covers the nitrogen demand. Furthermore, upon nitrogen depletion, *Chlamydomonas* expresses an extracellular amino acid oxidase (amino acid deaminase) that produces ammonium from a few distinct amino acids in the medium (Muñoz-Blanco et al. 1990, Vallon et al. 1993). However, the addition of several of those amino acids to HSP70B depleted cells (lysine, valine, leucine, isoleucine, methionine) was not sufficient to revert the growth arrest phenotype (Figure S7). In this case, nitrogen would be imported as ammonium and therefore would not require nitrate reductase or nitrite reductase, while only the latter is chloroplast localized and therefore could be a potential client of HSP70B (Fernandez and Galvan 2008). We therefore conclude that indeed anabolic pathways are affected and not nitrogen uptake itself is non-functional. Doubling time of arginine-supplied HSP70B underexpressing strains was still strongly reduced (24 hours) compared to control strains (8 hours). Other phenotypes than growth-arrest were also not reverted in HSP70B knock-down strains, for example VIPP1/2 accumulation, induction of stress genes and the cell size increase (Figure 7), indicating that further limitations repress further increased growth rates. However, *Chlamydomonas* lacks whole families of amino acid transporters present in higher plants, and consequently is only able to import arginine efficiently against gradient into the cell (Kirk and Kirk 1978, Tegeder and Ward 2012). The still decreased growth rate of arginine supplied HSP70B knock-down compared to wild-type strains could therefore be a result of the inability to take up further growth-limiting metabolites.

Stress responses are often accompanied by growth-arrests, also in *Chlamydomonas*, and might therefore also contribute to the observed growth-arrest (Muhlhaus et al. 2011, Perez-Perez et al. 2010). HSFs were thereby closely linked to the TOR (Target Of Rapamycin) kinase in yeast (Bandhakavi et al. 2008), a central regulator of cell growth upon exposure to different stresses, especially nutrient limitation (Loewith and Hall 2011). Additionally, a recent study showed that HSF1 is directly phosphorylated by the TOR kinase (Chou et al. 2012). Autophagy is also activated, in nutrient-limited, growth arrested cells, via the TOR signaling pathway (Chang et al. 2009, Perez-Perez et al. 2010).

Stromal HSP70s were found to contribute to chloroplast import in higher plants (Shi and Theg 2010, Su and Li 2010). Import of nuclear encoded proteins into the chloroplast is an essential process, as judged from phenotypes of knock-out plants depleted from central proteins of the translocons machinery (Bauer *et al.* 2000, Hust and Gutensohn 2006, Kovacheva *et al.* 2005). Accumulation of preproteins that still include the N-terminal extension was found in mutants defective in transport, as the precursor is cleaved in the stroma upon successful transport (Jarvis *et al.* 1998, Richter and Lamppa 1998). However, within our protein

investigations we analyzed many nuclear encoded chloroplast proteins, i.e. VIPP1/2, CGE1, CDJ1/2/4, HSP90C and we did not observe accumulation of pre-proteins. We therefore conclude that potential functions of HSP70B in import are either minor or can be compensated by other chaperones, i.e. HSP90C which is overexpressed in HSP70B knock-down strains (Figure 3), and therefore contribute only weakly to the growth arrest phenotype.

The chloroplast UPR is relayed in the HSF1-dependent stress response

Upon depletion of HSP70B, the HSF1-dependent HSR was induced during the accompanying growth-arrest period (Figure 6 and S6). Proteotoxic conditions in the chloroplast therefore appear to be integrated in cytosolic acclimation pathways, contrary to other compartments, where such conditions induce independent responses (Parmar and Schroder 2012, Pellegrino *et al.* 2012). Constitutive underexpression of HSP70B was already found before to desensitize the HSF1-dependent stress response already at ambient conditions resulting in reduced expression of heat shock proteins upon exposure to proteotoxic conditions (S.Schmollinger and M. Schroda, manuscript currently submitted for publication). The constitutive construct used for latter experiments and the inducible knock-down construct used here have different target regions within the HSP70B transcript, indicating the specificity of the response on HSP70B depletion. The inducible vector targets a region encoding for the N-terminal ATPase domain while the constitutive vector contains the 5'UTR and transit peptide region. In a recent microarray approach, many plastidic chaperones were identified whose transcript levels were dependent on the abundance of the central regulator of the HSR in *Chlamydomonas*, HSF1, similarly to HSP90C, where this was shown already in 2007 (Schulz-Raffelt *et al.* 2007). Additionally, the binding of HSF1 to promoter regions of potential plastidic chaperones HSP22F and CLPB3 was directly shown using chromatin immunoprecipitations (ChIP) (Strenkert *et al.* 2011) and (S.Schmollinger and M. Schroda, manuscript currently submitted for publication). Taken together, chloroplast stress appears to be integrated in cytosolic stress responses.

HSP70B-controlled VIPP1 assembly/disassembly is crucial for VIPP1 function in thylakoid biosynthesis

The so far only known client of the HSP70B chaperone system in the chloroplast of *Chlamydomonas* is the VIPP1 protein (Liu *et al.* 2005), where HSP70B was shown to play a role in mediating the distribution between oligomeric and monomeric states (Liu *et al.* 2007). This protein is strongly accumulating in inducibly HSP70B depleted cells (Figure 3), starting already early upon the beginning depletion of HSP70B. This clearly indicates that VIPP1 function is affected in HSP70B depleted cells, resulting in a feedback in order to increase functional VIPP1 levels. This is supported by the increased expression of the VIPP2 protein, a second homolog of the VIPP1 protein only present in green alga (Figure 3). VIPP2 is not expressed at ambient conditions and was shown to be expressed to high levels only in VIPP1 knock-down strains (Nordhues *et al.* 2012). Additional phenotypes of VIPP1 knock-down strains are also found in inducibly HSP70B-depleted cells, for example high light sensitivity (Figure 4) and, more

specifically, aberrant structures at the origin of thylakoid membranes (Figure 5). Probably the reason for this phenotype is the distribution between VIPP1 oligomers and monomers that is distorted in inducible HSP70B knock-down strains (Figure 4 and S2). Dependent on the HSP70B protein level, lower molecular weight isoforms of VIPP1 are depleted, while higher molecular weight isoforms are strongly increased. Either the low molecular weight isoforms themselves or the cycling between high and low molecular weight isoforms is therefore necessary for VIPP1 function.

Interestingly, even though total VIPP levels are increased, the feedback activation of VIPP1 did not revert the VIPP1 phenotypes. Remaining HSP70B is therefore not capable to maintain VIPP1 function. One reason for this observation might be the altered composition of the J-domain pool. While VIPP1 levels increase, CDJ2 levels are unaltered. Other CDJ proteins are strongly increased (CDJ1/CDJ4), therefore the chances for VIPP1/CDJ2 to attract a remaining HSP70B chaperone are even less pronounced.

Experimental procedures

Vector construction

The amiRNA targeting *Chlamydomonas HSP70B* was designed using the Web MicroRNA Designer (WMD3) webtool at <http://wmd3.weigelworld.org> (Ossowski *et al.* 2008) following the instructions for *Chlamydomonas* given by Molnar *et al.* 2009. The resulting oligonucleotides that met the criteria (5'-ctagtGCCGAGAACAACCTTTCTACTCActctgctgatcggcaccatgggggtgggtgatcagcgctaTGAGAAGAAAGTGTCTg-3' and 5'-ctagcGCCGAGAACAACCTTTCTTCTCAtagcgctgatcaccaccacccatggtgccgatcagcgagaTGAGTAGAAAGTGTCTCGGCa-3', uppercase letters indicate sequences targeting *HSP70B* mRNA) were annealed by a procedure of boiling to 100°C and slow reduction of the temperature to 60°C (0.3°C/min) in a thermocycler (Biometra). After purification, the annealed oligos were ligated into *SpeI*-digested pMS539 (Schmollinger *et al.* 2010), yielding pMS542.

Strains and culture conditions

Chlamydomonas reinhardtii strain cw15-325 (*cwd mt+ arg7*), kindly provided by R. Matagne (University of Liège, Belgium), was used as recipient strain for transformation with control constructs pCB412 (Schroda *et al.* 1999) and pMS539 (Schmollinger *et al.* 2010) or *HSP70B* amiRNA construct pMS542. All plasmids contain the wild-type *ARG7*, were linearized by digestion with *HindIII* and were transformed (1 µg) into cw15-325 by agitation with glass beads (Kindle 1990). If not stated otherwise strains were grown mixotrophically in TAP medium (Harris 1989) that contains 7.5 mM NH₄, referred to as TAP-NH₄, on a rotatory shaker at 25°C at ~30 µE m⁻² s⁻¹. To exchange the nitrogen source cells inoculated on TAP-NH₄ medium to a maximal cell density of 5 x 10⁶ cells/mL were centrifuged at 3100g for 2 min at 25°C. The resulting cell pellet was washed twice in 50 mL TAP medium without any nitrogen (-N) to remove remaining NH₄, involving two centrifugation steps at 3100g for 2 min at 25°C in between. Finally, the cell pellet was resuspended in TAP-NO₃ medium, containing 7.5 mM NO₃. If necessary, cells were diluted during the experiment in fresh nitrate containing medium to ensure that cell densities never exceeded 5 x 10⁶ cells/mL and cells remain in mid-log phase.

Cell number and cell size distribution

Cell number and cell size distribution were determined using a Coulter-Counter Z2 (Beckman-Coulter). Each measurement was carried out in two technical replicates and the average of both was used for further comparisons. The size distribution was monitored by counting cells in 256 windows between 4.4 µm and 12.2 µm. For comparison between different strains in different cell densities, the data was normalized to the highest number of cells in a single window, which was set to 1 (% max).

RNA extraction and analysis

RNA extraction was realized with a modified protocol using the TRIzol reagent (Invitrogen)

described previously (Strenkert *et al.* 2011). Following DNase treatment, reverse transcription and qPCR analysis was performed accordingly. RNA concentration was determined using a NanoDrop ND-1000 spectrophotometer (NanoDrop Technologies). Primers for qRT-PCRs were selected based on a single melt curve, a single band on a 1.5% agarose gel at the calculated amplicon size and maximal efficiency. Primer sequences and amplicon position are illustrated in Supplemental Figure 7 online. qRT-PCR was performed using the StepOnePlus RT-PCR system (Applied Biosystems) with the Maxima SYBR Green kit from Fermentas. Each reaction contained the vendor's master mix, 100 nM of each primer and 10 ng cDNA. A 10 min 95°C denaturation step was followed by 40 cycles of 95°C for 15 s and 65°C for 60 s. Template depleted controls were always included.

Protein extraction and analysis

Protein extraction and SDS-PAGE using 10% poly acrylamide gels for time course analysis and screenings for *HSP70B* underexpressing strains was performed as described previously (Laemmli 1970, Liu *et al.* 2005). Quantification of cellular protein concentrations was carried out as described. Proteins in gels were transferred to nitrocellulose membranes (Hybond-ECL, Amersham Biosciences) by semidry blotting by using a discontinuous transfer system. Immunodetection was realized using enhanced chemiluminescence (ECL) detected with Hyperfilm-ECL (Amersham, UK). Antisera described previously targeting HSP70B (Schroda *et al.* 1999), CGE1 (Schroda *et al.* 2001), CDJ1 (Willmund *et al.* 2008a), CDJ2 (Liu *et al.* 2005), CDJ4 (Dorn *et al.* 2010), VIPP1 (Liu *et al.* 2005), VIPP2 (S. Schmollinger and M. Schroda unpublished results), HSP90C (Willmund and Schroda 2005), CF1 α , CF1 β (Lemaire and Wollman 1989), CYTF (Pierre and Popot 1993), CLPB (Bukau), LHCSR3 (Naumann *et al.* 2007), HSP90A (Schulz-Raffelt *et al.* 2007), ATG8 (Perez-Perez *et al.* 2010), DEGP (S. Nick and M. Schroda unpublished results), D1(PSBA) (Agrisera, AS05 084), CP43, OEC33 (PSBO) (Agrisera, AS06 142-33), LHCI (Vallon *et al.* 1986), PETO (Hamel *et al.* 2000), PSAD (Agrisera, AS09 461), PSAG (Agrisera AS06 144), PSAL (M. Hippler), SECA (M. Possienke and M. Schroda, unpublished results).

Sucrose density centrifugation

Sucrose density centrifugation to separate high molecular weight oligomers of VIPP1 from soluble isoforms was performed as described previously (Liu *et al.* 2007). *Chlamydomonas* was grown in 500 mL TAP-NH₄ medium to a density of about 3 x 10⁶ cells/ml, harvested by centrifugation, washed twice in TAP-N medium and finally resuspended in TAP-NO₃ to a density of 2 x 10⁶ cells/ml. 2 x 10⁸ cells were harvested at the indicated timepoints and resuspended in 1 ml KH buffer containing 2% Triton X-100 and 0.25 x protease inhibitor cocktail (Roche). Cells were lysed by sonication on ice and centrifuged for 2 min at 16 100 g, 4°C in a table centrifuge to remove non-solubilized matter. The supernatant was transferred on top of a continuous 10 mL 10-30% sucrose gradient and centrifuged for 2 hours at 79000g, 4°C.

High light treatment

For the exposure to high light ($1000 \mu\text{E m}^{-2} \text{s}^{-1}$) a similar installation was used as already reported previously (Nordhues *et al.* 2012). 50 mL of cell cultures inoculated for 24-hours on TAP-NO₃ were transferred to 150-mL beakers and placed onto a water-cooled metal plate on a rotary shaker that was illuminated by Osram HLX 250W 64663 Xenophot bulbs. The temperature in the culture was kept constantly at 25°C. A glass plate nonpermissive to infrared and UV irradiation was placed in between light sources and beakers.

Transmission Electron Microscopy

Embedding for electron microscopy was performed according to a protocol published previously (Nordhues *et al.* 2012). 1×10^7 cells were harvested at the indicated timepoints after the exchange of the nitrogen source and fixed for 2 hours in 2.5% glutaraldehyde buffered with 100 mM Na-cacodylate (pH 7.2). After washing, cells were fixed for 1 hour in 1% OsO₄ at 4°C. After incubating the cells for 15 min in 20% BSA (w/v), the cell pellet was fixed for another 30 min with 2.5% glutaraldehyde. The cell pellet was fixed in 1.5% agarose and then cut into several pieces (~1 to 2 mm³ in size), dehydrated in ethanol and embedded in glycid ether 100 (Serva) with propylene oxide as intermediate solvent. Ultrathin sections (60 to 70 nm) were cut with a diamond knife (type ultra 358, Diatome) on an EM UC6 ultramicrotome (Leica) and mounted on single-slot Pioloformcoated copper grids (Plano). The sections were stained with uranyl acetate and lead citrate (Reynolds, 1963) and viewed with a JEM-2100 (Jeol) or EM 902A (Carl Zeiss) transmission electron microscope (both operated at 80 kV). Micrographs were taken using a 408034080-pixel or 1350 3 1040-pixel charge-coupled device camera (UltraScan 4000 or Erlangshen ES500W, respectively; Gatan) and Gatan Digital Micrograph software (version 1.70.16). Image brightness and contrast were adjusted and figures assembled using Adobe Photoshop 8.0.1.

Acknowledgments

We thank Olivier Vallon for several antisera. This work was supported by the Max Planck Society and grants from the Deutsche Forschungsgemeinschaft (Schr 617/5-1) and the Bundesministerium für Bildung und Forschung (Systems Biology Initiative FORSYS, project GoFORSYS).

References

- Ball, S.G., Dirick, L., Decq, A., Martiat, J.C. and Matagne, R.F.** (1990) Physiology of Starch Storage in the Monocellular Alga *Chlamydomonas-Reinhardtii*. *Plant Science*, **66**, 1-9.
- Bandhakavi, S., Xie, H., O'Callaghan, B., Sakurai, H., Kim, D.H. and Griffin, T.J.** (2008) Hsf1 activation inhibits rapamycin resistance and TOR signaling in yeast revealed by combined proteomic and genetic analysis. *PLoS one*, **3**, e1598.
- Bassham, D.C.** (2007) Plant autophagy--more than a starvation response. *Current opinion in plant biology*, **10**, 587-593.
- Bauer, J., Chen, K., Hiltbunner, A., Wehrli, E., Eugster, M., Schnell, D. and Kessler, F.** (2000) The major protein import receptor of plastids is essential for chloroplast biogenesis. *Nature*, **403**, 203-207.
- Bukau, B., Weissman, J. and Horwich, A.** (2006) Molecular chaperones and protein quality control. *Cell*, **125**, 443-451.
- Chang, Y.Y., Juhasz, G., Goraksha-Hicks, P., Arsham, A.M., Mallin, D.R., Muller, L.K. and Neufeld, T.P.** (2009) Nutrient-dependent regulation of autophagy through the target of rapamycin pathway. *Biochemical Society transactions*, **37**, 232-236.
- Cheetham, M.E. and Caplan, A.J.** (1998) Structure, function and evolution of DnaJ: conservation and adaptation of chaperone function. *Cell stress & chaperones*, **3**, 28-36.
- Chou, S.D., Prince, T., Gong, J. and Calderwood, S.K.** (2012) mTOR is essential for the proteotoxic stress response, HSF1 activation and heat shock protein synthesis. *PLoS one*, **7**, e39679.
- Dorn, K.V., Willmund, F., Schwarz, C., Henselmann, C., Pohl, T., Hess, B., Veyel, D., Usadel, B., Friedrich, T., Nickelsen, J. and Schroda, M.** (2010) Chloroplast DnaJ-like proteins 3 and 4 (CDJ3/4) from *Chlamydomonas reinhardtii* contain redox-active Fe-S clusters and interact with stromal HSP70B. *The Biochemical journal*, **427**, 205-215.
- Drzymalla, C., Schroda, M. and Beck, C.F.** (1996) Light-inducible gene HSP70B encodes a chloroplast-localized heat shock protein in *Chlamydomonas reinhardtii*. *Plant molecular biology*, **31**, 1185-1194.
- Fernandez, E. and Galvan, A.** (2008) Nitrate assimilation in *Chlamydomonas*. *Eukaryotic cell*, **7**, 555-559.
- Glover, J.R. and Lindquist, S.** (1998) Hsp104, Hsp70, and Hsp40: A novel chaperone system that rescues previously aggregated proteins. *Cell*, **94**, 73-82.
- Goloubinoff, P., Mogk, A., Zvi, A.P., Tomoyasu, T. and Bukau, B.** (1999) Sequential mechanism of solubilization and refolding of stable protein aggregates by a bichaperone network. *Proceedings of the National Academy of Sciences of the United States of America*, **96**, 13732-13737.
- Gruber, A.R., Lorenz, R., Bernhart, S.H., Neubock, R. and Hofacker, I.L.** (2008) The Vienna RNA websuite. *Nucleic acids research*, **36**, W70-74.
- Hamel, P., Olive, J., Pierre, Y., Wollman, F.A. and de Vitry, C.** (2000) A new subunit of cytochrome b6/f complex undergoes reversible phosphorylation upon state transition. *The Journal of biological chemistry*, **275**, 17072-17079.
- Harris, E.H.** (1989) *The Chlamydomonas sourcebook : a comprehensive guide to biology and laboratory use* 1. [Dr.]. edn. San Diego [u.a.]: Acad. Press.
- Harrison, C.** (2003) GrpE, a nucleotide exchange factor for DnaK. *Cell stress & chaperones*, **8**, 218-224.
- Hartl, F.U. and Hayer-Hartl, M.** (2009) Converging concepts of protein folding in vitro and in vivo. *Nature structural & molecular biology*, **16**, 574-581.
- Heide, H., Nordhues, A., Drepper, F., Nick, S., Schulz-Raffelt, M., Haehnel, W. and Schroda, M.** (2009) Application of quantitative immunoprecipitation combined with knockdown and cross-linking to *Chlamydomonas* reveals the presence of vesicle-inducing protein in plastids 1

in a common complex with chloroplast HSP90C. *Proteomics*, **9**, 3079-3089.

Hust, B. and Gutensohn, M. (2006) Deletion of core components of the plastid protein import machinery causes differential arrest of embryo development in *Arabidopsis thaliana*. *Plant Biol (Stuttg)*, **8**, 18-30.

Jarvis, P., Chen, L.J., Li, H., Peto, C.A., Fankhauser, C. and Chory, J. (1998) An *Arabidopsis* mutant defective in the plastid general protein import apparatus. *Science (New York, N.Y.)*, **282**, 100-103.

Kampinga, H.H. and Craig, E.A. (2010) The HSP70 chaperone machinery: J proteins as drivers of functional specificity. *Nature reviews*, **11**, 579-592.

Kindle, K.L. (1990) High-frequency nuclear transformation of *Chlamydomonas reinhardtii*. *Proceedings of the National Academy of Sciences of the United States of America*, **87**, 1228-1232.

Kirk, D.L. and Kirk, M.M. (1978) Carrier-mediated Uptake of Arginine and Urea by *Chlamydomonas reinhardtii*. *Plant physiology*, **61**, 556-560.

Kovacheva, S., Bedard, J., Patel, R., Dudley, P., Twell, D., Rios, G., Koncz, C. and Jarvis, P. (2005) In vivo studies on the roles of Tic110, Tic40 and Hsp93 during chloroplast protein import. *Plant J*, **41**, 412-428.

Kroll, D., Meierhoff, K., Bechtold, N., Kinoshita, M., Westphal, S., Vothknecht, U.C., Soll, J. and Westhoff, P. (2001) VIPP1, a nuclear gene of *Arabidopsis thaliana* essential for thylakoid membrane formation. *Proceedings of the National Academy of Sciences of the United States of America*, **98**, 4238-4242.

Laemmli, U.K. (1970) Cleavage of structural proteins during the assembly of the head of bacteriophage T4. *Nature*, **227**, 680-685.

Lemaire, C. and Wollman, F.A. (1989) The chloroplast ATP synthase in *Chlamydomonas reinhardtii*. I. Characterization of its nine constitutive subunits. *The Journal of biological chemistry*, **264**, 10228-10234.

Li, H.M., Kaneko, Y. and Keegstra, K. (1994) Molecular cloning of a chloroplastic protein associated with both the envelope and thylakoid membranes. *Plant molecular biology*, **25**, 619-632.

Liu, C., Willmund, F., Golecki, J.R., Cacace, S., Hess, B., Markert, C. and Schroda, M. (2007) The chloroplast HSP70B-CDJ2-CGE1 chaperones catalyse assembly and disassembly of VIPP1 oligomers in *Chlamydomonas*. *Plant J*, **50**, 265-277.

Liu, C., Willmund, F., Whitelegge, J.P., Hawat, S., Knapp, B., Lodha, M. and Schroda, M. (2005) J-domain protein CDJ2 and HSP70B are a plastidic chaperone pair that interacts with vesicle-inducing protein in plastids 1. *Molecular biology of the cell*, **16**, 1165-1177.

Loewith, R. and Hall, M.N. (2011) Target of rapamycin (TOR) in nutrient signaling and growth control. *Genetics*, **189**, 1177-1201.

Mayer, M.P. and Bukau, B. (2005) Hsp70 chaperones: cellular functions and molecular mechanism. *Cellular and molecular life sciences : CMLS*, **62**, 670-684.

Molnar, A., Bassett, A., Thuenemann, E., Schwach, F., Karkare, S., Ossowski, S., Weigel, D. and Baulcombe, D. (2009) Highly specific gene silencing by artificial microRNAs in the unicellular alga *Chlamydomonas reinhardtii*. *Plant J*.

Muhlhaus, T., Weiss, J., Hemme, D., Sommer, F. and Schroda, M. (2011) Quantitative shotgun proteomics using a uniform (1)N-labeled standard to monitor proteome dynamics in time course experiments reveals new insights into the heat stress response of *Chlamydomonas reinhardtii*. *Mol Cell Proteomics*, **10**, M110 004739.

Muñoz-Blanco, J., Hidalgo-Martínez, J. and Cárdenas, J. (1990) Extracellular deamination of l-amino acids by *Chlamydomonas reinhardtii* cells. *Planta*, **182**, 194-198.

Nakatogawa, H., Suzuki, K., Kamada, Y. and Ohsumi, Y. (2009) Dynamics and diversity in autophagy mechanisms: lessons from yeast. *Nature reviews*, **10**, 458-467.

Naumann, B., Busch, A., Allmer, J., Ostendorf, E., Zeller, M., Kirchhoff, H. and Hippler, M.

- (2007) Comparative quantitative proteomics to investigate the remodeling of bioenergetic pathways under iron deficiency in *Chlamydomonas reinhardtii*. *Proteomics*, **7**, 3964-3979.
- Nordhues, A., Miller, S.M., Muhlhaus, T. and Schroda, M.** (2010) New insights into the roles of molecular chaperones in *Chlamydomonas* and *Volvox*. *Int Rev Cell Mol Biol*, **285**, 75-113.
- Nordhues, A., Schottler, M.A., Unger, A.K., Geimer, S., Schonfelder, S., Schmollinger, S., Rutgers, M., Finazzi, G., Soppa, B., Sommer, F., Muhlhaus, T., Roach, T., Krieger-Liszky, A., Lokstein, H., Crespo, J.L. and Schroda, M.** (2012) Evidence for a Role of VIPP1 in the Structural Organization of the Photosynthetic Apparatus in *Chlamydomonas*. *The Plant cell*.
- Ossowski, S., Schwab, R. and Weigel, D.** (2008) Gene silencing in plants using artificial microRNAs and other small RNAs. *Plant J*, **53**, 674-690.
- Parmar, V.M. and Schroder, M.** (2012) Sensing endoplasmic reticulum stress. *Adv Exp Med Biol*, **738**, 153-168.
- Peers, G., Truong, T.B., Ostendorf, E., Busch, A., Elrad, D., Grossman, A.R., Hippler, M. and Niyogi, K.K.** (2009) An ancient light-harvesting protein is critical for the regulation of algal photosynthesis. *Nature*, **462**, 518-521.
- Pellegrino, M.W., Nargund, A.M. and Haynes, C.M.** (2012) Signaling the mitochondrial unfolded protein response. *Biochimica et biophysica acta*.
- Perez-Perez, M.E., Florencio, F.J. and Crespo, J.L.** (2010) Inhibition of target of rapamycin signaling and stress activate autophagy in *Chlamydomonas reinhardtii*. *Plant physiology*, **152**, 1874-1888.
- Pierre, Y. and Popot, J.L.** (1993) Identification of two 4-kDa miniproteins in the cytochrome b6f complex from *Chlamydomonas reinhardtii*. *Comptes rendus de l'Academie des sciences. Serie III, Sciences de la vie*, **316**, 1404-1409.
- Richter, S. and Lamppa, G.K.** (1998) A chloroplast processing enzyme functions as the general stromal processing peptidase. *Proceedings of the National Academy of Sciences of the United States of America*, **95**, 7463-7468.
- Rolland, N., Curien, G., Finazzi, G., Kuntz, M., Marechal, E., Matringe, M., Ravanel, S. and Seigneurin-Berny, D.** (2012) The Biosynthetic Capacities of the Plastids and Integration Between Cytoplasmic and Chloroplast Processes. *Annual review of genetics*.
- Rudiger, S., Germeroth, L., Schneider-Mergener, J. and Bukau, B.** (1997) Substrate specificity of the DnaK chaperone determined by screening cellulose-bound peptide libraries. *The EMBO journal*, **16**, 1501-1507.
- Schmollinger, S., Strenkert, D. and Schroda, M.** (2010) An inducible artificial microRNA system for *Chlamydomonas reinhardtii* confirms a key role for heat shock factor 1 in regulating thermotolerance. *Current genetics*, **56**, 383-389.
- Schroda, M.** (2004) The *Chlamydomonas* genome reveals its secrets: chaperone genes and the potential roles of their gene products in the chloroplast. *Photosynthesis research*, **82**, 221-240.
- Schroda, M. and Vallon, O.** (2008) *Chaperones and Proteases*. In: *The Chlamydomonas Sourcebook, Second Edition* San Diego, CA: Elsevier / Academic Press.
- Schroda, M., Vallon, O., Whitelegge, J.P., Beck, C.F. and Wollman, F.A.** (2001) The chloroplastic GrpE homolog of *Chlamydomonas*: two isoforms generated by differential splicing. *The Plant cell*, **13**, 2823-2839.
- Schroda, M., Vallon, O., Wollman, F.A. and Beck, C.F.** (1999) A chloroplast-targeted heat shock protein 70 (HSP70) contributes to the photoprotection and repair of photosystem II during and after photoinhibition. *The Plant cell*, **11**, 1165-1178.
- Schulz-Raffelt, M., Lodha, M. and Schroda, M.** (2007) Heat shock factor 1 is a key regulator of the stress response in *Chlamydomonas*. *Plant J*, **52**, 286-295.
- Sharma, S.K., Christen, P. and Goloubinoff, P.** (2009) Disaggregating chaperones: an unfolding story. *Current protein & peptide science*, **10**, 432-446.
- Shi, L.X. and Theg, S.M.** (2010) A stromal heat shock protein 70 system functions in protein import into chloroplasts in the moss *Physcomitrella patens*. *The Plant cell*, **22**, 205-220.

- Sousa, R. and Lafer, E.M.** (2006) Keep the traffic moving: mechanism of the Hsp70 motor. *Traffic*, **7**, 1596-1603.
- Strenkert, D., Schmollinger, S., Sommer, F., Schulz-Raffelt, M. and Schroda, M.** (2011) Transcription factor-dependent chromatin remodeling at heat shock and copper-responsive promoters in *Chlamydomonas reinhardtii*. *The Plant cell*, **23**, 2285-2301.
- Su, P.H. and Li, H.M.** (2008) Arabidopsis stromal 70-kD heat shock proteins are essential for plant development and important for thermotolerance of germinating seeds. *Plant physiology*, **146**, 1231-1241.
- Su, P.H. and Li, H.M.** (2010) Stromal Hsp70 is important for protein translocation into pea and Arabidopsis chloroplasts. *The Plant cell*, **22**, 1516-1531.
- Tegeder, M. and Ward, J.M.** (2012) Molecular Evolution of Plant AAP and LHT Amino Acid Transporters. *Frontiers in plant science*, **3**, 21.
- Vallon, O., Bulte, L., Kuras, R., Olive, J. and Wollman, F.A.** (1993) Extensive accumulation of an extracellular L-amino-acid oxidase during gametogenesis of *Chlamydomonas reinhardtii*. *European journal of biochemistry / FEBS*, **215**, 351-360.
- Vallon, O., Wollman, F.A. and Olive, J.** (1986) Lateral distribution of the main protein complexes of the photosynthetic apparatus in *Chlamydomonas reinhardtii* and in spinach: an immunocytochemical study using intact thylakoid membranes and PS II enriched membrane preparation. *Photobiochem Photobiophys*, **12**, 203-220.
- Weibezahn, J., Schlieker, C., Bukau, B. and Mogk, A.** (2003) Characterization of a trap mutant of the AAA+ chaperone ClpB. *The Journal of biological chemistry*, **278**, 32608-32617.
- Westphal, S., Heins, L., Soll, J. and Vothknecht, U.C.** (2001) Vipp1 deletion mutant of *Synechocystis*: a connection between bacterial phage shock and thylakoid biogenesis? *Proceedings of the National Academy of Sciences of the United States of America*, **98**, 4243-4248.
- Willmund, F., Dorn, K.V., Schulz-Raffelt, M. and Schroda, M.** (2008a) The chloroplast DnaJ homolog CDJ1 of *Chlamydomonas reinhardtii* is part of a multichaperone complex containing HSP70B, CGE1, and HSP90C. *Plant physiology*, **148**, 2070-2082.
- Willmund, F., Hinnenberger, M., Nick, S., Schulz-Raffelt, M., Muhlhaus, T. and Schroda, M.** (2008b) Assistance for a chaperone: *Chlamydomonas* HEP2 activates plastidic HSP70B for cochaperone binding. *The Journal of biological chemistry*, **283**, 16363-16373.
- Willmund, F., Muhlhaus, T., Wojciechowska, M. and Schroda, M.** (2007) The NH2-terminal domain of the chloroplast GrpE homolog CGE1 is required for dimerization and cochaperone function in vivo. *The Journal of biological chemistry*, **282**, 11317-11328.
- Willmund, F. and Schroda, M.** (2005) HEAT SHOCK PROTEIN 90C is a bona fide Hsp90 that interacts with plastidic HSP70B in *Chlamydomonas reinhardtii*. *Plant physiology*, **138**, 2310-2322.
- Zhao, T., Wang, W., Bai, X. and Qi, Y.** (2008) Gene silencing by artificial microRNAs in *Chlamydomonas*. *Plant J.*
- Zhu, X., Zhao, X., Burkholder, W.F., Gragerov, A., Ogata, C.M., Gottesman, M.E. and Hendrickson, W.A.** (1996) Structural analysis of substrate binding by the molecular chaperone DnaK. *Science (New York, N.Y.)*, **272**, 1606-1614.

Figure 1

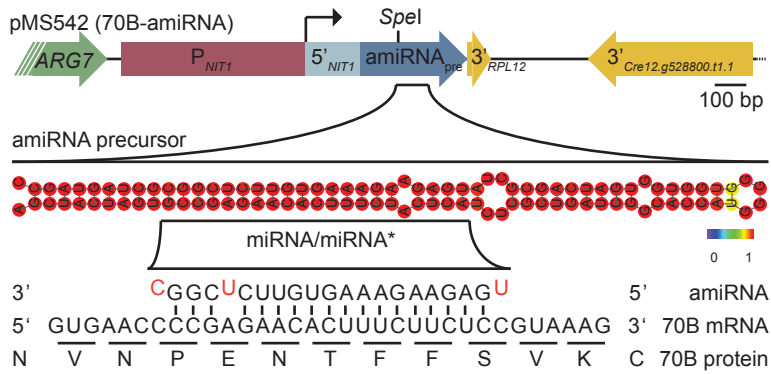


Figure 1: Vector expressing inducible amiRNA targeting *HSP70B*

Schematic overview of vector pMS542 harboring the amiRNA precursor targeting *HSP70B*, the *NIT1* promoter (P_{NIT1}) and 5'UTR (5'_{NIT1}) regulatory regions, two inverted 3'UTRs (from *RPL12* and the closeby gene *Cre12.g528800.t1.1*) as well as the *ARG7* gene used as selection marker conferring arginine prototrophy in respective mutant strains. The secondary structure of the introduced modified miRNA precursor targeting *HSP70B* was predicted using *RNAfold* on the Vienna webserver (Gruber *et al.* 2008). Sequence of the miRNA, the target region in the *HSP70B* mRNA and deduced protein sequence is denoted below.

Figure 2

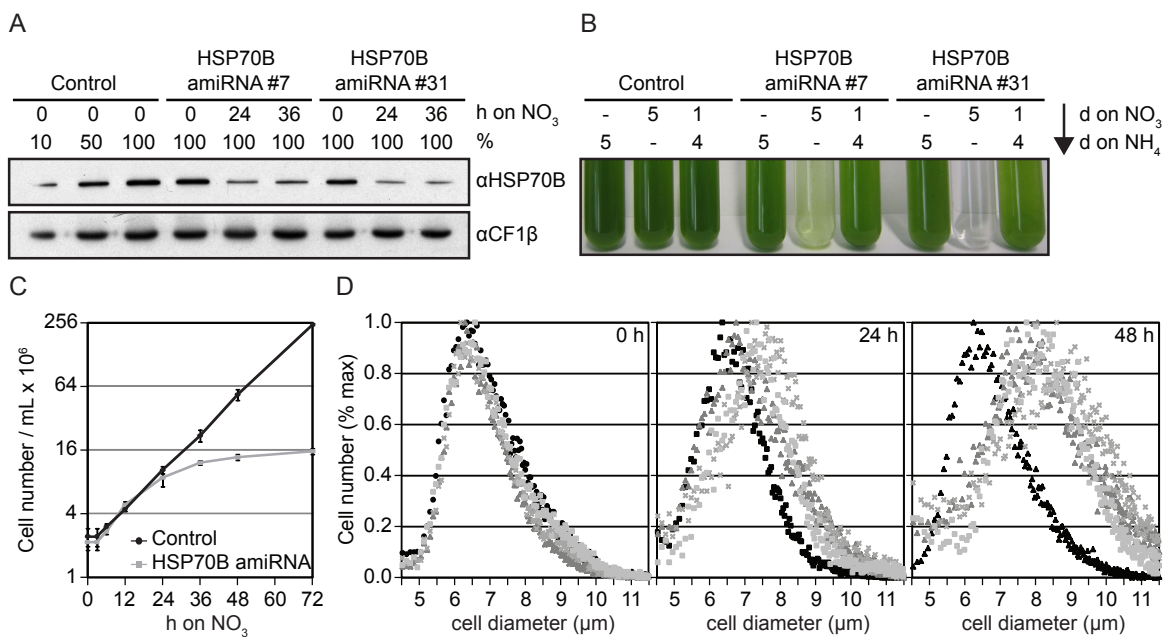


Figure 2: Underexpression of *HSP70B* results in a growth arrest and an increase in cell diameter

A: HSP70B protein levels: Total protein of a control and two independent *HSP70B* underexpressing strains (#7, #31) was extracted at different time points after induction of the amiRNA (h on NO₃). Protein was loaded corresponding to 0.5μg chlorophyll and subsequently separated on a 10% SDS-polyacrylamide gel. Amounts of HSP70B relative to loading control CF1β were analyzed by immunoblotting.

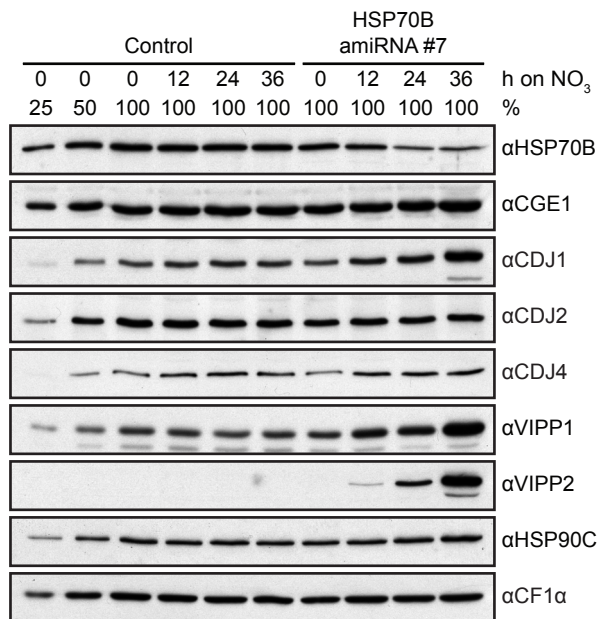
B: Growth analysis: Control and *HSP70B* amiRNA strains were grown for 5 days (d) either in ammonium-containing (TAP-NH₄, repressive), nitrate-containing (TAP-NO₃, inducing) media or re-subjected after 1 day of induction in TAP-NO₃ back to repressive conditions (TAP-NH₄).

C: Growth rate of inducible *HSP70B* amiRNA mutants upon switch to nitrate: The cell density (Cell number/ml x 10⁶, log scale) of three control strains (black circle), harboring pMS539 (empty vector), and three independent, inducible *HSP70B* amiRNA strains (grey square), harboring pMS542 (#7, #16, #31) was measured at the indicated time points after induction of the inducible amiRNA (time point 0). Cells were constantly diluted to 1x10⁶ cells/ml in fresh TAP-NO₃ when the cell density of 5x10⁶ cells/ml was reached, to keep the cells steadily in mid log-phase. Errors bars indicate standard errors within the respective group.

D: Cell size distribution of inducible *HSP70B* knockdown strains: The number of cells (% of max) with a given cell diameter (μm) is plotted against the cell diameter at the indicated time points after induction of the amiRNA in one control (black circle (0 h), square (24 h) and triangle (48)) and three independent, inducible *HSP70B* amiRNA strains (grey square (#2), triangle (#7), cross (#15)). Cell density and size distribution were measured using a Coulter-Counter Z2 (Beckman-Coulter).

Figure 3

A



B

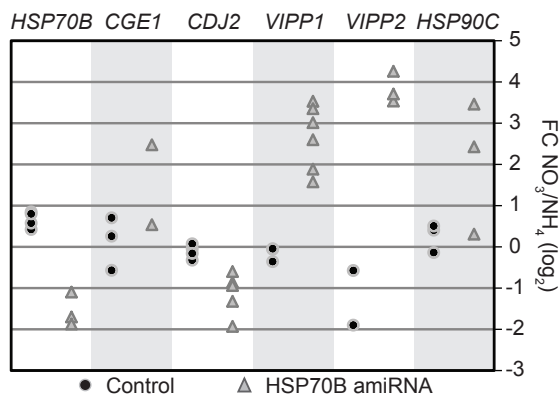


Figure 3: Co-chaperone and target protein abundance is altered upon HSP70B depletion

A: Time course analysis of co-chaperone and target protein levels in *HSP70B* knockdown strains: Total protein was extracted from control (empty vector) and inducible *HSP70B* knockdown strain #7 before and after switching the nitrogen source to induce the amiRNA. Protein was loaded corresponding to 2 μ g chlorophyll for CDJ1/2/4, VIPP2, CGE1 and HSP90C and 0.5 μ g chlorophyll for HSP70B, VIPP1 and CF1 α and separated on 10% SDS-polyacrylamide gels. Amounts of HSP70B, CGE1, CDJ1/2/4, VIPP1/2 and HSP90C relative to loading control CF1 α were analyzed by immunoblotting.

B: mRNA levels of co-chaperones and target proteins upon HSP70B depletion: RNA from three control (black circles) and at least three independent, inducible *HSP70B* underexpressing strains (grey triangle, #7, #31, #2, #15) was extracted for qRT-PCR analysis. After cDNA synthesis qPCR analysis was performed in three technical replicates and analyzed using the comparative C_T method with *CBLP2* as housekeeping gene. The log₂ fold change of transcripts (log₂) of *HSP70B*, *CGE1*, *CDJ2*, *VIPP1/2* and *HSP90C* to the 24-hours enduring exchange of TAP-NH₄ with TAP-NO₃ was analyzed.

Figure 4

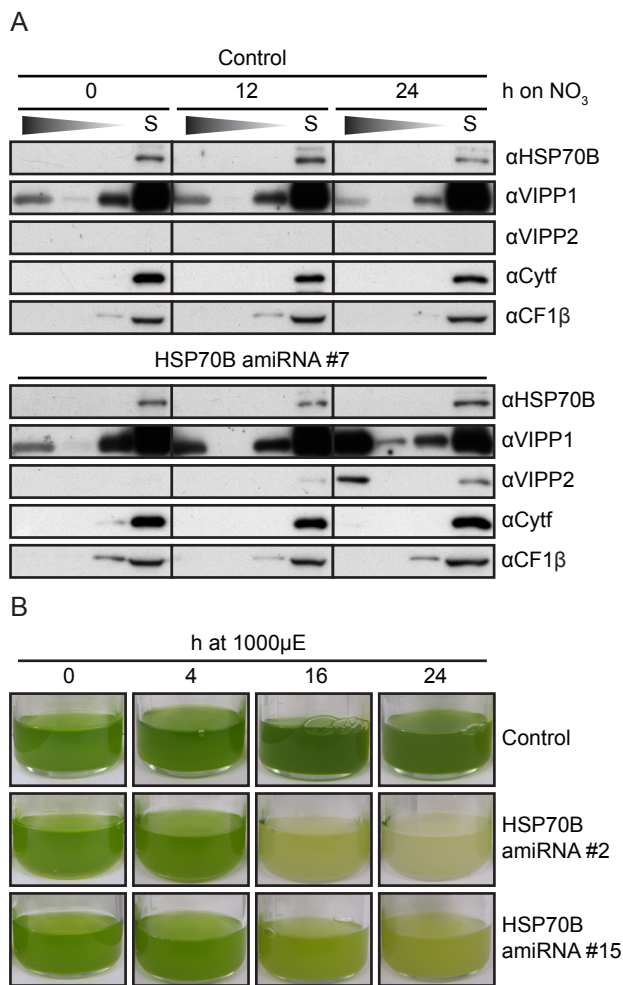


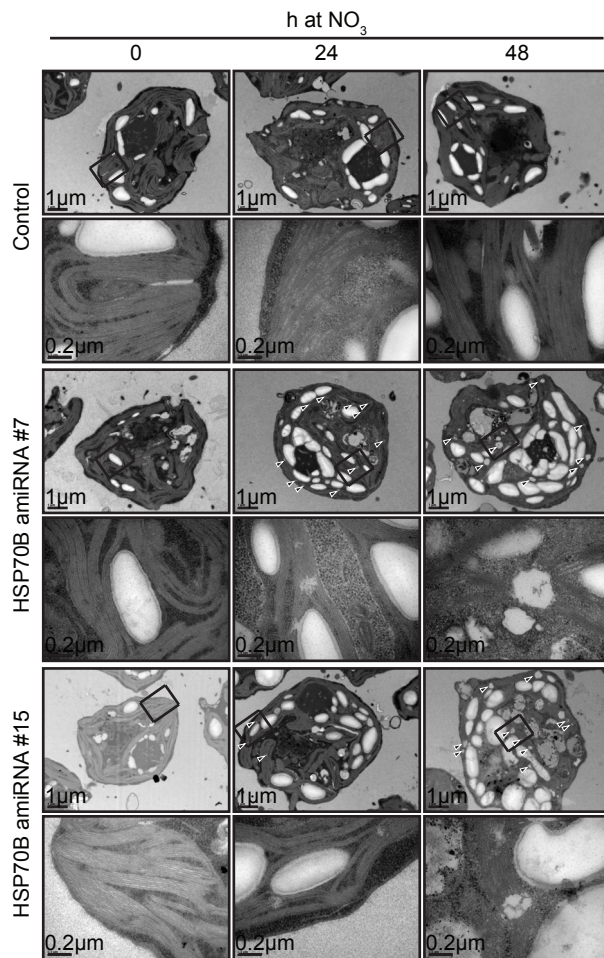
Figure 4: VIPP1 function is affected in inducible *HSP70B* knockdown strains

A: Analysis of high molecular weight oligomers of VIPP1/2: A control (empty vector) and inducible *HSP70B* knockdown strain #7 were solubilized with 2% Triton X-100 before and after switching the nitrogen source to induce the amiRNA. Lysates were loaded onto 10-30% sucrose gradients and centrifuged for 2h at 79000g. Fractions were separated on a 10% SDS-polyacrylamide gel and the amounts of HSP70B, VIPP1/2, CYTF and CF1β were analyzed with immunoblotting.

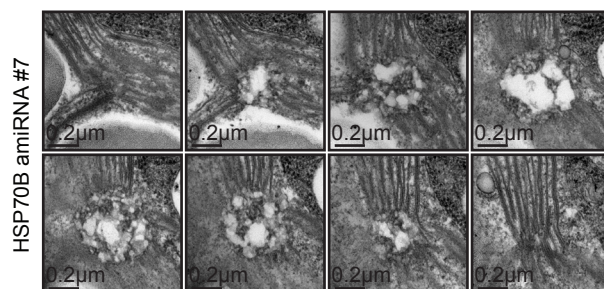
B: Adaptation to high light: After a 24-hour induction of the amiRNA targeting *HSP70B* on TAP-NO₃ one control and two inducible *HSP70B* underexpressing strains were transferred to high light conditions (1000 μE m⁻² s⁻¹) for additional 24 hours. Bleaching was analyzed at different time points after switch to higher light intensities (time point 0).

Figure 5

A



B

**Figure 5: Accumulation of starch and disordered thylakoid centers**

A: Electron microscopy: Representative electron microscopy images of cells from control and two independent inducible *HSP70B* knockdown strains (#7, #15) at different points after switching the nitrogen source to induce *HSP70B* underexpression. The black rectangle marks the region magnified below, triangles indicate divergent structures at the origin of thylakoid membranes.

B: Structures at origins of thylakoid membranes: Serial section of an exemplary aberrant structure in *HSP70B* underexpressing strain #7 48 hours after switching to nitrate to induce expression of the amiRNA.

Figure 6

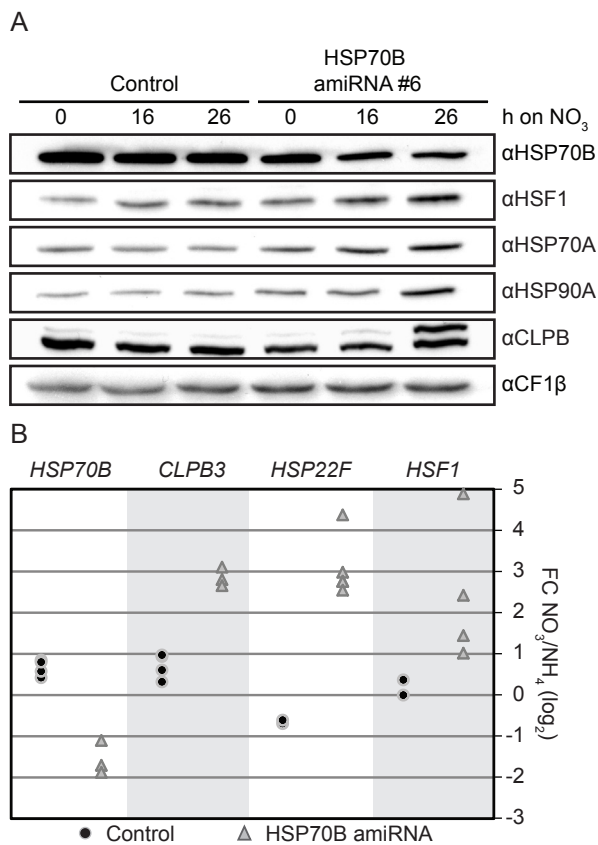


Figure 6: Salvage pathways

A: Time course analysis of heat stress related protein levels in an additional *HSP70B* knockdown strain: Total protein was extracted from control (empty vector) and inducible *HSP70B* knockdown strain #6 before and after switching the nitrogen source to induce the amiRNA. Protein was loaded corresponding to 2 μg chlorophyll and separated on 10% SDS-polyacrylamide gels. Amounts of HSP70A/B, HSF1, HSP90A and CLPB relative to loading control CF1β were analyzed by immunoblotting.

B: Transcripts of stress-related genes: RNA was extracted and analyzed from control (black circles) and HSP70B amiRNA strains (grey triangles) as already described in Figure 2B. The log₂ fold change of transcripts (log₂) of *CLPB3*, *HSF1* and *HSP22F* to the 24-hours enduring exchange of ammonium with nitrate was analyzed.

Figure 7

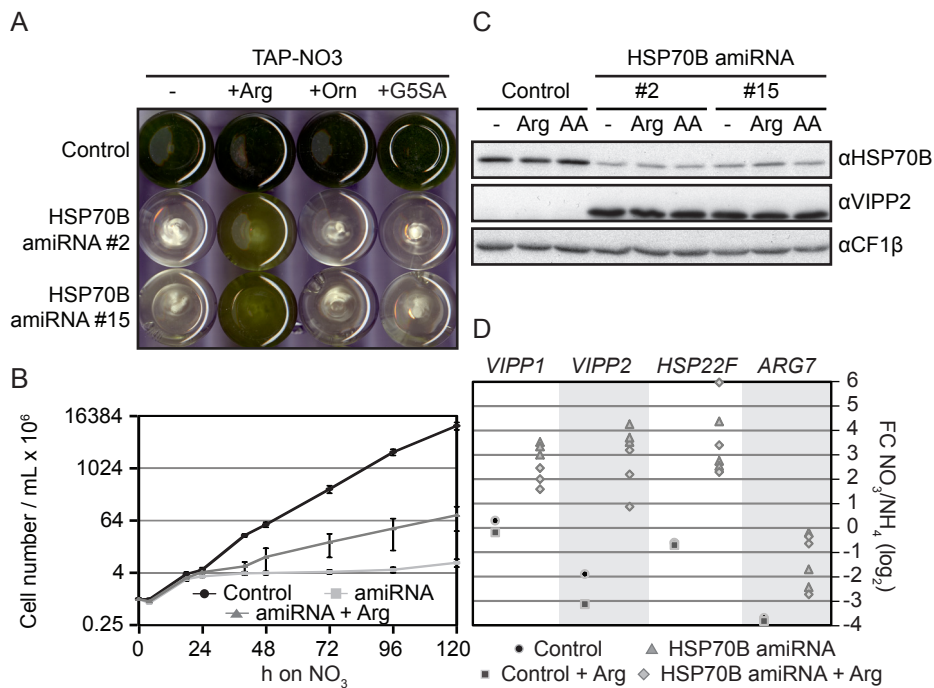


Figure 7: Supplying with arginine partially rescues growth arrest

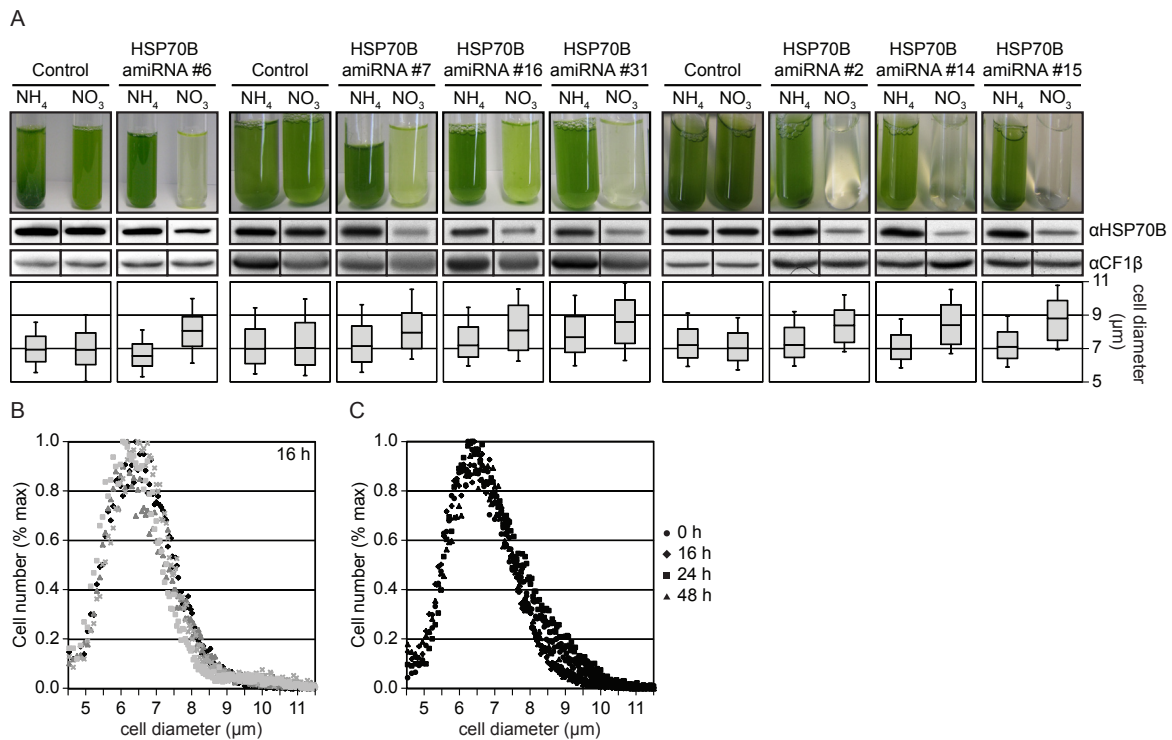
A: Growth analysis: Control and inducible *HSP70B* amiRNA strains (#2 and #15) were grown for 5 days in TAP-NO₃ media alone (-) or supplied with 7.5 mM arginine (Arg), ornithine (Orn) or L-glutamate 5-semialdehyde (G5SA).

B: Growth rate in inducible *HSP70B* amiRNA mutants supplied with arginine: Cell number of three control strains and three inducible *HSP70B* knockdown strains (#2, #7, #15) with or without addition of 7.5mM arginine (+/- Arg). Cell density was measured as described in Figure 1B at the indicated time points after induction of the inducible amiRNA targeting *HSP70B*. Errors bars indicate standard errors between control and mutant strains (+/- arginine), respectively.

C: *HSP70B* protein levels in arginine supplied cells: Total protein was extracted from a control and two inducible *HSP70B* knockdown strains (#2, #15). The cells were supplied with either no amino acids (-), 7.5mM of arginine (Arg) or 7.5mM each of 7 other amino acids (AA: Ile, Leu, Lys, Met, Pro, Thr, Val) and analyzed as already described in Figure 2A. Amounts of *HSP70B* and *VIPP2* relative to loading control *CF1β* were analyzed by immunoblotting.

D: Transcripts of *HSP70B* dependently regulated genes: RNA was extracted and analyzed as already described in Figure 2B. The log₂ fold change of transcripts (log₂) of *VIPP1*, *VIPP2*, *HSP22F* and *ARG7* to the 24-hours enduring exchange of ammonium with nitrate in presence or absence of arginine was analyzed.

Supplemental Figure 1

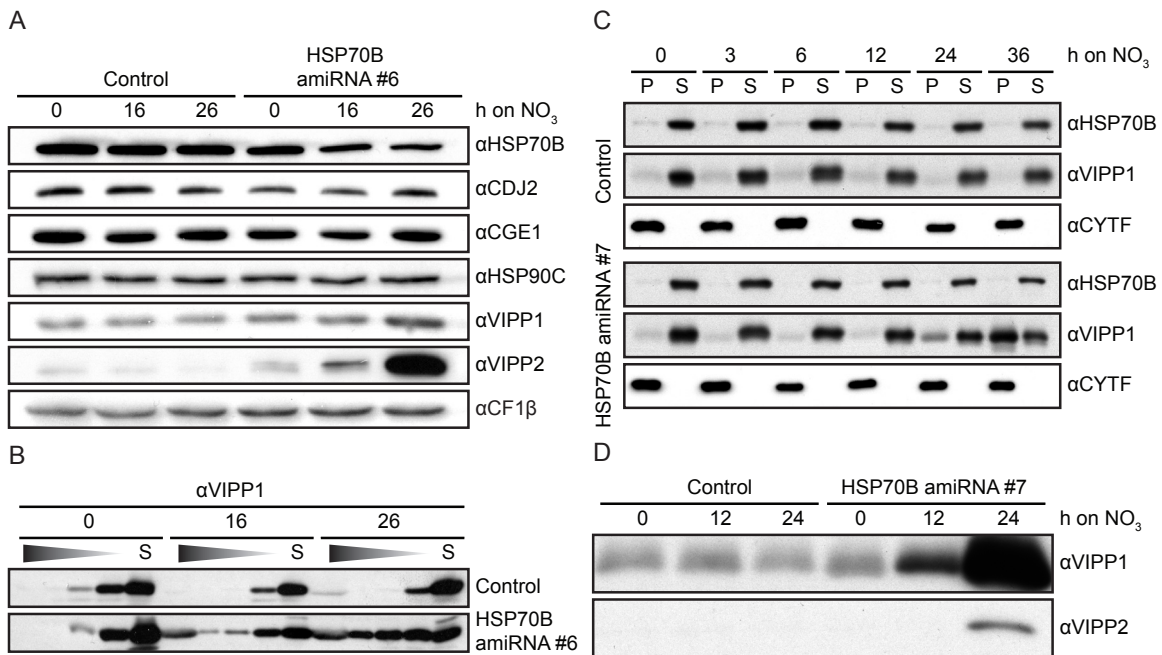
**Figure S1: Phenotypes of all *HSP70B* underexpressing strains used in this study**

A: Growth analysis, protein levels and cell size distribution of all seven *HSP70B* underexpressing strains used within this study: Control and *HSP70B* amiRNA strains were grown either in ammonium-containing (NH₄) or nitrate-containing media (NO₃). Cells were inoculated at 2x10⁴ cells/ml and grown for 3 days in the respective media. Total protein was extracted from control and *HSP70B* amiRNA strains grown either on TAP-NH₄ or TAP-NO₃. Protein was loaded corresponding to 0.5µg chlorophyll and subsequently separated on a 10% SDS-polyacrylamide gel. Amounts of *HSP70B* relative to loading control CF1β were analyzed by immunoblotting. Cell size distribution was analyzed for the different strains either on TAP-NH₄ or TAP-NO₃ using a Coulter-Counter Z2 (Beckman-Coulter). The distribution is illustrated with boxplots. From bottom to top plotted lines correspond to the 10th, 25th (Q₁), 50th (median), 75th (Q₃), and 90th percentiles.

B: Cell size distribution 16 h after the switch to inducing conditions: The number of cells (% of max) with a given cell diameter (µm) is plotted against the cell diameter 16 hours after the exchange of the nitrogen source in one control and three independent, inducible *HSP70B* amiRNA strains (grey square (#2), triangle (#7), cross (#15)). Cell size distribution was measured using a Coulter-Counter Z2 (Beckman-Coulter).

C: Cell size distribution in control strains upon shift to nitrate: Cell size distribution upon switch to TAP-NO₃ is compared in one control strain at different time points after the exchange of the nitrogen source (black circle (0 h), diamonds (16 h), square (24 h), triangle (48)).

Supplemental Figure 2

**Figure S2: Influence of *HSP70B* depletion on target proteins**

A: Total protein of co-chaperones and targets in an additional independent mutant strain: Total protein was extracted from one control and one inducible *HSP70B* knockdown strain #6 before and after switching the nitrogen source to induce the amiRNA. Protein was loaded corresponding to 2 μ g chlorophyll for CDJ2, VIPP2, CGE1, HSP90C and 0.5 μ g chlorophyll for HSP70B, VIPP1 and CF1 α and separated on 10% SDS-polyacrylamide gels. Amounts of HSP70B, CGE1, CDJ2, VIPP1/2 and HSP90C relative to loading control CF1 β were analyzed by immunoblotting.

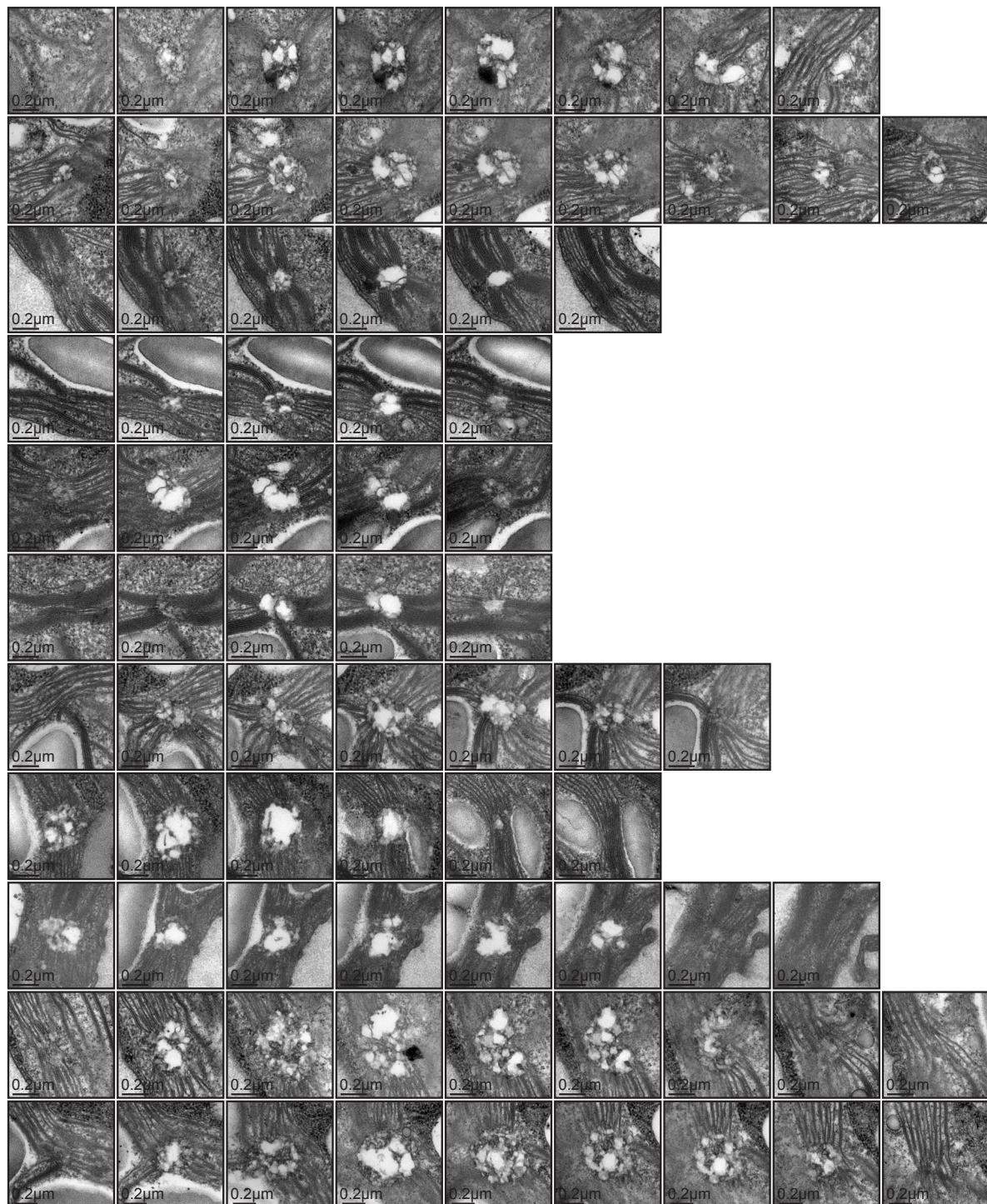
B: Analysis of VIPP1 high molecular weight complexes in an additional mutant strain: A control (empty vector) and inducible *HSP70B* knockdown strain #6 were solubilized with 2% Triton X-100 before and after switching the nitrogen source to induce the amiRNA. Lysates were loaded onto 10-30% sucrose gradients and centrifuged for 2h at 79000g. Fractions were separated on a 10% SDS-polyacrylamide gel and the amounts of VIPP1 were analyzed with immunoblotting.

C: Analysis of distribution between soluble and insoluble VIPP1: Total protein was extracted from control (empty vector) and inducible *HSP70B* knockdown strain #7 before and after switching the nitrogen source to induce the amiRNA. A 35-min centrifugation at 16.100 g separated proteins into a soluble (S) and pellet (P) fraction. Pelleted proteins were resuspended in equal amount of lysis buffer to soluble proteins to allow for quantitative comparison. Proteins were separated on a 10% SDS-polyacrylamide gel and the amounts of HSP70B and VIPP1 were analyzed with immunoblotting. The integral membrane protein CYTF was used as a control to ensure purity of the soluble fraction.

D: Amount of triton-insoluble protein complexes: Total protein was extracted from a control and an inducible *HSP70B* knockdown strain (#7) at different time points after exchanging the nitrogen source in the presence of 2% triton. A 1-hour centrifugation at 435.000 g separated proteins into a soluble and pellet fraction. The solubilized pellet was separated on a 10% SDS-polyacrylamide gels and the amounts of VIPP1/2 were analyzed by immunoblotting.

Supplemental Figure 3

A

**Figure S3: Disordered thylakoid centers**

A: Structures at origins of thylakoid membranes: Additional serial sections of aberrant structures at the origin of thylakoid membranes in *HSP70B* underexpressing strain #7 48 hours after switching to nitrate to induce expression of the amiRNA.

Supplemental Figure 4

A

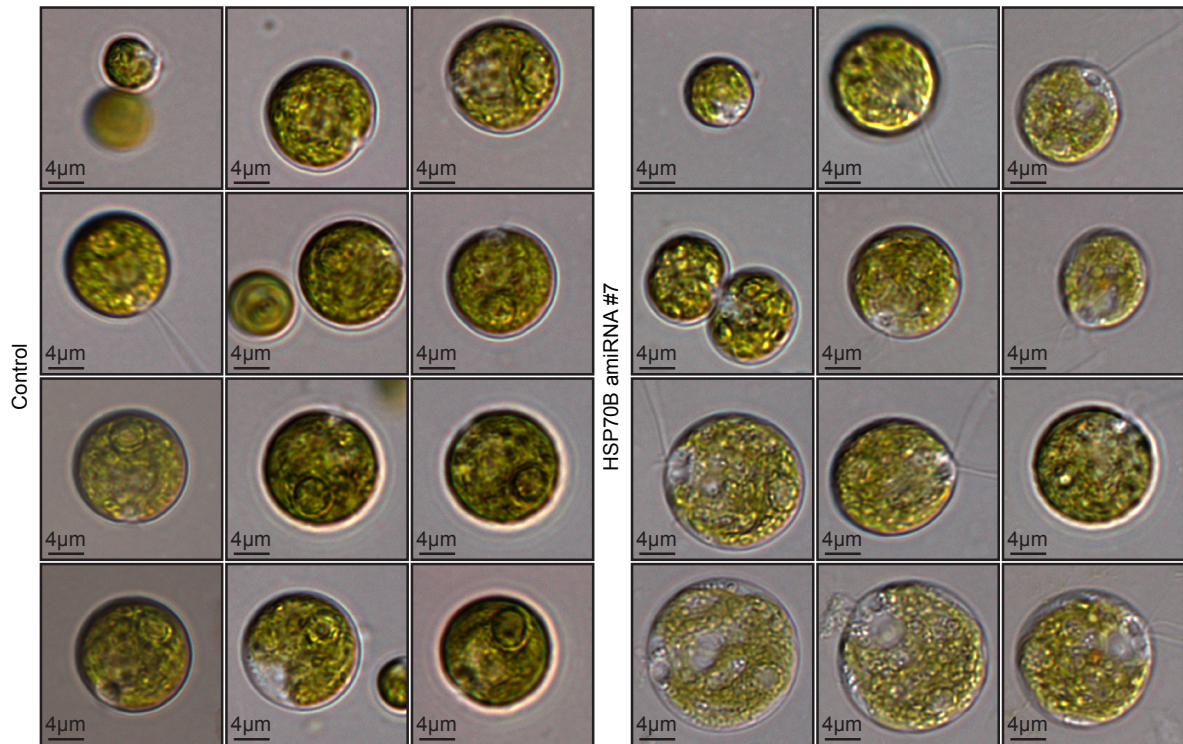
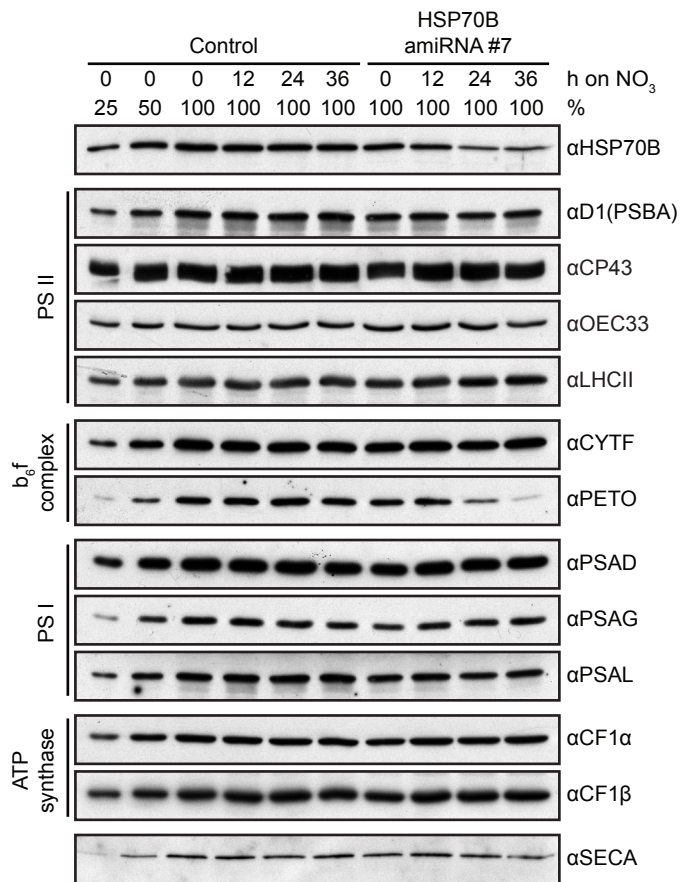


Figure S4: Light microscopy images of HSP70B underexpressing strains

A: Whole cell images: Nomarski images of a control and HSP70B amiRNA strain #7 25 hours after the switch to TAP-NO₃ at 100x magnification.

Supplemental Figure 5

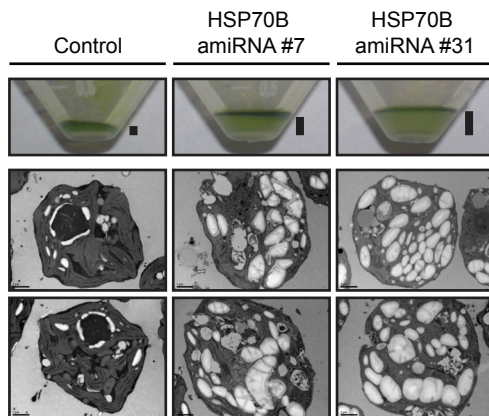
A

**Figure S5: Influence of *HSP70B* depletion on photosynthesis**

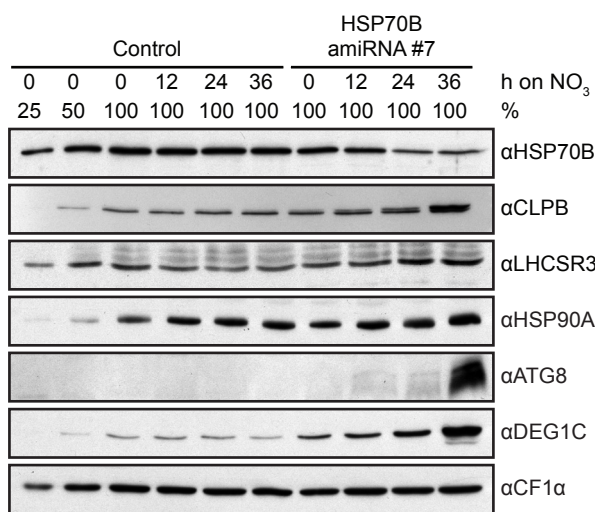
A: Effect of *HSP70B* depletion on proteins involved in photosynthesis: Total protein was extracted from one control and one inducible *HSP70B* knockdown strain #7 before and after switching the nitrogen source to induce the amiRNA. Protein was loaded corresponding to 2µg chlorophyll for CP43, OEC33, PSAG, PSAL and SECA and 0.5µg chlorophyll for PSBA, LHCII, CYTF, PETO, PSAD, CF1α and CF1β. Proteins were separated on 10% SDS-polyacrylamide gels and amounts of PSBA, CP43, OEC33, LHCII (components of photosystem II (PSII)), CYTF, PETO (part of b₆f complex), PSAD, PSAG, PSAL (components of photosystem I (PSI)), CF1α, CF1β (components of the ATPase) and SECA (involved in integration) were analyzed by immunoblotting.

Supplemental Figure 6

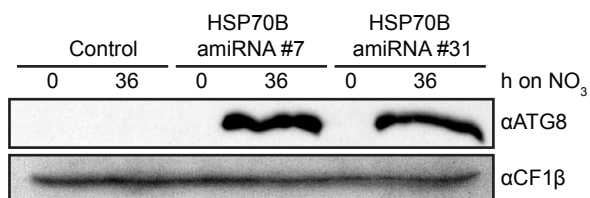
A



B



C

**Figure S6: Stress-related pathways**

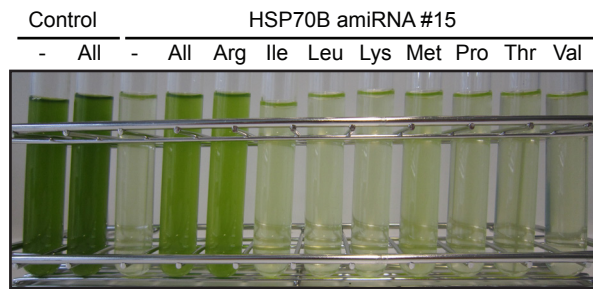
A: Accumulation of starch: Pellet after cell lysis of 1×10^9 *Chlamydomonas* cells from one control and two inducible *HSP70B* knockdown strains (#7, #31) 48 hours after induction of the amiRNA. Black lines indicate the height of the starch pellet. Below, additional representative electron microscopy images of cells from control and inducible *HSP70B* knockdown strains (#7, #15) are shown.

B: Time course analysis of stress related proteins: Total protein was extracted and analyzed as described in Figure 2A on 10% SDS-polyacrylamide gels except for ATG8 which was analyzed on a 15% SDS-polyacrylamide gel. Amounts of CLPB, LHCSR3, HSP90A, ATG8 and DEG1C relative to loading control CF1α were analyzed by immunoblotting.

C: ATG8 protein levels: Total protein was extracted from one control (empty vector) and inducible *HSP70B* knockdown strain #7/#31 before and after switching the nitrogen source to induce the amiRNA. Protein was loaded corresponding to $2 \mu\text{g}$ chlorophyll and separated on 10% SDS-polyacrylamide gels. Amounts of ATG8 relative to loading control CF1β were analyzed by immunoblotting.

Supplemental Figure 7

A

**Figure S7: Amino acids**

A: Growth analysis: Control and inducible *HSP70B* amiRNA strains #15) were grown for 5 days on nitrate-containing media with 7.5 mM arginine (Arg), isoleucine (Ile), leucine (Leu), lysine (Lys), methionine (Met), proline (Pro), threonine (Thr), valine (Val), no additional amino acid (-) or all amino acids together (All).

4. REFERENCES

1. **Harris, E.H.** *The Chlamydomonas sourcebook (Second edition)*, (Elsevier, Amsterdam [u.a.], 2008).
2. **Herrin, D.L. & Nickelsen, J.** Chloroplast RNA processing and stability. *Photosynthesis research* **82**, 301-314 (2004).
3. **Eberhard, S., Finazzi, G. & Wollman, F.A.** The dynamics of photosynthesis. *Annual review of genetics* **42**, 463-515 (2008).
4. **Snell, W.J., Pan, J. & Wang, Q.** Cilia and flagella revealed: from flagellar assembly in Chlamydomonas to human obesity disorders. *Cell* **117**, 693-697 (2004).
5. **Nagel, G., et al.** Channelrhodopsins: directly light-gated cation channels. *Biochemical Society transactions* **33**, 863-866 (2005).
6. **Yizhar, O., Fenno, Lief E., Davidson, Thomas J., Mogri, M. & Deisseroth, K.** Optogenetics in Neural Systems. *Neuron* **71**, 9-34 (2011).
7. **Akerfelt, M., Trouillet, D., Mezger, V. & Sistonen, L.** Heat shock factors at a crossroad between stress and development. *Annals of the New York Academy of Sciences* **1113**, 15-27 (2007).
8. **Morimoto, R.I.** Regulation of the heat shock transcriptional response: cross talk between a family of heat shock factors, molecular chaperones, and negative regulators. *Genes & development* **12**, 3788-3796 (1998).
9. **Ritossa, F.** A new puffing pattern induced by temperature shock and DNP in drosophila. *Cellular and Molecular Life Sciences* **18**, 571-573 (1962).
10. **Westerheide, S.D. & Morimoto, R.I.** Heat shock response modulators as therapeutic tools for diseases of protein conformation. *The Journal of biological chemistry* **280**, 33097-33100 (2005).
11. **Bukau, B., Weissman, J. & Horwich, A.** Molecular chaperones and protein quality control. *Cell* **125**, 443-451 (2006).
12. **Hartl, F.U., Bracher, A. & Hayer-Hartl, M.** Molecular chaperones in protein folding and proteostasis. *Nature* **475**, 324-332 (2011).
13. **Bukau, B. & Horwich, A.L.** The Hsp70 and Hsp60 chaperone machines. *Cell* **92**, 351-366 (1998).
14. **Hartl, F.U. & Hayer-Hartl, M.** Molecular chaperones in the cytosol: from nascent chain to folded protein. *Science (New York, N.Y)* **295**, 1852-1858 (2002).
15. **Hartl, F.U. & Hayer-Hartl, M.** Converging concepts of protein folding in vitro and in vivo. *Nature structural & molecular biology* **16**, 574-581 (2009).
16. **Kramer, G., Boehringer, D., Ban, N. & Bukau, B.** The ribosome as a platform for co-translational processing, folding and targeting of newly synthesized proteins. *Nature structural & molecular biology* **16**, 589-597 (2009).
17. **Sorger, P.K. & Pelham, H.R.** Purification and characterization of a heat-shock element binding protein from yeast. *The EMBO journal* **6**, 3035-3041 (1987).
18. **Sorger, P.K. & Pelham, H.R.** Yeast heat shock factor is an essential DNA-binding protein that exhibits temperature-dependent phosphorylation. *Cell* **54**, 855-864 (1988).
19. **Akerfelt, M., Morimoto, R.I. & Sistonen, L.** Heat shock factors: integrators of cell stress, development and lifespan. *Nature reviews* **11**, 545-555 (2010).
20. **Fujimoto, M. & Nakai, A.** The heat shock factor family and adaptation to proteotoxic stress. *The FEBS journal* **277**, 4112-4125 (2010).
21. **Harrison, C.J., Bohm, A.A. & Nelson, H.C.** Crystal structure of the DNA binding domain of the heat shock transcription factor. *Science (New York, N.Y)* **263**, 224-227 (1994).
22. **Littlefield, O. & Nelson, H.C.** A new use for the 'wing' of the 'winged' helix-turn-helix motif in the HSF-DNA cocystal. *Nat Struct Biol* **6**, 464-470 (1999).
23. **Nover, L., et al.** The Hsf world: classification and properties of plant heat stress transcription

- factors. *Cell stress & chaperones* **1**, 215-223 (1996).
24. **Schulz-Raffelt, M., Lodha, M. & Schroda, M.** Heat shock factor 1 is a key regulator of the stress response in *Chlamydomonas*. *Plant J* **52**, 286-295 (2007).
 25. **Sorger, P.K. & Nelson, H.C.** Trimerization of a yeast transcriptional activator via a coiled-coil motif. *Cell* **59**, 807-813 (1989).
 26. **Landschulz, W.H., Johnson, P.F. & McKnight, S.L.** The leucine zipper: a hypothetical structure common to a new class of DNA binding proteins. *Science (New York, N.Y)* **240**, 1759-1764 (1988).
 27. **Peteranderl, R. & Nelson, H.C.** Trimerization of the heat shock transcription factor by a triple-stranded alpha-helical coiled-coil. *Biochemistry* **31**, 12272-12276 (1992).
 28. **Treuter, E., Nover, L., Ohme, K. & Scharf, K.D.** Promoter specificity and deletion analysis of three heat stress transcription factors of tomato. *Mol Gen Genet* **240**, 113-125 (1993).
 29. **Doring, P., et al.** The role of AHA motifs in the activator function of tomato heat stress transcription factors HsfA1 and HsfA2. *The Plant cell* **12**, 265-278 (2000).
 30. **Fiorenza, M.T., Farkas, T., Dissing, M., Kolding, D. & Zimarino, V.** Complex expression of murine heat shock transcription factors. *Nucleic acids research* **23**, 467-474 (1995).
 31. **Ostling, P., Bjork, J.K., Roos-Mattjus, P., Mezger, V. & Sistonen, L.** Heat shock factor 2 (HSF2) contributes to inducible expression of hsp genes through interplay with HSF1. *The Journal of biological chemistry* **282**, 7077-7086 (2007).
 32. **Lin, Y.X., et al.** Genome-wide identification, classification and analysis of heat shock transcription factor family in maize. *BMC genomics* **12**, 76 (2011).
 33. **Guo, J., et al.** Genome-wide analysis of heat shock transcription factor families in rice and Arabidopsis. *Journal of genetics and genomics = Yi chuan xue bao* **35**, 105-118 (2008).
 34. **Nover, L., et al.** Arabidopsis and the heat stress transcription factor world: how many heat stress transcription factors do we need? *Cell stress & chaperones* **6**, 177-189 (2001).
 35. **Prandl, R., Hinderhofer, K., Eggers-Schumacher, G. & Schoffl, F.** HSF3, a new heat shock factor from Arabidopsis thaliana, derepresses the heat shock response and confers thermotolerance when overexpressed in transgenic plants. *Mol Gen Genet* **258**, 269-278 (1998).
 36. **Lee, J.H., Hubel, A. & Schoffl, F.** Derepression of the activity of genetically engineered heat shock factor causes constitutive synthesis of heat shock proteins and increased thermotolerance in transgenic Arabidopsis. *Plant J* **8**, 603-612 (1995).
 37. **Bharti, K., et al.** Tomato heat stress transcription factor HsfB1 represents a novel type of general transcription coactivator with a histone-like motif interacting with the plant CREB binding protein ortholog HAC1. *The Plant cell* **16**, 1521-1535 (2004).
 38. **Czarnecka-Verner, E., Yuan, C.X., Scharf, K.D., Englich, G. & Gurley, W.B.** Plants contain a novel multi-member class of heat shock factors without transcriptional activator potential. *Plant molecular biology* **43**, 459-471 (2000).
 39. **Chan-Schaminet, K.Y., Baniwal, S.K., Bublak, D., Nover, L. & Scharf, K.D.** Specific interaction between tomato HsfA1 and HsfA2 creates hetero-oligomeric superactivator complexes for synergistic activation of heat stress gene expression. *The Journal of biological chemistry* **284**, 20848-20857 (2009).
 40. **Scharf, K.D., et al.** The tomato Hsf system: HsfA2 needs interaction with HsfA1 for efficient nuclear import and may be localized in cytoplasmic heat stress granules. *Molecular and cellular biology* **18**, 2240-2251 (1998).
 41. **von Koskull-Doring, P., Scharf, K.D. & Nover, L.** The diversity of plant heat stress transcription factors. *Trends in plant science* **12**, 452-457 (2007).
 42. **Rabindran, S.K., Haroun, R.I., Clos, J., Wisniewski, J. & Wu, C.** Regulation of heat shock factor trimer formation: role of a conserved leucine zipper. *Science (New York, N.Y)* **259**, 230-234 (1993).
 43. **Westwood, J.T. & Wu, C.** Activation of Drosophila heat shock factor: conformational change

- associated with a monomer-to-trimer transition. *Molecular and cellular biology* **13**, 3481-3486 (1993).
44. **Ali, A., Bharadwaj, S., O'Carroll, R. & Ovsenek, N.** HSP90 interacts with and regulates the activity of heat shock factor 1 in *Xenopus* oocytes. *Molecular and cellular biology* **18**, 4949-4960 (1998).
 45. **Zou, J.Y., Guo, Y.L., Guettouche, T., Smith, D.F. & Voellmy, R.** Repression of heat shock transcription factor HSF1 activation by HSP90 (HSP90 complex) that forms a stress-sensitive complex with HSF1. *Cell* **94**, 471-480 (1998).
 46. **Bharadwaj, S., Ali, A. & Ovsenek, N.** Multiple components of the HSP90 chaperone complex function in regulation of heat shock factor 1 In vivo. *Molecular and cellular biology* **19**, 8033-8041 (1999).
 47. **Shi, Y., Mosser, D.D. & Morimoto, R.I.** Molecular chaperones as HSF1-specific transcriptional repressors. *Genes & development* **12**, 654-666 (1998).
 48. **Guettouche, T., Boellmann, F., Lane, W.S. & Voellmy, R.** Analysis of phosphorylation of human heat shock factor 1 in cells experiencing a stress. *BMC biochemistry* **6**, 4 (2005).
 49. **Holmberg, C.I., et al.** Phosphorylation of serine 230 promotes inducible transcriptional activity of heat shock factor 1. *The EMBO journal* **20**, 3800-3810 (2001).
 50. **Knauf, U., Newton, E.M., Kyriakis, J. & Kingston, R.E.** Repression of human heat shock factor 1 activity at control temperature by phosphorylation. *Genes & development* **10**, 2782-2793 (1996).
 51. **Hietakangas, V., et al.** PDSM, a motif for phosphorylation-dependent SUMO modification. *Proceedings of the National Academy of Sciences of the United States of America* **103**, 45-50 (2006).
 52. **Westerheide, S.D., Anckar, J., Stevens, S.M., Jr., Sistonen, L. & Morimoto, R.I.** Stress-inducible regulation of heat shock factor 1 by the deacetylase SIRT1. *Science (New York, N.Y)* **323**, 1063-1066 (2009).
 53. **Cotto, J., Fox, S. & Morimoto, R.** HSF1 granules: a novel stress-induced nuclear compartment of human cells. *Journal of cell science* **110** (Pt 23), 2925-2934 (1997).
 54. **Xiao, H. & Lis, J.T.** Germline transformation used to define key features of heat-shock response elements. *Science (New York, N.Y)* **239**, 1139-1142 (1988).
 55. **Amin, J., Ananthan, J. & Voellmy, R.** Key features of heat shock regulatory elements. *Molecular and cellular biology* **8**, 3761-3769 (1988).
 56. **Pelham, H.R.** A regulatory upstream promoter element in the *Drosophila* hsp 70 heat-shock gene. *Cell* **30**, 517-528 (1982).
 57. **He, Z., Eichel, K. & Ruvinsky, I.** Functional conservation of cis-regulatory elements of heat-shock genes over long evolutionary distances. *PloS one* **6**, e22677 (2011).
 58. **Yamamoto, A., Mizukami, Y. & Sakurai, H.** Identification of a novel class of target genes and a novel type of binding sequence of heat shock transcription factor in *Saccharomyces cerevisiae*. *The Journal of biological chemistry* **280**, 11911-11919 (2005).
 59. **Tamai, K.T., Liu, X., Silar, P., Sosinowski, T. & Thiele, D.J.** Heat shock transcription factor activates yeast metallothionein gene expression in response to heat and glucose starvation via distinct signalling pathways. *Molecular and cellular biology* **14**, 8155-8165 (1994).
 60. **Santoro, N., Johansson, N. & Thiele, D.J.** Heat shock element architecture is an important determinant in the temperature and transactivation domain requirements for heat shock transcription factor. *Molecular and cellular biology* **18**, 6340-6352 (1998).
 61. **Ernst, P. & Smale, S.T.** Combinatorial regulation of transcription. I: General aspects of transcriptional control. *Immunity* **2**, 311-319 (1995).
 62. **Britten, R.J. & Davidson, E.H.** Gene regulation for higher cells: a theory. *Science (New York, N.Y)* **165**, 349-357 (1969).
 63. **Xiao, H., Perisic, O. & Lis, J.T.** Cooperative binding of *Drosophila* heat shock factor to

- arrays of a conserved 5 bp unit. *Cell* **64**, 585-593 (1991).
64. **Bonner, J.J., Ballou, C. & Fackenthal, D.L.** Interactions between DNA-bound trimers of the yeast heat shock factor. *Molecular and cellular biology* **14**, 501-508 (1994).
 65. **Trinklein, N.D., Murray, J.I., Hartman, S.J., Botstein, D. & Myers, R.M.** The role of heat shock transcription factor 1 in the genome-wide regulation of the mammalian heat shock response. *Molecular biology of the cell* **15**, 1254-1261 (2004).
 66. **Hahn, J.S., Hu, Z., Thiele, D.J. & Iyer, V.R.** Genome-wide analysis of the biology of stress responses through heat shock transcription factor. *Molecular and cellular biology* **24**, 5249-5256 (2004).
 67. **Guertin, M.J. & Lis, J.T.** Chromatin landscape dictates HSF binding to target DNA elements. *PLoS genetics* **6**(2010).
 68. **Busch, W., Wunderlich, M. & Schoffl, F.** Identification of novel heat shock factor-dependent genes and biochemical pathways in *Arabidopsis thaliana*. *Plant J* **41**, 1-14 (2005).
 69. **Birch-Machin, I., et al.** Genomic analysis of heat-shock factor targets in *Drosophila*. *Genome biology* **6**, R63 (2005).
 70. **Taji, T., et al.** Important roles of drought- and cold-inducible genes for galactinol synthase in stress tolerance in *Arabidopsis thaliana*. *Plant J* **29**, 417-426 (2002).
 71. **Schramm, F., et al.** The heat stress transcription factor HsfA2 serves as a regulatory amplifier of a subset of genes in the heat stress response in *Arabidopsis*. *Plant molecular biology* **60**, 759-772 (2006).
 72. **Panchuk, II, Volkov, R.A. & Schoffl, F.** Heat stress- and heat shock transcription factor-dependent expression and activity of ascorbate peroxidase in *Arabidopsis*. *Plant physiology* **129**, 838-853 (2002).
 73. **Kumar, M., et al.** Heat shock factors HsfB1 and HsfB2b are involved in the regulation of Pdf1.2 expression and pathogen resistance in *Arabidopsis*. *Mol Plant* **2**, 152-165 (2009).
 74. **Sharma, S.K., Christen, P. & Goloubinoff, P.** Disaggregating chaperones: an unfolding story. *Current protein & peptide science* **10**, 432-446 (2009).
 75. **Sousa, R. & Lafer, E.M.** Keep the traffic moving: mechanism of the Hsp70 motor. *Traffic* **7**, 1596-1603 (2006).
 76. **Zhu, X., et al.** Structural analysis of substrate binding by the molecular chaperone DnaK. *Science (New York, N.Y)* **272**, 1606-1614 (1996).
 77. **Szabo, A., et al.** The ATP hydrolysis-dependent reaction cycle of the *Escherichia coli* Hsp70 system DnaK, DnaJ, and GrpE. *Proceedings of the National Academy of Sciences of the United States of America* **91**, 10345-10349 (1994).
 78. **Greene, M.K., Maskos, K. & Landry, S.J.** Role of the J-domain in the cooperation of Hsp40 with Hsp70. *Proceedings of the National Academy of Sciences of the United States of America* **95**, 6108-6113 (1998).
 79. **Craig, E.A., Huang, P., Aron, R. & Andrew, A.** The diverse roles of J-proteins, the obligate Hsp70 co-chaperone. *Reviews of physiology, biochemistry and pharmacology* **156**, 1-21 (2006).
 80. **Kampinga, H.H. & Craig, E.A.** The HSP70 chaperone machinery: J proteins as drivers of functional specificity. *Nature reviews* **11**, 579-592 (2010).
 81. **Jiang, J., et al.** Structural basis of J cochaperone binding and regulation of Hsp70. *Molecular cell* **28**, 422-433 (2007).
 82. **McCarty, J.S., Buchberger, A., Reinstein, J. & Bukau, B.** The role of ATP in the functional cycle of the DnaK chaperone system. *J Mol Biol* **249**, 126-137 (1995).
 83. **Harrison, C.** GrpE, a nucleotide exchange factor for DnaK. *Cell stress & chaperones* **8**, 218-224 (2003).
 84. **Rampelt, H., Mayer, M.P. & Bukau, B.** Nucleotide exchange factors for Hsp70 chaperones. *Methods Mol Biol* **787**, 83-91 (2011).
 85. **Sharma, S.K., De los Rios, P., Christen, P., Lustig, A. & Goloubinoff, P.** The kinetic

- parameters and energy cost of the Hsp70 chaperone as a polypeptide unfoldase. *Nat Chem Biol* **6**, 914-920 (2010).
86. Rudiger, S., Germeroth, L., Schneider-Mergener, J. & Bukau, B. Substrate specificity of the DnaK chaperone determined by screening cellulose-bound peptide libraries. *The EMBO journal* **16**, 1501-1507 (1997).
 87. Schroda, M. The Chlamydomonas genome reveals its secrets: chaperone genes and the potential roles of their gene products in the chloroplast. *Photosynthesis research* **82**, 221-240 (2004).
 88. Nordhues, A., Miller, S.M., Muhlhaus, T. & Schroda, M. New insights into the roles of molecular chaperones in Chlamydomonas and Volvox. *Int Rev Cell Mol Biol* **285**, 75-113 (2010).
 89. Drzymalla, C., Schroda, M. & Beck, C.F. Light-inducible gene HSP70B encodes a chloroplast-localized heat shock protein in Chlamydomonas reinhardtii. *Plant molecular biology* **31**, 1185-1194 (1996).
 90. Nordhues, A., *et al.* Evidence for a Role of VIPP1 in the Structural Organization of the Photosynthetic Apparatus in Chlamydomonas. *The Plant cell* (2012).
 91. Schroda, M., Vallon, O., Wollman, F.A. & Beck, C.F. A chloroplast-targeted heat shock protein 70 (HSP70) contributes to the photoprotection and repair of photosystem II during and after photoinhibition. *The Plant cell* **11**, 1165-1178 (1999).
 92. Su, P.H. & Li, H.M. Stromal Hsp70 is important for protein translocation into pea and Arabidopsis chloroplasts. *The Plant cell* **22**, 1516-1531 (2010).
 93. Shi, L.X. & Theg, S.M. A stromal heat shock protein 70 system functions in protein import into chloroplasts in the moss Physcomitrella patens. *The Plant cell* **22**, 205-220 (2010).
 94. Willmund, F., Muhlhaus, T., Wojciechowska, M. & Schroda, M. The NH₂-terminal domain of the chloroplast GrpE homolog CGE1 is required for dimerization and cochaperone function in vivo. *The Journal of biological chemistry* **282**, 11317-11328 (2007).
 95. Schroda, M., Vallon, O., Whitelegge, J.P., Beck, C.F. & Wollman, F.A. The chloroplastic GrpE homolog of Chlamydomonas: two isoforms generated by differential splicing. *The Plant cell* **13**, 2823-2839 (2001).
 96. Liu, C., *et al.* J-domain protein CDJ2 and HSP70B are a plastidic chaperone pair that interacts with vesicle-inducing protein in plastids 1. *Molecular biology of the cell* **16**, 1165-1177 (2005).
 97. Dorn, K.V., *et al.* Chloroplast DnaJ-like proteins 3 and 4 (CDJ3/4) from Chlamydomonas reinhardtii contain redox-active Fe-S clusters and interact with stromal HSP70B. *The Biochemical journal* **427**, 205-215 (2010).
 98. Willmund, F., Dorn, K.V., Schulz-Raffelt, M. & Schroda, M. The chloroplast DnaJ homolog CDJ1 of Chlamydomonas reinhardtii is part of a multichaperone complex containing HSP70B, CGE1, and HSP90C. *Plant physiology* **148**, 2070-2082 (2008).
 99. Cheetham, M.E. & Caplan, A.J. Structure, function and evolution of DnaJ: conservation and adaptation of chaperone function. *Cell stress & chaperones* **3**, 28-36 (1998).
 100. Liu, C., *et al.* The chloroplast HSP70B-CDJ2-CGE1 chaperones catalyse assembly and disassembly of VIPP1 oligomers in Chlamydomonas. *Plant J* **50**, 265-277 (2007).
 101. Willmund, F., *et al.* Assistance for a chaperone: Chlamydomonas HEP2 activates plastidic HSP70B for cochaperone binding. *The Journal of biological chemistry* **283**, 16363-16373 (2008).
 102. Sichting, M., Mokranjac, D., Azem, A., Neupert, W. & Hell, K. Maintenance of structure and function of mitochondrial Hsp70 chaperones requires the chaperone Hep1. *The EMBO journal* **24**, 1046-1056 (2005).
 103. Blamowska, M., *et al.* ATPase domain and interdomain linker play a key role in aggregation of mitochondrial Hsp70 chaperone Ssc1. *The Journal of biological chemistry* **285**, 4423-4431 (2010).

104. **Heide, H., et al.** Application of quantitative immunoprecipitation combined with knock-down and cross-linking to *Chlamydomonas* reveals the presence of vesicle-inducing protein in plastids 1 in a common complex with chloroplast HSP90C. *Proteomics* **9**, 3079-3089 (2009).
105. **Willmund, F. & Schroda, M.** HEAT SHOCK PROTEIN 90C is a bona fide Hsp90 that interacts with plastidic HSP70B in *Chlamydomonas reinhardtii*. *Plant physiology* **138**, 2310-2322 (2005).
106. **Pratt, W.B. & Toft, D.O.** Regulation of signaling protein function and trafficking by the hsp90/hsp70-based chaperone machinery. *Exp Biol Med (Maywood)* **228**, 111-133 (2003).
107. **Merchant, S.S., et al.** The *Chlamydomonas* genome reveals the evolution of key animal and plant functions. *Science (New York, N.Y)* **318**, 245-250 (2007).
108. **Maul, J.E., et al.** The *Chlamydomonas reinhardtii* plastid chromosome: islands of genes in a sea of repeats. *The Plant cell* **14**, 2659-2679 (2002).
109. **Vahrenholz, C., Riemen, G., Pratje, E., Dujon, B. & Michaelis, G.** Mitochondrial DNA of *Chlamydomonas reinhardtii*: the structure of the ends of the linear 15.8-kb genome suggests mechanisms for DNA replication. *Current genetics* **24**, 241-247 (1993).
110. **Debuchy, R., Purton, S. & Rochaix, J.D.** The argininosuccinate lyase gene of *Chlamydomonas reinhardtii*: an important tool for nuclear transformation and for correlating the genetic and molecular maps of the ARG7 locus. *The EMBO journal* **8**, 2803-2809 (1989).
111. **Kindle, K.L., Schnell, R.A., Fernandez, E. & Lefebvre, P.A.** Stable nuclear transformation of *Chlamydomonas* using the *Chlamydomonas* gene for nitrate reductase. *The Journal of cell biology* **109**, 2589-2601 (1989).
112. **Randolph-Anderson, B.L., et al.** Further characterization of the respiratory deficient dum-1 mutation of *Chlamydomonas reinhardtii* and its use as a recipient for mitochondrial transformation. *Mol Gen Genet* **236**, 235-244 (1993).
113. **Kindle, K.L.** High-frequency nuclear transformation of *Chlamydomonas reinhardtii*. *Proceedings of the National Academy of Sciences of the United States of America* **87**, 1228-1232 (1990).
114. **Kindle, K.L., Richards, K.L. & Stern, D.B.** Engineering the chloroplast genome: techniques and capabilities for chloroplast transformation in *Chlamydomonas reinhardtii*. *Proceedings of the National Academy of Sciences of the United States of America* **88**, 1721-1725 (1991).
115. **Shimogawara, K., Fujiwara, S., Grossman, A. & Usuda, H.** High-efficiency transformation of *Chlamydomonas reinhardtii* by electroporation. *Genetics* **148**, 1821-1828 (1998).
116. **Karpowicz, S.J., Prochnik, S.E., Grossman, A.R. & Merchant, S.S.** The GreenCutz resource, a phylogenomically derived inventory of proteins specific to the plant lineage. *The Journal of biological chemistry* **286**, 21427-21439 (2011).
117. **Gonzalez-Ballester, D., et al.** Reverse genetics in *Chlamydomonas*: a platform for isolating insertional mutants. *Plant Methods* **7**, 24 (2011).
118. **Molnar, A., et al.** Highly specific gene silencing by artificial microRNAs in the unicellular alga *Chlamydomonas reinhardtii*. *Plant J* (2009).
119. **Hardy, S., Legagneux, V., Audic, Y. & Paillard, L.** Reverse genetics in eukaryotes. *Biology of the cell / under the auspices of the European Cell Biology Organization* **102**, 561-580 (2010).
120. **San Filippo, J., Sung, P. & Klein, H.** Mechanism of eukaryotic homologous recombination. *Annual review of biochemistry* **77**, 229-257 (2008).
121. **Hinnen, A., Hicks, J.B. & Fink, G.R.** Transformation of yeast. *Proceedings of the National Academy of Sciences of the United States of America* **75**, 1929-1933 (1978).
122. **Huh, W.K., et al.** Global analysis of protein localization in budding yeast. *Nature* **425**, 686-691 (2003).
123. **Christie, K.R., Hong, E.L. & Cherry, J.M.** Functional annotations for the *Saccharomyces*

- cerevisiae genome: the knowns and the known unknowns. *Trends in microbiology* **17**, 286-294 (2009).
124. **Day, A. & Goldschmidt-Clermont, M.** The chloroplast transformation toolbox: selectable markers and marker removal. *Plant biotechnology journal* **9**, 540-553 (2011).
125. **Sodeinde, O.A. & Kindle, K.L.** Homologous recombination in the nuclear genome of *Chlamydomonas reinhardtii*. *Proceedings of the National Academy of Sciences of the United States of America* **90**, 9199-9203 (1993).
126. **Zorin, B., Hegemann, P. & Sizova, I.** Nuclear-gene targeting by using single-stranded DNA avoids illegitimate DNA integration in *Chlamydomonas reinhardtii*. *Eukaryotic cell* **4**, 1264-1272 (2005).
127. **Zorin, B., Lu, Y., Sizova, I. & Hegemann, P.** Nuclear gene targeting in *Chlamydomonas* as exemplified by disruption of the PHOT gene. *Gene* **432**, 91-96 (2009).
128. **Alonso, J.M., et al.** Genome-wide insertional mutagenesis of *Arabidopsis thaliana*. *Science (New York, N.Y)* **301**, 653-657 (2003).
129. **Pazour, G.J. & Witman, G.B.** Forward and reverse genetic analysis of microtubule motors in *Chlamydomonas*. *Methods* **22**, 285-298 (2000).
130. **Koornneef, M., Dellaert, L.W. & van der Veen, J.H.** EMS- and radiation-induced mutation frequencies at individual loci in *Arabidopsis thaliana* (L.) Heynh. *Mutation research* **93**, 109-123 (1982).
131. **Comai, L. & Henikoff, S.** TILLING: practical single-nucleotide mutation discovery. *Plant J* **45**, 684-694 (2006).
132. **McCallum, C.M., Comai, L., Greene, E.A. & Henikoff, S.** Targeted screening for induced mutations. *Nature biotechnology* **18**, 455-457 (2000).
133. **Cerutti, H., Ma, X., Msanne, J. & Repas, T.** RNA-mediated silencing in Algae: biological roles and tools for analysis of gene function. *Eukaryotic cell* **10**, 1164-1172 (2011).
134. **Schroda, M.** RNA silencing in *Chlamydomonas*: mechanisms and tools. *Current genetics* **49**, 69-84 (2006).
135. **Liu, Q. & Paroo, Z.** Biochemical principles of small RNA pathways. *Annual review of biochemistry* **79**, 295-319 (2010).
136. **Hamilton, A.J. & Baulcombe, D.C.** A species of small antisense RNA in posttranscriptional gene silencing in plants. *Science (New York, N.Y)* **286**, 950-952 (1999).
137. **Izant, J.G. & Weintraub, H.** Inhibition of thymidine kinase gene expression by anti-sense RNA: a molecular approach to genetic analysis. *Cell* **36**, 1007-1015 (1984).
138. **Hammond, S.M., Boettcher, S., Caudy, A.A., Kobayashi, R. & Hannon, G.J.** Argonaute2, a link between genetic and biochemical analyses of RNAi. *Science (New York, N.Y)* **293**, 1146-1150 (2001).
139. **Fire, A., et al.** Potent and specific genetic interference by double-stranded RNA in *Caenorhabditis elegans*. *Nature* **391**, 806-811 (1998).
140. **Malone, C.D. & Hannon, G.J.** Small RNAs as guardians of the genome. *Cell* **136**, 656-668 (2009).
141. **Ketting, R.F.** The many faces of RNAi. *Developmental cell* **20**, 148-161 (2011).
142. **Mourrain, P., et al.** *Arabidopsis* SGS2 and SGS3 genes are required for posttranscriptional gene silencing and natural virus resistance. *Cell* **101**, 533-542 (2000).
143. **Elbashir, S.M., Lendeckel, W. & Tuschl, T.** RNA interference is mediated by 21- and 22-nucleotide RNAs. *Genes & development* **15**, 188-200 (2001).
144. **Okamura, K. & Lai, E.C.** Endogenous small interfering RNAs in animals. *Nature reviews* **9**, 673-678 (2008).
145. **Bernstein, E., Caudy, A.A., Hammond, S.M. & Hannon, G.J.** Role for a bidentate ribonuclease in the initiation step of RNA interference. *Nature* **409**, 363-366 (2001).
146. **Schwarz, D.S., et al.** Asymmetry in the assembly of the RNAi enzyme complex. *Cell* **115**, 199-208 (2003).

147. **Khvorova, A., Reynolds, A. & Jayasena, S.D.** Functional siRNAs and miRNAs exhibit strand bias. *Cell* **115**, 209-216 (2003).
148. **Lee, R.C., Feinbaum, R.L. & Ambros, V.** The *C. elegans* heterochronic gene *lin-4* encodes small RNAs with antisense complementarity to *lin-14*. *Cell* **75**, 843-854 (1993).
149. **Wightman, B., Ha, I. & Ruvkun, G.** Posttranscriptional regulation of the heterochronic gene *lin-14* by *lin-4* mediates temporal pattern formation in *C. elegans*. *Cell* **75**, 855-862 (1993).
150. **Bartel, D.P.** MicroRNAs: genomics, biogenesis, mechanism, and function. *Cell* **116**, 281-297 (2004).
151. **Lagos-Quintana, M., Rauhut, R., Lendeckel, W. & Tuschl, T.** Identification of novel genes coding for small expressed RNAs. *Science (New York, N.Y)* **294**, 853-858 (2001).
152. **Lau, N.C., Lim, L.P., Weinstein, E.G. & Bartel, D.P.** An abundant class of tiny RNAs with probable regulatory roles in *Caenorhabditis elegans*. *Science (New York, N.Y)* **294**, 858-862 (2001).
153. **Lee, R.C. & Ambros, V.** An extensive class of small RNAs in *Caenorhabditis elegans*. *Science (New York, N.Y)* **294**, 862-864 (2001).
154. **Lee, Y., et al.** The nuclear RNase III Drosha initiates microRNA processing. *Nature* **425**, 415-419 (2003).
155. **Hutvagner, G., et al.** A cellular function for the RNA-interference enzyme Dicer in the maturation of the *let-7* small temporal RNA. *Science (New York, N.Y)* **293**, 834-838 (2001).
156. **Kurihara, Y. & Watanabe, Y.** Arabidopsis micro-RNA biogenesis through Dicer-like 1 protein functions. *Proceedings of the National Academy of Sciences of the United States of America* **101**, 12753-12758 (2004).
157. **Lau, N.C., et al.** Characterization of the piRNA complex from rat testes. *Science (New York, N.Y)* **313**, 363-367 (2006).
158. **Saito, K., et al.** Specific association of Piwi with rasiRNAs derived from retrotransposon and heterochromatic regions in the *Drosophila* genome. *Genes & development* **20**, 2214-2222 (2006).
159. **Aravin, A., et al.** A novel class of small RNAs bind to MILI protein in mouse testes. *Nature* **442**, 203-207 (2006).
160. **Djikeng, A., Shi, H., Tschudi, C. & Ullu, E.** RNA interference in *Trypanosoma brucei*: cloning of small interfering RNAs provides evidence for retroposon-derived 24-26-nucleotide RNAs. *RNA* **7**, 1522-1530 (2001).
161. **Cox, D.N., et al.** A novel class of evolutionarily conserved genes defined by piwi are essential for stem cell self-renewal. *Genes & development* **12**, 3715-3727 (1998).
162. **Girard, A., Sachidanandam, R., Hannon, G.J. & Carmell, M.A.** A germline-specific class of small RNAs binds mammalian Piwi proteins. *Nature* **442**, 199-202 (2006).
163. **Vagin, V.V., et al.** A distinct small RNA pathway silences selfish genetic elements in the germline. *Science (New York, N.Y)* **313**, 320-324 (2006).
164. **Brennecke, J., et al.** Discrete small RNA-generating loci as master regulators of transposon activity in *Drosophila*. *Cell* **128**, 1089-1103 (2007).
165. **Gunawardane, L.S., et al.** A slicer-mediated mechanism for repeat-associated siRNA 5' end formation in *Drosophila*. *Science (New York, N.Y)* **315**, 1587-1590 (2007).
166. **Song, J.J., Smith, S.K., Hannon, G.J. & Joshua-Tor, L.** Crystal structure of Argonaute and its implications for RISC slicer activity. *Science (New York, N.Y)* **305**, 1434-1437 (2004).
167. **Liu, J., et al.** Argonaute2 is the catalytic engine of mammalian RNAi. *Science (New York, N.Y)* **305**, 1437-1441 (2004).
168. **Fabian, M.R., Sonenberg, N. & Filipowicz, W.** Regulation of mRNA translation and stability by microRNAs. *Annual review of biochemistry* **79**, 351-379 (2010).
169. **Filipowicz, W., Bhattacharyya, S.N. & Sonenberg, N.** Mechanisms of post-transcriptional regulation by microRNAs: are the answers in sight? *Nat Rev Genet* **9**, 102-114 (2008).

170. **Kiriakidou, M., et al.** An mRNA m7G Cap Binding-like Motif within Human Ago2 Represses Translation. *Cell* **129**, 1141-1151 (2007).
171. **Behm-Ansmant, I., et al.** mRNA degradation by miRNAs and GW182 requires both CCR4:NOT deadenylase and DCP1:DCP2 decapping complexes. *Genes & development* **20**, 1885-1898 (2006).
172. **Giraldez, A.J., et al.** Zebrafish MiR-430 promotes deadenylation and clearance of maternal mRNAs. *Science (New York, N.Y)* **312**, 75-79 (2006).
173. **Verdel, A., Vasseur, A., Le Gorrec, M. & Touat-Todeschini, L.** Common themes in siRNA-mediated epigenetic silencing pathways. *The International journal of developmental biology* **53**, 245-257 (2009).
174. **Volpe, T.A., et al.** Regulation of heterochromatic silencing and histone H3 lysine-9 methylation by RNAi. *Science (New York, N.Y)* **297**, 1833-1837 (2002).
175. **Grewal, S.I.** RNAi-dependent formation of heterochromatin and its diverse functions. *Current opinion in genetics & development* **20**, 134-141 (2010).
176. **Napoli, C., Lemieux, C. & Jorgensen, R.** Introduction of a Chimeric Chalcone Synthase Gene into Petunia Results in Reversible Co-Suppression of Homologous Genes in trans. *The Plant cell* **2**, 279-289 (1990).
177. **Cerutti, H., Johnson, A.M., Gillham, N.W. & Boynton, J.E.** A eubacterial gene conferring spectinomycin resistance on *Chlamydomonas reinhardtii*: integration into the nuclear genome and gene expression. *Genetics* **145**, 97-110 (1997).
178. **Fuhrmann, M., Stahlberg, A., Govorunova, E., Rank, S. & Hegemann, P.** The abundant retinal protein of the *Chlamydomonas* eye is not the photoreceptor for phototaxis and photophobic responses. *Journal of cell science* **114**, 3857-3863 (2001).
179. **Xu, P., Zhang, Y., Kang, L., Roossinck, M.J. & Mysore, K.S.** Computational estimation and experimental verification of off-target silencing during posttranscriptional gene silencing in plants. *Plant physiology* **142**, 429-440 (2006).
180. **Vaistij, F.E., Jones, L. & Baulcombe, D.C.** Spreading of RNA targeting and DNA methylation in RNA silencing requires transcription of the target gene and a putative RNA-dependent RNA polymerase. *The Plant cell* **14**, 857-867 (2002).
181. **Yamasaki, T., Miyasaka, H. & Ohama, T.** Unstable RNAi effects through epigenetic silencing of an inverted repeat transgene in *Chlamydomonas reinhardtii*. *Genetics* **180**, 1927-1944 (2008).
182. **Schwab, R., Ossowski, S., Riester, M., Warthmann, N. & Weigel, D.** Highly specific gene silencing by artificial microRNAs in Arabidopsis. *The Plant cell* **18**, 1121-1133 (2006).
183. **Ghildiyal, M. & Zamore, P.D.** Small silencing RNAs: an expanding universe. *Nat Rev Genet* **10**, 94-108 (2009).
184. **Ossowski, S., Schwab, R. & Weigel, D.** Gene silencing in plants using artificial microRNAs and other small RNAs. *Plant J* **53**, 674-690 (2008).
185. **Zhao, T., et al.** A complex system of small RNAs in the unicellular green alga *Chlamydomonas reinhardtii*. *Genes & development* **21**, 1190-1203 (2007).
186. **Molnar, A., Schwach, F., Studholme, D.J., Thuenemann, E.C. & Baulcombe, D.C.** miRNAs control gene expression in the single-cell alga *Chlamydomonas reinhardtii*. *Nature* **447**, 1126-1129 (2007).
187. **Zhao, T., Wang, W., Bai, X. & Qi, Y.** Gene silencing by artificial microRNAs in *Chlamydomonas*. *Plant J* (2008).
188. **Sizova, I., Fuhrmann, M. & Hegemann, P.** A *Streptomyces rimosus* aphVIII gene coding for a new type phosphotransferase provides stable antibiotic resistance to *Chlamydomonas reinhardtii*. *Gene* **277**, 221-229 (2001).
189. **Moore, I., Samalova, M. & Kurup, S.** Transactivated and chemically inducible gene expression in plants. *Plant J* **45**, 651-683 (2006).
190. **Felenbok, B.** The ethanol utilization regulon of *Aspergillus nidulans*: the alcA-alcR system

- as a tool for the expression of recombinant proteins. *Journal of biotechnology* **17**, 11-17 (1991).
191. **Fillinger, S. & Felenbok, B.** A newly identified gene cluster in *Aspergillus nidulans* comprises five novel genes localized in the alc region that are controlled both by the specific transactivator AlcR and the general carbon-catabolite repressor CreA. *Molecular microbiology* **20**, 475-488 (1996).
 192. **Caddick, M.X., et al.** An ethanol inducible gene switch for plants used to manipulate carbon metabolism. *Nature biotechnology* **16**, 177-180 (1998).
 193. **Chen, S., Hofius, D., Sonnewald, U. & Bornke, F.** Temporal and spatial control of gene silencing in transgenic plants by inducible expression of double-stranded RNA. *Plant J* **36**, 731-740 (2003).
 194. **Koblenz, B. & Lechtreck, K.F.** The NIT₁ promoter allows inducible and reversible silencing of centrin in *Chlamydomonas reinhardtii*. *Eukaryotic cell* **4**, 1959-1962 (2005).
 195. **Pan, J.M., Haring, M.A. & Beck, C.F.** Dissection of the Blue-Light-Dependent Signal-Transduction Pathway Involved in Gametic Differentiation of *Chlamydomonas reinhardtii*. *Plant physiology* **112**, 303-309 (1996).
 196. **Hahn, A., Bublak, D., Schleiff, E. & Scharf, K.D.** Crosstalk between Hsp90 and Hsp70 chaperones and heat stress transcription factors in tomato. *The Plant cell* **23**, 741-755 (2011).
 197. **Zou, J., Guo, Y., Guettouche, T., Smith, D.F. & Voellmy, R.** Repression of heat shock transcription factor HSF1 activation by HSP90 (HSP90 complex) that forms a stress-sensitive complex with HSF1. *Cell* **94**, 471-480 (1998).
 198. **Taipale, M., Jarosz, D.F. & Lindquist, S.** HSP90 at the hub of protein homeostasis: emerging mechanistic insights. *Nature reviews* **11**, 515-528 (2010).
 199. **Rutherford, S.L. & Lindquist, S.** Hsp90 as a capacitor for morphological evolution. *Nature* **396**, 336-342 (1998).
 200. **Nathan, D.F., Vos, M.H. & Lindquist, S.** In vivo functions of the *Saccharomyces cerevisiae* Hsp90 chaperone. *Proceedings of the National Academy of Sciences of the United States of America* **94**, 12949-12956 (1997).
 201. **Sawarkar, R., Sievers, C. & Paro, R.** Hsp90 globally targets paused RNA polymerase to regulate gene expression in response to environmental stimuli. *Cell* **149**, 807-818 (2012).
 202. **Saidi, Y., et al.** The heat shock response in moss plants is regulated by specific calcium-permeable channels in the plasma membrane. *The Plant cell* **21**, 2829-2843 (2009).
 203. **Liu, H.T., et al.** The calmodulin-binding protein kinase 3 is part of heat-shock signal transduction in *Arabidopsis thaliana*. *Plant J* **55**, 760-773 (2008).
 204. **Wakabayashi, K., Ide, T. & Kamiya, R.** Calcium-dependent flagellar motility activation in *Chlamydomonas reinhardtii* in response to mechanical agitation. *Cell motility and the cytoskeleton* **66**, 736-742 (2009).
 205. **Tsien, R.Y.** New calcium indicators and buffers with high selectivity against magnesium and protons: design, synthesis, and properties of prototype structures. *Biochemistry* **19**, 2396-2404 (1980).
 206. **Saoudi, Y., et al.** Calcium-independent cytoskeleton disassembly induced by BAPTA. *European journal of biochemistry / FEBS* **271**, 3255-3264 (2004).
 207. **Berry, J. & Bjorkman, O.** Photosynthetic Response and Adaptation to Temperature in Higher Plants. *Annual Review of Plant Physiology* **31**, 491-543 (1980).
 208. **Tan, W., Meng, Q., Brestic, M., Olsovska, K. & Yang, X.** Photosynthesis is improved by exogenous calcium in heat-stressed tobacco plants. *J Plant Physiol* **168**, 2063-2071 (2011).
 209. **Pellegrino, M.W., Nargund, A.M. & Haynes, C.M.** Signaling the mitochondrial unfolded protein response. *Biochimica et biophysica acta* (2012).
 210. **Parmar, V.M. & Schroder, M.** Sensing endoplasmic reticulum stress. *Adv Exp Med Biol* **738**, 153-168 (2012).

211. **Su, P.H. & Li, H.M.** Arabidopsis stromal 70-kD heat shock proteins are essential for plant development and important for thermotolerance of germinating seeds. *Plant physiology* **146**, 1231-1241 (2008).
212. **Wielopolska, A., Townley, H., Moore, I., Waterhouse, P. & Helliwell, C.** A high-throughput inducible RNAi vector for plants. *Plant biotechnology journal* **3**, 583-590 (2005).
213. **Guo, H.S., Fei, J.F., Xie, Q. & Chua, N.H.** A chemical-regulated inducible RNAi system in plants. *Plant J* **34**, 383-392 (2003).
214. **Gupta, S., Schoer, R.A., Egan, J.E., Hannon, G.J. & Mittal, V.** Inducible, reversible, and stable RNA interference in mammalian cells. *Proceedings of the National Academy of Sciences of the United States of America* **101**, 1927-1932 (2004).
215. **Quinn, J.M., Kropat, J. & Merchant, S.** Copper response element and Crr1-dependent Ni(2+)-responsive promoter for induced, reversible gene expression in *Chlamydomonas reinhardtii*. *Eukaryotic cell* **2**, 995-1002 (2003).
216. **Pinsino, A., Turturici, G., Sconzo, G. & Geraci, F.** Rapid changes in heat-shock cognate 70 levels, heat-shock cognate phosphorylation state, heat-shock transcription factor, and metal transcription factor activity levels in response to heavy metal exposure during sea urchin embryonic development. *Ecotoxicology* **20**, 246-254 (2011).
217. **de Hostos, E.L., Togasaki, R.K. & Grossman, A.** Purification and biosynthesis of a derepressible periplasmic arylsulfatase from *Chlamydomonas reinhardtii*. *The Journal of cell biology* **106**, 29-37 (1988).
218. **Fujiwara, S., Fukuzawa, H., Tachiki, A. & Miyachi, S.** Structure and differential expression of two genes encoding carbonic anhydrase in *Chlamydomonas reinhardtii*. *Proceedings of the National Academy of Sciences* **87**, 9779-9783 (1990).
219. **Ohresser, M., Matagne, R.F. & Loppes, R.** Expression of the arylsulphatase reporter gene under the control of the nit1 promoter in *Chlamydomonas reinhardtii*. *Current genetics* **31**, 264-271 (1997).
220. **Fernandez, E., et al.** Isolation and characterization of the nitrate reductase structural gene of *Chlamydomonas reinhardtii*. *Proceedings of the National Academy of Sciences of the United States of America* **86**, 6449-6453 (1989).
221. **Fernandez, E. & Galvan, A.** Nitrate assimilation in *Chlamydomonas*. *Eukaryotic cell* **7**, 555-559 (2008).
222. **Quesada, A. & Fernandez, E.** Expression of nitrate assimilation related genes in *Chlamydomonas reinhardtii*. *Plant molecular biology* **24**, 185-194 (1994).
223. **Bloom, A.J., Sukrapanna, S.S. & Warner, R.L.** Root respiration associated with ammonium and nitrate absorption and assimilation by barley. *Plant physiology* **99**, 1294-1301 (1992).
224. **Camargo, A., et al.** Nitrate signaling by the regulatory gene NIT2 in *Chlamydomonas*. *The Plant cell* **19**, 3491-3503 (2007).
225. **Petroutsos, D., et al.** The chloroplast calcium sensor CAS is required for photoacclimation in *Chlamydomonas reinhardtii*. *The Plant cell* **23**, 2950-2963 (2011).
226. **Alvarez, J.P., et al.** Endogenous and synthetic microRNAs stimulate simultaneous, efficient, and localized regulation of multiple targets in diverse species. *The Plant cell* **18**, 1134-1151 (2006).
227. **Schroda, M., Beck, C.F. & Vallon, O.** Sequence elements within an HSP70 promoter counteract transcriptional transgene silencing in *Chlamydomonas*. *Plant J* **31**, 445-455 (2002).
228. **Lodha, M., Schulz-Raffelt, M. & Schroda, M.** A new assay for promoter analysis in *Chlamydomonas* reveals roles for heat shock elements and the TATA box in HSP70A promoter-mediated activation of transgene expression. *Eukaryotic cell* **7**, 172-176 (2008).
229. **Schroda, M., Blocker, D. & Beck, C.F.** The HSP70A promoter as a tool for the improved expression of transgenes in *Chlamydomonas*. *Plant J* **21**, 121-131 (2000).

230. Eberhard, S., *et al.* Generation of an oligonucleotide array for analysis of gene expression in *Chlamydomonas reinhardtii*. *Current genetics* **49**, 106-124 (2006).
231. Voss, B., *et al.* Hemin and magnesium-protoporphyrin IX induce global changes in gene expression in *Chlamydomonas reinhardtii*. *Plant physiology* **155**, 892-905 (2011).
232. May, P., *et al.* Metabolomics- and proteomics-assisted genome annotation and analysis of the draft metabolic network of *Chlamydomonas reinhardtii*. *Genetics* **179**, 157-166 (2008).
233. Reinbothe, S. & Reinbothe, C. The regulation of enzymes involved in chlorophyll biosynthesis. *European journal of biochemistry / FEBS* **237**, 323-343 (1996).
234. Kumar Tewari, A. & Charan Tripathy, B. Temperature-stress-induced impairment of chlorophyll biosynthetic reactions in cucumber and wheat. *Plant physiology* **117**, 851-858 (1998).
235. Phung, T.H., *et al.* Porphyrin biosynthesis control under water stress: sustained porphyrin status correlates with drought tolerance in transgenic rice. *Plant physiology* **157**, 1746-1764 (2011).
236. Li, X., Henry, R., Yuan, J., Cline, K. & Hoffman, N.E. A chloroplast homologue of the signal recognition particle subunit SRP54 is involved in the posttranslational integration of a protein into thylakoid membranes. *Proceedings of the National Academy of Sciences of the United States of America* **92**, 3789-3793 (1995).
237. Moseley, J.L., *et al.* Reciprocal expression of two candidate di-iron enzymes affecting photosystem I and light-harvesting complex accumulation. *The Plant cell* **14**, 673-688 (2002).
238. Guo, J. & Polymenis, M. Dcr2 targets Ire1 and downregulates the unfolded protein response in *Saccharomyces cerevisiae*. *EMBO reports* **7**, 1124-1127 (2006).
239. Shamu, C.E. & Walter, P. Oligomerization and phosphorylation of the Ire1p kinase during intracellular signaling from the endoplasmic reticulum to the nucleus. *The EMBO journal* **15**, 3028-3039 (1996).
240. Patil, C. & Walter, P. Intracellular signaling from the endoplasmic reticulum to the nucleus: the unfolded protein response in yeast and mammals. *Current opinion in cell biology* **13**, 349-355 (2001).
241. Hubel, A. & Schoffl, F. Arabidopsis heat shock factor: isolation and characterization of the gene and the recombinant protein. *Plant molecular biology* **26**, 353-362 (1994).
242. Scharf, K.D., Rose, S., Zott, W., Schoffl, F. & Nover, L. Three tomato genes code for heat stress transcription factors with a region of remarkable homology to the DNA-binding domain of the yeast HSF. *The EMBO journal* **9**, 4495-4501 (1990).
243. Lodha, M. & Schroda, M. Analysis of chromatin structure in the control regions of the *Chlamydomonas* HSP70A and RBCS2 genes. *Plant molecular biology* **59**, 501-513 (2005).
244. Ball, S.G., Dirick, L., Decq, A., Martiat, J.C. & Matagne, R.F. Physiology of Starch Storage in the Monocellular Alga *Chlamydomonas-Reinhardtii*. *Plant Science* **66**, 1-9 (1990).
245. Schroda, M. & Vallon, O. *Chaperones and Proteases*. In: *The Chlamydomonas Sourcebook, Second Edition*, (Elsevier / Academic Press, San Diego, CA, 2008).
246. Harris, E.H. *The Chlamydomonas sourcebook : a comprehensive guide to biology and laboratory use*, (Acad. Press, San Diego {[u.a.], 1989).
247. Hust, B. & Gutensohn, M. Deletion of core components of the plastid protein import machinery causes differential arrest of embryo development in *Arabidopsis thaliana*. *Plant Biol (Stuttg)* **8**, 18-30 (2006).
248. Bauer, J., *et al.* The major protein import receptor of plastids is essential for chloroplast biogenesis. *Nature* **403**, 203-207 (2000).
249. Kovacheva, S., *et al.* In vivo studies on the roles of Tic110, Tic40 and Hsp93 during chloroplast protein import. *Plant J* **41**, 412-428 (2005).
250. Jarvis, P., *et al.* An *Arabidopsis* mutant defective in the plastid general protein import apparatus. *Science (New York, N.Y)* **282**, 100-103 (1998).

251. **Richter, S. & Lamppa, G.K.** A chloroplast processing enzyme functions as the general stromal processing peptidase. *Proceedings of the National Academy of Sciences of the United States of America* **95**, 7463-7468 (1998).
252. **Rolland, N., et al.** The Biosynthetic Capacities of the Plastids and Integration Between Cytoplasmic and Chloroplast Processes. *Annual review of genetics* (2012).
253. **Bassham, D.C.** Plant autophagy--more than a starvation response. *Current opinion in plant biology* **10**, 587-593 (2007).
254. **Kirk, D.L. & Kirk, M.M.** Carrier-mediated Uptake of Arginine and Urea by *Chlamydomonas reinhardtii*. *Plant physiology* **61**, 556-560 (1978).
255. **Tegeder, M. & Ward, J.M.** Molecular Evolution of Plant AAP and LHT Amino Acid Transporters. *Frontiers in plant science* **3**, 21 (2012).
256. **Remacle, C., et al.** The ARG9 gene encodes the plastid-resident N-acetyl ornithine aminotransferase in the green alga *Chlamydomonas reinhardtii*. *Eukaryotic cell* **8**, 1460-1463 (2009).
257. **Vallon, O., Bulte, L., Kuras, R., Olive, J. & Wollman, F.A.** Extensive accumulation of an extracellular L-amino-acid oxidase during gametogenesis of *Chlamydomonas reinhardtii*. *European journal of biochemistry / FEBS* **215**, 351-360 (1993).
258. **Muñoz-Blanco, J., Hidalgo-Martínez, J. & Cárdenas, J.** Extracellular deamination of l-amino acids by *Chlamydomonas reinhardtii* cells. *Planta* **182**, 194-198 (1990).
259. **Muhlhaus, T., Weiss, J., Hemme, D., Sommer, F. & Schroda, M.** Quantitative shotgun proteomics using a uniform (1)N-labeled standard to monitor proteome dynamics in time course experiments reveals new insights into the heat stress response of *Chlamydomonas reinhardtii*. *Mol Cell Proteomics* **10**, M110 004739 (2011).
260. **Perez-Perez, M.E., Florencio, F.J. & Crespo, J.L.** Inhibition of target of rapamycin signaling and stress activate autophagy in *Chlamydomonas reinhardtii*. *Plant physiology* **152**, 1874-1888 (2010).
261. **Bandhakavi, S., et al.** Hsf1 activation inhibits rapamycin resistance and TOR signaling in yeast revealed by combined proteomic and genetic analysis. *PLoS one* **3**, e1598 (2008).
262. **Loewith, R. & Hall, M.N.** Target of rapamycin (TOR) in nutrient signaling and growth control. *Genetics* **189**, 1177-1201 (2011).
263. **Chou, S.D., Prince, T., Gong, J. & Calderwood, S.K.** mTOR is essential for the proteotoxic stress response, HSF1 activation and heat shock protein synthesis. *PLoS one* **7**, e39679 (2012).
264. **Chang, Y.Y., et al.** Nutrient-dependent regulation of autophagy through the target of rapamycin pathway. *Biochemical Society transactions* **37**, 232-236 (2009).
265. **Markham, K., Bai, Y. & Schmitt-Ulms, G.** Co-immunoprecipitations revisited: an update on experimental concepts and their implementation for sensitive interactome investigations of endogenous proteins. *Anal Bioanal Chem* **389**, 461-473 (2007).
266. **Gavin, A.C., Maeda, K. & Kuhner, S.** Recent advances in charting protein-protein interaction: mass spectrometry-based approaches. *Curr Opin Biotechnol* **22**, 42-49 (2011).
267. **Selbach, M. & Mann, M.** Protein interaction screening by quantitative immunoprecipitation combined with knock-down (QUICK). *Nat Methods* **3**, 981-983 (2006).
268. **Ong, S.E. & Mann, M.** A practical recipe for stable isotope labeling by amino acids in cell culture (SILAC). *Nat Protoc* **1**, 2650-2660 (2006).
269. **Mayer, M.P. & Bukau, B.** Hsp70 chaperones: cellular functions and molecular mechanism. *Cellular and molecular life sciences : CMLS* **62**, 670-684 (2005).

5. SUMMARY / ZUSAMMENFASSUNG

Wechselnde Umweltbedingungen wie Temperaturveränderungen oder der Zugang zu Nährstoffen erfordern spezielle genetische Anpassungsprogramme, vor allem von sessilen Organismen wie Pflanzen. Ein solcher hochkonservierter Mechanismus, der unter anderem vor Temperaturspitzen schützt, ist die von Hitzeschockfaktoren (HSF) kontrollierte Hitzeschockantwort (HSR). Dabei werden vermehrt spezifische Hitzestressproteine (HSPs, Chaperone) gebildet, die die zelluläre Proteinhomeostase aufrecht erhalten. In Pflanzen hat sich ein hochkomplexes regulatorisches Netzwerk evolviert, das aus über 20 HSFs besteht und eine genaue Feinabstimmung der HSR auf die jeweiligen Stressbedingungen erlaubt.

Das hohe Maß an Komplexität der HSR in Pflanzen erschwert die wissenschaftliche Zugänglichkeit jedoch erheblich. Um die grundlegenden Prinzipien der HSR in Pflanzen zu verstehen griffen wir deshalb auf einen einfacheren Modellorganismus zurück, der einzelligen Grünalge *Chlamydomonas reinhardtii*, der Pflanzen sehr nahe steht aber nur einen kanonischen HSF (HSF1) enthält. Im Rahmen dieser Arbeit wurden dazu drei Ansätze verfolgt:

Als erstes wurden verschiedene chemische Substanzen eingesetzt, die unterschiedliche Schritte während der Aktivierung und Abschaltung der HSR hemmen, um darüber die Regulation der HSR aufzuklären. Dabei wurde festgestellt, dass die Phosphorylierung von HSF1 eine entscheidende Rolle bei dessen Aktivierung spielt, das auslösende Momentum die Anhäufung von falsch gefalteten Proteinen ist und HSP90A aus dem Cytosol eine wichtige modulierende Rolle bei der HSR spielt.

Als zweites wurden mit Hilfe von Microarrays und HSF1-RNAi-Stämmen potentielle Zielgene ermittelt, um vor allem pflanzenspezifische Prozesse zu identifizieren, die während eines Hitzeschocks gezielt angepasst werden. Dabei konnte die Chlorophyll-Biosynthese und der Transport von Proteinen in den/im Chloroplasten als neue, pflanzenspezifische Ziele der Stressantwort identifiziert werden. Des Weiteren konnte gezeigt werden, dass HSF1 auch die Expression plastidäre Chaperone reguliert.

Als letztes wurde gezielt die Expression wichtiger Gene für die Stressantwort (HSF1/HSP70B) unterdrückt, um den Einfluss dieser Gene auf die HSR genauer zu studieren. Dazu habe ich ein System entwickelt, das auf künstlichen microRNAs beruht und es erlaubt induzierbar Gene auszuschalten, abhängig von der Stickstoffquelle im Nährmedium. Dieses System erlaubte es zu zeigen, dass HSF1 selbst während der HSR die Expression seiner mRNA erhöht um die Stressantwort weiter zu verstärken. Mithilfe des induzierbaren microRNA Systems konnte ich weiter zeigen, dass das plastidäre HSP70B ein essentielles Protein für das Zellwachstum ist. Dabei konnte ich feststellen, dass die HSP70B-vermittelte Assemblierung und Disassemblierung von makromolekularen Komplexen des VIPP1 Proteins für dessen Funktion im Chloroplasten entscheidend ist. Des Weiteren konnte ich zeigen, dass HSP70B sehr wahrscheinlich für die Faltung eines oder mehrerer noch unbekannter Enzyme der Arginin Biosynthese oder der Stickstofffixierung verantwortlich ist, und das dies wahrscheinlich der Grund dafür ist, dass HSP70B ein essentielles Protein ist.

6. ERKLÄRUNG

Hiermit erkläre ich, dass die vorliegende Arbeit ohne unzulässige Hilfe Dritter und ohne Benutzung anderer als der hier angegebenen Hilfsmittel von mir persönlich angefertigt wurde. Die aus anderen Quellen direkt oder indirekt übernommenen Daten und Konzepte sind unter Angabe der Quellen gekennzeichnet.

Insbesondere habe ich hierfür nicht die entgeltliche Hilfe von Vermittlungs- beziehungsweise Beratungsdiensten (Promotionsberater oder anderer Personen) in Anspruch genommen. Niemand hat von mir unmittelbar oder mittelbar geldwerte Leistungen für Arbeiten erhalten, die im Zusammenhang mit dem Inhalt der vorgelegten Dissertation stehen.

Die Arbeit wurde bisher weder im In- noch im Ausland in gleicher oder ähnlicher Form einer anderen Prüfungsbehörde vorgelegt.

Die Bestimmungen der Promotionsordnung des Fachbereichs Biologie der Universität Kaiserslautern sind mir bekannt, insbesondere weiß ich, dass ich vor Vollzug der Promotion zur Führung des Dokortitels nicht berechtigt bin.

Stefan Schmollinger

Kaiserslautern, den 17.10.2012

7. CURRICULUM VITAE

Personal dates

Name: Stefan Schmollinger
Gender: Male
Nationality: German

Education

School:

1986 – 1990 Elementary school
1990 – 1999 Gymnasium, major in mathematics & physics (Abitur, grade 1.3)

University:

2000 – 2003 University of Karlsruhe: Study of Biology
(Vordiplom, grade 1.7)
2003 – 2007 University of Freiburg: Study of Biology with major in biochemistry
(Diploma, grade 1.2)
2007 – 2008 Department of Plant Biochemistry, Freiburg: Diploma thesis, entitled:
“Characterization of the VIPP2 protein from *Chlamydomonas reinhardtii*.”
(Diploma thesis, grade 1.0)
2008 – 2012 Max Planck Institute for Molecular Plant Physiology, Potsdam:
PhD thesis in the group of PD. Dr. M. Schroda

Attended scientific conferences and contributions

13th International Conference of the Cell and Molecular Biology of *Chlamydomonas*, Hyères-les-Palmiers (France), 2008. Poster presentation with the title:
„Characterisation of *Chlamydomonas reinhardtii* VIPP2 protein”

German Symposium on Systems Biology, Heidelberg (Germany), 2009. Poster presentation:
“Evidence for a role of heat shock factors in *HSP70A* promoter mediated activation of transgene expression”

14th International Conference of the Cell and Molecular Biology of *Chlamydomonas*, Boston (USA), 2010. Oral presentation with the title:
“An inducible artificial microRNA system for *Chlamydomonas reinhardtii* as a tool to investigate essential gene function”

14th International Conference of the Cell and Molecular Biology of Chlamydomonas, Boston (USA), 2010. Oral presentation with the title:

"Modeling of the HSF1-dependent heat shock response in *Chlamydomonas reinhardtii* "

Havel-Spree-Colloquium, Potsdam (Germany), 2012. Oral presentation with the title:

"An inducible artificial microRNA system for *Chlamydomonas reinhardtii* as a tool to investigate (essential) protein function"

Research Initiative Membrane Biology (RIMB) Meeting, Kaiserslautern (Germany), 2012. Oral presentation with the title:

"Shedding new light onto the functions of the HSP70B chaperone in the chloroplast of *Chlamydomonas reinhardtii*"

15th International Conference of the Cell and Molecular Biology of Chlamydomonas, Potsdam (Germany), 2012. Poster presentation with the title:

"*HSF1*-dependent stress response - Specific acclimation strategies in *Chlamydomonas*. Regulation of chloroplast import, tetrapyrrole biosynthesis and a unique positive feedback loop"

